An Improved Ebullioscope for High Polymers

RAYMOND L. ARNETT, MELVIN E. SMITH, and BARRY O. BUELL, *Phillips Petroleum Company, Bartlesville, Oklahoma*

Synopsis

A description is given of an ebullioscope which was calibrated and found satisfactory for determining the number-average molecular weight of several unbranched polyethylenes. It employs a benzene-filled Menzies differential vapor pressure thermometer having a detection limit of 5×10^{-6}°C. In order to obtain a close approach to solvent–vapor and solution–vapor equilibria, the boiler design incorporates a means of preheating the liquid solvent returning from the condenser and a mechanical lift pump to extract liquid solution from the boiler. In addition, time stability of these equilibria is provided by insulation to reduce heat conduction, reflectors to exclude radiant energy, constant pressure control, and constant wall temperature. An analysis of the observed temperature fluctuations shows that these features result in thermometer noise which is lower by an order of magnitude than any heretofore reported. Full advantage from this improvement has not been realized in interrupted (3-day) experimental runs which gave a standard deviation of 400 at the 10,000 molecular weight level. Indications are that full benefit of the reduced thermometer noise with severalfold further reduction in standard deviation, could be realized in uninterrupted runs.

I. INTRODUCTION

The direct measurement of number-average molecular weights in the range from a few thousand to several tens of thousands has proven to be difficult. Osmometry, the most logical approach, is ruled out for many applications because low molecular weight species diffuse through available membranes. Of the next most popular techniques, ebullioscopy and cryoscopy, the latter carries the inherent disadvantage of the possibility of solid solution formation. We were thus led to consider an ebullioscope for the determination of number-average molecular weights of synthetic polymeric materials.

Adequate thermometer sensitivity appeared not to be a problem; on the contrary, the high sensitivities that can be obtained with suitable thermometers would seem to require that the designer take steps to provide for a closer approach to and better time stability of the vapor–liquid equilibria whose temperature difference is to be measured. The first notable accomplishments in this direction are perhaps those of Ray,[1] whose modifications of the Menzies-Wright apparatus[2] resulted in considerable improvement for polymer application. More recently, Dimbat and Stross[3] designed a micro apparatus with two separate boilers which, although not intended

for high polymer work, included several desirable features, such as a partially silvered vacuum jacket surrounding the regions whose temperatures are measured, a vapor jacket around the whole, and provision for operating at constant pressure.

The single-boiler apparatus of Menzies and Wright seemed to us to be more susceptible of careful control than a two-boiler set-up. In general, those controls which result in the closest approach to equilibrium at the two thermometer positions will give the greatest accuracy, and those resulting in time stability of the equilibrium conditions will increase precision. Our analysis of the problems led us to believe that of the two difficulties the former had received less direct attention by previous workers than had the latter. Our design features aimed at the former problem are described below.

II. DESCRIPTION OF EBULLIOSCOPE

Thermometry

The sheer simplicity of the differential vapor pressure thermometer described by Menzies,[4] together with the obvious ability freely to select its sensitivity noted by Kitson and Mitchell[5] and by Hill and Brown[6] strongly recommended itself to us. If benzene is the thermometric fluid, the thermometer sensitivity is calculated[7] to be 1×10^{-3} °C./mm. (of benzene) in a solvent boiling in the neighborhood of 130°C. With a precision

WIRE (COILS TO PERMIT HEIGHT ADJUSTMENT)

GLASS HOOK AT TOP OF HELIX FITS LOOP IN END OF WIRE HOOKED INSIDE PUMP DISCHARGE

1 mm PRECISION CAPILLARY

2 CONCENTRIC GLASS SPIRALS OF SAME PITCH APPROX. 1/8". MAKING 20 TURNS

FIDUCIARY MARK
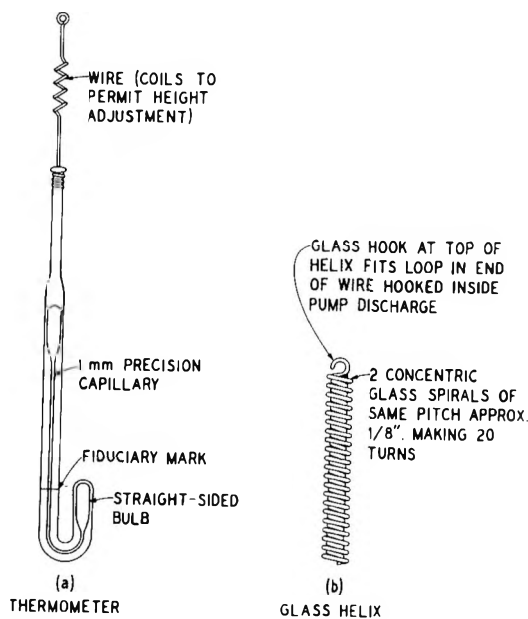
STRAIGHT-SIDED BULB

(a) THERMOMETER

(b) GLASS HELIX

Fig. 1. Thermometer and helix.

cathetometer distances may be reproducibly measured to 0.005 mm. thus, a temperature difference of 5×10^{-6}°C. should be the detection limit. This would allow the determination of the molecular weight of a polymer having $M_n = 100,000$ to a precision of 1% for solutions (in ethylbenzene, say) whose concentrations did not exceed 1 wt.%. The inherent sensitivity of such a thermometer is gratifyingly adequate for the task and hence we prepared J-shaped thermometers filled with carefully degassed reagent grade benzene (see Fig. 1a). The problem now was development of a boiler assembly sufficiently stable to utilize as much as possible of this inherent sensitivity. It may be mentioned here that these thermometers have been used at temperatures where the benzene vapor pressure exceeded four atmospheres, and no difficulty of the kind experienced by Kitson and Mitchell[5] was encountered.

Boiler

The boiler assembly finally evolved is composed of a tube provided with a heater at the lower closed end and a condenser at the upper open end (Fig. 2a). This tube is provided with all the stability controls and isolation found necessary by Dimbat and Stross.[3] In addition, we control the temperature of the condenser water. The inside walls of the tube are covered with powdered glass (lightly sintered in place) in the heater region. This region and a sufficient length of the tube to accommodate the thermometer are enclosed in an evacuable jacket although we have preferred to operate it at atmospheric pressure to reduce the temperature of the heater wire. The vapor jacket of an outer boiler, which maintains all walls at the boiling temperature of the pure solvent, surrounds this jacket and extends further up the inner tube.

The top end of the tube is closed with a machined aluminum fitting connected directly with the pressure regulator. In operation, both boilers and a 25-liter reservoir are sealed in a nitrogen atmosphere at 760 ± 1 mm. Hg. Sample additions are made through Teflon-stoppered holes drilled in a Lucite window at the top of the aluminum fitting. The whole tube assembly is housed in an aluminized cabinet to shield the thermometer from outside radiation.

The following features have been incorporated to allow for a closer approach to the vapor–pure liquid solvent equilibrium. The liquid solvent returning to the boiler from the condenser runs down the uninsulated section of the wall (above the ground glass joint) which is directly heated by the vapor jacket. Here the liquid is brought nearly to the equilibrium temperature without having to extract all its heat from the vapor. In this condition the liquid is diverted from the tube wall by a carefully ground joint (Fig. 2b) and allowed more intimate exchange with vapor within the male portion of the joint. The final delicate adjustments to equilibrium are made here before the liquid flows onto the upper bulb of the thermometer. The thermometer is suspended from this male joint assembly.
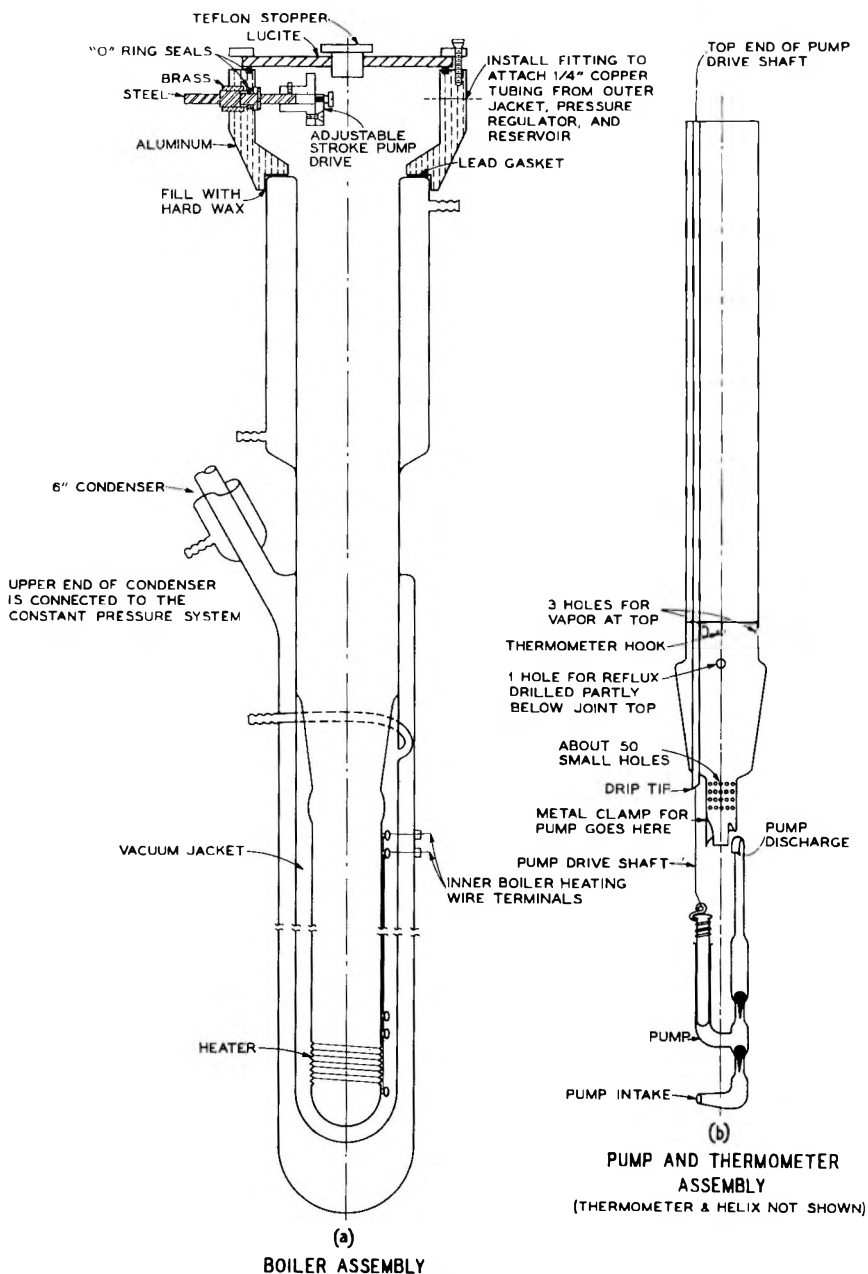
Fig. 2. Ebullioscope assembly.

Lift Pump

In modern ebullioscopes a Cottrell-type pump brings the liquid solution from the boiler to a thermometer located in the vapor region. However, for polymer work, surface tension changes accompanying the addition of

solute cause variations in the size of the liquid slugs lifted by the pump; in severe cases of foaming, the pump may fail to operate. The resulting changes in hydrostatic head make it more difficult to obtain a close approach to the desired solution-vapor equilibrium.

To overcome this difficulty we replaced the Cottrell pump with a powered mechanical lift pump (Fig. 2b) of all-glass construction. The upstroke of the piston takes liquid from the boiler into the pump, and the downstroke delivers it into the vapor region about 12 cm. above the boiler level. Here, in order to allow a close approach to equilibrium at the lower thermometer bulb, the solution is discharged dropwise onto a glass helix (Fig. 1b) around which the drop runs until at the lower end it touches and flows over the thermometer. In order to reduce the tendency of the drop to fly off the spiral under the centrifugal field we have found it expedient to use two concentric helicies of the same pitch so that capillarity confines the drop to the annular space. About 3 sec. is required for the liquid to descend the helix. The piston is driven by a small electric motor turning (1 rps) an eccentric which connects with the piston by a long stainless steel rod extending from the aluminum fitting to the pump.

III. METHOD OF OPERATION

The amount of solvent, both liquid and vapor, which is held in the upper regions of the boiler tube cannot be precisely determined during operation. Thus, although the mass of solute in the solution is precisely known, its concentration is not known. This lack of information need not lend uncertainty to the data if the amount of solvent in contact with the solute is kept constant. This constant may then become part of the instrument constant. To insure this constancy, at the start of a calibration or molecular weight determination, the pump, boiler tube, and all its components are dry, and a fixed amount (40.00 ml.) of solvent is added. As equilibrium reflux conditions are approached, the power supplied to the heaters is adjusted to a fixed value which is constant throughout a determination and from run to run. A slow boiling rate is used.

A solute addition is made and by means of a long-handled dipper, placed at the returning solvent hole just above the ground joint. At this time the reflux rate may be increased to hasten solution of the addition, and also to prevent cessation of boiling because of the pressure adjustment made after the system is opened to the atmosphere to add the solute. After a constant thermometer reading is obtained at the higher reflux rate (nominally 2 hr.), the heater power is reset to its fixed value and an additional hour or so is allowed for the new equilibrium to be established. The thermometer is then read at 1-min. intervals during a 30-min. period. With no trend evident, the mean of these readings is taken as the thermometer reading.

Treatment of Data

The quantitative expression used to interpret data taken under the above conditions of operation is

$$\lambda = (1/\bar{M}_n) \ [RT_0{}^2 \ V_0(dp/dt)/\Delta H_0 v] \ (m + am^2) + \lambda_0 \qquad (1)$$

where λ is the measured difference in heights (millimeters) of the thermometric fluid in the two thermometer arms; ΔH_0 is the heat of vaporization of the pure solvent at its boiling point, T_0; V_0 is the molar volume of the pure solvent at T_0; v is the volume, at T_0, of solution containing m grams of solute whose number-average molecular weight is $\bar{M}_n$; dp/dT is the temperature rate of change of vapor pressure, at T_0, of the thermometric fluid in millimeters of thermometric fluid, at T_0; a is a constant arising from the mathematical expansion of the nonideal factor in the thermodynamic expression for boiling point elevation, it being assumed that further terms in the expansion are negligible at the concentrations used.

The most common method of treating data would be to use the reading obtained for pure solvent at the beginning of a run as the numerical value for λ_0, and to plot $(\lambda - \lambda_0)/m$ versus m, fit a straight line to the data, and read the intercept according to the rearrangement of eq. (1),

$$(\lambda - \lambda_0)/m = (1/\bar{M}_n) \ K \ (1 + am) \qquad (2)$$

where K is written for the factor in square brackets in eq (1). Because of the possibility of occurrence of a "zero-point" error,[8,9] we prefer to take the derivative of eq. (1),

$$d\lambda/dm = (1/\bar{M}_n) \ K \ (1 + 2am) \qquad (3)$$

eliminating λ_0, and plot $(\lambda_{i+1} - \lambda_i)/(m_{i+1} - m_i)$ versus $m_{i+1} + m_i$, even though this increases the scatter of the plotted points. With a little practice in comparing visually fitted lines with least-square fitted lines, curves can be fitted visually in close agreement with those obtained by statistical treatment of the data.

In statistical adjustment of the data it is assumed that relative to the thermometer readings, solute masses are free of errors. The quantities, $\Delta\lambda/\Delta m$, are given statistical weights proportional to $(\Delta m)^2$ so that the $\Delta\lambda$ receive just that notice due them. In order to determine what that notice should be, we have plotted (Fig. 3) estimates, s_λ (obtained from the sets of 30 readings) of the standard deviations of thermometer readings against the total moles of solute added. The solutes included contain examples of branched and linear polyolefins and a low molecular weight calibration compound. Although several of the sets of points appear to show a trend of increasing noise with increasing solute concentration, others would appear to go through a maximum and still others have no pattern. We have not discovered a correlation between thermometer noise and solute type or concentration. It may be noted that in the

absence of solute the noise is nearly down to that expected from rounding error (for speed of reading, the thermometer is read to the nearest 0.01 mm.) and that, in general, the presence of solute increases the noise over this. Blackmore[10] has made this same observation and concluded that the increase in noise is inherently associated with the polymer solutions. For comparison with the noise figures reported by Blackmore, the ordinate scale of Figure 3 may be multiplied by 10 to give (very approximately) the noise level in microdegrees. Blackmore suggests that a well constructed ebullioscope of his design using thermistors would be operating
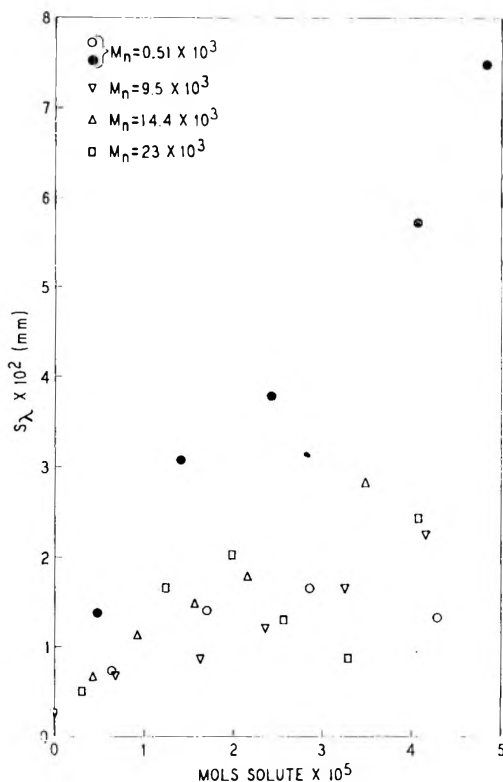

Fig. 3. Thermometer noise.

satisfactorily if the temperature uncertainty of the mean obtained over a 30-min. interval was 20×10^{-6}°C. for pure solvent; a 10% polymer solution would raise this uncertainty by a factor of 4 to 5. The corresponding figure obtained from Figure 3 is 0.7×10^{-6}°C. as the uncertainty of the mean of 30 readings; those data also confirm the 4 to 5 factor in the presence of solute.

Since there is no apparent correlation of thermometer noise with solute concentration, we have given all thermometer readings, hence the $\Delta\lambda$'s, equal weight in statistical fitting of data to eq. (3).

Calibration

It is apparent that, with the proper λ_0 for eq. (2), the determination of the intercept from data plotted according to either eq. (2) or (3) would constitute a measurement of $\bar{M}_n$ if the numerical value of K were known. We estimated K by measurement of the intercept of eq. (3) using suitable compounds as solutes for which $\bar{M}_n(=M)$ is known. The results of ten determinations are given in Table I for the case of n-octane as solvent and benzene as the thermometer fluid with the pressure adjusted to 760 mm. Three compounds are included: n-hexatriacontane ($C_{36}H_{74}$) and a single determination with each of 19,28-hexatetracontadione ($C_{46}H_{90}O_2$) and perchloropentacyclodecane ($C_{10}Cl_{12}$). The values for K are obtained from least-square fits of the several sets of data, and w_K are the relative statistical weights to be associated with each value. The weighted mean has a standard deviation of 3×10^3 estimated from 26 degrees of freedom. A calculated value for K assuming no solvent hold-up in the boiler tube is 168×10^3 mm./mole.

TABLE I
Determination of Instrument Constant

Compound	$K \times 10^{-3}$	w_K
$C_{36}H_{74}$	162	1.7
	155	2.5
	150	4.6
	164	1.0
	163	2.0
	181	4.9
	161	5.0
	161	1.8
$C_{46}H_{90}O_2$	167	1.4
$C_{10}Cl_{12}$	170	1.9
Mean	164	a

a The standard deviation for the mean of K is 3×10^3 mm./mole, estimated from 26 degrees of freedom.

IV. RESULTS FOR SOME LINEAR POLYETHYLENES

The data shown in Figure 4 are typical of those obtained for polymer runs. The solvent, thermometer and pressure are the same as those used in calibration. In Table II we present values of $\bar{M}_n$ obtained in this way for several unbranched polyethylenes together with estimates s of the standard deviations of the number-average molecular weights.

The standard deviations were estimated by the following procedure. Since $M_n = K/I$, where I is the intercept in a plot of eq. (3), then

$$s \simeq (\bar{M}_n/K)(s_K{}^2 + \bar{M}_n{}^2 s_I{}^2)^{1/2} \tag{4}$$

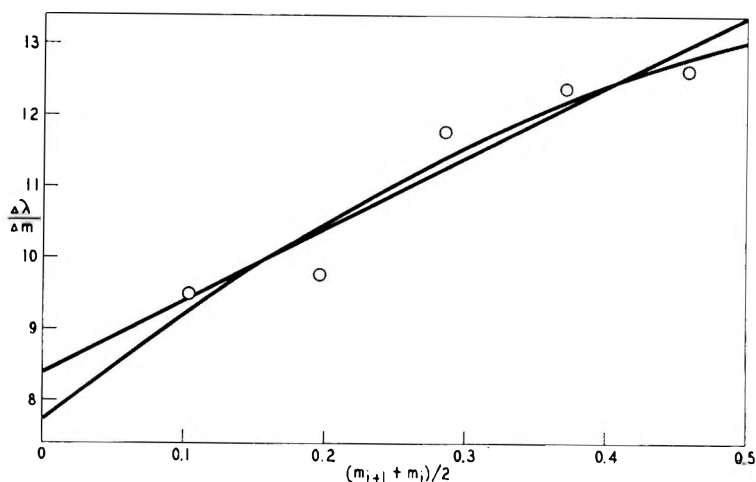where s_K and s_I are estimates of the standard deviations of K and I,

Fig. 4. Plot of data from a typical polymer $\bar{M}_n$ determination.

respectively. A few values of s_I, obtained from the least squares fit of data to eq. (3), are plotted in Figure 5 against $\bar{M}_n$. No dependence on $\bar{M}_n$ is apparent, hence a root-mean-square value of 0.57 mm./g. is used in eq. (4); other needed values are obtained from Table I.

That part of the uncertainty in I arising from the scatter of the data about the fitted line would be expected to come from the uncertainty in thermometer readings plus (1) the scatter occasioned by the failure of the data to follow the assumed straight-line relation eq. (3) and (2) the scatter occasioned by possible bias introduced in a random manner each time a solute addition is made. Although none of the data obtained on poly-ethylenes of unbranched or lightly branched structure (the limit of our investigation) shows any indication that eq. (3) is inadequate to describe the observations, a few runs were examined in some detail to give quantitative estimates of items (1) and (2) above as possible sources of scatter. A discussion of one of these will be informative.

TABLE II
Results for Some Linear Polyethylenes

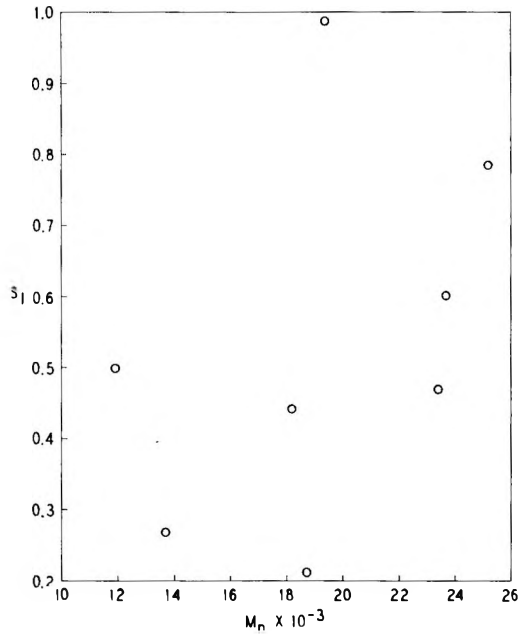| Poly-mer	$M_n \times 10^{-3}$	$s \times 10^{-3}$	Polymer	$M_n \times 10^{-3}$	$s \times 10^{-3}$
1	8.0	0.25	9	13.5	0.68
2	8.1	0.25	10	7.8	0.25
3	8.5	0.28	Fractions		
4	8.6	0.28	A	3.0	0.06
5	10.0	0.39	B	9.1	0.31
6	10.2	0.39	C	16.5	1.0
7	10.6	0.42	D	26.0	2.4
8	11.2	0.47	E	35.	4.3

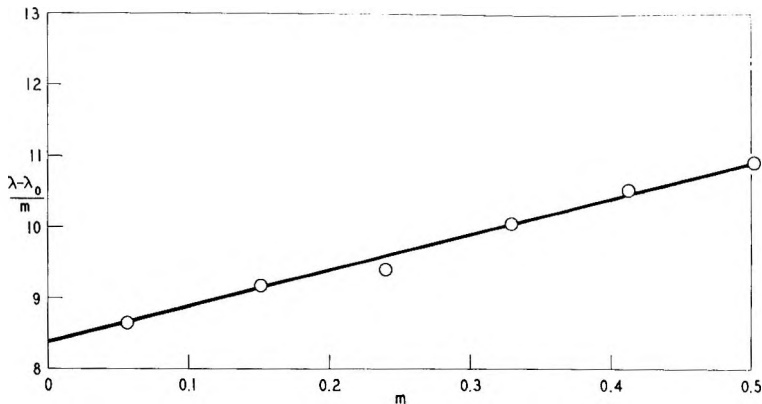Fig. 5. Uncertainty of intercept of eq. (3).

Fig. 6. Conventional plot of same data as in Fig. 4.

On the basis of the several sets of 30 thermometer readings, the mean square deviation of the data about a fitted line is estimated to be 4×10^{-5} mm.^{2} for a particular run.   As a result of fitting a straight line, the mean-square deviation of the five points (3 degrees of freedom) is estimated to be 220×10^{-5} mm.^{2} (Fig. 4).   It is highly improbable that these are estimates of the same quantity.   If we argue that the large magnitude of the second of the two estimates is due to an inadequacy of the straight line to represent the data and so include a quadratic term in eq. (3) to be fitted, the new mean-square deviation is 280×10^{-5} mm.^{2}, a value not significantly

different from that obtained with the linear relation. The statistical result that no improvement in fit is gained by adding the additional parameters is also immediately obvious from Figure 4, where both fitted curves are displayed, and from Figure 6, where the same data are plotted according to eq. (2). The curve in Figure 6 is drawn with the use of the constants obtained from the fit of eq. (3). In order to plot the observed data as $(\lambda - \lambda_0)/m$ without introducing a zero-point error, the parameter λ_0 was also fitted to the 6 observations by using the I and a values obtained from fitting eq. (3).

Figure 6 permits the illustration of two points. In comparison with Figure 4, which has the same coordinate scales, it allows a visual estimate of the amount of apparent scatter introduced by the derivative plot; by itself it allows examination of each primary observation. The lion's share of sum-of-squares is about equally divided between two observations, the second and fourth highest concentrations. It happens the data for this run were collected during three days and the two points in question were the first observations made after the two overnight breaks. If these are omitted, the mean-square deviation, estimated from one degree of freedom, drops from 220 to 7×10^{-5} mm.^{2}, a value in agreement with that expected from thermometer noise alone. Examination of other records reveals that an overnight break does not always result in a large fluctuation, but where a large deviation occurs, it is associated with such a break in operations; further these deviations seem to be random in magnitude and sign.

Although the mechanism responsible for the large deviations remains a mystery to us, the suggested means of avoiding them, namely completion of a run at one sitting, will allow full benefit of the reduced thermometer noise of our instrument.

References

1. Ray, N. H., *Trans. Faraday Soc.*, **48**, 809 (1952).
2. Menzies, A. W. C., and S. L. Wright, *J. Am. Chem. Soc.*, **43**, 2314 (1921).
3. Dimbat, M., and F. H. Stross, *Anal. Chem.*, **29**, 1517 (1957).
4. Menzies, A. W. C., *J. Am. Chem. Soc.*, **43**, 2309 (1921).
5. Kitson, R. E., and J. Mitchell, Jr., *Anal. Chem.*, **21**, 401 (1949).
6. Hill, F. N., and A. Brown, *Anal. Chem.*, **22**, 562 (1950).
7. Rossini, F. D., et al., *Selected Values of Physical and Thermodynamic Properties of Hydrocarbons and Related Compounds*, Carnegie Press, Pittsburgh, 1953.
8. Smith, H., *Trans. Faraday Soc.*, **52**, 402 (1956).
9. Bonnar, R. U., M. Dimbat, and F. H. Stross, *Number-Average Molecular Weights*, Interscience, New York, 1958.
10. Blackmore, W. R., *Rev. Sci. Instr.*, **31**, 317 (1960).

Résumé

On donne une description d'un ébullioscope qui a été calibré et trouvé satisfaisant pour la détermination du poids moléculaire moyen en nombre de plusieurs polyéthylènes linéaires. On utilise un thermomètre de Menzies rempli de benzène, qui mesure la tension de vapeur différentielle et qui possède une limite de détection de 5×10^{-6}

degrés. Afin d'approahcer le plus possible l'équilibre solvant–vapeur et solution–vapeur, on a conçu un appareil de chauffage qui contient un moyen de préchauffage du solvant liquide qui reflue du réfrigérant et une pompe mécanique pour extraire la solution liquide du ballon de chauffage. De plus, on assure une stabilité de ces équilibres en fonction du temps par isolation, pour diminuer la conduction thermique, à l'aide de réflecteurs pour exclure l'énergie de radiation, à l'aide d'un manostat et d'une température de paroi constante. L'analyse des fluctuations de température observées indique que celles-ci consistent dans des écarts du thermomètre qui sont inférieurs d'un ordre de grandeur par rapport à celles obtenues précédemment. Cette amélioration ne donne pas son avantage intégral lorsqu'on effectue des séries d'expériences interrompues (3 jours). Dans ce cas on observe une déviation standard de 400 pour une valeur de poids moléculaire de 10.000. On possède des indications que l'avantage complet de la diminution de l'imprécision du thermomètre peut être réalisé dans des expériences continues; ceci réduit encore plusieurs fois la déviation standard.

Zusammenfassung

Ein Ebullioskop, das geeicht wurde und sich zur Bestimmung des Zahlenmittels des Molekulargewichts mehrerer unverzweigter Polyäthylene als geeignet erwies, wird beschrieben. Es benützt ein benzol-gefülltes Differentialdampfdruckthermometer nach Menzies mit einer Erfassungsgrenze von 5×10^{-6} Grad. Um eine gute Annäherung an das Lösungsmittel-Dampf- und Lösungs-Dampfgleichgewicht zu erhalten, besitzt das Siedegefäss eine Einrichtung zur Vorheizung des aus dem Kühler zurückkehrenden flüssigen Lösungsmittels und eine mechanische Umlaufpumpe zur Abführung der flüssigen Lösung aus dem Siedegefäss. Zusätzlich wird eid zeitliche Beständigkeit der Gleichgewichte durch Isolierung zur Herabsetzung der Wärmeleitung, durch Reflektoren zum Ausschluss von Strahlungsenergie, sowie durch Aufrechterhaltung von konstantem Druck und konstanter Wandtemperatur gewährleistet. Eine Analyse der beobachteten Temperaturschwankungen zeigt, dass diese Anordnung zu einem um eine Grössenordnung kleineren Thermometergeräusch als bisher berichtet führt. Es war nicht möglich diese Verbesserung bei unterbrochenen (3 Tage) Versuchen, die eine Standardabweichung von 400 in Molekulargewichtsbereich um 10000 ergaben, voll auszunützen. Es bestehen Anzeichen dafür, dass eine volle Ausnützung des herabgesetzten Thermometergeräusches, mit mehrfacher weiterer Reduktion der Standardabweichung, bei ununterbrochenen Bestimmungen möglich sein sollte.

Crystallization and Melting Behavior of Polyacrylonitrile

R. CHIANG, *Chemstrand Research Center, Durham, North Carolina*

Synopsis

Dilatometric measurements have been carried out on the crystallization of polyacrylonitrile from propylene carbonate solutions at concentrations of 1.0, 4.2, and 8.4% and temperatures of 40, 70, 95, 104, and 108°C. Contrary to expectation, the volume of the solution actually increases upon crystallization, although the increase is extremely small (about 1% based on polymer). This small change in volume is consistent with the partial specific volume of polyacrylonitrile in solution and the specific volume of the polymer measured directly by a flotation method. Recent investigation by Holland, et al. revealed that polyacrylonitrile, upon crystallization from dilute solution, forms crystalline platelets resembling the single crystals observed in other polymers. It appears that the small change in volume on transformation from the dissolved state into the crystalline state is due to the closeness of the specific volumes in the two different states. These unusual density data of polyacrylonitrile resemble those of poly(methylmethacrylate), where isotactic, syndiotactic, and atactic polymers have about the same density. The fact that the difference in density of polyacrylonitrile is so small might well explain a number of related phenomena: the lack of abrupt volume change on melting, the absence of amorphous regions, the narrow range of the density values of different samples prepared by different methods, and the fact that crystallization conditions exert practically no effect on the density of the sample.

INTRODUCTION

Crystallization of nonpolar organic polymers is usually accompanied by a decrease in volume of about 10–15%. Examples in which the density of a semicrystalline polymer is nearly equal or even lower than that of the liquid polymer are not common.

Polyacrylonitrile has a number of exceptional properties. Various samples have bulk densities invariably in the range of 1.17–1.18 cc./g. at 25°C., irrespective of the method of preparation and the condition of crystallization (of course, cases in which structural irregularities are effected by branching, crosslinking or formation of condensed rings[1] are not included here). Because of its diffuse x-ray diffraction pattern and very small volume change on melting, polyacrylonitrile has long been considered a crystalline polymer with a low degree of crystallinity.

Recently it has been found that, upon crystallization from dilute propylene carbonate solutions, polyacrylonitrile forms crystalline platelets resembling the single crystals observed in other polymers.[2] Since the

molecular properties of polyacrylonitrile in the dissolved state[3] and the microstructure of the crystalline platelets are better defined than in any other state, it is of interest to study the change that takes place between the two states.

In this investigation dilatometric measurements were made on the crystallization of polyacrylonitrile from propylene carbonate solutions at different concentrations and temperatures. The same techniques were used to study the melting behavior of the sample which had been crystallized. Results obtained dilatometrically are compared with those obtained by direct measurements.

These results indicate that the volume of the solution increases upon crystallization over a wide range of temperature, although the change is small.

EXPERIMENTAL

Sample Preparation

The sample used in this work, unless otherwise stated, was prepared by using a redox catalyst system containing potassium persulfate and sulfur dioxide. The sample was purified by dissolving in N,N-dimethylformamide at 50°C., followed by precipitation, washing, and drying. The intrinsic viscosity was 1.06 dl./g. determined in DMF at 25°C.

The disks used for density measurements were prepared by compression molding under vacuum at 150°C.

Density Measurement

Densities of PAN disks and powders were determined by different methods. The density of the disk was determined by a flotation method, aqueous NaBr solution being used as the immersion liquid. The density of the powder was determined by means of a pycnometer as described by Culbertson and Weber,[4] and the results were rechecked by the flotation method used by Hermans et al.,[5b] with propylene carbonate as the immersion liquid.

Partial Specific Volume

In order to determine the partial specific volume of PAN in solution, the specific volumes of the solutions at different concentrations were determined with the use of a pycnometer similar to the type described by Heller and Thompson.[6] A flask of 25 cc. and a precision tubing of 1.000 mm. bore were used. The temperature of the bath was controlled to the nearest ± 0.005°C. The pycnometer was calibrated with Hg at 30.0°C. and 115.0°C. All the weights were corrected for air buoyancy. After necessary corrections for the thermal expansion of the pycnometer, the values obtained at these two temperatures are found to be in excellent agreement.

Solutions of different concentrations were prepared by diluting the stock solution with the purified solvent of the same batch. Dilution factors were determined by direct weighing.

The solutions were kept in sealed tubes and heated to 150°C. for half an hour to obtain uniform mixing prior to measurement. The solutions, when hot, were introduced into the pycnometer by means of a hypodermic syringe.

Crystallization

PAN crystallized from dilute solutions dissolves in propylene carbonate at approximately 125°C. A degree of supercooling of about 30°C. below the solubility point is necessary to achieve an appreciable rate of crystallization. The crystallization was carried out in a dilatometer at the highest practical temperature to promote growth of crystals of high perfection, specifically 95, 104, and 108°C. for the solutions at concentrations of 1.0, 4.2, and 8.4%, respectively. The rate of crystallization was measured by following the volume change in the dilatometer.

Melting Curve

Melting curves were obtained on samples which had been crystallized by the method described above. A slow heating procedure was used; namely 5°C./hr. before melting, 2° C./hr. during melting, and 10°C./hr. after melting was complete. Although prolonged heating at 150°C. causes chemical reaction (decomposition can be detected at approximately 130°C.), no noticeable change was observed at this temperature within the few hours required for a measurement.

The conversion of dilatometer capillary readings to specific volumes of the sample was based on reading at 140°C. at which only homogeneous solution was present. The volume of the dilatometer was calculated from the amount and the specific volume of the solution and the mercury present in the dilatometer.

Volume of Mixing

The volume of mixing was measured in an apparatus described by Hildebrand and Carter.[7] It consisted of two pear-shaped bulbs connected by a U-tube, with a precision tubing of 1.514 mm. bore sealed to the top of each bulb. The capacity of each bulb was about 20 cc. The solution and the solvent were placed in each side, separated by mercury which had been degassed by vacuum distillation. After the temperature had become constant, the readings of the liquid levels in the capillaries were taken by means of a cathetometer. The liquids were then mixed by allowing the mercury to flow from one side to the other several times. The readings were taken again after uniform mixing. The limit of detection was in the order of ± 0.01 cm., corresponding to a volume of $\pm 1.08 \times 10^{-4}$ cc.

RESULTS

Specific Volume

The specific volumes of polyacrylonitrile (disks) as determined by flotation methods were in the range of 0.849–0.852 (Table I), in close agreement with the values given by Kolb and Izard.[8] These values were found to be insensitive to the method of preparation and the condition of crystallization.

TABLE I
Specific Volume of Polyacrylonitrile (Disks)

			Specific volume	
Polymer	Initiator	$\bar{M}_v$	25°C.	47.6°C.
A	Persulfate–SO$_2$	70,000	0.849[a]	0.850[b]
B	Also free radical	—	0.852	
C	n-BuLi at -78°C.[c]	—	0.852	

[a] Flotation method in aqueous sodium bromide solution.
[b] In propylene carbonate.
[c] See ref. 9.

The specific volume of polyacrylonitrile in powder form depends upon the immersion liquid. As shown in Table II, the same sample has a specific volume of 0.853, 0.857, and 0.862 at 25°C. when determined in propylene carbonate, succinonitrile, and octyl alcohol, respectively.

TABLE II
Specific Volume of Polyacrylonitrile (Powders)

	Specific volume		
Immersion liquid	34.0°C.	95.0°C.	115.0°C.
Succinonitrile	—	0.853 ± 0.001[b]	—
Propylene carbonate	0.8399 ± 0.0004[a]	0.857 ± 0.001[b]	0.864[c]
Octyl alcohol	—	0.862 ± 0.004[b]	—

[a] Flotation method.
[b] Pycnometer method.
[c] Extrapolated by using the value of $dv/dt = 3.0 \times 10^{-4}$ cc./g. °C.

The variation in specific volume of the same sample in different liquids is undoubtedly due to the absorption of the liquid by the sample. Hermans et al.,[5] in studying the density of cellulose fibers in various organic liquids (helium, water, etc.), draw the conclusion that the most important factor in selecting a liquid for density measurement is its solvent power. Correct density of cellulose fibers can only be obtained by using a liquid which does not penetrate into the sample. When penetration occurs, a higher value is invariably obtained. The same phenomenon has indeed been observed in the present case; the density of polyacrylonitrile power in-

creases with the solvent power (as expressed by the cohesive energy density[10]) in the order: succinonitrile > propylene carbonate > octyl alcohol. The value obtained in octyl alcohol at 95°C. is identical, within the experimental error, with the density of the disk obtained dilatometrically.

Partial Specific Volume

The specific volumes of polyacrylonitrile solutions in propylene carbonate at 115.0°C. are given in Table III, together with the apparent

TABLE III
Specific Volumes of PAN Solution in Propylene Carbonate at 115.0°C.

Weight fraction of PAN, w_2	v, cc./g.	v_2^*
0.000	0.90506[a]	(0.8482)[b]
0.024722	0.90366	0.8482
0.030178	0.90335	0.8483
0.034330	0.90307	0.8482
0.040576	0.90277	0.8486
0.052148	0.90204	0.8471

[a] Average of two determinations, 0.90506 and 0.90507.
[b] Extrapolated value.

specific volumes, v_2^*, defined by the relation, $v_2^* = (v - v_1°w_1)/w_2$. The partial specific volume of polyacrylonitrile can then be calculated from the value of v_2^* by using eq. (1) given by Schulz and Hoffmann:[11]

$$\bar{v}_2 = v_2^* + w_1w_2(dv_2^*/dw_2) \tag{1}$$

where v is the specific volume of the solution and w_1 and w_2 are the weight fraction of the solvent and the polymer, respectively. The constancy of the value v_2^*, i.e., $dv_2^*/dw_2 = 0$, means that the partial specific volume of PAN in propylene carbonate remains constant throughout the range of concentration investigated, and has a value of 0.848 cc./g. at 115.0°C. In other words, when 1 g. of polyacrylonitrile (a liquid in hypothetical case) is added to a large excess of propylene carbonate or its dilute solution, the increase in volume is 0.848 cc. at this temperature.

Theoretically, the same conclusion can be reached by way of Scatchard's equation:[12]

$$v = v_1°w_1 + v_2°w_2 + kw_1w_2 \tag{2}$$

where v, $v_1°$, and $v_2°$ are the specific volumes of the solution, the solvent, and the polymer (in liquid state), respectively, kw_1w_2 being the correction term for the deviation from additivity of the specific volumes. Equation (2) can be rearranged to read:

$$v_2^* = (v - v_1°w_1)/w_2 = v_2° + kw_1 \tag{3}$$

According to eq. (3), when v_2^* is plotted against w_2, a straight line should be obtained, the slope of which is the value of $-k$ and the intercept is the value of $k + v_2^\circ$. In actual practice, however, an accurate extrapolation can not be made since all our measurements were made in the concentration range below 8% and values at higher concentrations are unattainable.

By using eq. (2), it can be shown readily that:

$$v_D = k[m_1 m_2/(m_1 + m_2)](w_2)^2 \qquad (4)$$

where v_D is the volume of mixing when m_2 grams of solution of concentration w_2 are mixed with m_1 grams of pure solvent.

It is evident from eq. (4) that the accuracy of k is determined only by the value of v_D since m_1, m_2, and w_2 can be determined easily with high accuracy. The values obtained (Table IV) are complementary to the value of dv_2^*/dw_2 obtained by the specific volume measurement.

TABLE IV

Volume of Dilution of 20 g. of Solution and 20 g. of Solvent at 115.0°C.

w_2	$v_D \times 10^{-4}$, cc.		k
0 0149	−0.54		−0.024
0.0298	+0.54		+0.006
0 0434	−5.9		−0.031
0.0518	+2.0		+0.008
0.0652	−3.1		−0.007
		Avg.	−0.009₆

From these results it is concluded that the value of k can be ignored within the concentration range of interest and that the basis of the additivity of specific volumes is established for the present discussion.

Crystallization

Figure 1 represents the rate of crystallization of polyacrylonitrile from a 1.0% solution at 95.0°C. The volume of the solution remained unchanged
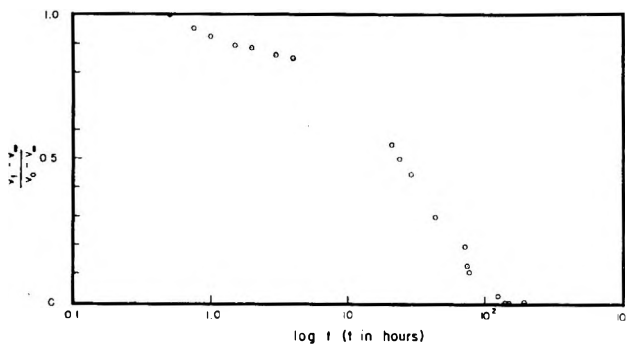

Fig. 1. Crystallization of polyacrylonitrile from a 1.0% propylene carbonate solution at 95.0°C.

TABLE V
Volume Change Upon Crystallization

Temperature of crystallization, °C.	w_2	Time of crystallization, hr.[a]	Volume increase, cc./g. polymer
40	0.010	117	0.010
70	0.010	167	0.008
95	0.010	189	0.014
104	0.042	238	0.013
108	0.084	234	0.011

[a] Crystallization was allowed to take place until no further change in volume was observed. In one experiment, approximately 80-85% of the polymer was crystallized out from the solution.

within the first $3/4$ hr., then increased at an accelerating rate, and finally remained almost constant, giving a typical sigmoid curve characteristic of the crystallization of high polymers.

Experiments carried out at 40 and 70°C. gave the same type of curve. However, the rate of crystallization varied considerably with the temperature of crystallization; for example, the times required for the onset of crystallization were approximately 2, 0.5, and 0.8 hr., and the half times of crystallization were approximately 7.0, 1.5, and 3.0 hr. at 40, 70, and 95°C., respectively. The fact that there exists a temperature for a maximum rate of crystallization to occur suggests there are more than one factor that determines the rate, a fact generally observed in studying the rate of crystallization.

In all cases, the volume of the solution increased by an amount ranging from 0.008 to 0.014 cc., depending upon the concentration and the temperature of crystallization, hence the degree of crystallinity and the perfection of the crystals formed (Table V).

It is of interest to note that, assuming the degree of crystallization is constant, crystallization at higher temperature promotes growth of crystals of higher perfection while the rapid crystallization at lower temperatures yields crystals of lower perfection; this relation is indicated by the volume change obtained at their respective temperatures: 0.008 cc./g. at 70°C. as compared to 0.014 cc./g. at 95°C.

Melting of Polyacrylonitrile

Figure 2, in which the specific volume is plotted against temperature, represents the melting curve for a sample crystallized at 108°C. The apparent specific volume increases linearly with the temperature up to 90°C. The melting began at 90°C. and ended at 135°C., as evidenced by the change of the opacity of the solution. The melting is accompanied by a decrease in volume, but this decrease is almost compensated by the increase in volume due to expansion, with the net result that the volume almost remains constant during melting.
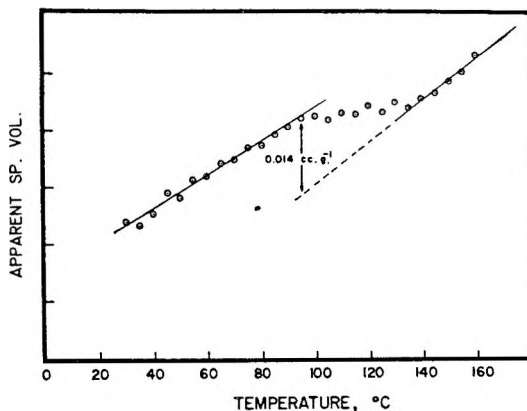
Fig. 2. Melting curve for polyacrylonitrile in propylene carbonate (concn. = 8.4%).

If a straight line is drawn through the points above the melting point and extrapolated to 95°C., the difference in specific volumes between the solid and the liquidus line represents the decrease in volume upon melting (Fig. 2). A value of 0.014 cc./g. is obtained which is identical with the value obtained under similar conditions by crystallization.

These values compare favorably with the specific volumes by direct measurements. The specific volume of polyacrylonitrile as determined in powder form is 0.857 at 95°C. and the partial specific volume in solution is 0.848 at 115.0°C. or 0.841 at 95°C. by extrapolation, the difference being 0.016 cc./g.

All these measurements give internally consistent results, showing that polyacrylonitrile expands when crystallized from propylene carbonate solution in the amount of: 0.014 as measured by crystallization, 0.014 by melting, and 0.016 cc./g. by direct measurements. In view of the uncertainties involved in determining the exact value of the volume of mixing, this agreement should be considered excellent. It is therefore established that the volume of the solution increased upon crystallization, although the increase was extremely small.

It should be mentioned here that Krigbaum and Tokita,[13] when measuring the rate of crystallization of polyacrylonitrile in dimethylformamide, also observed that the volume change is extremely small, about 0.005% (based on the amount of solution used), but with a sign different from ours. This discrepancy is believed to be due to the fact that different solvents were used. In any event the volume change is much smaller than in the case of nonpolar polymer where a difference of 10–15% is often observed.

DISCUSSION

Volume of Mixing

The crystallization of polyacrylonitrile from propylene carbonate solution is identical with a reverse process of the two steps: the melting of the

crystalline polymer and the subsequent mixing of the liquid polymer with the solvent. The volume change observed dilatometrically must be equal to the sum of the changes in the two steps involved: $\Delta V_{total} = \Delta V_{melting} + \Delta V_{mixing}$.

The precise value of ΔV_{mixing} is difficult to obtain since it requires data at higher concentrations. We have demonstrated only that ΔV_{mixing} is nearly zero up to a concentration of 8%.

However, indirect evidence can be found in Schulz and Hoffmann's report[11] that in the cases of polystyrene and poly(methyl methacrylate) a contraction in volume is usually observed upon mixing.

These same authors also indicated that the specific volume of the polymer is really equal to the partial specific volume of the polymer in dilute solution when the solvent is sufficiently poor, but higher than the partial specific volume in good solvents. In all the cases they studied, 14 solvents for poly(methylmethacrylate) and 16 solvents for polystyrene, the specific volume of the polymer exceeds the partial specific volume of the polymer in solution by not more than 2%.

If the same situation prevails here, the specific volume of liquid polyacrylonitrile at 95°C. will have a value not smaller than 0.841, and the shape of the melting curve will not be altered.

Crystalline State of Polyacrylonitrile

The question naturally arises as to whether the small volume change is due to the low degree of crystallinity or to the small difference in specific volume in dissolved and crystalline state or to both.

Bohn, Schaefgen, and Statton,[14] on the basis of x-ray diffraction data and swelling experiments, emphasized the fact that there are no conventional amorphous areas in polyacrylonitrile and the polymer can be thought of as being a single phase.

Recent investigation by Holland, et al.[2] revealed that polyacrylonitrile crystallized from dilute solution, when examined under the electron microscope, forms crystalline platelets closely resembling the "single crystals" observed in other polymers. Polyacrylonitrile crystallized from dilute solution of propylene carbonate at 95°C., glutaronitrile at 130°C., and succinonitrile at 64°C. all gave fairly sharp x-ray diffraction patterns. The two equatorial reflections ordinarily observed can be split into two doublets; one at 5.22 and 5.01 and the other at 3.05 and 2.95 A., indicating improved lateral order.

It thus appears that the small change in volume upon crystallization is due to the closeness of the partial specific volume in the dissolved state and the specific volume in the crystalline state.

Although the crystal structure of PAN is not accurately known, it has been suggested[14] that the polymer chains are coiled in a more or less kinked or helical manner and these chains are then packed laterally in a regular hexagonal or pseudohexagonal pattern. The average conformation of the chains may be such that they do not occupy appreciably more volume in

solution than in the crystal, and the regular packing of these chains may actually result in a greater occupied volume in the crystal.

The fact that the difference in specific volume in different states is so small serves to explain a number of observations: the lack of abrupt volume change on melting, the absence of amorphous regions, the narrow range of the density among different samples prepared by different methods, and the fact that crystallization conditions exert a marked effect on the x-ray intensity distribution, but practically no effect on the density of the sample.

In conclusion, the unusual melting behavior of polyacrylonitrile has not received much attention in the past. The phenomenon may not be unique for polyacrylonitrile alone. Poly(methyl methacrylate) serves as another example in which syndiotactic, isotactic, and atactic forms have about the same density.[15] There are probably other polymer systems, especially polymers of polar monomers, which have a high degree of crystallinity but a very small volume change on melting.

References

1. See, for example, N. Grassie and J. N. Hay, *J. Polymer Sci.*, **56**, 189 (1962).

2. Holland, V. F., S. B. Mitchell, W. L. Hunter, and P. H. Lindenmeyer, *J. Polymer Sci.*, **62**, 145 (1962).

3. Krigbaum, W. R., and A. M. Kotliar, *J. Polymer Sci.*, **32**, 323 (1958); W. R. Krigbaum, *J. Polymer Sci.*, **28**, 213 (1958).

4. Culbertson, J. L., and M. K. Weber, *J. Am. Chem. Soc.*, **60**, 2695 (1938).

5. (a) Hermans, P. H., and D. Vermass, *J. Polymer Sci.*, **1**, 149 (1946); (b) P. H. Hermans, J. J. Hermans, and D. Vermass, *Ibid.*, **1**, 162 (1946).

6. Heller, W., and A. C. Thompson, *J. Colloid Sci.*, **6**, 57 (1951).

7. Hildebrand, J. H., and J. M. Carter, *J. Am. Chem. Soc.*, **54**, 3592 (1932).

8. Kolb, H. J., and E. F. Izard, *J. Appl. Phys.*, **20**, 564 (1949).

9. Miller, M. L., *J. Polymer Sci.*, **56**, 203 (1962).

10. Walker, E. E., *J. Appl. Chem.*, **2**, 470 (1952).

11. Schulz, G. V., and M. Hoffmann, *Makromol. Chem.*, **33**, 220 (1957).

12. Scatchard, G., *Chem. Revs.*, **44**, 7 (1948).

13. Krigbaum, W. R., and N. Tokita, *J. Polymer Sci.*, **43**, 467 (1960).

14. Bohn, C. R., J. R. Schaefgen, and W. O. Statton, *J. Polymer Sci.*, **55**, 531 (1961).

15. Stroupe, J. D., and R. E. Hughes, *J. Am. Chem. Soc.*, **89**, 2341 (1958).

Résumé

On a fait des mesures dilatométriques de la cristallisation du polyacrylonitrile à partir de solutions dans le carbonate de propylène à des concentrations de 1.0, 4.2 et 8.4% et à des températures de 40, 70, 95, 104, et 108°C. Contrairement à ce qu'on attendait, le volume de la solution augmente par cristallisation, quoique l'augmentation soit extrêmement petite (environ 1% par rapport au polymère). Ce léger changement de volume s'accorde avec le volume spécifique partiel du polyacrylonitrile en solution et le volume spécifique du polymère mesuré directement par la méthode de flotation. Une étude récente de Holland et collaborateurs a montré que le polyacrylonitrile forme, par cristallisation au départ d'une solution diluée, des plaques cristallines qui ressemblent aux

monocristaux observés dans d'autres polymères.   Il semble que le petit changement en volume par transformation de l'état dissous à l'état cristallin est dû aux valeurs voisines des volumes spécifiques dans les doux états différents.   Ces résultats inhabituels de la densité du polyacrylonitrile sont comparables à ceux du polyméthacrylate de méthyle où les polymères isotactique, syndiotactique et atactique ont à peu près la même densité. Le fait que la différence en densité du polyacrylonitrile est si minime, pourrait bien expliquer quelques phénomènes similaires: l'absence d'un changement brusque du volume par fusion, l'absence de régions amorphes, la gamme étroite des valeurs de la densité de différents échantillons préparés par des méthodes différentes et le fait que les conditions de cristallisation n'exercent pratiquement pas d'effet sur la densité de l'échantillon.

Zusammenfassung

Die Kristallisation von Polyacrylnitril aus Propylenkarbonatlösung bei Konzentrationen von 1,0, 4,2 und 8,4% und Temperaturen von 40°, 70°, 95°, 104° und 108° wurde dilatometrisch untersucht.   Entgegen der Erwartung nimmt das Volumen der Lösung bei der Kristallisation tatsächlich zu, obgleich die Zunahme äusserst gering ist (etwa 1% bezogen auf das Polymere).   Diese kleine Volumsänderung stimmt mit dem partiellen spezifischen Volumen von Polyacrylnitril in Lösung und dem nach einer Flotationsmethode direkt gemessenem spezifischen Volumen des Polymeren überein. Eine neuere Untersuchung von Holland et al. zeigte, dass Polyacrylnitril bei der Kristallisation aus verdünnter Lösung Plättchen, ähnlich den bei anderen Polymeren beobachteten "Einkristallen" bildet.   Es scheint, dass die kleine Volumsänderung beim Übergang von gelösten kum kristallinen Zustand auf der Ähnlichkeit der spezifischen Volumina in den beiden verschiedenen Zuständen beruht.   Die ungewöhnlichen Dichteverhältnisse beim Polyacrylnitril äaneln denjenigen von Polymethylmethacrylat, wo isotaktische, syndiotaktische und ataktische Polymere etwa die gleiche Dichte besitzen.   Die Tatsache, dass der Dichteunterschied bei Polyacrylnitril so klein ist, kann eine Anazhl verwandter Phänomene gut erklären: das Fehlen einer plötzlichen Volumsänderung beim Schmelzen, die Abwesenheit amorpher Bereiche, der enge Bereich der Dichtewerte bei nach verschiedenen Methoden dargestellten Proben und die Tatsache, dass die Kristallisationsbedingungen praktisch keinen Einfluss auf die Dichte der Probe haben.

Polymerization of Alicyclic Epoxides with Aluminum Alkyl Catalysts

R. BACSKAI, *California Research Corporation, Richmond, California*

Synopsis

The polymerization of alicyclic epoxides with aluminum alkyls has been investigated. In many cases, fast polymerization rates were observed at $-78°C$., leading to high molecular weight compounds in good yield. The infrared spectra of the polymers are consistent with the proposed polyether structure. It was found that the molecular weight of the polymers obtained in these reactions is a function of the alicyclic ring size. This was interpreted by considering the variation of molecular strain during the polymer-forming reaction. The following order of reactivity based on estimated propagation rates has been established for the monomers: cyclohexene oxide > cyclopentene oxide > cycloheptene oxide $\gg$ cyclooctene oxide. A reaction mechanism is proposed where initiation occurs through coordination of the aluminum alkyl with the epoxide, followed by successive addition of monomers to the electrophilic centers. The absence of phenyl endgroups in a relatively low molecular weight polycyclohexene oxide, prepared with $Al(C_6H_5)_3$ catalyst, precludes one of the possible alternative mechanisms. The proton magnetic resonance spectra of polycyclohexene oxide, *cis*-1,2-cyclohexanediol, and *trans*-1,2-cyclohexanediol were determined in dilute chloroform solution and suggest a stereoregular poly-*trans*-ether structure for the polymers.

The polymerization of ethylene and propylene oxide by aluminum alkyls has been reported from various laboratories.[1] Relatively high temperatures and long reaction times were employed in these reactions probably to obtain reasonable yields.

The activating action of water in metal alkyl catalyzed epoxide polymerizations was first observed by Furukawa[2] and more recently by Vandenberg.[3] By using the reaction product of an aluminum alkyl and water, Vandenberg polymerized *cis*- and *trans*-2-butene oxide and cyclohexene oxide at $-78°C$. to high molecular weight polymers.

Polymers of alicyclic epoxides have received only little attention, although the patent literature describes the polymerization of cyclohexene oxide[4] and 4-vinylcyclohexene oxide[5] by Friedel-Crafts type catalysts. From the mode of preparation, it is believed that these polymers had relatively low molecular weights.

We have found that certain alicyclic epoxides react instantaneously with aluminum alkyls at temperatures as low as $-78°C$. to give high molecular weight polymers in nearly quantitative yield. The remarkably facile polymerization of these monomers by unmodified aluminum alkyls has not been observed previously. In the present work, the synthetic and mecha-

nistic aspects of the polymerization and the stereochemistry of the products will be discussed.

EXPERIMENTAL

Materials

Monomers were either purchased or synthesized by known methods.

Cyclopentene oxide was prepared both by the peroxytrifluoracetic acid[6] and the peracetic acid[7] methods; b.p. 100.7°C.

Cyclohexene oxide was obtained from Arapahoe Chemicals, Inc., and redistilled before use; b.p. 131–132°C.

Cycloheptene oxide was prepared by the peracetic acid method;[8] b.p. 77–78°C./50 mm.

cis-Cyclooctene oxide was prepared by the peroxytrifluoracetic acid method;[6] b.p. 90°C./30 mm. The infrared spectrum of the compound was identical to that reported in the literature.[9]

trans-Cyclooctene oxide was prepared by the peracetic acid method;[9] b.p. 95–97°C./33 mm. The infrared spectrum of the compound was identical to that reported in the literature.

Cyclododecene oxide, obtained from Aldrich Chemical Company, Inc., was used without further purification. The compound is probably a mixture of cis and trans isomers.

4-Vinylcyclohexene oxide was obtained from Aldrich Chemical Company, Inc. Before use, it was redistilled; b.p. 75–76°C./30 mm.

Vinylcyclohexene dioxide, 3,4-epoxycyclohexane carbonitrile, 3,4-epoxy-6-methylcyclohexylmethyl acetate, and 3-oxatricyclo-[3·2·1·0^{2,4}]-octane-6-carboxylate were obtained from Union Carbide Chemicals Company and used as received.

Indene epoxide was prepared by the method of Whitmore and Gebhart;[10] b.p. 90–93°C./4 mm.

cis-2-Butene oxide was prepared by the method of Wilson and Lucas;[11] b.p. 60–61°C.

Propylene oxide was obtained from the Matheson, Coleman, and Bell Company. Before use, it was redistilled from KOH; b.p. 34.5°C.

Cyclohexene sulfide was obtained from Aldrich Chemical Company, Inc. and was used without further purification.

Cyclohexene imine was prepared by the method of Paris and Fanta;[12] b.p. 60–70°C./30 mm. The infrared spectrum of the compound was identical to that reported in the literature.

The aluminum alkyls were obtained from Texas Alkyls, Inc.

All polymerizations were conducted under a nitrogen atmosphere. The n-hexane, Phillips Pure Grade, used as a solvent in the polymerizations, was stored over sodium wire.

Polymer Preparation

In a typical experiment, 1 ml. of triethylaluminum in 100 ml. of n-hexane was cooled to −78°C. with the exclusion of air and moisture. Addition of

cyclohexene oxide to the stirred homogeneous solution resulted in an exothermic reaction and solid polymer precipitated instantaneously. The monomer addition was continued at such a rate that, in spite of the heat evolved, the temperature of the reaction mixture never rose above $-70°C$. After 20 g. of cyclohexene oxide had been added and the increasing amount of polymer prevented proper mixing, the unreacted catalyst was decomposed with methanol and concentrated HCl. The reaction product was washed several times with methanol and dried in vacuum. For purification, the polymer was dissolved in benzene, filtered through sintered glass, and precipitated with methanol; the yield was 16.8 g. (82% of theory) and $[\eta] = 2.28$ (in benzene at 30°C.). For further experimental details, see Table I.

Copolymerization

A 2-g. portion of total monomers was dissolved in 10 ml. of n-hexane. At 20°C. a solution of 0.01 ml. AlEt₃ in 0.49 ml. n-hexane was added with stirring. In about 20 sec., the reaction temperature rose to 23–24°C., and the copolymerization was stopped by the addition of methanol–concentrated HCl. The copolymer was precipitated with methanol, dried, and purified by dissolving in benzene and after filtration precipitating with methanol. Monomer conversion varied between 6% and 12%. Since one of the comonomers was always 4-vinylcyclohexene oxide, the composition of the copolymer was determined by measuring the absorbance of 5 mg. copolymer/ml. CS_2 solutions at 910 cm.$^{-1}$ (characteristic vinyl absorption) in the infrared. For calibration, synthetic mixtures of poly-4-vinylcyclohexene oxide and polycyclohexene oxide were used.

Polymer Characterization

Infrared spectra of the polymers were obtained with a Perkin-Elmer Infracord spectrophotometer on films cast from benzene solution onto a sodium chloride plate.

Intrinsic viscosities $[\eta]$ were determined in benzene at 30°C.
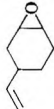
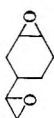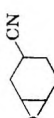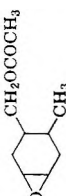Softening points were measured by the penetrometer method.[13]

Proton magnetic resonance spectra were obtained with a Varian A-60 proton magnetic resonance spectrometer. The chloroform used as solvent was filtered through activated alumina to remove the ethanol stabilizer.

RESULTS AND DISCUSSION

Results of our polymerization experiments are summarized in Table I.

One of the most remarkable features of these reactions is the rapid conversion of certain monomers to high molecular weight polymer at low temperatures. Instantaneous polymer formation accompanied by a strong exotherm was observed upon the addition of the epoxide to an aluminum alkyl solution. In order to obtain good temperature control, only small portions of the monomer were added at a time. In contrast, published

TABLE 1
Polymerization of Alicyclic Epoxides with Aluminum Alkyls

Monomer	Wt. monomer, g.	Vol. n-hexane, ml.	Catalyst	Vol. catalyst, ml.	Reaction temp., °C.	Reaction time, min.	Polymer yield, %	$[\eta]$	Polymer softening point, °C.	Remarks
	1.0	6	AlEt₃	0.1	−60	10	29	1.27		Tacky solid at room temperature
	5.46	5	AlEt₃	0.2	−75 → +30ᵃ	5	98.8	0.87		
	20.5	100	AlEt₃	1.0	−70	25	82	2.28	70	
	4.87	5	AlEt₂Cl	0.2	−75 → +30	5	86	2.16		
	19.5	100	Al(i-Bu)₃	1.85	−70	25	66.3			
	1.92	2	AlEt₃	0.1	−78 → +30	5	93.7	0.83ᵇ	65	Polymer partially crosslinked
							86.3			
	2.2	2	AlEt₃	0.1	−75 → +30		0.16			Crosslinked solid polymer
CN	1.0	c	AlEt₃	0.1	−20 → +30	5	25			Methanol-insoluble, viscous oil
CH₂OCOCH₃	2.19	2	AlEt₃	0.1	0 → +40	3				Reaction product yellow solid
CH₃	2.14	2	AlEt₃	0.1	0 → +40	5				Reaction product: white solid

Epoxide	Monomer	Solvent (ml)	Catalyst	(mole)	Temp. (°C)			[η]	%	Remarks
[epoxide, fused bicyclic]	1.0	6	AlEt₃	0.1	−60	10	32	0.7	60	
[epoxide] *cis*	0.95	—	AlEt₃	0.1	+125	960	47	0.04	65	No polymer formation in hexane at −78°C.
[epoxide] *trans*	1.0	1	AlEt₃	0.1						No polymer formation at −78°C. Reaction mixture reacts violently at room temperature, becomes viscous but no methanol insoluble polymer is formed.
[spiro/cross epoxide]	1.0		AlEt₃	0.1						Solid formation after prolonged heating at 125°C.
[S]	2.0	2	AlEt₃	0.1	−75 → +30	5	69	0.15		
	1.0	6	AlEt₃	0.1	−60	10	54	0.25	71	
[NH]	0.5	0.5	AlEt₃	0.05						No reaction observed at room temperature. Reaction mixture solidifies after 16 hr. of standing.

[a] Due to the exotherm, the temperature rose to +30°C. during the reaction.
[b] Refers to the benzene-soluble portion of the product.
[c] *m*-Xylene (1 ml.) used.

results indicate that rather strenuous conditions are required to polymerize aliphatic epoxides with aluminum alkyls.[1]

From Table I, it is evident that the lowering of temperature favors the formation of high molecular weight products. Most of the polymers reported here are amorphous solids that soften at 60–70°C. Interestingly, polycyclopentene oxide is an exception; even higher molecular weight samples of this compound ($[\eta] > 1$) are tacky solids at room temperature. No crystallinity was found in the polymers by x-ray analysis. In the polymerization of 4-vinylcyclohexene oxide, the formation of considerable amounts of benzene insoluble products was observed. Considering the very high purity of the monomer used in these experiments (99.88%; no detectable amounts of vinylcyclohexene dioxide), it is possible that the olefinic double bond is involved to a certain extent in the reaction, causing crosslinking. Similarly, vinylcyclohexene dioxide would not be expected to form crosslinked polymers, since terminal epoxides, like propylene oxide, do not react under these conditions.

cis- and *trans*-Cyclooctene oxide did not polymerize at low temperature; but solid, low molecular weight polymer was isolated when undiluted *cis*-cyclooctene oxide was heated with AlEt$_3$ at 125°C. for 16 hr. Cyclododecene oxide (probably a mixture of the *cis*- and *trans*-isomer) behaved similarly. Cyclohexene oxides bearing polar substituents like 3,4-epoxy-cyclohexane carbonitrile and 3,4-epoxy-6-methylcyclohexylmethyl acetate reacted violently with AlEt$_3$ at room temperature. Solid, probably polymeric, products were obtained.

Indene epoxide and 3-oxatricyclo [3·2·1·0^{2,4})-octane-6-carboxylate did not give solid polymers with AlEt$_3$.

Cyclohexene sulfide is somewhat less reactive than the corresponding oxygen analog, but it polymerized to a fairly high molecular weight polymer. Cyclohexeneimine is more reluctant to undergo polymerization; 16 hr. was required for a sample to solidify at room temperature in the presence of AlEt$_3$.

B$_2$H$_6$ and B(C$_2$H$_5$)$_3$ are also good catalysts for the polymerization of alicyclic epoxides, but the intrinsic viscosity of the solid polymers formed is relatively low.

BF$_3$ etherate or AlEt$_3$–TiCl$_4$, [Al]/[Ti] = 1.5, did not convert cyclohexene oxide at −78°C. to a methanol-insoluble polymer.

Structure of Polymers

The polymerization of alicyclic epoxides proceeds through the opening of the epoxide ring, and the products are linear polyethers. Evidence for the polyether structure was obtained by studying the infrared spectra of the polymers. Typical epoxide bands[14] characteristic of the monomers are missing from the polymer spectra, and a new very powerful band associated with the ether linkage[15] is present. This new band is the strongest in the spectrum, and its position varies slightly with chemical structure of the polymer (Table II).

TABLE II

Ether Bands in the Infrared Spectrum of Alicyclic Epoxide Polymers

Polymer	Ether band, μ
Polycyclopentene oxide	9.05
Polycyclohexene oxide	9.15
Polycycloheptene oxide	9.08, 9.40
Poly-cis-cyclooctene oxide	8.95, 9.35
Poly-4-vinylcyclohexene oxide	9.27
Poly-cis-2-butene oxide	9.05

The polyether obtained from 4-vinylcyclohexene oxide has strong absorption bands also at 1650, 995, and 910 cm.$^{-1}$, indicating the presence of vinyl groups in the polymer.

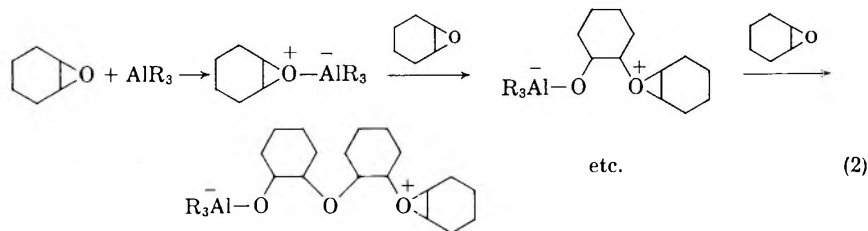### Reaction Mechanism and Polymerizability

In view of the high polymerization rates observed at low temperature, only reaction mechanisms with ionic or metal organic intermediates are considered.

One of the possibilities, mechanism A, involves the addition of an aluminum alkyl to the epoxide through the opening of the three-membered ring followed by rapid successive addition of monomer molecules to the alcoholate intermediate, as shown in eq. (1) (al = $^1/_3$ Al):

$$(1)$$
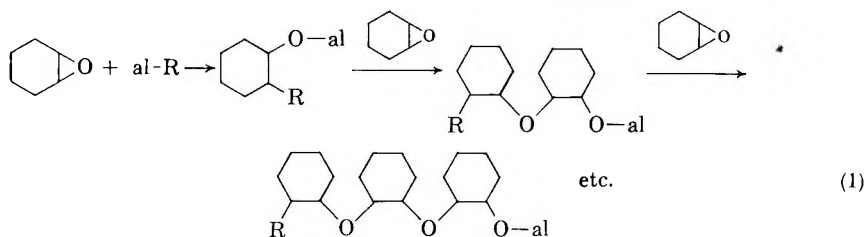
In support of this speculation is the fact that the addition of metal alkyls to the epoxide ring is known;[16] this reaction may account for the initiation. The polymerizing power of aluminum alcoholates recently discovered by Osgan and Price[17] supports the proposed propagation reaction.

Alternatively (Mechanism B), initiation may occur through coordination of the aluminum alkyl (a weak Lewis acid) with the epoxide followed by rapid addition of monomer molecules to the complex, as shown in eq. (2):

$$(2)$$

The nature of the termination step is not clear, but it can be easily seen that each reaction mechanism leads to polymer end groups with different hydrolytic stabilities. During the isolation of the product, the polymerization mixture was treated with HCl containing methanol. On the basis of mechanism A the polymer should contain as one endgroup the alkyl group originally present in the aluminum catalyst. On the other hand, if the reaction proceeds through mechanism B, no such endgroup should be detected in the polymer. It was possible to differentiate between these alternatives by conducting a polymerization experiment in the presence of a catalyst which introduces end groups that can be easily identified.

The triphenyl aluminum catalyzed polymerization of cyclohexene oxide in n-hexane between 25 and 50°C. gave a polymer in 97% yield. The intrinsic viscosity of the material was 0.16, and the number-average molecular weight was 5900. The infrared spectrum of this polymer was examined for aromatic absorption. Considering one phenyl endgroup per molecule, the concentration of phenyl groups in this particular polymer would exceed by 10 times the limit of detectability under the analytical conditions used. However, the polymer solution in CS_2 showed no absorption at 730 cm.$^{-1}$. Therefore, we must rule out mechanism A and propose that mechanism B is the most probable for the polymerization of alicyclic epoxides.

The chemical structure of the alicyclic epoxide has a great influence on the outcome of the polymerization reaction. It is particularly interesting to compare the results obtained with unsubstituted alicyclic epoxides of different ring size. These data are summarized in Table III; for comparison, two aliphatic epoxides have been included in the list.

For alicyclic epoxides, the relative ease of polymer formation, as reflected in the yields and intrinsic viscosities, is greatest for cyclohexene oxide. Under the same experimental conditions, cis-cyclooctene oxide does not polymerize at all, while cyclopentene and cycloheptene oxides occupy an intermediate position regarding both yield and intrinsic viscosity.

TABLE III
Polymerization of Epoxides with AlEt₃ in n-Hexane at $-60°C.$[a]

Monomer	Monomer purity (by vapor phase chromatography), %	Yield of methanol-insoluble polymer, %	$[\eta]$
Cyclopentene oxide	99.4	29	1.27
Cyclohexene oxide	100.0	92	1.88
Cycloheptene oxide	100.0	32	0.7
cis-Cyclooctene oxide	99.0	0	—
Propylene oxide	100.0	0	—
cis-2-Butene oxide	100.0	12	1.20

[a] Time of reaction: 10 min. Monomer added dropwise during the first 5 min.

The yields in Table III are not a measure of the over-all rates of polymerization, since no increase in polymer yields was found after the indicated reaction time.   In view of the high purity of the monomers used in these experiments, it is unlikely that the low yields are caused by contaminants.   Different complexing abilities of the polymers with the aluminum alkyls which result in autoinhibition could be the cause of this phenomenon.

To discuss the differences observed in the intrinsic viscosities, we assume that the functional relationship between the average degree of polymerization and intrinsic viscosity is identical for homologous alicyclic epoxides. It follows that either the rate of chain propagation or the rate of chain termination is different for the epoxides under consideration.

We prefer to interpret our experimental data in terms of differences in the propagation rates.   One can argue on the basis of heats of combustion studies[18] that the polymer of cyclohexene oxide, comprised of long sequences of cyclohexane rings interlinked by oxygen atoms, is relatively strain-free, while the five-, seven-, and eight-membered analog due to nonbonded interactions, retains considerable strain even after polymerization.   It is likely that in these reactions the transition state of each individual propagation step closely resembles the product formed by the addition of a new monomer molecule to the growing chain.   Transition states with less strain will have a lower energy content, and we may write that

$$E_{P_6} < E_{P_5} < E_{P_7} \ll E_{P_8}$$

(where E_P is the activation energy of propagation, and the subscripts refer to the number of carbon atoms in the alicyclic ring), from which it follows that the rates of propagation, V_P, have the reverse order:

$$V_{P_6} > V_{P_5} > V_{P_7} \gg V_{P_8}$$

This treatment of experimental data established a definite order of reactivity according to ring size among alicyclic epoxides based on rates of propagation in polymerization.   It might be interesting to note that the corresponding alicyclic ketones show the same order of reactivity in their reaction with sodium borohydride.[19]

Copolymerization Studies

Copolymerization results obtained with the monomer systems: 4-vinylcyclohexene oxide–cyclopentene oxide and 4-vinylcyclohexene oxide–cyclohexene oxide are illustrated in Figures 1 and 2.

We have found that over the entire composition range these epoxides enter the copolymer in approximately the same proportion as they are present in the monomer feed.   From this observation, it follows that the monomer reactivity ratios as defined by the copolymerization equation[20] are very close to unity.   Looking at the system, 4-vinylcyclohexene oxide–cyclopentene oxide and using the usual notation,[20] we may write for the propagation steps:
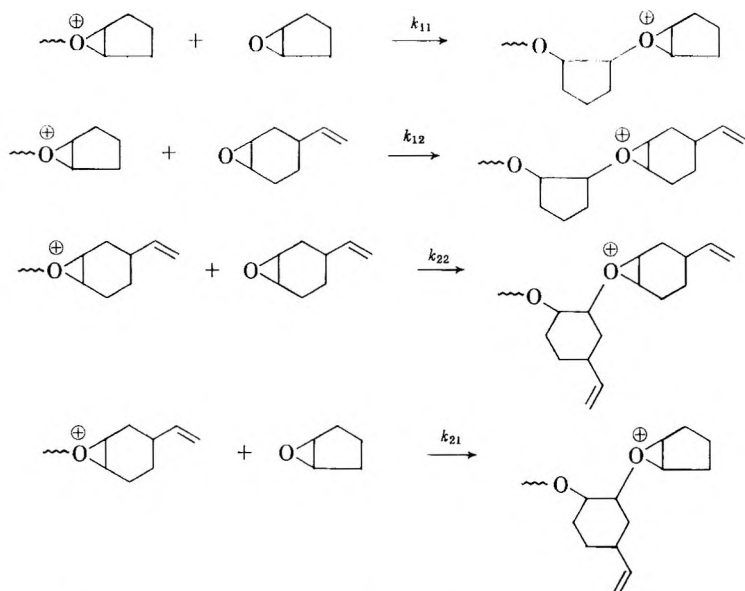
where $O\!\!<\!\!\square$ = Monomer 1, $O\!\!<\!\!\bigcirc\!\!\diagup$ = Monomer 2, k denotes the propagation rate constant, and

$$k_{11}/k_{12} = r_1 \cong 1$$
$$k_{22}/k_{21} = r_2 \cong 1$$

The same argument that was used to explain the different rates of propagation in the homopolymerization of homologous alicyclic epoxides can be applied for copolymerization as well. Accordingly, in the previous example, k_{11} and k_{12} are small, and k_{22} and k_{21} are large because the corresponding reactions involve the opening of five- and six-membered ring epoxides, respectively.
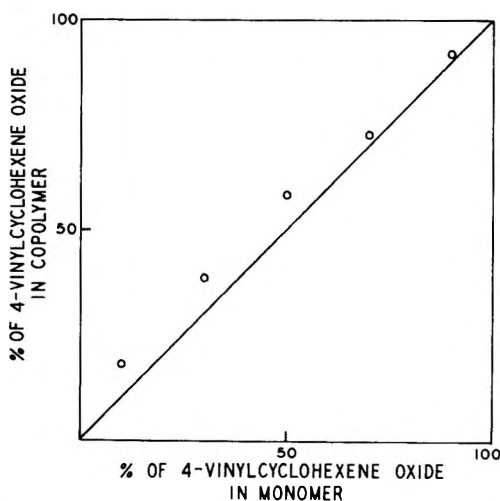
Fig. 1. Copolymerization of 4-vinylcyclohexene oxide with cyclopentene oxide.
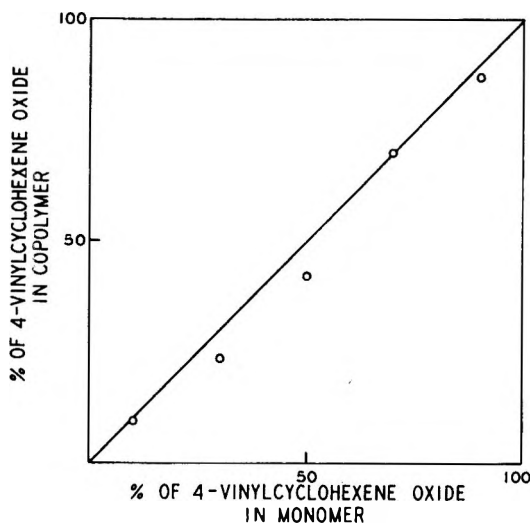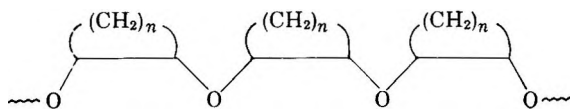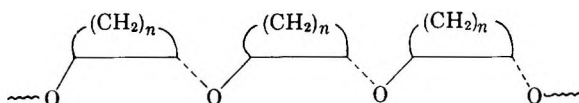
Fig. 2. Copolymerization of 4-vinylcyclohexene oxide with cyclohexene oxide.

Stereochemical Considerations

There are numerous possibilities for stereoisomerism in polymers of alicyclic epoxides. Theoretically, these compounds can exist in the pure poly-*cis* form:

or in the pure poly-*trans* form:

and a random or some ordered copolymer containing *cis*- and *trans*-structural units is equally conceivable. However, careful stereochemical studies lead to the conclusion that the ring opening of alicyclic epoxides[21] and sulfides[22] always yields the *trans*-addition product; *trans*-addition should occur for polymerization reactions as well.

Proton magnetic resonance studies on polycyclohexene oxide furnished evidence for the steric course of the polymerization. The spectra of polycyclohexene oxide, *cis*-1,2-cyclohexanediol and *trans*-1,2-cyclohexanediol measured in dilute $CHCl_3$ solution are presented in Figure 3. The positions of the characteristic main peaks are summarized in Table IV.

The assignment of peaks for the CH_2 and CH protons was done by comparison with appropriate literature values;[24] while the OH proton was identified by the dilution technique.[25] No effort was made to interpret the splitting of the CH_2 band.

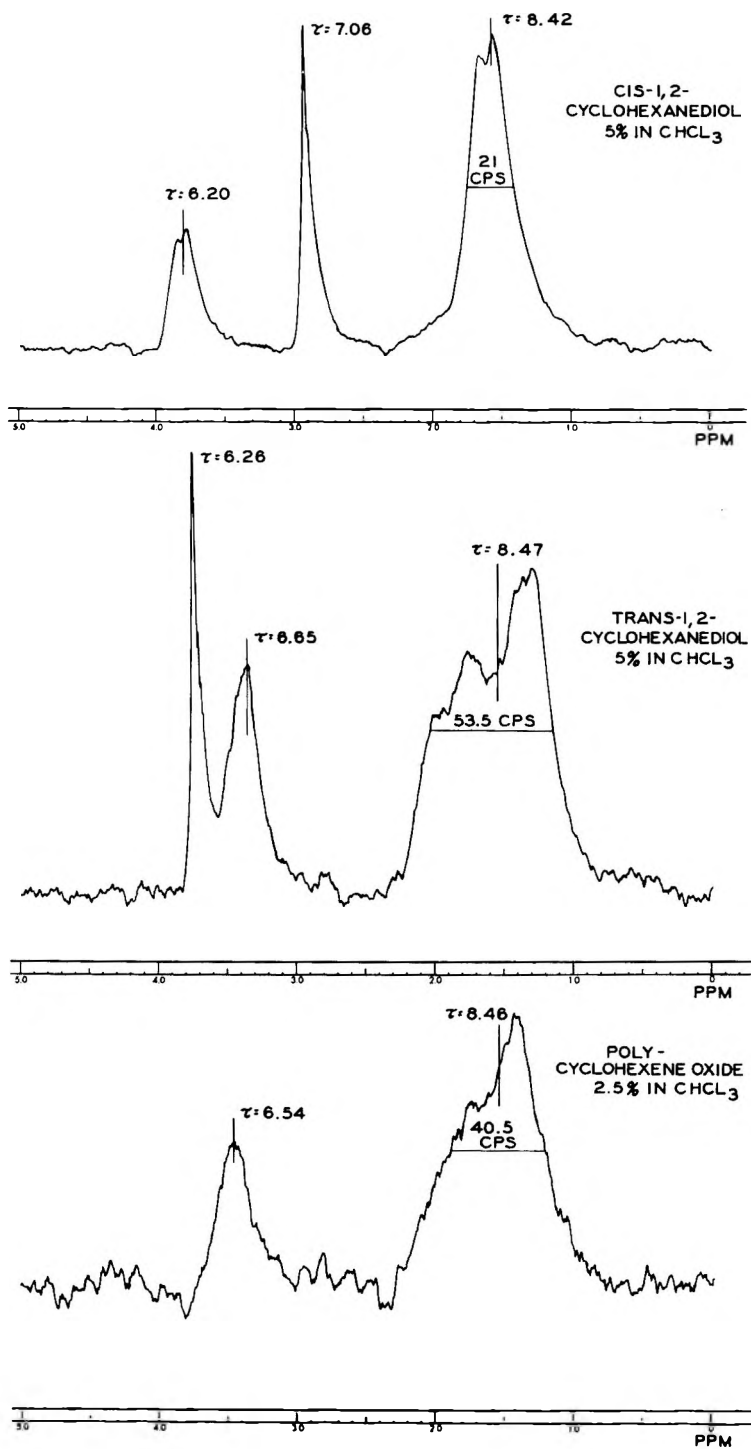Both the position of the CH proton resonance peak and the broadness of

Fig. 3. Proton magnetic resonance spectrum of polycyclohexene oxide, *cis*-1,2-cyclohexanediol, and *trans*-1,2-cyclohexanediol in CHCl₃.

TABLE IV

Characteristic Proton Resonance Absorptions in the Spectrum of Polycyclohexene Oxide,
cis-1,2-Cyclohexanediol and *trans*-1,2-Cyclohexanediol

		τ^a		Width of CH_2 band at half height,
Compound	CH_2	CH	OH	cycles/sec.
cis-Diol	8.42	6.20	7.06	21
trans-Diol	8.47	6.65	6.26	53.5
Polymer	8.46	6.54	—	40.5

[a] Data of Jackman.[23]

the CH_2 band point to the close stereochemical relationship between the *trans*-diol and the polymer. This observation strongly suggests that the polymerization of alicyclic epoxides follows established stereochemical principles for these compounds to yield the stereoregular poly-*trans*-ether. Based upon this analogy, we propose that the polymer of cyclohexene sulfide also has the stereoregular poly-*trans* structure:
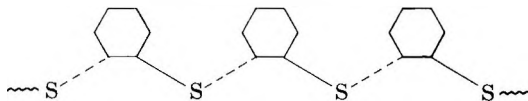
References

1. (*a*) Ebert, P. E., and C. C. Price, *J. Polymer Sci.*, **34**, 157 (1959); (*b*) S. Kambara and M. Hatano, *J. Polymer Sci.*, **27**, 584 (1958); (*c*) R. A. Miller, and C. C. Price, *J. Polymer Sci.*, **34**, 161 (1959).

2. Furukawa, J., T. Tsuruta, R. Sakata, T. Saegusa, and A. Kawasaki, *Makromol. Chem.*, **32**, 90 (1959).

3. Vandenberg, E. J., *J. Polymer Sci.*, **47**, 486 (1960): *ibid.*, **47**, 489 (1960); *J. Am. Chem. Soc.*, **83**, 3538 (1961).

4. Rothrock, H. S., U.S. Pat. 2,054,099 (1936), to E. I. du Pont de Nemours and Company.

5. Foster, R. E., U.S. Pat. 2,687,406 (1954), to E. I. du Pont de Nemours and Company.

6. Emmons, W. D., and A. S. Pagano, *J. Am. Chem. Soc.*, **77**, 89 (1955).

7. Cope, A. C., S. W. Fenton, and C. F. Spencer, *J. Am. Chem. Soc.*, **74**, 5887 (1952).

8. Cope, A. C., and W. N. Baxter, *J. Am. Chem. Soc.*, **76**, 280 (1954).

9. Cope, A. C., A. Fournier, Jr., and H. E. Simmons, Jr., *J. Am. Chem. Soc.*, **79**, 3907 (1957).

10. Whitmore, W. F., and A. I. Gebhart, *J. Am. Chem. Soc.*, **64**, 914 (1942).

11. Wilson, C. E., and H. J. Lucas, *J. Am. Chem. Soc.*, **58**, 2399 (1936).

12. Paris, O. E., and R. E. Fanta, *J. Am. Chem. Soc.*, **74**, 3007 (1952).

13. Edgar, O. B., and E. Ellery, *J. Chem. Soc.*, **1952**, 2633.

14. Bomstein, J., *Anal. Chem.*, **30**, 544 (1958).

15. Jones, R. N., and C. Sandorfy, in *Chemical Applications of Spectroscopy*, W. West, Ed., Interscience, New York, 1956, p. 575.

16. Winstein, S., and R. B. Henderson, in *Heterocyclic Compounds*, Vol. I, R. C. Elderfield, Ed., Wiley, New York, 1953, p. 57.

17. Osgan, M., and C. C. Price, *J. Polymer Sci.*, **34**, 153 (1959).

18. Kilpatrick, J. E., K. S. Pitzer, and R. Spitzer, *J. Am. Chem. Soc.*, **69**, 2483 (1947).

19. Brown, H. C., and K. Tchikawa, *Tetrahedron*, **1**, 221 (1959).

20. Billmeyer, F. W., Jr., *Textbook of Polymer Chemistry*, Interscience, New York, 1957, p. 222.

21. Elderfield, R. C., Ed., *Heterocyclic Compounds*, Vol. I, Wiley, New York, 1953, p. 30.

22. VanTamelen, E. E., *J. Am. Chem. Soc.*, **64**, 2716 (1942).

23. Jackman, L. M., *Applications of Nuclear Magnetic Resonance Spectroscopy in Organic Chemistry*, Pergamon, New York, 1959, p. 47.

24. Jackman, L. M., *Applications of Nuclear Magnetic Resonance Spectroscopy in Organic Chemistry*, Pergamon, New York, 1959, pp. 52 and 55.

25. Roberts, J. D., *Nuclear Magnetic Resonance Applications to Organic Chemistry*, McGraw-Hill, New York, 1959, p. 23.

Résumé

On a étudié la polymérisation des époxydes alicycliques en présence d'alkyl aluminium. Très souvent on a observé de grandes vitesses de polymérisation à la température de −78°C et la formation de produits de haut poids moléculaire avec de très bons rendements. Les spectres infra-rouges des polymères sont en accord avec les structures polyéthers proposées. On a trouvé que le poids moléculaire des polymères obtenus dans ces réactions était fonction de la taille du cycle acyclique. Ceci a été expliqué par l'examen de la variation de tension moléculaire au cours de l'étape de formation du polymère. On a établi l'ordre de réactivité suivant en se basant sur des estimations des vitesses de propagation: oxyde de cyclohexène > oxyde de cyclopentène > oxyde de cycloheptène ≫ oxyde de cyclooctène. On propose un mécanisme de réaction dans lequel l'initiation est provoquée par la coordination du dérivé alkylaluminum avec l'époxyde et est suivie d'additions successives des monomères aux centres électrophiliques. L'absence de groupes phényles terminaux dans un oxyde de polycyclohexène de poids moléculaire assez bas exclut un des mécanismes possibles. Les spectres de résonance magnétique des protons de l'oxyde de polycyclohexène, du *cis*-1,2-cyclohexanediol et du *trans*-1,2-cyclohexanediol ont été déterminés en solution chloroformique diluée et suggèrent une structure stéréorégulière poly-*trans*-éther pour ces polymères.

Zusammenfassung

Die Polymerisation alicyclischer Epoxyde mit Aluminiumalkylen wurde untersucht. In vielen Fällen wurden bei −78°C grosse Polymerisationsgeschwindigkeiten bei Bildung hochmolekularer Produkte in guter Ausbeute beobachtet. Die Infrarotspektren der Polymeren stimmen mit der vorgeschlagenen Polyätherstruktur überein. Es wurde gefunden, dass das Molekulargewicht der bei diesen Reaktionen erhaltenen Polymeren eine Funktion der Grösse des alicyclischen Ringes ist. Dieses Verhalten liess sich durch eine Betrachtung der Änderung der Molekülspannung während der polymerbildenden Reaktion erklären. Auf Grund der Wachstumsgeschwindigkeit wurde folgende Reaktivitätsreihe für die Monomeren aufgestellt: Cyclohexenoxyd > Cyclopentenoxyd > Cycloheptenoxyd ≫ Cyclooctenoxyd. Ein Reaktionsmechanismus mit Start durch Koordination des Aluminiumalkyls mit dem Epoxyd und darauffolgender stufenweiser Addition des Monomeren an die elektrophilen Zentren wird vorgeschlagen. Das Fehlen von Phenylendgruppen in einem verhältnismässig niedermolekularen, mit AlPh$_3$ als Katalysator dargestellten Polycyclohexenoxyd schliesst einen der möglichen, alternativen Mechanismen aus. Die protonmagnetischen Resonanzspektren von Polycyclohexenoxyd, *cis*-1,2-Cyclohexandiol und *trans*-1,2-Cyclohexandiol wurden in verdünnter Chloroformlösung aufgenommen und sprechen für eine stereoreguläre Poly-*trans*-äther-Struktur der Polymeren.

Effect of Ions on the Dielectric Dispersion of Ovalbumin Solution

SHIRO TAKASHIMA,* *Institute for Protein Research, Osaka University, Osaka, Japan*

Synopsis

The dielectric dispersion of ovalbumin solution was studied in the presence of various ions. It was found that ions such as tetraethylammonium, ammonium, Na, and K which are not bound to the protein had no effect on the dielectric increment or on the relaxation time. On the contrary, the addition of ions such as Cu, Ca, Mg, and H ions had a considerable effect on the dielectric increment as well as on the binding of the ions to the protein. These results indicate that ions do not affect the dielectric dispersion parameters of this protein unless they have specific interaction with the polar sites of the ovalbumin molecule. The electric polarization of protein solutions is discussed and it is suggested that the ion fluctuation process including the Maxwell-Wagner effect is not necessarily the essential mechanism of dielectric polarization of isoelectric protein solutions.

Introduction

It is known that the configurations of linear polyelectrolytes are strongly dependent on the presence of ions in the solution. This may be due to the fact that the addition of electrolytes apparently neutralizes the charges of the molecules and decreases the electrostatic interaction between segments. Although hydrogen bonds, hydrophobic bonds, or other bonds may play an important role in stabilizing the tertiary structure of the globular proteins,[1] it is still plausible that the electrostatic interaction is an important factor in determining the configuration of these molecules. Thus, the addition of salts to protein solutions may change the structure of the globular protein molecules and as a consequence, it may change also the dielectric behavior of their solutions.

The dielectric properties of aqueous protein solutions have been investigated in the past at as low ionic strength as possible,[2] since electrolytes increase the conductivity of the solution and render dielectric measurement extremely difficult. However, the recent development of an impedance bridge in the kilocycle and megacycle region now enables us to measure the dielectric dispersion of aqueous protein solutions with reliable accuracy even in the presence of electrolytes. We carried out a number of measure-

ments of the dielectric dispersion of some proteins in the presence of various salts, and the results with ovalbumin will be reported in this article.

Experiments

An Ando TR-IB impedance bridge was used in all the experiments. The bridge was designed for the measurement of conductive solutions and suitable for the measurement of protein solutions of moderate ionic strength. The bridge covered the frequency range from 30 cycles/sec. to 5 Mcycles/sec., and the precision of the capacity and conductivity readings were 0.1 $\mu\mu$f and 0.003 μmho, respectively.

Although ovalbumin solutions were thoroughly dialyzed before the measurement, they had considerable conductivity and this gave rise to an electrode polarization in the low frequency region which obscured the determination of the static dielectric constant (ϵ_0) of protein solutions. The electrode polarization could best be eliminated by plating the electrodes carefully with platinum black. However, the electrode polarization could not be corrected satisfactorily even by extremely careful plating. The following method was applied for further correction. If one plots the logarithm of the measured capacity of the polyelectrolyte solution log C against log frequency, log C begins to rise at low frequency where the effect of electrode polarization is not negligible. As shown in eq. (1),

$$C = C_s + [1/(1 + \omega^2 R^2 C_p)] \tag{1}$$

the effect of the electrode polarization is more pronounced in the lower frequency region, and the capacity which is due to the electrode polarization tends to increase to infinite value, and no tendency of leveling off of this capacity has ever been observed. (Here ω and R are the angular frequency and resistance, respectively, and C_s and C_p are the true capacity of the solutions and the electrode capacity.) The limiting slope of log C with the abscissa has been confirmed to be 1.5 provided the electrodes are carefully plated with platinum black. Poor plating shifts the electrode polarization toward the higher frequency region as eq. (1) indicates, and also, according to Imai and Minakata,[3] the slope changes from 1.5 to approximately 1.8. They found that the 1.5 slope could be obtained only when the electrodes were carefully plated. Our measurements were carried out between 60 cycles/sec. and 5 Mcycles/sec. which made the correction by taking the difference between the observed capacity and the limiting 1.5 slope possible. However, even this correction is not sufficient to eliminate the effect of electrode polarization completely, as is shown in Figure 1, in which one observes a gradual increase of the dielectric constant of the solution in the lower frequency region instead of the plateau as indicated by the broken line which probably is the true static dielectric constant ϵ_0 of the solution. Whether this increase of the dielectric constant is really due to the electrode polarization or to the presence of an unknown dielectric dispersion in the protein solution is not certain. However, we have fairly good reasons to conclude that this is not due to the protein molecule but due only to the
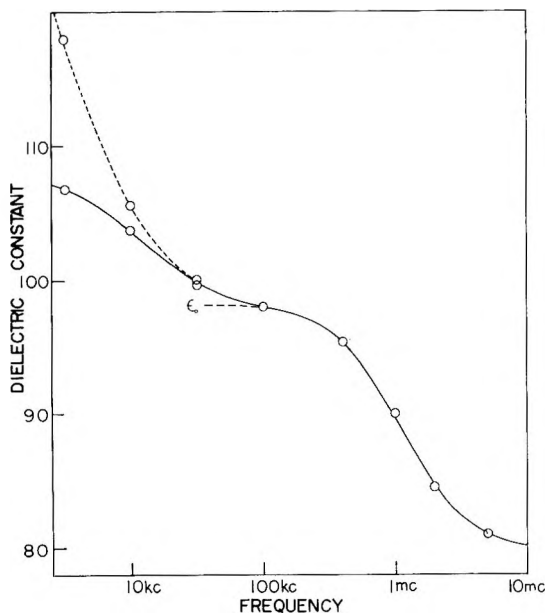
Fig. 1. Dielectric dispersion of ovalbumin at 12°C.: (——) curve corrected from the 1.5 limiting slope; (--) measured value; (—) (ϵ_0) supposed static dielectric constant of the protein solution.

residual electrode polarization which cannot be corrected by the method mentioned above and, therefore, the static dielectric constant ϵ_0 was obtained by the most probable extension of the dispersion curve as is indicated by the broken line designated ϵ_0.

Ovalbumin was prepared by two methods. When ovalbumin was prepared by fractional precipitation with ammonium sulfate (preparation I), this protein gave a large dielectric increment (curve *1* in Fig. 2) of 0.45 which is much larger than the value Oncley[4] reported (0.14). However, ovalbumin which was crystallized by the addition of sodium sulfate solution (preparation II) gave a dielectric dispersion shown by curve *2* in Figure 2 with a value of 0.202 for the dielectric increment which is appreciably closer to Oncley's observation. Although there was no decisive reason to conclude that the preparation I was a denatured protein (the intrinsic viscosity of this preparation was 4.3 cc./g.), we used preparation II throughout the experiments because this preparation had similar dielectric properties to that of the preparation used by Oncley. Furthermore, as is shown by curve *3* in Figure 2, the dielectric dispersion of ovalbumin solutions changed with the time after dissolution and the aged solution gave a still lower dielectric increment (0.17) and larger relaxation time (Table I). The ions examined in this experiment were hydrogen ion, potassium, sodium, ammonium, and tetraethylammonium (TEA) and also Ca, Mg, Hg, and Cu ions. The TEA ion was chosen since it is supposed to have no specific interaction with polyelectrolytes and seemed to be the best reagent with
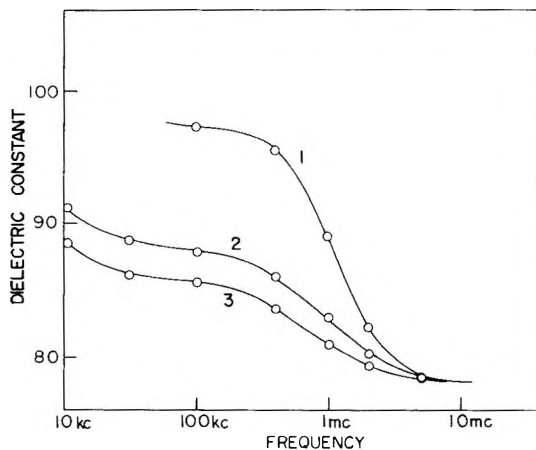
Fig. 2. The dielectric dispersion of ovalbumin: (*1*) dispersion of ovalbumin which is purified with ammonium sulfate; (*2*) dispersion of ovalbumin crystallized with sodium sulfate (fresh solution); (*3*) dispersion of ovalbumin crystallized with sodium sulfate (aged solution).

which to examine the effect of ionic strength on the physical properties of protein solutions without secondary effects due to ion binding.

The pH of the dialyzed ovalbumin solution was about 5.5, which is the isoelectric point of this protein. As will be shown in the following section (Fig. 8), the dielectric increment of ovalbumin is sensitive to the pH of the solution and a shift of pH from 5.5 to 4.5 caused an appreciable decrease in the dielectric increment. Thus one has to keep the pH of the solution as constant as possible without adding any buffering reagent. Therefore, the salts used were carefully purified and it was confirmed that the addition of these salts did not change the pH of the protein solution. A decrease of pH (0.2–0.3) was observed for some ions, but it was confirmed that this was not due to impurities in the salts but may have been due to the release of protons from the protein due to the binding of the added ions. Since direct contact of the dielectric cell with a water bath increases the external capacity, the temperature of the solution was controlled by circulating thermostatted water in a jacket which surrounded the dielectric cell. Also, many of the measurements were carried out in an air-conditioned room at a temperature which was slightly higher than room temperature. The fluctuation of temperature during the measurements was very small, and this turned out to be sufficient for the capacity reading, although it is by no means satisfactory for the conductivity reading. We noticed a considerable drift of conductivity during the measurement, and this made the determination of the dispersion of conductivity which is related to the imaginary part of the dielectric constant ϵ'' extremely difficult.

By measuring the dielectric dispersion of protein solution, one obtains three dielectric parameters: (*1*) the dielectric increment which is related to the dipole moment of the molecules by $\mu = AT \ (\delta_0 - \delta_\infty)$, where A is a constant and δ_0 and δ_∞ are the specific dielectric increments at low and high

TABLE I

Dielectric Dispersion Parameters of Ovalbumin in the Absence and Presence of Various Ions

Salt added	Time after dissolution, days	$\Delta\epsilon/g$, no salt (δ_0)	$\Delta\epsilon/g$, with salt (δ)	δ/δ_0 ratio	$\tau_0 \times 10^8$, no salt	$\tau \times 10^8$, with salt	τ/τ_0 ratio	Maximum concn. of salt added, $M \times 10^3$
HCl	4	0.202	0.118	0.584	13.8	11.5	0.83	2
CuSO$_4$	6	0.202	0.142	0.73	13.8	8.71	0.63	2
AgNO$_3$	7	0.200	0.174	0.87	13.6	11.8	0.85	2
HgCl$_2$	9	0.192	0.174	0.88	12.1	12.6	1.0	2
KCl	11	0.200	0.174	0.87	15.2	15.7	1.0	1
NaCl	12	0.174	0.150	0.86	15.1	15.7	1.0	2
NH$_4$Cl	14	0.174	0.167	0.97	17.5	17.0	0.95	2
TEAB	17	0.156	0.155	0.99	19.2	19.7	1.0	5
CaCl$_2$	18	0.163	0.087	0.53	25.2	8.36	0.33	1
MgCl$_2$	20	0.163	0.105·	0.64	21.5	13.3	0.61	1

frequency, respectively; (2) the relaxation time; and (3) the distribution of the relaxation times. The dielectric increment is obtained from $(\epsilon_0 - \epsilon_\infty)/g$ where ϵ_0 and ϵ_∞ are the dielectric constants of the solution at very low and high frequencies, respectively. The relaxation time is obtained from $\tau = 1/2\pi f_c$ where f_c is the critical frequency. The distribution of relaxation times is usually obtained by a simple calculation from a Cole-Cole circular plot in which ϵ' and ϵ'' are plotted in a complex plane. However, the determination of ϵ'' requires an accurate measurement of the conductivity of the solution in a dispersion frequency region, and even a small error in the conductivity reading, especially in the low frequency region, can cause a serious error in the value of ϵ'' since $\epsilon'' = \epsilon_r(\sigma_\infty - \sigma_0)/2\pi f$, where σ_∞ and σ_0 are high and low frequency conductivities, respectively, and $\epsilon_r = {}^1/_9 \times 10^{11} \times 4\pi$. As already mentioned, the fluctuation of temperature has to be strictly controlled for the precise conductivity measurement, and unfortunately our temperature control was insufficient for this purpose so that the determination of the dielectric loss ϵ'' had to be abandoned.

Results

It is known that TEA does not interact specifically with polyions, and this reagent is widely used to increase the ionic strength of the solutions without causing secondary effects due to ion binding. Ammonium ions are also believed to have little affinity for proteins. Therefore, prior to the investigation of the effect of other ions which are known to be specifically bound, the effect of TEA and simple ammonium ion were investigated. The dielectric increment of ovalbumin in the presence of these ions is illustrated in Figure 3, and the dielectric dispersion with and without these
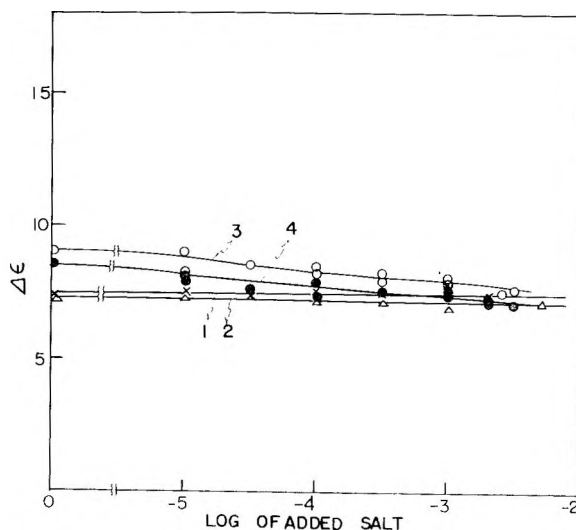

Fig. 3. The dielectric increment of ovalbumin in the presence of various ions: (1) TEA bromide; (2) ammonium chloride; (3) AgNO₃; (4) HgCl₂.
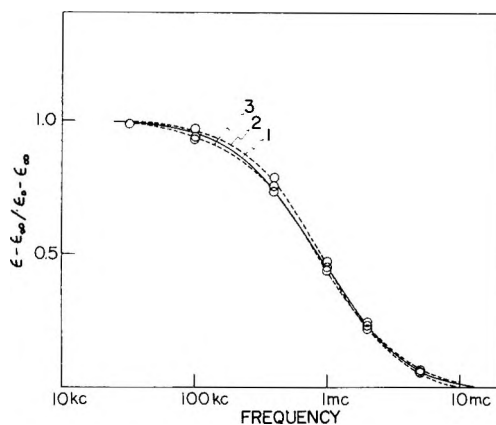
Fig. 4. The dielectric dispersion of ovalbumin (*1*) without salt and in the presence of (*2*) TEA and (*3*) ammonium ion.
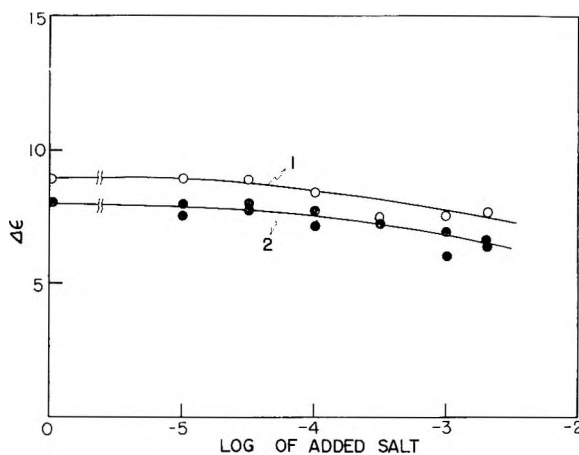
Fig. 5. Dielectric increment of ovalbumin in the presence of (*1*) NaCl; (*2*) KCl.

ions is shown in Figure 4.   TEA and ammonium ions are found to have no effect either on dielectric increment or on dielectric relaxation of ovalbumin solutions.   These results are clear evidence that the mere increase of ionic strength does not change the dielectric properties of an ovalbumin solution.   As further evidence, the effect of Ag and Hg ions was investigated.

Ovalbumin has no titratable sulfhydryl group in the native state,[5] which means that Ag or Hg ions which are known to be SH reagents are not bound to ovalbumin; accordingly, these ions should have no effect on the dielectric properties of this protein in analogy with TEA and ammonium ions. As shown in Figure 3, the decreases in the dielectric increment due to these ions are only slightly beyond the experimental error.

These results indicate that the ions which are known to have no interaction with ovalbumin have no effect on the dielectric properties of this

Fig. 6. Dielectric increment of ovalbumin in the presence of (1) $MgCl_2$; (2) $CaCl_2$.
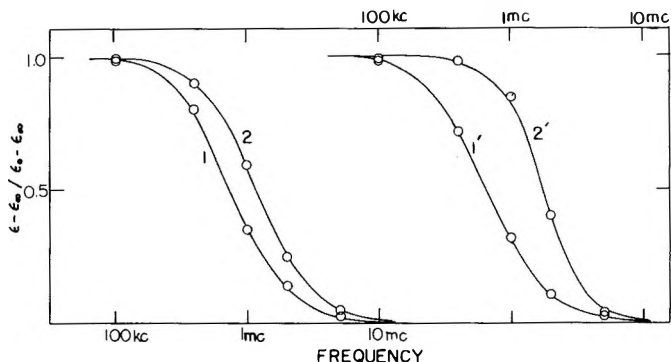
Fig. 7. Dielectric dispersion of ovalbumin in the presence of (left) $MgCl_2$ and (right) $CaCl_2$: (1) control; (2) with $10^{-3}M$ $MgCl_2$; (1') control; (2') with $10^{-3}M$ $CaCl_2$.

protein solution. However, unfortunately, we have little information on the ion binding of ovalbumin except for the few ions such as TEA, ammonium, Ag, and Hg. Therefore, we cannot easily conclude that ions are bound to the protein even when we observe some change in the dielectric properties of the solution. However, the results with TEA, ammonium, and also Ag and Hg may substantiate the postulate that ions have no effect on the dielectric properties of proteins unless they are bound to them, and we may be able to assume that ions may have fairly strong interaction with the protein when they change the dielectric increment or relaxation time of the solution.

KCl and NaCl. The binding of these ions to bovine serum albumin were studied by many workers, and no binding has been detected, even at fairly high concentration.[6] As shown in Figure 5, both KCl and NaCl have only little effect on the dielectric increment; they have no effect on
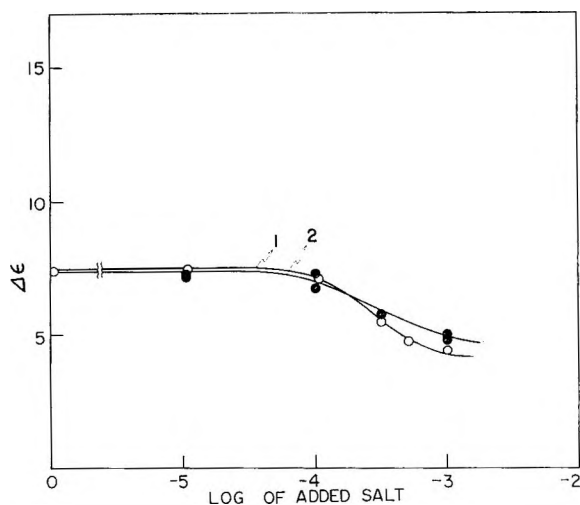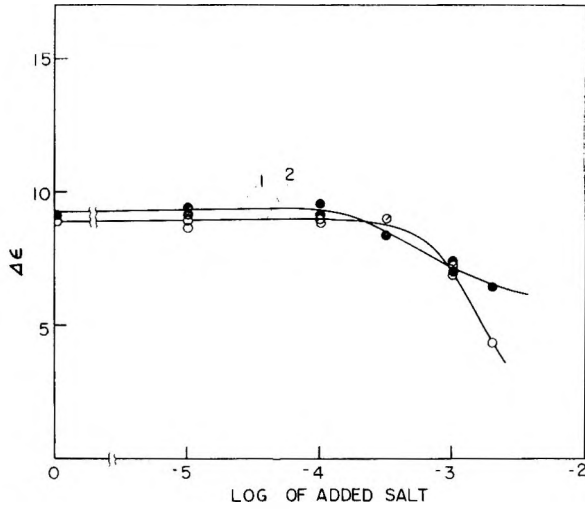
Fig. 8. Dielectric increment of ovalbumin in the presence of (1) CuSO₄; (2) HCl.
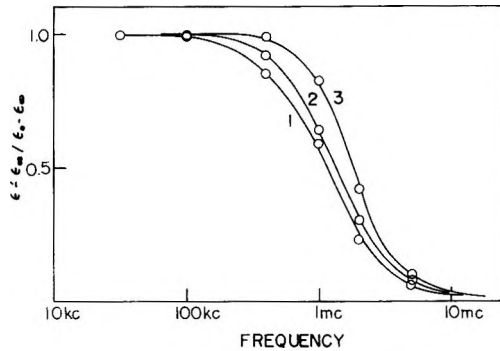
Fig. 9. Dielectric dispersion of ovalbumin: (1) control; (2) with $2 \times 10^{-3}M$ HCl; (3) with $2 \times 10^{-3}M$ CuSO₄.

the relaxation time (Table I), and their behavior is similar to that of Hg and Ag ions. These results indicate that KCl and NaCl, as in the case of serum albumin, have little or no interaction with ovalbumin.

CaCl₂, MgCl₂, and CuSO₄. Ca and Mg are ions which are widely distributed in living organisms and they are of physiological importance. Both of them play a specific role in many biological activities and consequently we have good reason to believe that these ions interact strongly with many proteins although no detailed experiments on binding with ovalbumin have been reported. The dielectric increments of ovalbumin in the presence of various concentrations of these ions are shown in Figure 6. As shown, the dielectric increments decreases markedly at added ion concentrations above $10^{-4}\ M$, and we observe also a distinct change in the dielectric dispersion in the presence of these ions (Fig. 7). Particularly calcium ion changes both relaxation time and the shape of the dispersion

curve; this is indicative of a direct binding of these ions to ovalbumin The data are also tabulated in Table I.

Cupric ion is also known to bind with proteins, often irreversibly,[7] with the precipitation of these proteins.   As shown in Figure 8, Cu ion has a considerable effect on the dielectric increment of ovalbumin at a concentration above $10^{-4}M$.   The effect of Cu ion on the relaxation time is shown in Figure 9.   Although the shape of the dispersion curve is changed, the shift of the relaxation time is not pronounced compared to that produced with $CaCl_2$.

HCl.   The binding of protons to carboxyl groups of proteins has been extensively studied, but very little work has been done on the effect of binding on the structure of protein molecules.   Kauzman[8] observed that the binding of hydrogen ions to serum albumin and ovalbumin caused an increase of specific volumes of these proteins.   On the other hand, Shutt[9] observed a marked decrease of static dielectric increment of ovalbumin in the pH region between 5.5 and 4.5 which was followed by a sudden increase on further decrease of pH of the solution.   However, he did not study the effect of proton binding on the dielectric dispersion and the main objective of this measurement is to investigate how the proton binding affects the dispersion parameters of this protein.   As illustrated in Figure 8, the dielectric increment decreases very rapidly between 3×10^{-4} and $3 \times 10^{-3}M$ (between pH 5.5 and 4.48), which confirms Shutt's observation.

However, contrary to our expectation, the binding of protons does not affect the dielectric dispersion of this protein significantly, and the relaxation time decreases only from 13.8×10^{-8} to 11.5×10^{-8} sec.   The results are shown in Figure 9 and also tabulated in Table I.   Although HCl has as much effect on the static dielectric increment as Ca, Mg, and Cu it has only a slight effect on the relaxation time and its distribution.   In spite of Kauzman's observation, no volume increase of ovalbumin was observed in this concentration range.   However, this does not seem to contradict his results, since the concentration of hydrochloric acid used in this experiment differs drastically from that of Kauzman's experiments.

Discussion

The mechanism of dielectric polarization of protein solutions has long been studied and discussed by many workers.   Oncley explained his experimental results on the assumption that the dielectric polarization of protein solution was due to the orientation of the whole molecule in the electric field.   However, there are several alternative hypotheses which are based on the assumption that the orientation of the whole protein molecule is restricted because of the high molecular weights of the proteins and that the orienting torque is not sufficient to overcome the potential barrier which prevents the molecules from orienting along the direction of the field.   These hypotheses assume a polarization caused by the fluctuation of ions on the surface of the protein molecules, and Kirkwood and Shu-

maker[10] showed that the dipole moment of proteins could be accounted for by this effect alone. They emphasized that the orientational polarization was not necessarily the only mechanism of dielectric polarization of protein solutions.

According to the Maxwell-Wagner theory,[11,12] the dielectric polarization and the dispersion of these particles can be accounted for by assuming a boundary which separates two regions having different dielectric constants and conductivities, namely, the dielectric constant and conductivity of the solvent (ϵ_1 and σ_1, respectively) and the dielectric constant and conductivity of the particle (ϵ_2 and σ_2, respectively).

We obtain:

$$\epsilon' = \epsilon_\infty + \left(1 + \frac{k}{1 + w^2\tau^2}\right) \qquad (2)$$

where ϵ' is the real part of the dielectric constant, ϵ_∞ is the high frequency dielectric constant, $\omega = 2\pi f$, and τ is the relaxation time. k is given by eq. (3):

$$k = 9q[(\epsilon_1\sigma_2 - \epsilon_2\sigma_1)/\epsilon_1(2\epsilon_1 + \epsilon_2)(2\sigma_1 + \sigma_2)] \qquad (3)$$

where q is the volume fraction of the particle.

We can assume $\epsilon_1 = \epsilon_2$ for most dilute polyelectrolytes,[13] and then $\sigma_1 \neq \sigma_2$ is the condition which must be fulfilled in order that these particles have dielectric polarization. Ordinarily, the measurements of the dielectric constant of protein solutions are performed in distilled water, and we may safely assume that the conductivity of the double layer is larger than that of solvent, since the counterions are supposedly confined in this region because of the electrostatic potential. Accordingly, we have reason to believe proteins to have Maxwell-Wagner type polarization under these circumstances.

If the polarization of protein solution is due to the Maxwell-Wagner effect, the addition of electrolytes will decrease the dielectric increment of protein solutions by decreasing the difference between the conductivities of the solvent and proteins, i.e., $\sigma_1 \simeq \sigma_2$.

As was already mentioned, the addition of TEA or simple ammonium ions which have little or no affinity for the polar groups of proteins does not change the dielectric increment of the ovalbumin solution. The highest concentration used was $0.5 \times 10^{-2}M$ and the equivalent conductivity was increased from 600 μmho to 2500 μmho, which should be sufficient to cause a measurable change in the dielectric increment if the dielectric polarization of ovalbumin is due to the Maxwell-Wagner effect. Also, the addition of other ions which are not supposed to bind with ovalbumin, such as potassium or sodium ions, does not change the dielectric increment. These results would offer sufficient evidence for the conclusion that the Maxwell-Wagner effect is not important in the dielectric polarization of ovalbumin.

Furthermore, the fact that the addition of the ions does not change the relaxation time of the ovalbumin solution is inconsistent with the postulate

of the Maxwell-Wagner theory in which the relaxation time is expressed by eq. (4):

$$\tau = [(2\epsilon_1 + \epsilon_2)/4(\sigma_1 + \sigma_2)] \tag{4}$$

where σ_1 is the conductivity of the solvent and σ_2 is that of particle. If one increases σ_1, the conductivity of the solvent, it increases the denominator of eq. (4), and consequently there would result a decrease of the relaxation time of the solution. The facts that the addition of salts changes neither the dielectric increment nor the relaxation time seem to be sufficient to eliminate the possibility that the Maxwell-Wagner effect is a major dielectric polarization mechanism of ovalbumin, although we cannot extend this conclusion to other globular proteins without further investigation.

Although the Maxwell-Wagner effect is almost ruled out by the observations mentioned above, it does not necessarily mean that the dielectric polarization of protein solutions is due to the orientations of the permanent dipole. However, Takashima[14] observed that the relaxation time of protein solutions depends on the viscosity of the solvent rather than the conductivity. We are, therefore, led to the conclusion that the polarization of protein solutions is possibly due to the orientation of permanent dipole. However, the experiment is so far limited to the isoelectric region, and the above conclusion must be confined to the isoelectric proteins. The behavior of Ca, Mg, and Cu is entirely different from that of TEA, ammonium, Na, and K, and this difference seems to be due to binding of these ions to ovalbumin, since hydrogen ion which is known to bind with proteins has similar effect as these ions. These ions, as well as hydrogen ion, cause a decrease in the dielectric increment and relaxation time. However, the extent of change depends largely on each ion, and the effect seems to be specific. Apparently the effect, particularly on the relaxation time, increases with increasing ionic radius, and the most pertinent explanation for this effect seems to be to attribute it to the binding of these ions to the protein. However, the results mentioned above have to be supplemented by the direct measurement of ion binding in order to draw a definite conclusion as to the behavior of these ions.

These ions cause the decrease in the relaxation time, and according to Stoke's law ($\tau = 4\pi\eta ab^2/RT$, where η is the viscosity of the solvent, a and b are the semiaxes of ellipsoid of revolution), the decrease of relaxation time is indicative of the decrease in semiaxes, i.e., the decrease of the specific volume. However, the semiaxes which are used in Stoke's law are those of hydrated molecules, and the change of volume of the molecule does not necessarily mean a change in structure, but there may well be a decrease of volume by the removal of water of hydration by these ions.

References

1. Tanford, C., *Physical Chemistry of Macromolecules*, Wiley, New York, 1961, p. 129.

2. Oncley, J. L., in *Proteins, Amino Acids and Peptides*, Cohn and Edsall, Eds., Reinhold, New York, 1953.

3. Imai, N., and A. Minakata, private communication.

4. Oncley, J. L., J. D. Ferry, and J. Shack, *Ann. N.Y. Acad. Sci.*, **40**, 371 (1940).

5. Cecil, R., and J. R. McPhee, *Advan. Protein Chem.*, **14**, 343 (1959).

6. Carr, C. W., and L. Topol, *J. Phys. Colloid Chem.*, **54**, 176 (1950).

7. Klotz, I. M., and H. G. Vurme, *J. Am. Chem. Soc.*, **70**, 939 (1948).

8. Kauzman, W., *Biochim. Biophys. Acta*, **28**, 87 (1958).

9. Shutt, W. J., *Trans. Faraday Soc.*, **30**, 893 (1934).

10. Kirkwood, J., and J. B. Shumaker, *Proc. Natl. Acad. Sci., U.S.*, **38**, 855 (1952).

11. Maxwell, J. C., *Treatise on Electricity and Magnetism, 3rd Ed.*, Vol. 1, Clarendon, Oxford, 1892, p. 451.

12. Wagner, K. W., *Arch. Electrotech.*, **2**, 371 (1914).

13. Dintzis, H. M., J. L. Oncley and R. M. Fuoss, *Proc. Natl. Acad. Sci. U.S.*, **40**, 62 (1954).

14. Takashima, S., *J. Polymer Sci.*, **56**, 257 (1962).

Résumé

On a étudié la dispersion diélectrique d'une solution d'ovalbumine en présence d'ions différents. On a trouvé que des ions tels que ammonium tétraéthyle, ammonium, Na et K qui n'étaient pas liés à la protéine n'avaient aucun effet ni sur l'incrément diélectrique ni sur le temps de rélaxation. Par contre, l'addition d'ions tels que Cu, Ca, Mg et H exerce une influence considérable aussi bien sur l'incrément diélectrique que sur le temps de rélaxation. L'effet de ces ions était évidemment dû aux liaisons des ions avec la protéine. Les résultats ci-dessus indiquent que les ions n'affectent pas les paramètres de dispersion diélectrique de la protéine, à moins que ceux-ci soient liés spécifiquement aux endroits polaires de la molécule d'ovalbumine. Sur la base de ces résultats la polarisation électrique d'une solution de protéine est discutée; on suppose que la variation dans le processus ionique comprenant l'effet Maxwell Wagner n'est pas nécessairement le mécanisme essentiel de la polarisation diélectrique de solutions isoélectriques de protéine.

Zusammenfassung

Die dielektrische Dispersion einer Ovalbuminlösung wurde in Gegenwart verschiedener Ionen untersucht. Es wurde gefunden, dass Ionen wie Tetraäthylammonium, Ammonium, Na und K, die nicht an das Protein gebunden wurden, keinen Einfluss auf das dielektrische Inkrement oder auf die Relaxationszeit besitzen. Im Gegensatz dazu hat der Zusatz von Ionen wie Cu, Ca, Mg und H-Ionen beträchtlichen Einfluss auf dielektrisches Inkrement und Relaxationszeit. Der Einfluss dieser Ionen wird offenbar durch die Bindung der Ionen an das Protein verursacht. Die angeführten Ergebnisse zeigen, dass Ionen die Parameter der dielektrischen Dispersion dieses Proteins nur dann beeinflussen, wenn sie spezifisch an die polaren Stellen des Ovalbuminmoleküls gebunden werden. Auf Grundlage dieser Ergebnisse wird die elektrische Polarisation von Proteinlösungen diskutiert und es wird angenommen, dass der Ionenschwankungsprozess einschliesslich des Maxwell-Wagner-Effekts nicht notwendigerweise der wesentliche Mechanismus der dielektrischen Polarisation in isoelektrischen Proteinlösungen ist.

Effects of High Energy Irradiation on Polypropylene

S. E. CHAPPELL, J. A. SAUER, and A. E. WOODWARD, *Department of Physics, The Pennsylvania State University, University Park, Pennsylvania*

Synopsis

Isotactic polypropylene (Profax) film samples irradiated in the Pennsylvania State University (PSU) reactor at ambient temperatures were examined by solvent extraction and infrared absorption techniques. At low irradiation doses, samples annealed (density = 0.909 g./cc. at 24°C.) prior to irradiation were found to have a lower gel content and a higher concentration of oxidation products than quenched samples (density = 0.899 g./cc. at 24°C.) irradiated under identical conditions. Similar gel fraction results were obtained for electron irradiated samples of polypropylene. These effects are believed to arise from the accumulation of a greater concentration of free macroradicals in the higher density samples. At higher reactor dosages the irradiation effects in the annealed and quenched films appear to be about the same. The gel content as a function of dose was found to be independent of the irradition intensity level over a twofold range. Irradiations in the PSU reactor were also carried out on high density polyethylene (Marlex 50) pellets at two temperatures, viz., 40 ± 10°C. and 150°C. Irradiation at 150°C. led to a greater gel content at any given dose, a result in agreement with that reported by Lawton, Balwit, and Powell for electron-irradiated specimens. Nuclear magnetic resonance spectra were obtained for molded annealed samples of partially isotactic polypropylene, irradiated in the Brookhaven reactor, at temperatures of 90–330°K. The observed shifts in the line narrowing process that occur in the 270–330°K. region are explained in terms of the decrease in crystallinity and the increasing density of crosslinks that accompany irradiation.

INTRODUCTION

In a study of the effects of electron irradiation on linear polyethylene (Marlex 50) Lawton, Balwit, and Powell[1] reported a marked increase in gel content for samples irradiated at temperatures in the vicinity of the melting point over that found for samples irradiated at lower temperatures whereas double bond formation was little affected by a temperature change. The lower reactivity towards free radical crosslinking reactions for the chains in the crystalline regions implied by these results was attributed to their relative rigidity as compared to that for the chains in the amorphous (or disordered) parts.[1] This explanation also accounted for the accumulation of free macroradicals in samples of high crystallinity as observed by reactivity with oxygen and other gases[2] and by electron paramagnetic resonance.[3]

Although a number of investigations concerned with the effects of high energy irradiation on polypropylene have been reported,[4–11] the effect of

physical state on the reactions occurring has received no systematic study to date. A property of partially isotactic polypropylene which makes it especially useful for such a study is that by quenching from the melt it can be made to exist in a metastable state[12] in which the properties of the material differ from those for annealed samples of the same material. Therefore, one part of the investigation to be reported herein was concerned with the determination of gel contents by solvent extraction of both quenched and annealed samples of partially isotactic polypropylene (Profax) film irradiated in a nuclear reactor at ambient temperature. To obtain further information, similar irradiated specimens were subjected to infrared absorption measurements. In addition, gel fraction determinations were carried out on annealed and on quenched polypropylene samples irradiated with an electron source at 25°C. and on linear polyethylene pellets (Marlex 50) irradiated in a reactor at 30–50°C. and at 150°C.

Dynamic mechanical, density, and gel fraction measurements have been given previously for a series of reactor-irradiated polypropylene samples.[11] At the dosages employed, marked alterations of the mechanical loss peaks accompanied by room temperature density changes were observed, and these changes were interpreted in terms of two competing processes, destruction of crystallinity and crosslink formation. To obtain further information nuclear magnetic resonance (NMR) measurements were carried out on four such specimens, and the results are presented and discussed herein.

EXPERIMENTAL

A. Samples

The polypropylene (Profax) samples used in this investigation were supplied by Hercules Powder Company in the form of powder and film. The powder was used to prepare sample rods which were irradiated in the Brookhaven reactor at 50–75°C. as described previously.[11] Pieces of these rods were subjected to NMR measurements in the as-received condition after prolonged storage in air.

Three batches of polypropylene film were received, the difference in them presumably being only the film thickness. Samples of all three were found to be 91% nonextractable in boiling n-heptane (98–99°C.). Density determinations were carried out at 25°C. on specimens 0.076 mm. in thickness 135 days and 150 days after arrival, and values of 0.879 and 0.892 g./cc., respectively, were obtained. Upon annealing such specimens at 140°C. for 3 hr. under vacuum followed by cooling in the oven, the density at 25°C. attained a value of 0.913 ± 0.001 g./cc. Samples of this film were used for the irradiations with the electron source. For irradiations in the PSU reactor, film samples of 0.15 mm. were generally used, although in a few cases film of 0.025 mm. was employed. The irradiations were carried out with quenched, as-received samples, found to have a density at 24°C. of 0.899 ± 0.001 g./cc., and samples annealed at 140°C.

having a density of 0.909 g./cc. at 24°C. Heating of such specimens at 75°C., the highest ambient temperature reached during the reactor irradiations, for 5 hr. caused no change in density.

High density polyethylene (Marlex 50) was supplied by the Phillips Petroleum Company in the form of pellets (density at 25°C. of 0.966 g./cc.).

B. Irradiation Facilities and Procedures

The electron irradiations were carried out at High Voltage Engineering Corporation with the use of a Van Der Graaff accelerator. The samples were enclosed in containers under nitrogen, the container and plate on which they rested, being kept at 25°C. during irradiation by a water cooling coil. The full dose was imparted to the samples in bursts of 2×10^7 rad, the instantaneous dose rate being 4.75×10^8 rad/sec., and the average dose rate being 3.8×10^6 rad/sec.

The details of irradiations carried out in the Brookhaven reactor have been given elsewhere.[11]

In the PSU irradiation facility, a swimming pool-type reactor, the samples were located about 15 cm. above the grid plate and 4.4 cm. from the face of the reactor core. Power levels of 100 and 200 kw. were used. At 100 kw. the irradiation conditions were as follows: thermal neutron flux 10^{12} neutrons/cm.²-sec., fast neutron flux (>0.1 m.e.v.) 3×10^{11} neutrons/cm.²-sec., γ-ray dose rate 1.3×10^3 rad/sec., and rate of energy deposition 2.3×10^3 rad/sec. At 200 kw. the fluxes and dose rates are double those at 100 kw. The total dose rate is based on the value measured for polyethylene by Jacobs and Kline[13] at the position employed. The energy deposited per unit mass in polypropylene was assumed to be identical to that for polyethylene, the total dose assigned to the irradiated samples being calculated on the basis of this assumption.

The irradiation temperature was measured with a copper–constantan thermocouple which was mounted between two of the irradiation containers. For the samples irradiated at 100 kw., the temperature increased from about 25°C., the temperature before irradiation, to 30°C. after approximately 20 min.; however, the temperature never exceeded about 47°C., even for the longest irradiation times at this power level. When the power level of the reactor was at 200 kw., the temperature of the irradiation containers increased to approximately 64°C., within 30 min., after which the temperature increased to a maximum of 75°C. after 3 hr. and remained at this value during the remainder of the irradiation period.

The irradiation containers were aluminum cylinders about 1.5 cm. long and 3.1 cm. in diameter. An attempt was made to seal the samples in these containers from the atmosphere. This was accomplished by first pumping on the containers, including the samples, in a vacuum desiccator at about 10^{-4} mm. of mercury for about 2 hr. Nitrogen gas was then allowed to fill the desiccator, and the containers were sealed by threaded lids which seated on a lead gasket. Quenched and annealed samples irradiated to the

same dose at 200 kw. were exposed simultaneously in the same container at the same time.

After irradiation, the samples were stored in the reactor pool for a period of at least one week to allow the induced radioactivity in the aluminum containers to decay to a level which was safe for handling. The samples were then unloaded from the irradiation containers and stored in a vacuum desiccator until subjected to analysis.

C. Analytical Procedures

Gel contents were determined by solvent extraction with boiling (111°C.) toluene for the polyethylene and polypropylene samples irradiated in the PSU reactor and xylene (at 120-135°C.) for the samples irradiated with the electron source. The apparatus consisted of an Alundum–RA98 coarse extraction thimble suspended in a large volume of liquid. For the samples irradiated in the PSU reactor the thimbles were removed from the solvent after 6–12 hr. of extraction, dried for approximately 1 hr. in a vacuum oven at 100°C. and then weighed, after which the extraction was repeated, the solvent being changed periodically throughout the extraction process. The length of time required for complete extraction varied but was never less than 50 hr. for any sample. Extraction was assumed to be complete when the content of extracted polypropylene varied no more than ±0.2% in three consecutive extraction–weighing determinations. For the samples irradiated with the electron source, extraction was carried out for a period of approximately 8 hr.

The infrared absorption spectrum between 2 and 15 μ was measured at room temperature for the film samples with a Perkin-Elmer Model 21 spectrometer using a sodium chloride prism. The spectrometer was calibrated by employing frequencies of absorption bands from polystyrene in the region of interest, the accuracy of the bands used, as reported by Plyler[14] and co-workers, being within ±0.3 cm.$^{-1}$.

The NMR measurements were made with the use of equipment and procedures described previously.[15,16]

Densities were measured by a displacement technique with ethanol as the liquid.

RESULTS AND DISCUSSION

A. Solvent Extraction Studies

1. Polyethylene. In Figure 1 plots of the gel content versus irradiation time in the PSU reactor are given for polyethylene irradiated at 100 kw. at ambient temperatures (30–50°C.) and at 150°C. At all doses used irradiation in the molten state at 150°C. led to a greater amount of gel formation than for the corresponding irradiation at 30–50°C., temperatures well below the melting point. The greatest difference occurs at an irradiation time of 2000 sec., a twelvefold difference being found.

These results are in agreement with those given by Lawton, Balwit, and Powell[1] for electron-irradiated polyethylene.

2. Polypropylene. The variation of gel content with irradiation time in the PSU reactor is shown for annealed (density = 0.909 g./cc. at 24°C.) and quenched (density = 0.899 g./cc. at 24°C.) samples of polypropylene
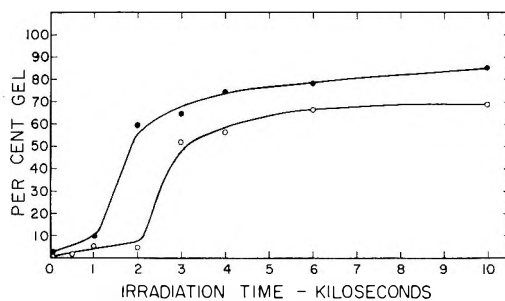
Fig. 1. Effect of irradiation in PSU reactor at 100 kw. on gel content for polyethylene (Marlex 50): (O) at 30–50°C.; (●) at 150°C.
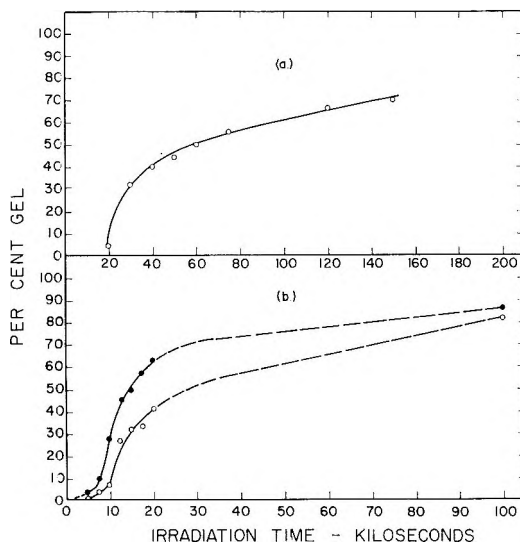
Fig. 2. Effect of irradiation in PSU reactor on gel content in (●) quenched and (O) annealed polypropylene film at power levels of: (a) 100 kw.; (b) 200 kw.

in Figure 2. Comparison of Figures 2a and 2b shows that power level (or dose rate) has little if any effect on the gel content versus irradiation time plot for annealed polypropylene. As is readily apparent in Figure 2b, however, at any given irradiation dose used the gel content for the quenched material is greater than that for the annealed polymer film. The ratio of the two is greatest at an irradiation time of 10,000 sec., where it is a four-

fold one, whereas at the highest dosage used (10^5 sec.), the gel contents are nearly the same.

When irradiations were carried out with the electron source at $25°C.$, quenched samples also yielded higher gel contents than those obtained for annealed samples. The samples irradiated in the quenched state (density ≤ 0.879 g./cc. at $25°C.$) were found to have the following gel contents: 3% for 2×10^7 rad, 53% for 10^8 rad, and 72% for 2×10^8 rad. A quenched sample irradiated to a dose of 5×10^8 rad at a later time had a gel content of only 65%. For the annealed samples (density $= 0.913$ g./cc. at $25°C.$), the gel contents corresponding to electron doses of 5×10^7, 2×10^8, and 5×10^8 rad were 4, 32, and 52%, respectively. It should be noted that these results are qualitatively consistent with those obtained for the reactor-irradiated series; however, since the characteristics of the samples irradiated by the two methods were different, direct comparisons cannot be made.

Miller[12] has reported on the physical properties of partially isotactic polypropylene quenched from the melt and held at room temperature. X-ray analysis, density measurements, and NMR spectra indicated that the quenched material (density $= 0.874$ g./cc.) was in a state of lower order than that for annealed samples of the same polymer (density $= 0.895$ g./cc.). It would be expected that at temperatures above the glass transition temperature the polymer chains in the less ordered regions would be more mobile than those in the crystalline parts. As a consequence of this, macroradicals present in the former regions would possess a higher mobility and therefore the probability of macroradical coupling to form crosslinks would be greater. Upon irradiation of samples which differ initially in long-range order, an increase in gel content with decreasing order would be expected, as found experimentally. There is ample evidence available[17] to show that, as irradiation of a high polymer proceeds, crystallinity is progressively destroyed, and therefore the restrictions to radical mobility imposed by these regions decrease. This would mean that at sufficiently high doses the gel contents for samples having difference physical states at the outset will tend to approach the same value, as observed in this study.

The production of free macroradicals is not expected to be affected by the physical state of the material except due to changes in concentration of available sites for radical formation due to density changes. However, the macroradicals "trapped" in the regions of higher order are less able to undergo coupling and may exist for extended periods of time. Upon heating the material to temperatures near the melting point or by exposure of the sample to small reactive molecules capable of diffusing into the crystal, decay of the radical concentration will occur. That free macroradicals can be stored in irradiated polypropylene at room temperature has been shown by electron paramagnetic resonance[9] and solvent extraction techniques.[7] As is discussed below, the infrared absorption results presented here are in agreement with this interpretation.

B. Infrared Absorption Studies

1. The 770–1050 cm.$^{-1}$ Frequency Regions. In Figure 3 infrared absorption spectra in the 770 to 1050 cm.$^{-1}$ range are shown for: (a) quenched (b) annealed, and (c) quenched and irradiated (100 ksec. in PSU reactor at 200 kw.) film samples (0.025 mm. thick) of partially isotactic polypropylene. It is observed that the bands centered at 997, 841, and 809 cm.$^{-1}$ are sensitive to changes in sample density [compare (a) and (b)] and to irradiation [compare (a) and (c)], while the band centered at 973 cm.$^{-1}$ is unaltered. That the band centered at 973 cm.$^{-1}$ is nearly independent of a density change has been noted previously.[18,19] Also, Quynn and coworkers[18] have shown that absorbance ratios for the 997, 841, and 809 cm.$^{-1}$ bands, taking the 973 cm.$^{-1}$ band as a standard, are linear functions of the sample density. Absorbance ratios have been calculated by the procedure of Quynn et al.[18] for various irradiated quenched and annealed film samples (0.15 mm. thick), and these are given in Figure 4. It is noted that at all three frequencies in question above a dose of about 10 ksec. the absorbance ratio is reduced at a given dose by roughly the same amount in both the annealed and unannealed samples. Assuming that the decrease in absorbance ratio is due entirely to changes in sample density, the data suggest that a reduction in long-range order is occurring which, following a
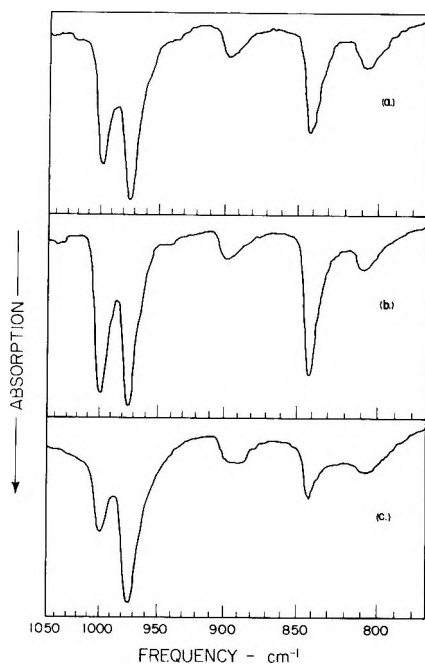
Fig. 3. Absorption spectra in the 1050–780 cm.$^{-1}$ region for (a) quenched, (b) annealed, and (c) irradiated (100 ksec. at 200 kw. in PSU reactor) quenched polypropylene film.
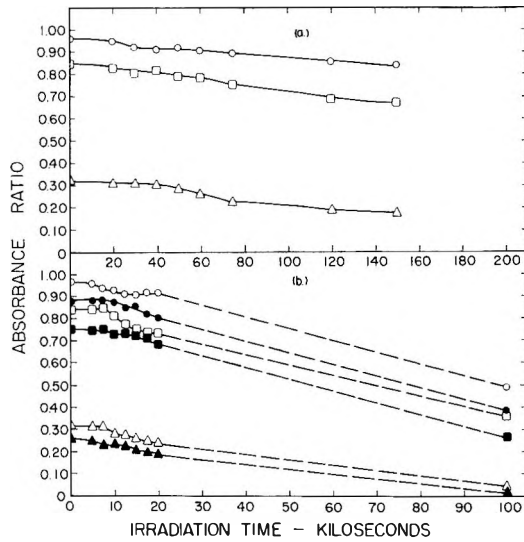
Fig. 4. Ratio of absorbance at $(0, \bullet)$ 997 cm.$^{-1}$, $(\square, \blacksquare)$ 841 cm.$^{-1}$, and $(\triangle, \blacktriangle)$ 809 cm.$^{-1}$ to absorbance at 973 cm.$^{-1}$ in $(\bullet, \blacksquare, \blacktriangle)$ quenched and $(O, \square, \triangle)$ annealed irradiated polypropylene at PSU reactor power levels of (a) 100 kw. and (b) 200 kw.
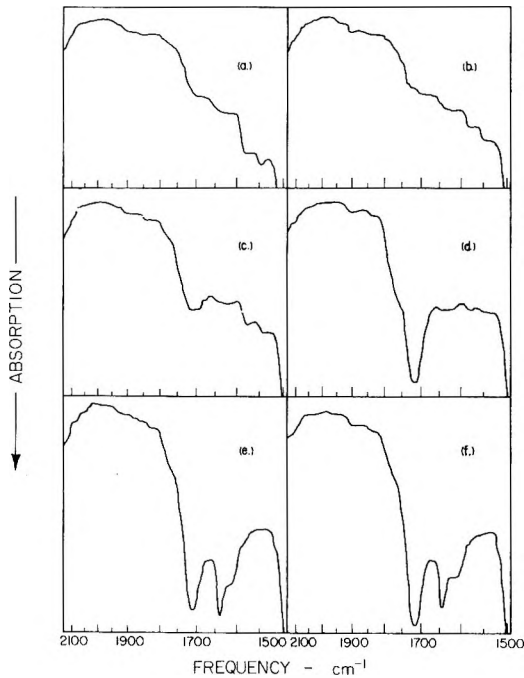
Fig. 5. Effect of irradiation in PSU reactor (200 kw.) on absorption spectra in the 2100–1500 cm.$^{-1}$ region for (a, c, e) quenched and (b, d, f) annealed polypropylene receiving dose of (a, b) 0 nvt; (c, d) 0.15 × 10^{17} nvt; (e, f) 2 × 10^{17} nvt.

certain minimum dose, is proportional to the irradiation dose and is independent of the initial state of order.

Whether or not a dose rate effect exists cannot be established from the limited data available. The decrease in absorbance ratio at 841 and 809 cm.$^{-1}$ for the samples given at 20,000 sec. dose at 200 kw. is somewhat greater than that for the samples given a 40,000 sec. dose at 100 kw. However, no such difference appears for the 997 cm.$^{-1}$ band.

2. The 1500–4000 cm.$^{-1}$ Frequency Region. In Figure 5 infrared spectra in the 1500–2100 cm.$^{-1}$ region are given for six polypropylene specimens (0.15 mm. thick). Irradiation is seen to lead to an increase in absorbance for two bands centered at 1640 and 1715 cm.$^{-1}$ which are not distinct in the unirradiated material. The 1715 cm.$^{-1}$ band is found to be much more pronounced in the annealed specimen for a comparatively low irradiation dose than for the quenched sample receiving an identical dose. An absorption band centered at 3380 cm.$^{-1}$ also becomes apparent in irradiated films. The increase in absorbance over that for the unirradiated controls at 1640, 1715, and 3380 cm.$^{-1}$ for 16 irradiated specimens are recorded in Table I. Examination of the raw data reveals little consistency in the absorbance as a function of total dose. However, upon taking the ratio of the absorbance for the quenched to that for the annealed sample at each dose and frequency of interest, one finds a more consistent and interpretable behavior with first a decrease and then an increase in this

TABLE I

Absorbance for Quenched and Annealed Polypropylene Film ($\sim$0.15 mm. Thick) Irradiated in PSU Reactor at 200 Kilowatts

Sample No.[a]	Irradiation time, ksec.	Absorbance[b] and ratio					
		1640 cm.$^{-1}$	Ratio	1715 cm.$^{-1}$	Ratio	3380 cm.$^{-1}$	Ratio
1	5.0	0.053	0.67	0.280	0.59	0.150	0.48
1*		0.079		0.471		0.316	
2	7.5	0.025	0.61	0.045	0.30	0.003	0.08
2*		0.041		0.150		0.098	
3	10.0	0.041	0.73	0.089	0.48	0.018	0.20
3*		0.056		0.185		0.091	
4	12.5	0.040	0.93	0.042	0.58	0.005	0.31
4*		0.043		0.073		0.016	
5	15.0	0.066	0.82	0.206	0.63	0.949	0.39
5*		0.081		0.326		0.125	
6	17.5	0.061	0.77	0.143	0.53	0.026	0.28
6*		0.075		0.269		0.092	
7	20.0	0.053	0.88	0.062	0.58	0.007	0.41
7*		0.060		0.106		0.017	
8	100	0.171	1.16	0.156	0.97	0.013	1.08
8*		0.147		0.161		0.012	

[a] The starred numbers (*) designate the samples annealed prior to irradiation.

[b] Net absorbance greater than that exhibited by the unirradiated sample at the frequency given.

ratio with increasing dose.   This trend is present for all three bands, but is more marked for the 1715 and 3380 cm.$^{-1}$ bands.   It can be seen that the ratios at the highest doses (100 ksec.) are of the order of 1.

Exact assignments for bands centered at these frequencies have not been made previously for polypropylene, although Black and Lyons[4] attributed bands at 1642 and 1710 cm.$^{-1}$ to carbon-carbon double bond stretching and carbonyl stretching, respectively.   Bands found at these frequencies in polyethylene have been identified as indicative of carbon-carbon double bonds (1640 cm.$^{-1}$), ketonic carbonyl groups (1715–1720 cm.$^{-1}$), and hydroxyl groups (3380–3388 cm.$^{-1}$).[20]   Although attempts were made in the present study to exclude air from the samples before, after, and during irradiation, the procedures adopted were not expected to exclude all traces of oxygen, and therefore the appearance of some oxidation products was expected.   The irregularities in the absorbances with increasing dose given in Table I are attributed to the nonuniformity of oxidation conditions in going from one container to another.   Since the quenched and annealed samples receiving any specific dose were irradiated together in the same container, equal opportunity existed for reaction with available oxygen. The time lapse between irradiation and infrared analysis for all but samples 8 and 8* was nine months.   Samples 8 and 8* were analyzed after two months' storage and then again after five months' storage, and the spectra were found to be the same in each case.

A greater concentration of oxidation products in the annealed than in the quenched specimens is in keeping with the explanations given in the preceding section accounting for the gel fraction results.   The lower reactivity of the macroradicals towards coupling reactions, due to a lower chain mobility in the more ordered regions of the polymer, results in a greater number of radicals being present in the annealed samples.   These in turn then react with the oxygen which is available and which diffuses into these regions. At high irradiation dosages most of the crystalline order has been destroyed, and therefore samples with different amounts of initial long-range order will compete more or less equally for the available oxygen after long exposure.

If the assignment for the 1640 cm.$^{-1}$ band as due to carbon-carbon double bonds is the correct one, then it would appear from the present data that formation of such bonds may be a function of both the amount of oxidation taking place and the physical state of the material.   Black and Lyons[4] have reported that the total number of carbon-carbon bonds as well as that of vinylidene double bonds in polypropylene increases with increasing dose.

C. Nuclear Magnetic Resonance

NMR spectra were obtained at temperatures of 90–330°K. for four polypropylene specimens irradiated in the Brookhaven (BNL) reactor. The results in terms of the peak-to-peak width of the derivative of the absorption, herein called line width, are shown in Figure 6.   Second
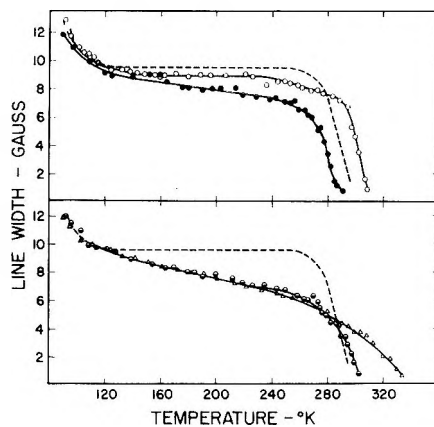
Fig. 6. Effect of irradiation in BNL reactor on NMR line width for partially isotactic polypropylene (- -) unirradiated; (O) 1.1×10^{18} nvt; (●) 3.2×10^{18} nvt; (◒) 5.7×10^{18} nvt; (△) 14×10^{18} nvt.
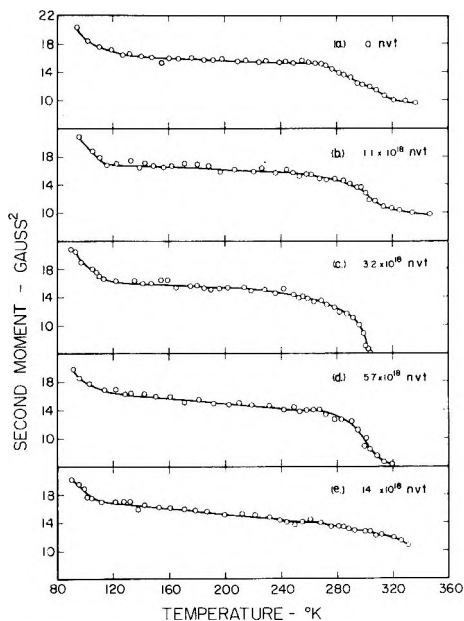
Fig. 7. Effect of irradiation in BNL reactor on NMR second moment for partially isotactic polypropylene.

moment values, calculated from the derivative shapes, are given in Figure 7.

It was not possible to decompose the derivative line shapes into two components above the glass transition (255°K. for unirradiated material[21]), although in the spectra for the unirradiated specimen considerable tail portions were evident. With reference to Figures 6 and 7, the irradiation is

seen to have little effect on the line narrowing process occurring at low temperatures, previously attributed to the onset of methyl group rotation.[22,23]

However, the line narrowing found at $\geq 280°$K., due to the onset of reorientational motions accompanying the glass transition,[22,23] is markedly altered by the irradiation. Interpreting these changes in terms of two competing effects, that is, the formation of intermolecular crosslinks and the destruction of crystallinity, indicates that at the lowest dose the second effect is small and the first effect, which adds additional restraints to the chains in amorphous regions, causes a shifting of the line narrowing process to higher temperatures. The fact that the second moment levels off at about the same value at temperatures above the glass transition for both the 0 and 1.1×10^{18} nvt samples is evidence that little destruction in long range order has been facilitated by that dose. On the other hand, the density at 25°C. of the 1.1×10^{18} nvt sample is lower than that for the unirradiated one,[11] indicating some loss of crystallinity. However, in dynamic mechanical measurements carried out on a sample given a dose of 5.4×10^{17} nvt in the same hole in the Brookhaven reactor, a shift of the mechanical loss peak associated with the glass transition to higher temperatures was found.[11]

For the sample irradiated to 3.2×10^{18} nvt, the second effect, viz., destruction of crystallinity, is now the most significant factor, and the NMR line narrowing process is found to occur at temperatures below that for the unirradiated sample. A lower crystallinity for this sample than for the preceding one is also indicated by the greater decrease in second moment (by ≥ 2 gauss^2) occurring in this temperature region. At still higher doses, an increase of crosslinking[11] is the predominant effect, and this causes a shift to higher temperatures with increasing dose of both the NMR line width and second moment values in agreement with the observed increases found in the density.[11] Dynamic mechanical studies carried out on samples given doses of 3.2×10^{18}, 5.7×10^{18}, and 14×10^{18} nvt, but heated to temperatures of 450–480°K. before testing show similar shifts in the position of the principal loss maximum and associated modulus dispersion.[11]

Two specimens (8 and 8*) irradiated in the PSU reactor were also examined by the NMR method in the temperature range of 240–300°K. The line narrowing process was found to occur at temperatures about 10–15°K. lower than that for the unirradiated annealed one. This behavior would imply, on the basis of the results discussed above, that the film samples had lost most of their crystalline content.

References

1. Lawton, E. J., J. S. Balwit, and R. S. Powell, *J. Polymer Sci.*, **32**, 257 (1958).
2. Lawton, E. J., R. S. Powell, and J. S. Balwit, *J. Polymer Sci.*, **32**, 277 (1958).
3. Lawton, E. J., J. S. Balwit, and R. S. Powell, *J. Chem. Phys.*, **33**, 395 (1960).
4. Black, R. M., and B. J. Lyons, *Proc. Roy. Soc. (London)*, **A253**, 322 (1959).
5. Waddington, F. B., *J. Polymer Sci.*, **31**, 221 (1958).
6. Dole, M., T. J. Stolki, and T. F. Williams, *J. Polymer Sci.*, **48**, 61 (1961).
7. Sobue, H., and Y. Tazima, *Nature*, **188**, 315 (1960).
8. Libby, D., M. G. Ormerod, and A. Charlesby, *Polymer*, **1**, 212 (1960).
9. Ohnishi, S., Y. Ikeda, M. Kashiwagi, and I. Nitta, *Polymer*, **2**, 119 (1961).
10. Fischer, H., and K. H. Hellwege, *J. Polymer Sci.*, **56**, 33 (1962).
11. Sauer, J. A., L. J. Merrill, and A. E. Woodward, *J. Polymer Sci.*, **58**, 19 (1962).
12. Miller, R. L., *Polymer*, **1**, 135 (1960).
13. Jacobs, A., and D. E. Kline, *J. Polymer Sci.*, **6**, 605 (1962).
14. Plyler, E. K., A. Danti, L. R. Blaine, and E. D. Tidwell, *J. Res. Natl. Bur. Std.*, **64A**, 29 (1960).
15. Odajima, A., A. E. Woodward, and J. A. Sauer, *J. Polymer Sci.*, **55**, 181 (1961).
16. Odajima, A., J. A. Sauer, and A. E. Woodward, *J. Polymer Sci.*, **57**, 107 (1962).
17. Charlesby, A., *Atomic Radiation and Polymers*, Pergamon, London, 1960.
18. Quynn, R. G., J. L. Riley, D. A. Young, and H. D. Noether, *J. Appl. Polymer Sci.*, **2**, 166 (1959).
19. Luongo, J. P., *J. Appl. Polymer Sci.*, **3**, 302 (1960).
20. Luongo, J. P., *J. Polymer Sci.*, **42**, 139 (1960).
21. Reding, F. P., *J. Polymer Sci.*, **21**, 547 (1956).
22. Slichter, W. P., and E. R. Mandell, *J. Appl. Phys.*, **29**, 1438 (1958).
23. Woodward, A. E., A. Odajima, and J. A. Sauer, *J. Phys. Chem.*, **65**, 1384 (1961).

Résumé

On a examiné par extraction dans différents solvants et par les techniques infrarouges des échantillons de films de polypropylène isotactique (profax) irradiés à température ambiante dans le réacteur de l'université d'état de Pensylvanie (PSU). Pour des doses faibles d'irradiation, les échantillons précuits (densité = 0.909 g/cc à 24 °C) avant irradiation ont un contenu en gel plus faible et une concentration en produits d'oxydation plus élevée que les échantillons brusquement refroidis (densité = 0.899 g/cc à 24 °C) irradiés dans les mêmes conditions. On obtient des contenus en gel similaires dans les échantillons de polypropylène irradiés par des électrons. Ces effets sont probablement dús à l'accumulation plus grande de macroradicaux dans les échantillons à densité plus grande. Pour des doses plus élevées en irradiations, les effets dans les films recuits et refroidis semblent être à peu près semblables. On a trouvé que le taux de gélification en fonction de la dose était indépendant du niveau d'intensité de l'irradiation dans un double domaine. On a aussi entrepris d'irradier du polyéthylène haute densité (Marlex 50) en pastilles à deux températures, à savoir 40 ± 10 °C et 150 °C. Pour n'importe quelle dose d'irradiation à 150 °C on obtient un taux de gélification plus élevé, ce qui est en accord avec les résultats de Lawton, Balwitt et Powell pour des spécimens irradiés par électrons. On a obtenu des spectres de résonance magnétique nucléaire pour des échantillons fondus recuits de polypropylène partiellement isotactique, irradiés dans le réacteur de Brookhaven à des températures allant de 90° à 330°K. Les glissements observés dans le processus de rétrécissement des lignes observé dans la région 270-330°K, sont expliqués en termes de diminution de la cristallinité et de l'augmentation de la densité du pontage qui accompagnent l'irradiation.

Zusammenfassung

Folien aus isotaktischem Polypropylen (Profax) wurden im Reaktor der Pennsylvania State University (PSU) bei Raumtemperatur bestrahlt und durch Lösungsmittelextraktion und Infrarotabsorption untersucht. Bei niedriger Bestrahlungsdosis zeigten vor der Bestrahlung getemperte Proben (Dichte = 0,909 g/cc bei 24°C) einen niedrigeren Gelgehalt und eine höhere Konzentration an Oxydationsprodukten als abgeschreckte Proben (Dichte = 0,899 g/cc bei 24°C) unter identischen Bedingungen. Ähnliche Ergebnisse bezüglich der Gelfraktion wurden an elektronenbestrahlten Polypropylenproben erhalten. Es wird angenommen, dass diese Effekte durch die Ausbildung einer grösseren Konzentration an freien Makroradikalen in den Proben mit höherer Dichte hervorgerufen werden. Bei höherer Reaktordosis scheinen die Bestrahlungseffekte in getemperten und abgeschreckten Folien etwa die gleichen zu sein. Der Gelgehalt erwies sich als Funktion der Dosis über einen zweifachen Bereich als unabhängig von der Bestrahlungsintensität. Bestrahlungen im PSU-Reaktor wurden auch an Pellets von Polyäthylen hoher Dichte (Marlex 50) bei zwei Temperaturen, nämlich 40 ± 10°C und 150°C ausgeführt. Bestrahlung bei 150°C führte bei allen Dosen zu einem grösseren Gelgehalt, was mit dem von Lawton, Balwit und Powell für elektronenbestrahlte Proben berichteten Ergebnis übereinstimmt. Kernmagnetische Resonanzspektren wurden an getemperten, im Brookhaven-Reaktor bei Temperaturen zwischen 90 und 330°K bestrahlten Pressmussen aus partiell isotaktischem Polypropylen erhalten. Die beobachtete Verschiebung der Linienverengung, die im Bereich von 270–300°K auftritt, wird durch die Abnahme der Kristallinität und die Zunahme der Vernetzungsdichte bei der Bestrahlung erklärt.

Tracer Techniques for the Determination of Monomer Reactivity Ratios.   IV.   Monomer Reactivity Ratios for Styrene–Isoprene Copolymerization

RICHARD H. WILEY and BURNS DAVIS, *Department of Chemistry, College of Arts and Sciences, University of Louisville, Louisville, Kentucky*

Synopsis

The ionization chamber-vibrating reed electrometer assay technique has been improved in precision ($\pm 0.25\%$ average deviation) and used to determine monomer reactivity ratios for the styrene–isoprene copolymerization.   Values of r_1 (styrene) = 0.50 (100°) and 0.54 (80°) and $r_2 = 1.92$ (100°, 80°) have been obtained for the radical initiated copolymerization.   For γ-irradiation initiation at 22°, $r_1 = 0.66$ and $r_2 = 1.88$.   For butyllithium initiation, $r_1 = 0.03$ and $r_2 = 5.9$.   The difference in the radical and γ-radiation initiation values is considered in terms of possible partial ionic character of the radiation initiation process and possible temperature dependence of the reactivity ratios (r_1) over the 22–100°C. range.   The latter indicates a difference in activation energy of 0.8 kcal./mole for the radical to styrene and radical to isoprene propagation steps.

Several values for the monomer reactivity ratios of the styrene–isoprene copolymerization have been reported.   These include values of r_1 (styrene) = 1.38 ± 0.54 and $r_2 = 2.05 \pm 0.45$, at 50°C. with benzoyl peroxide initiator;[1] $r_1 = 0.44$, $r_2 = 1.98$ for emulsion copolymerization;[2] $r_1 = 0.42$, $r_2 = 2.02$ for bulk copolymerization;[2] and $r_1 = 0.48 \pm 0.01$, $r_2 = 1.30 \pm 0.02$ at -18°C. for emulsion copolymerization.[3,4]

We have determined the reactivity ratios for this pair at 80 and 100°C. With benzoyl peroxide initiator, at 30°C. with *n*-butyllithium initiator, and at 22°C. with γ-radiation initiation.   The peroxide-initiated copolymer produced at 80° has been fractionated by a previously described method[5] to establish the constancy of composition at various molecular weights. The copolymer composition was determined by radioactive assay of its C^{14}-labeled styrene content by means of the ionization chamber-vibrating reed electrometer assay technique[6] which has been previously used by us.[7]

Experimental

Monomers

Styrene-β-C^{14}, supplied (Tracerlab, Inc.) with a specific activity of 0.13 mc./mmole, was diluted, with 150 vol. (0.445:67 ml.) of freshly distilled styrene (Distillation Products Industries), n_D^{20} 1.5463, to a specific activity

of approximately 8.50×10^{-4} mc./mmole, and stored at $-8.0°C$. with di-(*tert*-butyl)-*p*-cresol stabilizer until used in the peroxide-initiated copolymerizations and butyllithium-initiated copolymerizations and in the preparation of the copolymer for the fractionation experiment. For the radiation-initiated copolymerizations, styrene-β-C^{14} (Tracerlab, Inc.) with a specific activity of 0.24 mc./mmole was diluted with 270 vol. (0.241:65 ml.) of freshly distilled styrene, n_D^{20} 1.5468, to a specific activity of approximately 8.80×10^{-4} mc./mmole and stored at $-8.0°C$. with di(*tert*-butyl)-*p*-cresol stabilizer. Isoprene (Distillation Products Industries) was obtained commercially and stored at 2.7°C. until used. A sample distilled by the technique used in copolymerization studies gave n_D^{20} 1.4217.

Polymerization Procedures

The monomers for polymerization with the use of free-radical initiator were distilled under vacuum at room temperature from stock solution into the polymerization cells just prior to use. The reaction cells were weighed before and after the addition of each monomer under a nitrogen atmosphere. After the addition of solid benzoyl peroxide (0.2% by weight of monomers) the cells were degassed and sealed under vacuum. Polymerization to 3.5–9.8% conversion was accomplished by immersing the cells in a constant-temperature oil bath for a length of time estimated from control runs to give the desired conversion. At 80°C. this required 3.5 hrs. for high styrene content to 7.5 hrs. for low styrene content. At 100°C. the time varied from 0.5 hr. to 2.5 hrs. Data for these copolymers are given in Tables I and II.

TABLE I

Peroxide-Initiated Copolymerization of Styrene (M_1) with Isoprene (M_2) at 80°C.; Ionization Chamber Assay

Monomer mole ratio	Conversion, %	Specific charge rate, mv./sec./mg.[a]	Molar ratio[b]
0.8702	4.9	1.3116	
		1.3098	2.1732
0.7778	5.1	1.2422	
		1.2369	
		1.2279	2.3976
0.2316	4.1	0.4994	
		0.5013	8.1666
0.2499	4.6	0.5231	
		0.5258	7.7208
3.3548	5.6	2.3113	
		2.3215	0.5658
4.0680	9.3	2.4400	
		2.4333	0.4621

[a] Based on an average of 3–9 readings for 4–15-mg. samples at charge times of 150–700 sec. at a charge of 240 to 8000 mv. The specific charge is the (charge/charge time-background)/weight. Background was determined daily and was about 0.0885 mv./sec. Control on labeled polystyrene, 3.1734 ± 0.004 mv./sec./mg.

[b] Copolymer composition average of the two determinations.

TABLE II

Peroxide-Initiated Copolymerization of Styrene (M_1) with Isoprene (M_2) at 100°C.; Ionization Chamber Assay[a]

Monomer mole ratio	Conversion, %	Specific charge rate, mv./sec./mg.[a]	Molar ratio[b]
0.8760	9.8	1.3008	
		1.2923	2.2125
0.8701	9.3	1.2939	
		1.2937	2.2223
0.2383	6.1	0.5040	
		0.5073	8.0639
0.2262	6.9	0.4806	
		0.4791	8.5840
1.2455	3.5	1.5650	
		1.5520	1.5843
2.0931	4.8	1.9597	
		1.9532	0.9512

[a] Footnotes: see Table I.

The monomers used in the n-butyllithium-initiated copolymers were dried over calcium hydride prior to use and vacuum distilled at room temperature into the reaction cells. n-Butyllithium (Foote Mineral Company) was obtained in a pentane and heptane solution (15.5% n-butyllithium by weight). A syringe was used to add the initiator (0.25–0.50 mole-% of monomer) to the reaction cell. The cell was blanketed with nitrogen during this process and then frozen, degassed, and sealed under vacuum. Polymerization at 30°C. required 14–38 min. to give conversions of 2.6–9.3%. Data for the copolymers are given in Table III.

TABLE III

Butyllithium-Initiated Copolymerization of Styrene (M_1) with Isoprene (M_2) at 30°C.; Ionization Chamber Assay[a]

Monomer mole ratio	Conversion, %	Specific charge rate, mv./sec./mg.[a]	Molar ratio[b]
0.2530	2.6	0.1807	
		0.1808	25.2956
0.8430	9.3	0.5441	
		0.5427	7.4021
0.8059	4.3	0.4892	
		0.4866	8.4190
3.4672	5.5	1.2459	
		1.2523	2.3557
2.5164	2.6	1.0217	
		1.0179	3.2283
0.1918	8.3	0.1523	
		0.1542	30.1273
0.1365	5.8	0.1042	
		0.1058	44.6644

[a] Footnotes: see Table I.

The copolymer was isolated by pouring the reaction mixture into methanol. The precipitated copolymer was dissolved in benzene and reprecipitated with methanol four times. This product was dissolved in benzene, frozen to the side of a centrifuge tube, evacuated under 1 mm. vacuum at room temperature to remove benzene, and dried to constant weight under 1 mm. vacuum at 60°C. (8 hrs.).

The copolymers with high isoprene content and prepared with benzoyl peroxide initiator were sticky rubbery materials. With high styrene content, they were white solids. The n-butyllithium-initiated copolymers highly viscous liquids.

For the γ-radiation-induced polymerizations, the monomers were distilled into reaction cells, degassed, and sealed under vacuum. The cells were irradiated at 22°C. for 48–144 hrs. at intensities of 1.63×10^5 rep, to obtain conversions of 2.9–5.4%. A total dose varying from 7.87×10^6 rep for high styrene content to 24.42×10^6 rep for low styrene copolymers was required. The copolymers, which resembled the peroxide-initiated styrene–isoprene copolymers, were isolated, purified, and dried as described above. Data for these copolymers are given in Table IV.

TABLE IV

γ-Radiation-Initiated Copolymerization of Styrene (M_1) with Isoprene (M_2) at 22°C.; Ionization Chamber Assay

Monomer mole ratio	Conversion, %	Specific charge rate, mv./sec./mg.[a]	Molar ratio[b]
0.2564	5.3	0.8338	
		0.8319	4.7632
0.2498	4.2	0.8081	
		0.8170	4.9198
0.9578	4.1	1.7985	
		1.8004	1.3828
0.9400	5.4	1.7830	
		1.7811	1.4114
3.3739	2.9	2.6857	
		2.6992	0.4178
3.6380	3.7	2.7519	
		2.7590	0.3727

[a] Footnotes: see Table I.

Analysis

A previously described method[6] for radioactivity assay with the use of a vibrating-reed electrometer (Applied Physics Corporation Cary Model 31) and ionization chamber technique with a recorder (Honeywell Electronik Strip Chart Model 153X12) was made by the rate of charge procedure. The copolymer samples were dissolved in a minimum amount of benzene (0.5–1.0 ml.) and portions of these solutions containing 4.016–15.934 mg. of copolymer were dried to a constant weight in a porcelain boat (± 6 μg.) at 60°C. under 1 mm. vacuum. The samples were burned to carbon diox-

ide in medical oxygen containing 5% carbon dioxide with a previously described[8] micro combustion train having a combination filling and an absorption trap for removing the water. The rate of combustion was followed by a flowmeter controlled with the needle valve of a previously evacuated 500-ml. spherical or cylindrical Borkowski ionization chamber used with all copolymer analyses. Combustion required 40–50 min. for the size samples used (see Tables I, II, III, and IV). Duplicate analysis gave values which checked from ±0.008–0.8% with an average value of ±0.25%.

Copolymer Fractionation

For fractionation of copolymer, 2.7542 g. of styrene-β-C^{14} (specific activity about 8.50×10^{-4} mc./mmole) and 4.7343 g. of isoprene were copolymerized at 80°C. with solid benzoyl peroxide as initiator (0.15% by weight of monomers), and yielded 0.5386 g. of copolymer (7.2% yield) in 12 hrs. By a previously described procedure,[5] 0.4060 g. of the copolymer were fractionated, with 100% ethanol as the nonsolvent and benzene as the solvent. A volumetric fraction collector (Rinco Instrument Company) was used to collect 25 fractions (19 ml. each) at a rate of 8 ml./hr. A 34 cm. by 20 mm. glass column packed with glass beads (0.25–0.80 mm. in diameter) was used. The column, having a 45-mm. outside diameter bronze jacket was maintained at centrigrade temperatures of 57.6 ± 0.6, 33.3 ± 1.2, and 14.5 ± 1.0°C. at the top, middle, and bottom, respectively, as determined by a copper–Constantan thermocouple placed inside the bronze jacket. Adjacent samples were combined (see Table V), when necessary, to obtain enough copolymer for analysis. The solvent was removed from the copolymer by evaporation. The copolymer was purified by precipitation and viscosities were determined in benzene solu-
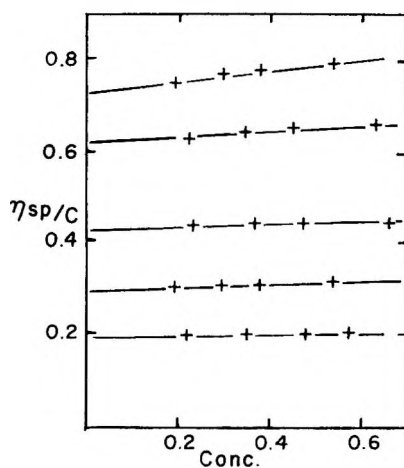

Fig. 1. Reduced viscosity ($\eta_{sp/c}$) vs. concentration (g./100 ml.) for styrene–isoprene copolymer fractions in benzene.

TABLE V
Styrene–Isoprene Copolymer Fractionation

Copolymer fraction number[a]	Wt., mg.	Limiting viscosity number	Styrene, %
4-5-6-7-8-9-	0.0405	0.20	21.75
10-11	0.0462		
12-13[b]			
14-15	0.0547	0.30	22.51
16[b]	0.0385		
17-18	0.0668	0.43	22.43
19	0.0953	0.62	22.53
20-21-22-23-	0.0378	0.73	22.63
24-25			

[a] Fractions 1–3 contained no copolymer.
[b] Not analyzed for viscosity or composition.

tion (concentrations 0.1929–0.6680 g./100 ml. benzene) at 30°C. The Ubbelohde viscometer used gave a benzene efflux time of 253.1 sec. Analysis for styrene content was made by the ionization chamber-vibrating reed electrometer technique. The results are given in Figure 1. Data for the copolymer are given in Table V.

Discussion

The data available from the present studies (summarized in Table VI) establish values of $r_1 = 0.50$ (100°C.) and 0.54 (80°C.) and $r_2 = 1.92$ (100°C.) and 1.92 (80°C.) for the radical-initiated copolymerization of styrene with isoprene. The graphical solutions of the copolymerization equation are given in Figures 2–9. The accuracy of our measurements has been improved over those reported previously, by the use of a recorder for measurement of the rate of charge and by the use of longer charge times to give an average deviation of ±0.25%. Fractionation of a typical copolymer gave fractions of viscosities varying from 0.2 to 0.73 (Fig. 1) which showed no alteration in composition (Table V) with viscosity and thus no heterogeneity of initiation mechanism or structural distribution. These values are in fair agreement with some previous reports[2-4] but not others.[1]

By means of r values obtained by the Fineman-Ross method (Figs. 3 and 5), Q and e values for isoprene are 1.97 and −0.83 at 80°C. and 2.34

TABLE VI
Monomer Reactivity Ratios for Styrene (r_1) and Isoprene (r_2)

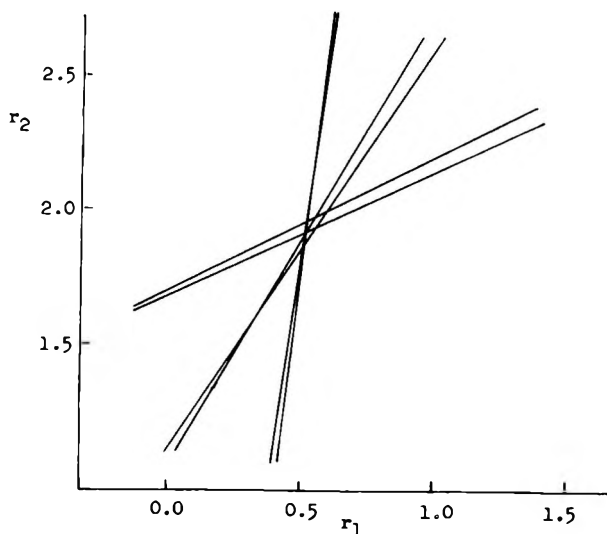|	Fineman-Ross data		Graphical data	
	r_1	r_2	r_1	r_2
Peroxide at 80°C.	0.54	1.92	0.55	1.93
Peroxide at 100°C.	0.50	1.92	0.50	1.93
Gamma radiation at 22°C.	0.66	1.18	0.66	1.19
Butyllithium at 30°C.	0.03	5.89	0.04	5.90

Fig. 2. Intersect plot for copolymerization of styrene ($r_1 = 0.55$) and isoprene ($r_2 = 1.93$), benzoyl peroxide initiator at 80°C.
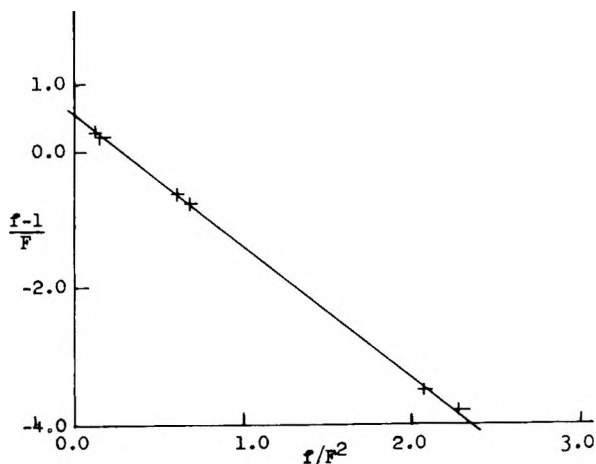

Fig. 3. Fineman-Ross Plot for copolymerization of styrene ($r_1 = 0.54$) and isoprene ($r_2 = 1.92$); benzoyl peroxide initiator at 80°C.

and -1.00 at 100°C., respectively. These values are based on a styrene Q and e values of 1.00 and -0.8. The $r_1 r_2$ product for the r values at 80°C. was taken as slightly less than one (0.999) to give a real solution. Averaging these values, $Q = 2.16$ and $e = 0.92$ for isoprene. These values differ from those reported previously[9] ($Q = 3.33$, $e = -1.22$), probably because different values were used for the previous averages.

Values of the reactivity ratios from the γ-irradiation-initiated copolymerization ($r_1 = 0.66$, $r_2 = 1.18$; see Figs. 6 and 7) are distinctly
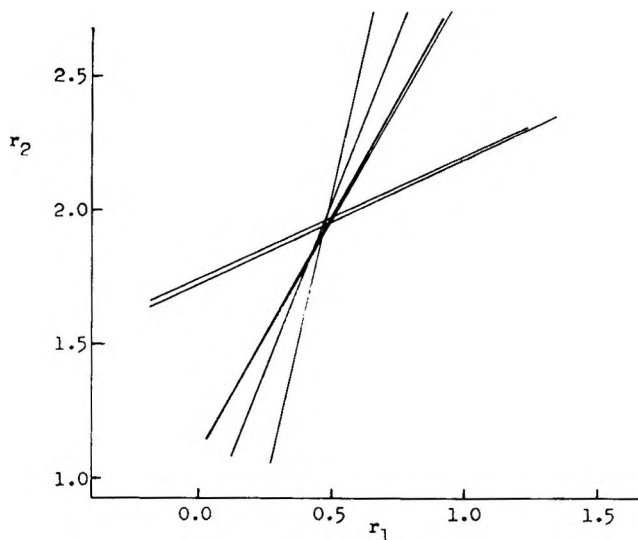
Fig. 4. Intersect plot for copolymerization of styrene ($r_1 = 0.50$) and isoprene ($r_2 = 1.93$); benzoyl peroxide initiator at 100°C.
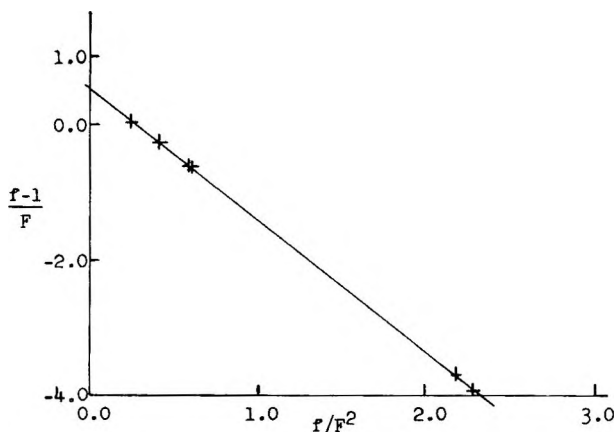

Fig. 5. Fineman-Ross plot for copolymerization of styrene ($r_1 = 0.50$) and isoprene $r_2 = 1.92$); benzoyl peroxide initiator at 100°C.

different from those for the radical-initiated copolymerization. It has been suggested previously[10] that the radiation-initiated polymerization of isoprene appears to involve both ionic and radical initiation mechanisms and this is confirmed by our observations for the copolymerizations. Both the r_1 (0.66) and r_2 (1.18) values deviate from the radical initiated values (0.5, 1.9) in the opposite direction from the values for the butyllithium-initiated copolymerization (0.03, 5.9; see Figs. 8 and 9). This indicates, but perhaps not without reservation, a cationic mechanism

Fig. 6. Intersect plot for copolymerization of styrene (r_1 = 0.66) and isoprene (r_2 = 1.19); gamma radiation initiator at 22°C.
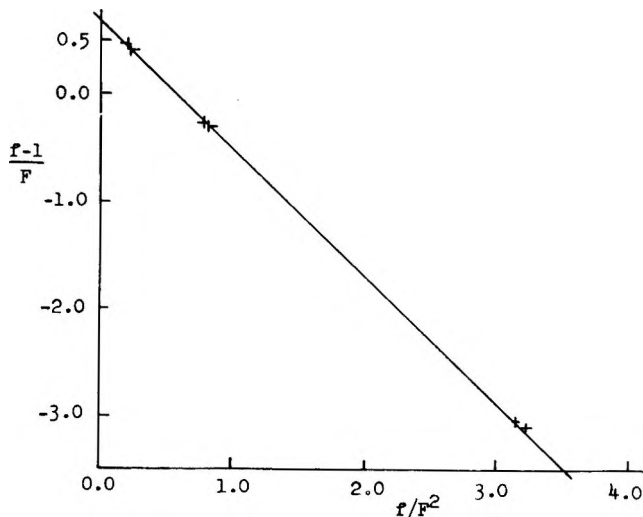
Fig. 7. Fineman-Ross plot for copolymerization of styrene (r_1 = 0.66) and isoprene (r_2 = 1.18); gamma radiation initiator at 22°C.

for the gamma initiation consistent with irradiation-induced copolymerization of styrenes[11] and homopolymerization of isoprene[10-12] which show cationic initiation characteristics. Some reservations must be made in evaluating the relative significance of these values in view of condition-dependent deviations in the reactivity ratios that others have observed in copolymerizations involving ionic initiators. The butyllithium values are
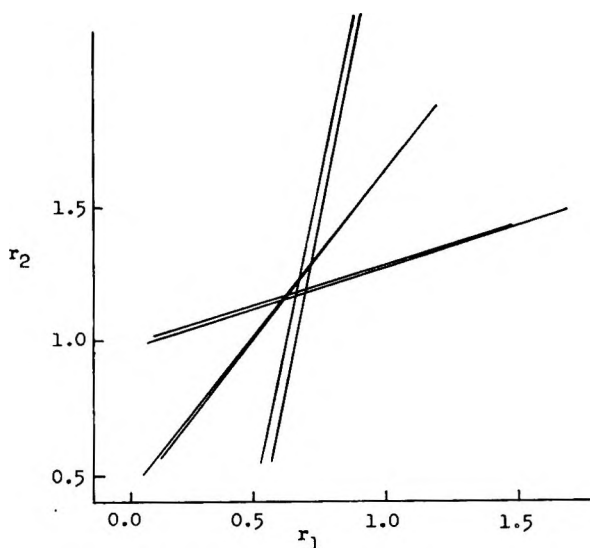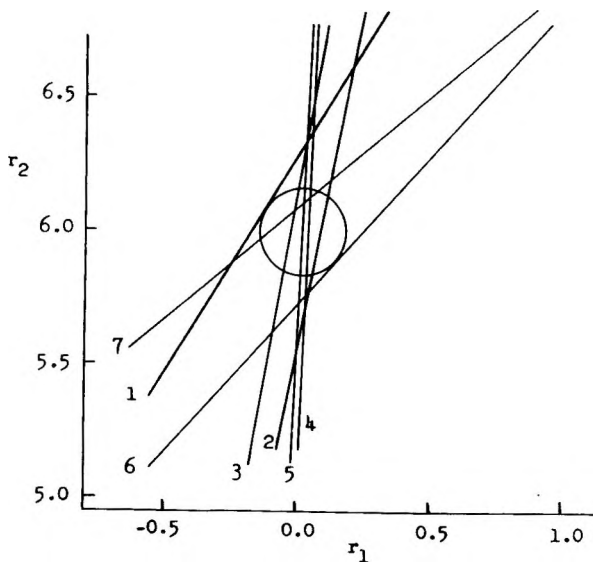
Fig. 8. Intersect plot for copolymerization of styrene ($r_1 = 0.04$) and isoprene ($r_2 = 5.90$); n-butyllithium initiator at 30°C.
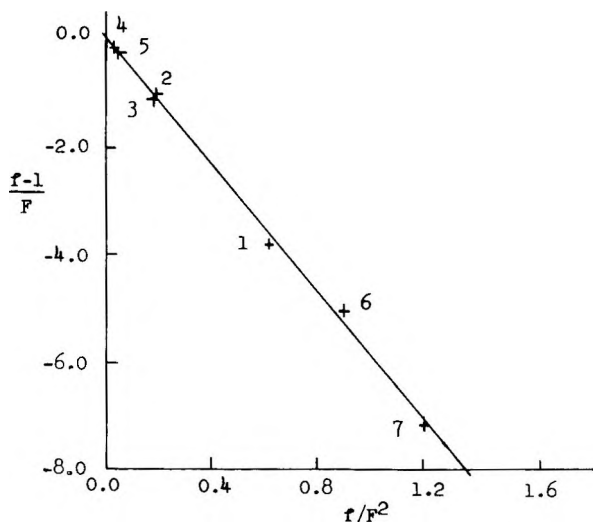
Fig. 9. Fineman-Ross plot for copolymerization of styrene ($r_1 = 0.03$) and isoprene ($r_2 = 5.89$), n-butyllithium initiator at 30°C.

more like those reported[13] ($r_1 = 0.12$, $r_2 = 6.4$) for the styrene–methyl methacrylate copolymerization than those reported ($r_1 = 2.5$, $r_2 = 0.26$) for the styrene-p-methylstyrene pair.[14,15] Our values agree well with those ($r_1 = 0.12$, $r_2 = 8.0$) reported recently[16] for the anionic copolymerization.

It has been pointed out to the authors by Dr. J. E. Guillet that the differences in reactivity ratios for the peroxide and radiation initiated copoly-

merizations may be accounted for by temperature effects. The slope of an Arrhenius plot of the r_1 values at $22°$, $80°$, and $100°$ corresponds to an activation energy of 0.8 kcal./mole. The values for r_2 do not give a linear Arrhenius plot but are of opposite sign and may be about 1.3 kcal./mole This magnitude of difference in activation energy for the rate constants for the addition of the radical to styrene and of radical to isoprene seems reasonable in relation to the propagation rate constants (7.8; 9.8 kcal./mole) for these monomers in homopolymerizations. Apparently, the refined technique for determining reactivity ratios gives values of sufficient precision to detect the temperature dependence of reactivity ratios and the styrene-isoprene copolymerization shows a detectable difference in the ratios of rates. Further studies over wider temperature ranges and with other monomer pairs are in progress.

References

1. Henery-Logan, K. R., and R. V. V. Nicholls, quoted by R. Simha, and L. A. Wall, *J. Res. Natl. Bur. Std.*, **41**, 521 (1948).

2. Zverev, M. P., and M. F. Margaritova, *Ukrain. Khim. Zh.*, **24**, 626 (1958); *Chem. Abstr.*, **53**, 10823f (1959).

3. Orr, R. J., and H. L. Williams, *Can. J. Chem.*, **30**, 108 (1952).

4. Gilbert, R. D., and H. L. Williams, *J. Am. Chem. Soc.*, **74**, 4114 (1952).

5. Baker, C. A., and H. L. Williams, *J. Chem. Soc.*, **1956**, 2352.

6. Tolbert, B. M., *Ionization Chamber Assay of Radioactive Gasses*, U.S. At. Energy Comm. Rept., UCRL-3499, March 5, 1956.

7. Wiley, R. H., and B. Davis, *J. Polymer Sci.*, **46**, 423 (1960).

8. Niederl, J. B., and V. Niederl, *Organic Quantitative Microanalysis*, Wiley, New York, 1942, p. 107.

9. Young, L. J., *J. Polymer Sci.*, **54**, 411 (1961).

10. Burlant, W. J., and D. H. Green, *J. Polymer Sci.*, **31**, 227 (1958); Kelley, D. J., and A. V. Tobolsky, *J. Am. Chem. Soc.*, **81**, 1597 (1959).

11. Chen, C. S. H. (Mrs.), and R. F. Stamm, *Abst., Intern. Symp. on Polymer Chem.*, Montreal, 1961, p. 69, 70.

12. Tabata, Y., R. Shimozawa, and H. Sobue, *J. Polymer Sci.*, **54**, 201 (1961).

13. Landler, Y., *Compt. Rend.*, **230**, 539 (1950); *J. Polymer Sci.*, **8**, 64 (1952).

14. Tobolsky, A. V., and R. J. Boudrean, *J. Polymer Sci.*, **51**, S53 (1961).

15. Seitzer, W., R. Goeckermann, and A. Tobolsky, *J. Am. Chem. Soc.*, **75**, 755 (1953).

16. O'Driscoll, K. F., and I. Kuntz, papers presented at the Washington meeting of the Division of Polymer Chemistry of the American Chemical Society, March 1962; Vol. **3**, No. 1, p. 54.

Résumé

La précision de la technique utilisant une chambre d'ionisation et un électromètre à plume vibrante a été améliorée ($\pm 0.25\%$ d'écart moyen) et utilisée à la détermination des rapports de réactivité de monomère au cours de la copolymérisation styrène–isoprène. Les valeurs r_1 (styrène) = 0.50 (100°) et 0.54 (80°) et r_2 = 1.92 (100°, 80°) ont été obtenus pour des copolymérisations radicalaires. Sous irradiation-γ à 22°C, r_1 = 0.66 et r_2 = 1.88. Par initiation au lithium-butyle, r_1 = 0.03 et r_2 = 5.9. La différence des

valeurs obtenues suivant le mode d'initiation radicalaire sous irradiation-γ peut résulter du caractère ionique partiel de l'initiation par radiation et de la dépendance thermique des rapports de réactivité (r_1) dans le domaine de 22 à 100°C. Ce dernier effet indique une différence d'énergie d'activation de 0.8 Kcal/mole entre l'étape de propagation d'un radical à une unité styrénique par rapport à celle d'un radical à une unité isoprénique.

Zusammenfassung

Die Genauigkeit der Bestimmungsmethode mit dem Ionisationskammer-Vibratorstab-Elektrometer wurde verbessert ($\pm 0.25\%$ mittlere Abweichung) und mit dieser Methode die Reaktivitätsverhältnisse für die Styrol–Isopren-Copolymerisation ermittelt. Für die radikalische Copolymerisation wurden die r_1-Werte (Styrol) 0,50 (100°) und 0,54 (80°) und der r_2-Wert 1,92 (100°, 80°) erhalten. Bei Anregung mit γ-Strahlen bei 22° ist $r_1 = 0,66$ und $r_2 = 1,88$. Bei Anregung mit Butyllithium ergibt sich r_1 zu 0,03 und r_2 zu 5,9. Der Unterschied zwischen den Werten bei Radikal- und γ-Strahlenanregung ist möglicherweise auf einen teilweise ionischen Charakter des strahlungs-induzierten Prozesses, möglicherweise aber auch auf die Temperaturabhängigkeit der Reaktivitätsverhältnisse (r_1) im Bereich von 22–100° zurückzuführen. Im letzteren Falle ergibt sich ein Unterschied von 0,8 kcal/Mol für die Aktivierungsenergie des Wachstumsschrittes zwischen Radikal und Styrol und Radikal und Isopren.

The Preparation and Polymerization of Suberaldehyde

JERRY N. KORAL and EDWIN M. SMOLIN, *Stamford Research Laboratories, American Cyanamid Company, Stamford, Connecticut*

Synopsis

A study of the controlled polymerization of suberaldehyde has been carried out. The monomer was prepared by a new route, the catalytic reduction of the ozonate of cyclooctene. By the proper choice of catalyst and conditions, three different types of polymers could be prepared from suberaldehyde. A Tischenko condensation resulted in a pure linear polyester. The sodium hydroxide-catalyzed polymerization of the aldehyde produced an aldol condensation polymer that was partially crosslinked through hemiacetal groups. The use of carbonyl polymerization catalysts such as triethylaluminum and boron trifluoride etherate, resulted in a polyacetal type of polymer containing free pendent carbonyl groups.

INTRODUCTION

There have been no reported studies on the controlled polymerization of aliphatic dialdehydes. Early German workers[1,2] observed that during their preparation of certain aliphatic dialdehydes some undirected polymerization took place, but they made no attempt to characterize the polymers. There are at least three possible mechanisms by which aliphatic dialdehydes can polymerize. These are (*a*) aldol condensation reactions, (*b*) Tischenko reactions, and (*c*) carbonyl-type polymerization. In order to investigate these reactions, a pure stable sample of suberaldehyde was prepared and its polymerization was studied under various conditions.

EXPERIMENTAL

Suberaldehyde

Ozonation

A charge of 11.0 g. (0.1 mole) of cyclooctene (Cities Service Co.) in 100 ml. of solvent which was either purified dry hexane (washed 3 times with H_2SO_4 and then H_2O, dried with $CaCl_2$, and distilled) or absolute methanol was placed in a Mini-lab wide-mouth flask fitted with a hollow-shaft gas-delivery stirrer and a Dry Ice condenser. The other end of the condenser led to a back-pressure manometer and a bubbler containing about 100 ml. of 4% aqueous KI. The flask was cooled in Dry Ice–acetone to

−78°C.   Hexane solutions remained homogeneous; methanol solutions became slurries.   A stream of O_2 was sent through the Wellsbach Model T-23 ozonator at a rate of about 1 l./min. until the KI bubbler started to color.   Hexane solutions precipitated heavy white solids; methanol solutions became homogeneous unless either the temperature was allowed to rise too high (−35°C.) or the stirring was inadequate, as in the case of a fritted gas-delivery tube with no stirring.   The completed ozonate was kept at Dry Ice temperature and stoppered until it was transferred to a hydrogenation vessel.

Reduction of the Ozonate

The cold ozonate solution from above was charged to a 300-ml. standard Aminco autoclave with 0.1 g. of PtO_2 (Adams catalyst) with 20 ml. of absolute methanol for rinsing.   At this point the temperature within the clave was about −35°C.   The clave was purged 4 or 5 times with hydrogen, pressured to 500 psig, and rocked for 1 hr.   At the end of this period, the reaction was complete.   The solution of crude suberaldehyde was filtered to remove the catalyst and distilled, whereupon there was obtained 12.8 g. of colorless mobile liquid (89% based on 100% cyclooctene), b.p. 77–82°/0.4 mm. Hg (lit.,[1a] 140–145°C. at 30 mm. Hg).

1,8-Dihydroxyoctane

A sample of crude suberaldehyde in methanol prepared, as described above, by ozonation and reduction of 11.0 g. (0.10 mole) of cyclooctene in 100 ml. of absolute methanol, was charged to a 300-ml. standard Aminco stainless-steel autoclave.   Then 1.5 g. of Raney Ni (W-6, freshly prepared), 0.3 ml. of 10N NaOH, and 0.11 g. of K_2PtCl_6 were added, in that order. The clave was sealed, flushed well with hydrogen, and pressured to 500 psig with hydrogen.   It was rocked at room temperature for 210 min., during which time several repressurings were necessary to keep the pressure between 400 and 500 psig.   The hydrogen uptake was 315 psig, or 75.5% of theory.   The clave was vented and the contents were removed, filtered, and concentrated on a rotary film evaporator.   The crude material was distilled in Bantamware equipment.   The major portion was collected at 109°C. at 0.4 mm. Hg and weighed 11.0 g. (75% yield).   Upon recrystallization from twice the weight of ethyl acetate, colorless needles were obtained; m.p. 58.5–59.5°C., corr. (lit.,[1b] 58.5°C.).

Polymerization of Suberaldehyde

Tischenko Reaction

A 100-ml. micro reaction apparatus fitted with a rubber serum stopper, stirrer, and nitrogen inlet tube was used for the polymerizations.   The apparatus was dried in a 140°C. oven for 2 hr. prior to use.   In a typical polymerization run, 10 ml. of CCl_4 (spectro grade) and 10 ml. of suberalde-
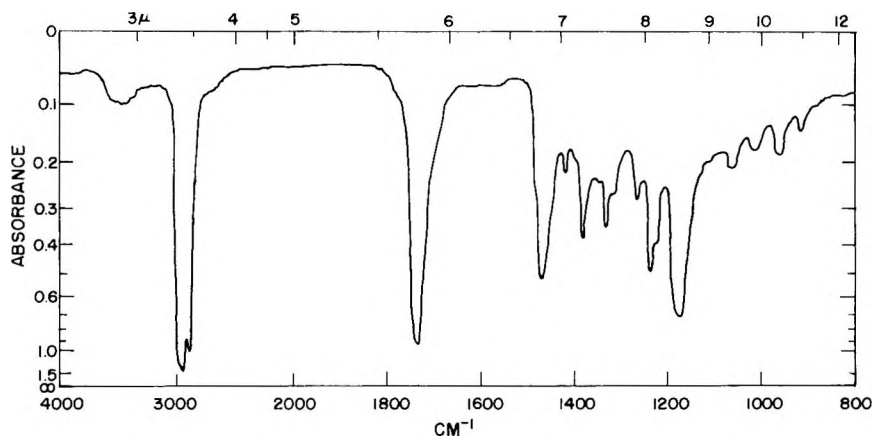
Fig. 1. Suberaldehyde polymer: aluminum isopropoxide catalyst.

hyde were placed in the apparatus which was immersed in an ice-water bath to maintain 0°C. Prepurified dry nitrogen was bubbled through the solution for 10 min. and then 10 ml. of a catalyst solution, containing 1.355 g. of freshly distilled aluminum isopropoxide in 15 ml. of CCl_4, was added. The reaction mixture was stirred for 17 hr. and a slight increase in viscosity was observed. The polymer was precipitated by pouring the reaction mixture into a large excess of heptane, washed with fresh heptane, and dried in a vacuum oven at 40°C. for 24 hr. A yield of 5.1 g. of a white powdery resin was obtained, corresponding to a 53% conversion. The infrared spectrum of the polymer indicated that it was a pure polyester (see Fig. 1). The polymer melted sharply at 50°C. and its x-ray diffraction pattern indicated a high degree of crystallinity. The number-average molecular weight of the polymer, determined in benzene at 30°C. by a thermistor method,[3] was 2,300. These results together with those from other runs appear in Table I.

TABLE I
The Tischenko Polymerization of Suberaldehyde (S)

Run No.	Moles cat./ moles S.	Monomer concn., vol.-%	Temp., °C.	Conver., % (19 hr.)	Polymer characteristics		
					M.p., °C.	Crystal.	Mol. wt. ($\overline{M}_n$)
1	0.056	9.1	0	23	50	+	—
2	0.056	33.0	0	53	50	+	—
3	0.029	40.0	0	53	50	+	2,300
4	0.029	40.0	25	55	50	+	2,050

Aldol Condensation

The aldol polymerizations were carried out in 2-oz. bottles containing Teflon-coated magnetic stirring bars and fitted with rubber serum stoppers.
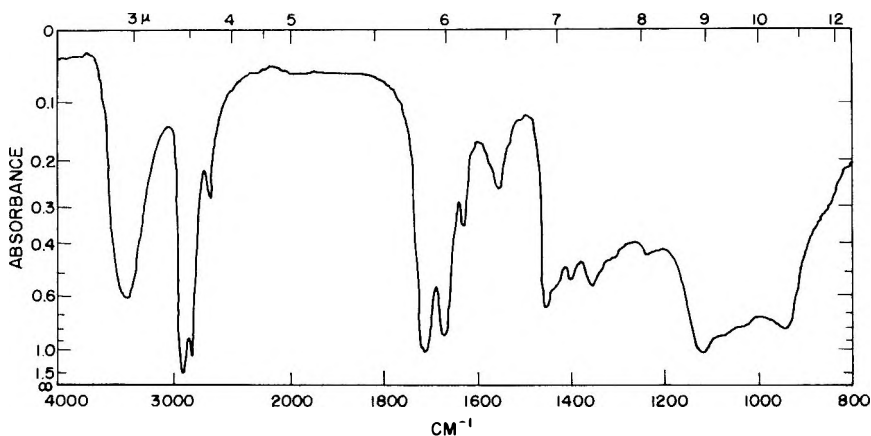
Fig. 2. Suberaldehyde polymer: potassium hydroxide catalyst.

In a typical reaction, a charge of 1.0 ml. of suberaldehyde, 1.0 ml. of methanol, and 2.0 ml. of distilled water was placed in the bottle and prepurified nitrogen was bubbled through the solution for 10 min. The bottle was placed in a 0°C. bath and 0.07 ml. of a 25% aqueous solution of KOH was added. Precipitation appeared approximately 1 min. after the catalyst addition. After 30 min. the polymer was removed from the bottle, washed several times with water, filtered, and dried in a vacuum oven at 45°C. for 24 hr. A yield of 0.97 g. of a fine white powder was obtained, corresponding to a 100% conversion. The infrared spectrum of the polymer appears in Figure 2. The polymer softened near 95°C. and had a melting

TABLE II

The Effect of the Basicity of the Catalyst on the Aldol Condensation of Suberaldehyde

Catalyst	pK_a	React. time, hr.	Conver., %
TMG[a]	13.6	0.5	100
KOH	13.5	0.5	100
NaOH	13.5	0.5	98
$(C_2H_5)_3N$	10.6	76.0	75
$(C_4H_9)_3P$	8.4	18.0	68
TEDA[b]	8.6	24.0	0

[a] Tetramethyl guanidine.
[b] Triethylenediamine.

point of 110°C. X-ray diffraction measurements indicated that it was amorphous. The polymer was insoluble in most common organic solvents but was soluble in benzyl alcohol. The intrinsic viscosity of the polymer in benzyl alcohol at 30.4°C. was 0.07 dl./g. Attempts to reprecipitate the polymers were unsuccessful, indicating that some structural change had occurred during the solution process.

The effect of the basicity of the catalyst on the aldol condensation polymerization of suberaldehyde was studied with such catalysts as tetramethyl guanidine, sodium hydroxide, triethylamine, etc. These polymerizations were carried out at 0°C. with a catalyst concentration of 4.5 mole-% based on the monomer, and a monomer concentration of 25% in 2:1 water/methanol, by volume. The results are shown in Table II.

Several runs were made in order to study the effect of monomer concentration on the aldol polymerization of suberaldehyde. Polymerizations were carried out at 0°C. in a 2:1 water/methanol solvent. The catalyst was 9 mole-% sodium hydroxide based on the monomer. These results are summarized in Table III.

TABLE III
The Effect of Monomer Concentration on the Aldol Condensation
Polymerization of Suberaldehyde

Monomer concn., vol.-%	React. time, hr.	Conver., %
6.2	1.0	70
12.5	0.5	83
25.0	0.25	94
100.0	1.0	100

Some work was carried out in which the effect of the solvent composition on the rate of polymerization of suberaldehyde at 0°C. and the melting points of the resultant polymers was studied by varying the ratios of water–methanol solvent. The catalyst concentration was 4.5 mole-% sodium hydroxide based on monomer. The results appear in Table IV.

TABLE IV
The Effect of the Solvent Composition on the Aldol Condensation
Polymerization of Suberaldehyde

H_2O in solvent, %	React. time, hr.	Conver., %	M.p. of resin, °C.
0	1.0	72	Infusible
4	76.0	75	Softens at 129°C.; does not melt.
6	20.0	65	Softens at 133°C.; does not melt.
8	3.0	78	108
33	0.5	58	111
67	0.25	98	110
100[a]	0.25	100	110

[a] Suberaldehyde is water-insoluble and the reaction was run as a dispersion of the monomer in water.

Carbonyl Polymerizations

A 100-ml. micro reaction apparatus fitted with a rubber serum stopper, stirrer, and nitrogen inlet tube was charged with 2 ml. of suberaldehyde
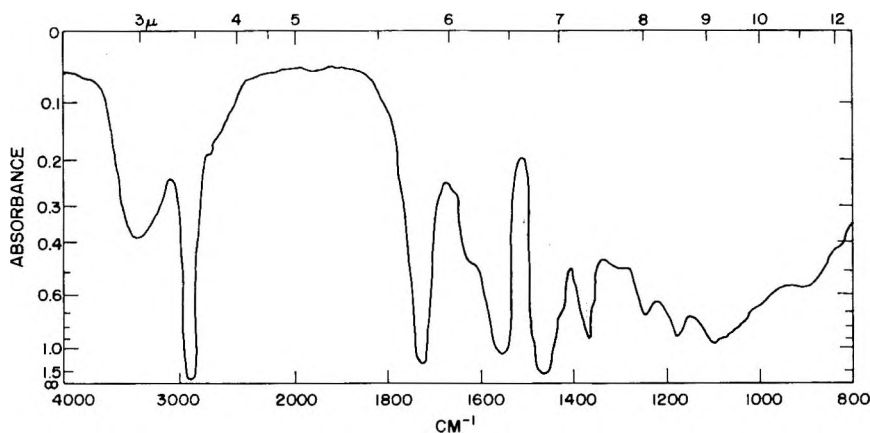
Fig. 3. Suberaldehyde polymer: boron trifluoride etherate catalyst.

and 10 ml. of toluene. The toluene had been dried over CaH_2, distilled, and the fraction that boiled at 110°C. was used in the polymerization studies. The apparatus was placed in a controlled temperature bath[4] at −20°C. and prepurified dry nitrogen was bubbled through the solution for 10 min. Then 0.1 ml. of distilled $BF_3 \cdot O(C_2H_5)_2$ was added through the serum stopper by means of a hypodermic syringe. Immediate polymerization was observed and the solution gelled within 1 min. After 2 hr. the gelled solution was added to a large excess of vigorously stirred, cold heptane. A fine white powder was obtained. The resin was washed several times with fresh heptane and then dried in a vacuum oven at 45°C.

TABLE V
The Carbonyl Polymerization of Suberaldehyde

Catalyst	Moles cat./ moles S.	Mono- mer concn., vol.-%	React. time, hr.	Con- ver., %	Polymer characteristics	
					Soft p., °C.	Infrared C—O—C/ C=O
$(C_2H_5)_3Al$	0.068	9.1	16	53	160	1
$BF_3 \cdot O(C_2H_5)_2$	0.083	9.1	2	69	120	1
$BF_3 \cdot O(C_2H_5)_2$	0.083	3.5	2	91	87	3–4
$BF_3 \cdot O(C_2H_5)_2$	0.083	1.7	1	76	92	3–4

for 24 hr. The dry sample weighed 1.32 g., corresponding to a 69% conversion. The infrared spectrum of this polysuberaldehyde is shown in Figure 3. The polymer softened at about 120°C. under pressure but did not completely melt at 300°C. It was insoluble in dimethylformamide, acetone, toluene, Cellosolve, and dioxane. The results of several other polymerizations carried out with $BF_3 \cdot O(C_2H_5)_2$ and $(C_2H_5)_3Al$ as catalysts are listed in Table V.

Polyesterification of Suberic Acid and 1,8-Dihydroxyoctane

The suberic acid used was obtained by H_2O_2 oxidation of the cyclooctene ozonate according to the procedure of Bailey.[5] Yields were 96% crude. A method similar to that of Marvel and Johnson[6] was used for the preparation of the polyester. A 1:1 molar ratio of suberic acid and 1,8-dihydroxyoctane was heated for 2 hr. at 170°C. Then, over a period of 3 hr., the pressure was lowered to 8 mm. and the temperature raised to 200°C. The polymer was isolated by precipitation from methanol of a $CHCl_3$ solution of the reaction mixture. A 38% conversion to a white powdery polymer whose infrared spectrum was characteristic of a polyester was obtained. An x-ray diffraction pattern indicated a high degree of crystallinity. The number-average molecular weight of the polymer determined in CH_2Cl_2 by a thermistor method was 2,210.

DISCUSSION

A necessary condition for the study of the controlled polymerization of linear aliphatic dialdehydes was the preparation of a stable monomer. It was felt that the synthesis of a fairly high molecular weight dialdehyde would offer the best chance for obtaining a pure monomer with the desired stability.

Early German workers[1] had prepared suberaldehyde by the decarboxylation of 2,9-dihydroxysebacic acid but an appreciable amount of polymerization occurred during the synthesis. Therefore, a different synthetic approach, the ozonation of cyclooctene, was selected. The 6-C analog, adipaldehyde, has been prepared in 50% overall yield by the ozonation of cyclohexene in methanol at Dry Ice temperatures followed by a reduction of the ozonide.[7] Criegee,[8] in ozonizing cyclooctene, obtained exclusively a polymeric ozonide using hexane solvent at 0°C. He stated that hexane, in general, reduces the tendency toward polymer formation during ozonation.

A short series of ozonation experiments with cyclooctene was carried out in hexane at Dry Ice temperature. In every case copious amounts of a white solid polymer were obtained. Attempts to reduce this with hydrogen and Ni or Co catalysts led only to other polymeric products. Reduction with Pd/C gave a H_2 uptake equal to 20% of theory. When hexane was replaced by methanol as the ozonation solvent, cyclooctene was converted smoothly to an ozonide, giving a clear colorless solution. All subsequent runs were made in methanol. Reduction of the ozonide to suberaldehyde was accomplished in satisfactory yields in a Paar low-pressure hydrogenation apparatus with PtO_2. Other catalysts such as Pd/C and $Pd/BaCO_3$ were not as effective. Maximum yields of suberaldehyde of 85–89% were obtained, however, when the reduction was carried out under pressures of the order of 500 psi in an autoclave.

The polymerization of aliphatic dialdehydes should proceed by three distinct mechanisms which are illustrated below:
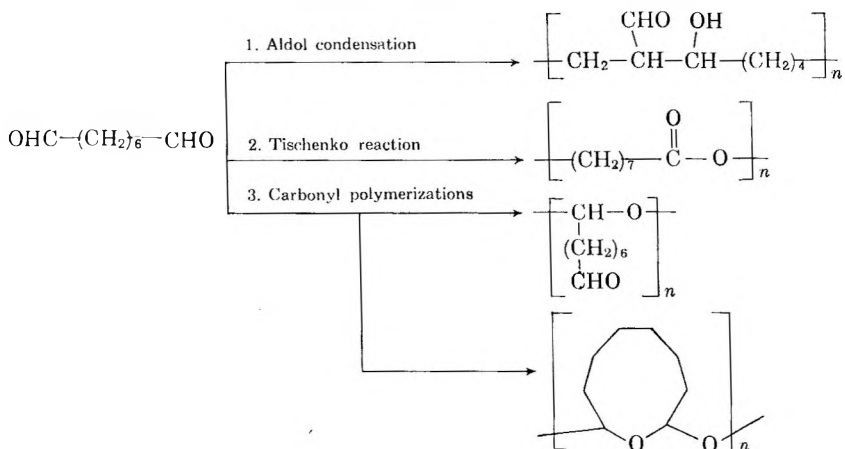
No study of the controlled polymerization of aliphatic dialdehydes has been reported in the literature. The only analogous work was reported in a recent Russian article,[9] the polymerization of aromatic dialdehydes such as terephthalic and isophthalic aldehyde to high molecular weight polyesters under the influence of aluminum ethoxide and similar catalysts.
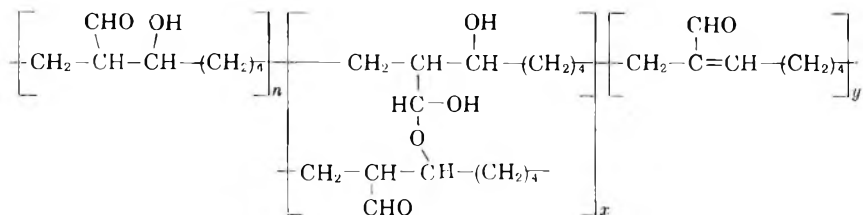
The Tischenko polymerization of suberaldehyde with aluminum isopropoxide as catalyst resulted in a pure polyester having a number-average molecular weight of about 2,000 (see Fig. 1). The infrared spectrum and x-ray diffraction pattern of this polymer were indentical with those of the polyester prepared from the condensation of 1,8-dihydroxyoctane and suberic acid.

We found that aluminum isopropoxide is a good catalyst for the polymerization of suberaldehyde. This contrasts with the finding by Russian workers[9] that aluminum isopropoxide is without catalytic activity for the polymerization of aromatic dialdehydes. However, our results are in agreement with those obtained by Child and Adkins[10] from the Tischenko condensation of simple aldehydes (i.e., acetaldehyde, butyraldehyde, etc.). They found that aluminum isopropoxide and aluminum butoxide are much more effective catalysts for the condensation than aluminum ethoxide.

The effect of monomer and catalyst concentration on the rate of reaction was significantly different in Tischenko condensation with suberaldehyde and with a simple aldehyde such as butyraldehyde. Child and Adkins[10] observed that the change in rate on doubling the amount of aldehyde or catalyst was surprisingly small. A 100% increase in aluminum alkoxide or aldehyde concentration caused a 3–5% increase in rate. Our results showed that the yield of polysuberaldehyde was doubled when the monomer concentration was tripled (Table II). Only a small increase in the rate of polymerization was obtained when the catalyst concentration was increased.

Suberaldehyde was readily polymerized to polyester in solution with little temperature effect on the rate at 0–25°C. in contrast to high-temperature bulk polymerization conditions[9] necessary for aromatic dialdehydes.

The addition of small amounts of strong bases such as KOH, tetramethyl guanidine, etc., to a water–methanol solution of suberaldehyde resulted in an extremely rapid polymerization (see Table II). The infrared spectra of these polymers were different from the product prepared with aluminum isopropoxide (compare Figs. 1 and 2). A typical spectrum contained hydroxyl groups (3400 cm.[-1]), carbonyl groups (1720 cm.[-1]), conjugated carbonyl groups (1675 cm.[-1], ether groups (1150 cm.[-1], and some unsaturation (1625 cm.[-1]). A structure containing these groups and in their relative amounts is consistent with the product expected from an aldol condensation type of polymerization of suberaldehyde in which, to some degree, water elimination and crosslinking has taken place via hemiacetal formation. This structure may be represented as:

$$\left[\begin{array}{c} \underset{\diagdown}{CHO}\ \underset{|}{OH} \\ \text{-CH}_2-\text{CH}-\text{CH}-(\text{CH}_2)_4- \end{array}\right]_n \left[\begin{array}{c} OH \\ | \\ \text{CH}_2-\text{CH}-\text{CH}-(\text{CH}_2)_4- \\ | \\ \text{HC}-\text{OH} \\ | \\ \text{O} \\ \diagdown \\ \text{-CH}_2-\text{CH}-\text{CH}-(\text{CH}_2)_4- \\ | \\ \text{CHO} \end{array}\right]_x \left[\begin{array}{c} CHO \\ | \\ \text{-CH}_2-\text{C}=\text{CH}-(\text{CH}_2)_4- \end{array}\right]_y$$

The elimination of water in aldol condensation reactions of simple aldehydes is well known and probably accounts for the presence of the conjugated carbonyl groups observed in the infrared spectra. Under the basic conditions of the polymerization, the formation of hemiacetal crosslinks would be quite favorable. A partially crosslinked polymer would also account for the limited solubility of the polymer. Some additional evidence of crosslinking was obtained from molding experiments. It was observed that a sample of polysuberaldehyde molded into a transparent bar was extremely flexible, even after equilibrating to room temperature; however, after two days it became quite stiff. It is suggested that heatlabile but reversible hemiacetal crosslinking may account for the increased rigidity with time.

The rate of aldol condensation with suberaldehyde was very fast and similar to that obtained by Bell[11] with acetaldehyde. When KOH (pK_a = 13.5) was used for polymerizing suberaldehyde, a 100% conversion to polymer was obtained in 30 min. at 0°C. The reaction was slower when weaker bases such as triethylamine (pK_a = 10.6) and tributyl phosphine (pK_a = 8.4) were used as catalysts. Triethylenediamine (pK_a = 8.6), whose basicity is in the same range as tributyl phosphine, did not initiate polymerization.

The effect of suberaldehyde concentration and solvent composition on the polymerization rate was also investigated. An examination of Table III shows that the monomer concentration has only a small effect on the

rate of reaction in the range studied. However, the solvent composition profoundly affected both the rate and the melting behavior of the resultant polymer (see Table IV). The sodium hydroxide-catalyzed polymerization of suberaldehyde in pure methanol was extremely fast and gave an infusible polymer. Small increments of water caused large decreases in polymerization rates. The resultant polymers softened under pressure but without melting. The use of still larger amounts of water in the solvent resulted in faster reaction rates and produced a polymer which had a fairly sharp melting point of 110°C. It is difficult to explain the drastic effect of water concentration on the rate of polymerization, but the fusibility of the polymers is probably related to the degree of hemiacetal formation. The polymer prepared in pure methanol was probably highly crosslinked, and even the application of heat and pressure was not sufficient to cause complete fusion. As the water concentration in the system was increased, the resulting polymer could be melted, probably as a result of less crosslinking. Further work is being carried out in these laboratories to elucidate this and other phenomena. The effects of different solvents, temperature, and catalyst concentration on the polymerization of suberaldehyde is being studied, together with the aldol condensation polymerization of other aliphatic dialdehydes and their copolymerization. These results will be reported in the future.

The last type of dialdehyde polymerization investigated can be classified as carbonyl polymerization. Much has been published on the carbonyl polymerization of simple aldehydes,[12-14] but no work has been reported with dialdehydes. The carbonyl polymerization of dialdehydes should proceed by the two different mechanisms previously illustrated: (1) polymerization through one carbonyl group leaving the other as a free pendent group and (2) an inter-intramolecular carbonyl polymerization analogous to the cyclopolymerization of certain divinyl monomers.[15] With suberaldehyde one would expect the first mechanism to predominate because the second would necessitate formation of nine-membered rings along the chain.

The rate of polymerization of suberaldehyde with typical carbonyl polymerization catalysts and conditions was extremely fast, even when the monomer concentration was only 3.5% (Table V). The infrared spectrum of a typical polymer (Fig. 3) shows the presence of carbonyl groups (1720 cm.$^{-1}$), ether groups (1150 cm.$^{-1}$), and a low concentration of hydroxyl groups (3400 cm.$^{-1}$). No solvent was found for these polymers, perhaps because of crosslinking of some pendent carbonyl groups. It was felt that polymerizations carried out at high dilution might result in some cyclopolymerization, even though nine-membered ring formation is not energetically favored. The increase in the observed ratio of ether to carbonyl groups in the infrared spectra of the polymers provides evidence of some cyclopolymerization. Further studies are being carried out in this area in order to obtain more quantitative data.

The results of this preliminary investigation have shown that the poly-

merization of aliphatic dialdehydes can be controlled, and that polymers of different structure and properties can be prepared from the same monomer. These facts suggest the broad possibilities of dialdehyde polymers.

References

1. (a) Baeyer, A., *Chem. Ber.*, **30**, 1962 (1897); (b) Scheuble, R., and E. Loebl, *Monatsh.*, **25**, 345 (1904).

2. Harries, C., and L. Tank, *Chem. Ber.*, **41**, 1701 (1908).

3. Wilson, A., L. Bini, and R. Hofstader, *Anal. Chem.*, **33**, 135 (1961).

4. Kell, R. M., *J. Appl. Polymer Sci.*, **4**, 252 (1960).

5. Bailey, P., *Ind. Eng. Chem.*, **50**, 993 (1958).

6. Marvel, C. S., and J. H. Johnson, *J. Am. Chem. Soc.*, **72**, 1674 (1950).

7. Fisher, E. E., U.S. Patent 2,733,270 (Jan. 1956); G. W. Rigby, U.S. Patent 2,657,239 (Oct. 1953); R. E. Foster and H. E. Schroeder, U.S. Patent 2,657,240 (Oct. 1953).

8. Criegee, R., A. Kerchon, and H. Zinke, *Cnem. Ber.*, **88**, 1878 (1955).

9. Mitim, Yu. V., Y. N. Sazanov, G. P. Vlasov, and M. M. Koton, *Vysokomolekul. Soedin.*, **15**, 716 (1960).

10. Child, W. C., and H. Adkins, *J. Am. Chem. Soc.*, **47**, 798 (1925).

11. Bell, R. P., *J. Chem. Soc.*, **1937**, 1637.

12. Vogl, O., *J. Polymer Sci.*, **46**, 261 (1960).

13. Natta, G., G. Mazzanti, P. Corradini, and I. W. Bassi, *Makromol. Chem.*, **37**, 156 (1960).

14. Furukawa, J., T. Saegusa, and H. Fujii, *Makromol. Chem.*, **44**, 398 (1961).

15. Barnett, M. D., A. Crawshaw, and G. B. Butler, *J. Am. Chem. Soc.*, **81**, 5946 (1959).

Résumé

On a étudié la polymérisation contrôlée de l'aldéhyde subérique. On a préparé le monomère par une voie nouvelle, par réduction catalytique de l'ozonate de cyclooctène. Au moyen d'un choix judicieux du catalyseur et des conditions, on peut préparer trois types différents de polymères à partir de l'aldéhyde subèrique. Par condensation de Tischenko il en résulte un polyester purement linéaire. La polymérisation de l'aldéhyde, catalysée par l'hydroxyde de sodium, fournit un polycondensat aldolique qui est partiellement ramifié par les groupes hémiacétals. Enfin l'emploi de catalyseurs de polymérisation carbonylique comme le triéthyl aluminium et l'éthérate de trifluorure de bore, donne un polymère du type polyacétal renfermant des groupes carbonyles libres.

Zusammenfassung

Eine Untersuchung der Polymerisation von Suberaldehyd unter kontrollierten Bedingungen wurde durchgeführt. Das Monomere wurde auf einem neuen Weg, nämlich durch katalytische Reduktion des Cyclooctenozonids, dargestellt. Durch geeignete Wahl des Katalysators und der Versuchsbedingungen konnten aus Suberaldehyd drei verschiedene Arten von Polymeren hergestellt werden. Eine Tischenko-Kondensation lieferte ein rein lineares Polymeres. Die durch Natriumhydroxyd katalysierte Polymerisation des Aldehyds ergab ein Aldolkondensations-Polymeres, das zum Teil durch Hemiacetalgruppen vernetzt war. Schliesslich entstand mit Carbonylpolymerisationskatalysatoren, wie Triäthylaluminium und Bortrifluorid-Ätherat, ein Polymeres vom Polyacetaltyp mit anhängenden, freien Carbonylgruppen.

Growth of Single Crystals of Polytetrafluoroethylene from the Melt*

N. K. J. SYMONS, *Plastics Department, E. I. du Pont de Nemours and Co. Inc., Wilmington, Delaware*

Synopsis

The melt crystallization of dispersion-based polytetrafluoroethylene, in amounts varying from single dispersion particles to continuous films, has been studied by electron microscopy, electron diffraction, and optical microscopy. Since the maximum temperature used was only 350°C., negligible thermal degradation of the polymer is believed to have occurred during the crystallization. Using very small amounts of the polymer, single crystals with thicknesses of about 150–900 A. having their molecular chains oriented perpendicularly to the basal plane of the crystal have been observed; this shows that the melt crystallization of polytetrafluoroethylene occurs by a chain-folding mechanism as reported previously for other high polymers. This new knowledge allows a more positive interpretation of the striated band structures previously observed on fracture surfaces of bulk specimens of both dispersion-based and granular types of this polymer. Such bands which show striations perpendicular to their length probably represent individual crystal plates which have been fractured in planes perpendicular to their bases, while bands showing longitudinal striations result from the splitting apart of stacks of such plates, or lamellae, along fracture planes approximately parallel with their surfaces. The present observation of isolated and well defined single crystals from a polymer melt, as distinct from a solution, is believed quite novel. Although seen so far with polytetrafluoroethylene only, the growth of such single crystals from the melt might be possible with other polymers also, if these were studied in very small quantities.

INTRODUCTION

Over the past decade, a number of papers have been published concerning the morphology and structure of high polymers as revealed by optical and electron microscopy. Many of these papers, reporting studies with various polymers crystallized either from solution or from the molten state, were summarized in a review by Keller[1] in 1959, and additional work in this field has continued to appear since that time. However, in this literature, studies dealing with the crystallization of polytetrafluoroethylene (PTFE) seem to have lagged considerably behind those with other polymers, such as polyethylene, polyoxymethylene, and the nylons. One reason for this may be that solution crystallization studies with PTFE are not as attractive as those with other polymers because of the insolubility

---

of PTFE in the solvents customarily used. Consequently, for PTFE there are no published reports of the solution-grown single crystals which have contributed so much to our knowledge of the crystallization of other more soluble polymers; the only published work in this area appears to be that of Symons,[2] in which dendritic growths only were observed. In the area of melt crystallization, the most significant work with PTFE is probably that of Bunn, Cobbold, and Palmer,[3] reporting various banded structures seen on fracture surfaces of annealed bulk specimens of granular and dispersion-based types of the polymer. However, a disadvantage of such bulk specimens is that they can be studied in the electron microscope in the form of surface replicas only and are not suitable for examination by electron diffraction. Consequently, although some general information is available from optical evidence, positive interpretation of these bands is hampered by lack of precise knowledge of the orientation of the polymer molecular chains from which they are formed.

The work described here was undertaken to gain a better understanding of the manner in which PTFE crystallizes from the melt. To this end, it appeared best to start with observation of the crystallization behavior of small and isolated portions of the polymer, as conveniently provided by deposits of small groups of the polymer particles formed in dispersion polymerization. In this manner, crystallization could be expected to proceed unhampered by the influence of surrounding material, and also, in amounts suitable for examination by electron diffraction, as well as by direct observation, in the electron microscope. This approach has proved fruitful, enabling us to grow single crystals directly from the polymer melt, and to show that, with the dispersion-based material at least, crystallization apparently occurs by the chain folding which is now the generally-accepted mechanism of crystallization of other high polymers.

This work appears also of interest in a somewhat wider context, in that the present observation of separate and well defined single crystals formed from a polymer melt is believed to be quite novel, being distinct from either the single crystals grown from other polymer solutions or the composite lamellar structures from the polymer melts, which have been reported previously. Although demonstrated for PTFE only, this suggests the possibility that single crystals from the molten state might be formed with other polymers also, if these were studied in very small quantities, comparable with those provided by the dispersion particles used here.

EXPERIMENTAL DETAILS

The polymer used in these studies was dispersion-based material, derived from Teflon 41BX TFE-fluorocarbon resin dispersion (du Pont) and Fluon GP-1 (I.C.I.). These two independent sources were used to provide specimens representative of this polymer, the similarity of the experimental results with both supporting the general validity of the conclusions.

The polymer was deposited on glass slides in amounts ranging from isolated dispersion particles and groups of particles to continuous films by

drying different sized portions of the aqueous dispersions, after dilution
with distilled water.   To obtain scanty polymer deposits, minute droplets
of the dispersions, diluted to 0.5% solids content, were sprayed on the
slides with an atomizer.   Somewhat heavier, but still isolated, deposits
were obtained from the same dilute dispersions when dried as single drops
from an eye dropper   Continuous films of the particles were obtained by
drying thin layers of the dispersions diluted to 7.5% solids content.   These
slides were next enclosed in an air atmosphere in an electrically heated
brass block.   The block was then heated to a maximum temperature of
350°C.   Finally, the molten polymer was allowed to crystallize during
cooling of the block under various controlled conditions from this tempera-
ture to below its 327°C. crystalline melting point.

The discrete crystal formations obtained on heating the isolated deposits
of polymer were examined by direct transmission in the electron micro-
scope, after application of evaporated support and shadowing films of
carbon and chromium, respectively.   In this manner, both normal electron
micrographs and also selected area electron diffraction patterns were
recorded.   The film specimens, being too thick to permit transmission of
the electron beam, were examined by means of shadowed carbon replicas
made by conventional methods.   For optical examination, the heated
slides were examined directly with the polarizing microscope, transmitted
or reflected light optics being used for the discrete crystals and the con-
tinuous film specimens, respectively.

RESULTS

The evidence to be presented below supports the belief that when PTFE
dispersion polymer is cooled from temperatures above its crystalline melting
point, the molecular chains tend to align themselves to form plates or
lamellae, which, in the idealized case, show a hexagonal habit with the
chains oriented normal to the basal plane of the hexagon.   The extent to
which this chain alignment occurs in any given case probably depends on
a number of factors, including the time and temperature of heating, the
rate of cooling, the molecular weight of the polymer specimen, and the
amount of polymer involved in the crystallization.   Although no systematic
investigation has been made of the influence of these factors on the form
and perfection of the polymer crystals finally obtained, fairly pronounced
differences in behavior have been observed with respect to the amount of
polymer involved, i.e., the size of the discrete portions of polymer which
are physically separate during their crystallization.   Therefore, the ob-
servations below are described in order of increasing amounts of the dis-
persion particles heated, going from isolated particles or clusters of particles
to continuous films.   In each case, observations with the electron micro-
scope are given first, followed by those with the optical microscope.

1. Scanty Polymer Deposits

Figures 1 and 2 are electron micrographs showing typical crystal forma-
tions observed when light deposits of particles, sprayed from dilute Teflon

Fig. 1. Crystals formed from Teflon 41BX dispersion particles sprayed on glass and heated for 2 hr. at 350°C.; not annealed. Chromium shadowed 30°; original magnification 10,000×.
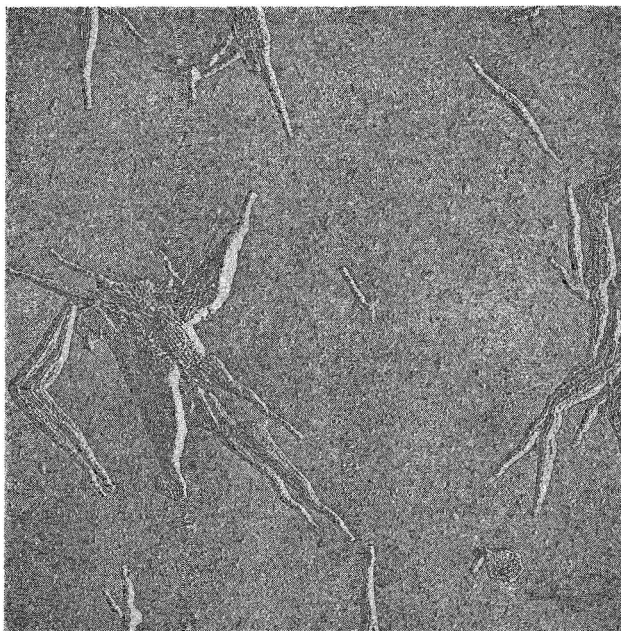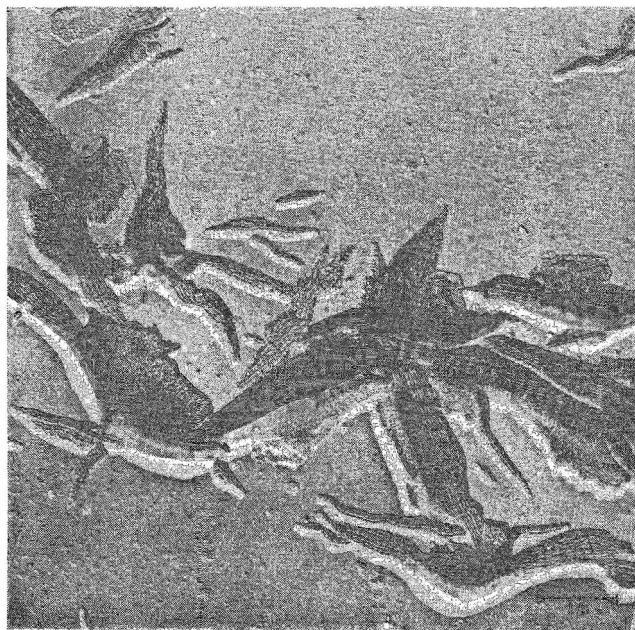

Fig. 2. Crystals formed from Fluon GP-1 dispersion particles sprayed on glass and heated for 2 hr. at 350°C.; not annealed. Chromium shadowed 30°; original magnification 10,000×.

Fig. 3. Single PTFE crystal from Teflon 41BX dispersion particles sprayed on glass and heated for 2 hr. at 350°C.; not annealed. The framed region shows the selected area which gave the inset 80 kv. electron diffraction pattern. Chromium shadowed 30°; original magnification 10,000×.
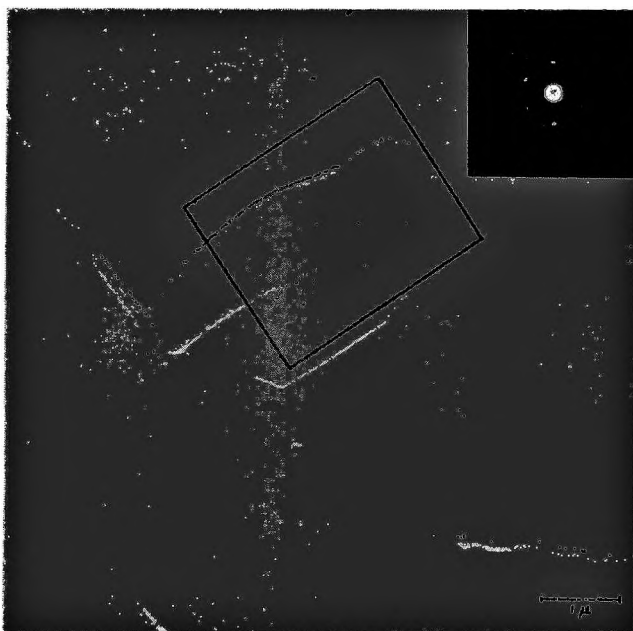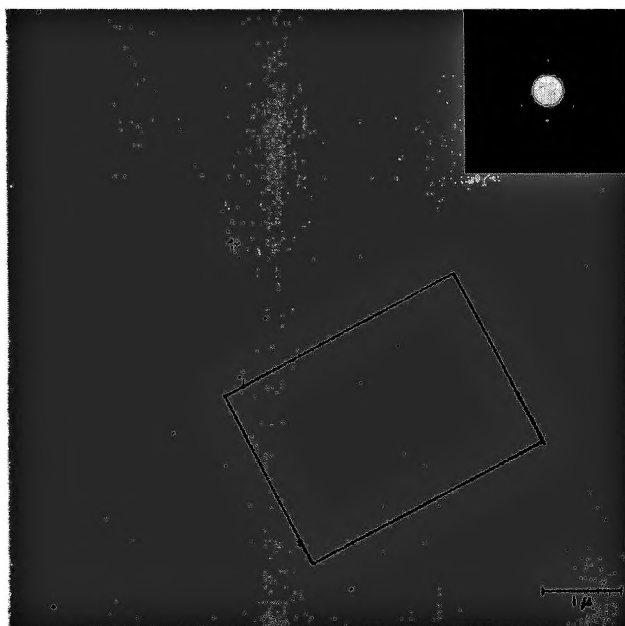

Fig. 4. Single PTFE crystal from Fluon GP-1 dispersion particles sprayed on glass and heated for 2 hr. at 350°C.; not annealed. The framed region shows the selected area which gave the inset 80 kv. electron diffraction pattern. Chromium shadowed 30°; original magnification 10,000×.

41BX and Fluon GP-1 dispersions, respectively, were heated for 2 hr. at 350°C. and then allowed to cool to below the 327°C. melting point in approximately 15 min. These pictures show that the dispersion particles from both sources had coalesced on melting and subsequently crystallized as flat plates and forms resembling broad needles, the latter often having a number of parallel striations along their lengths. In these pictures, as well as in some of the later figures, the surface of the crystals shows a sort of cobbled appearance, in the size range about 250–500 A. While this may represent the real structure of the crystals, it might also arise from a possible greater tendency for the shadow metal to granulate on the PTFE surface than on the substrate material, and positive interpretation does not appear possible at this time.

In several places in Figures 1 and 2 the flat plates have assumed a clearly hexagonal habit, and in other regions of the slides, where even less polymer had been deposited originally, isolated crystals with quite well defined hexagonal outlines were observed. Examples of these are shown in Figures 3 and 4, in which the crystal platelets are about 2–4 μ in extent and have a thickness of about 150 A., as measured from their shadow lengths. Rough calculation of the volume of such crystals shows them to correspond to clusters of some 100 or so dispersion particles of typical diameter about 0.2 μ; however, the volume of some of the smallest crystals observed, such as that seen in the lower right corner of Figure 1, indicates that these may actually have been formed from a single dispersion particle.

The selected area electron diffraction patterns in Figures 3 and 4 show that, as strongly suggested by their hexagonal outlines, these plates consist of single crystals, and also that the crystallographic c axis and so the direction of the PTFE molecular chains is perpendicular to their basal plane. The striated needlelike crystals, of the type shown in Figures 1 and 2, on the other hand, were found to give complicated, multispot diffraction patterns, showing them to have a more complex crystal structure than the single crystal plates. As has been reported previously[1] for crystals of other polymers such as polyethylene, exposure of the present PTFE crystals to the electron beam caused a fairly rapid disappearance of the diffraction pattern, without any great change in the normal electron microscope image. The magnitude of this effect with the PTFE crystals did not appear greatly different from that seen with polyethylene, despite the approximately 200°C. higher melting point of the former polymer, but insufficient evidence is available at present to allow a quantitative comparison.

Although some of the crystals from these scanty polymer deposits could be seen with the optical microscope, most of them were too small for convenient study; more fruitful observations were possible with the similar but larger crystals obtained from the somewhat heavier deposits described below.

2. Moderate Polymer Deposits

Heating heavier, but still isolated deposits of polymer obtained from larger drops of the same dilute dispersions, again resulted in flat plates and striated, needlelike crystals, but these were larger and thicker than
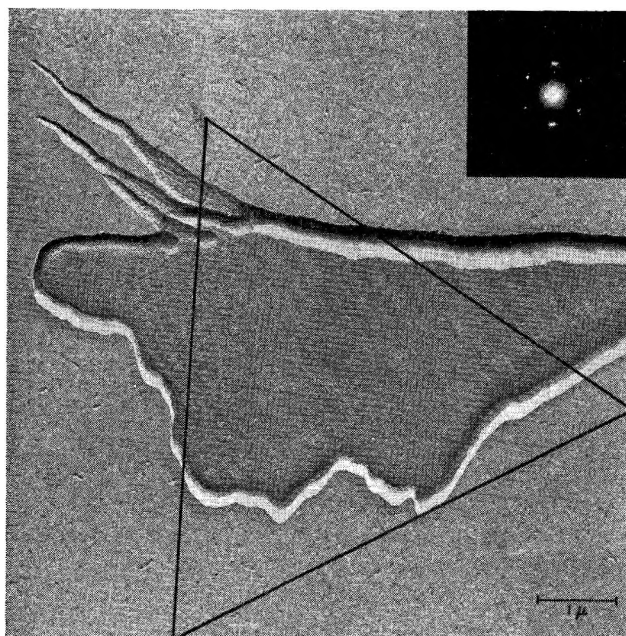
Fig. 5. Single crystal plate, ca. 900 A. thick, from Teflon 41BX dispersion particles heated on glass for 2 hr. at 350°C. and then annealed for 20 hr. at 334°C. The framed region shows the selected area which gave the inset 100 kv. electron diffraction pattern. Chromium shadowed 30°; original magnification 10,000×.

those seen in the specimens prepared with the atomizer, and, in this case, thin hexagonal crystals were not observed. If not annealed, these crystals gave complicated electron diffraction patterns which showed them to have a composite crystalline structure. However, if the preparation included an annealing treatment at a temperature above the 327°C. crystalline melting point, many of the thick plates were found to give single crystal diffraction patterns.

Figure 5 shows an electron micrograph and the corresponding selected area electron diffraction pattern of a typical plate observed on heating polymer from Teflon 41BX for 2 hr. at 350°C., followed by 20 hr. at 334°C., and then cooling to below the melting point at the rate of 0.1°C./min. The shadow length shows this plate to be about 900 A. thick. Although it does not have the regular outlines of the thinner hexagonal plates described above, the electron diffraction pattern shows that this, also, is essentially a single crystal, with the molecular chain direction again perpendicular to the basal plane. Single crystal plates of similar thickness were also observed when moderate deposits of polymer from Fluon GP-1 dispersion were heated in the same manner.

With these moderate deposits of polymer, many of the crystal plates and needles were fairly large (e.g., 10–20 μ), and this allowed further evidence regarding their molecular structure to be obtained by examination with the polarizing microscope. The pictures in Figure 6 are optical micrographs of a group of the crystals from the annealed Teflon 41BX preparation described above; in Figure 6a, taken with unpolarized light, a typical
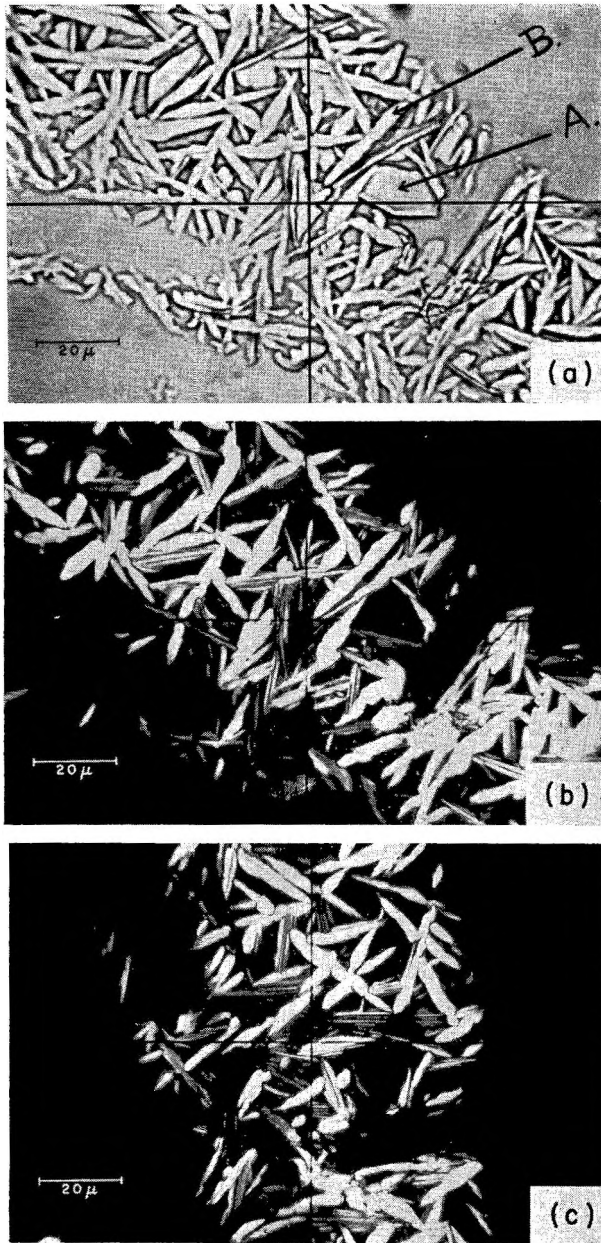
Fig. 6. Crystals formed from Teflon 41BX dispersion particles heated on glass for 2 hr. at 350°C. and then annealed for 20 hr. at 334°C.: (a) transmitted light, no polarizers; (b) as (a), but between crossed polarizers, crystal B at position of maximum illumination; (c) as (b), but crystals rotated 45°; crystal B now at position of maximum extinction. Original magnification 500×.

crystal plate and a needle are denoted by A and B, respectively. Between crossed polarizers, the plates appeared dark in all rotation positions of the microscope stage, as illustrated for crystal A in Figures 6b and 6c, showing this group of crystals in two positions of the stage between the crossed

polarizers.   Thus, in their customary position, lying flat on the microscope slide, these plates presented an isotropic view, along an optic axis perpendicular to their bases.   In contrast to the plates, the needles showed fairly marked birefringence; this is illustrated by Figure 6b.   Needle B is seen in a position of maximum illumination, lying at 45° to the polarizer and analyzer vibration directions, indicated by the crosshairs in this picture.   Examination with the use of the quartz wedge showed the birefringence to be negative, the higher refractive index being in the direction perpendicular to the length of the needles.   The overall needles showed parallel extinction, as shown by Figure 6c.   Needle B is seen in a position of maximum extinction, lying parallel to the vibration direction of the polarizer in this case.   However, this extinction was not complete, the needles showing a series of light and dark striations, as can be seen with needle B in this picture.

The significance of this evidence from the polarizing microscope is discussed later.

3. Continuous Films

The electron micrograph of Figure 7 shows a surface replica of a continuous film obtained by drying a layer of Fluon GP-1 dispersion, heating to 350°C., and immediately cooling at a rate of 0.1°C./min. until a temperature below the melting point was reached.   This picture shows the film surface to consist of lamellae and broad needles, or bands; as may be seen at the right center portion of the picture, the bands often had a fine structure of parallel striations running along their length.   Similar features

Fig. 7. Surface replica of a thin film from Fluon GP-1 dispersion particles heated to 350°C. and cooled slowly.   Germanium shadowed 30°; original magnification 4000×.

were also observed with films prepared in the same manner from Teflon 41BX dispersion.   Since the original polymer films were too thick to permit penetration by the electron beam, electron diffraction examination of their structure was not feasible.   However, on examination with the optical microscope with the use of reflected polarized light, the bands were found to show weak negative birefringence.

The lamellae and bands observed on the surface of these films are believed to correspond to the single crystal plates and the broad striated needles described earlier.   The crystal forms seen in the films were less well defined than those obtained when isolated portions of dispersion polymer were heated.   However, this is to be expected, because in each region of the film the crystallization of the molten polymer was constrained by the material in adjacent regions.

DISCUSSION

1. Interpretation of the Optical Evidence

The appearance of the larger crystal plates in the polarizing microscope is confirmation of the electron diffraction evidence that these are polymer single crystals, and that their molecular chains are oriented perpendicularly to their basal plane.   Since PTFE is known[4] to have a hexagonal unit cell, a single crystal of the polymer would be expected to show uniaxial properties, with the optic axis coincident with the chain direction, and thus to present the isotropic view actually observed when viewed along this direction with the plate lying flat on the microscope slide.

Further consideration of the optical properties of these single crystal plates leads to tentative conclusions regarding the structure of the separate striated needles (Figs. 2 and 6) and the rather similar striated bands on the surface of the continuous films of the type seen in Figure 7.   Thus, polymer chains have, in general, a higher refractive index for light vibrating in a direction parallel with their length than for light vibrating perpendicular to the chains; that this is the case for PTFE has been shown by Bunn and co-workers.[3,4]   Therefore, the optical properties of a single crystal plate of the polymer should be represented by a positive uniaxial indicatrix. Consequently, minimum (zero) birefringence will be shown when the plate transmits light along the optic axis and parallel with the chain direction, the specimen then showing equal and minimal refractive indices in all directions perpendicular to the chains; this corresponds to the isotropic view described above.   Maximum birefringence would be expected when the plate transmits light in a direction normal to the chain direction, with the maximum and minimum refractive indices shown for light vibrating in planes parallel and perpendicular, respectively, to the chain direction.   To observe this, it would be necessary to view the crystal plates edge-on; we have not yet attempted to mount one of the plates in this manner.   For all other transmission directions, corresponding to various inclinations of the plate to the microscope stage, intermediate birefringence

would be observed, the index for light vibrating in planes across the chains having the minimum value, and that for light vibrating in the perpendicular direction having some intermediate value, depending on the inclination of the plate. In these cases, it is evident that the direction of this intermediate, highest observed, refractive index will also be the direction of the projection of the molecular chains on the microscope stage. A more or less parallel arrangement of such inclined crystal plates, in which the striations seen in the electron microscope represent inclined edge views of the individual plates or lamellae, seems to provide the most probable interpretation of the separate needles, and also, of the bands on the film surface. The fact that the needles showed parallel extinction indicates that they had a considerable degree of crystalline order, with the molecular chains oriented in a definite direction. Moreover, this molecular chain direction was apparently such that its projection in the base plane was perpendicular to the length of the needle; this follows from the considerations above and the fact that the highest refractive index was observed in this direction. The feeble negative birefringence of the bands in the film surface may signify that in these the crystalline sheets are inclined at rather small angles to the film surface. This does, in fact, appear to be the case in the bands seen in Figure 7. Although this model, resembling a stack of planks which has been pushed over sideways, does not explain the bright striations seen when the needles are at their position of maximum extinction between crossed polarizers, these striations may signify that not all of the polymer sheets are parallel, some being skewed from the direction of the length of the needle.

2. Evidence for Molecular Chain Folding

The thickness of the single crystal plates observed in this work varied in the range of about 150–900 A. As shown by the electron diffraction and polarizing microscope evidence, the PTFE molecular chains in these crystals were oriented vertically within the plate thickness. The observed thicknesses, therefore, represent chain segments of about 115–690 CF_2 groups, corresponding to molecular weights of about 5,750–34,500. Since the crystal plates were formed directly from molten clusters of dispersion particles, the molecular weight of the constituent polymer must have been that of the whole dispersion polymer after heating, as there appears no possibility for molecular fractionation, such as might occur during recrystallization from a solvent. The original dispersion polymer is known[5] to have a molecular weight of several million. If it preserved a comparable value after the heating, it is evident that, for the molecular chains to be accommodated vertically within the plate thickness, they must have assumed the folded configuration previously reported[1] for single crystals of other polymers. In fact, such folding must have occurred unless the heating reduced the molecular weight of the thinnest plates to a value as low as the 5,750 figure mentioned above. Such extensive thermal degradation seems very improbable under the comparatively mild conditions used,

First, although involving longer heating times, these conditions were at a maximum temperature some 30°C. below those customarily used in the commercial fabrication of this polymer. Moreover, published studies[6,7] have shown that the rate of thermal decomposition of the polymer to form monomer is negligible at temperatures below about 400°C., the velocity constant for this reaction being only about 10^{-8}/sec. at this temperature. Although the present interest is not so much in the formation of monomer as in degradation to form lower molecular species, which are not necessarily volatile, these data indicate that little decomposition occurred at the 350°C. temperature used here.

While it thus seems fairly certain that the melt crystallization of PTFE occurs by a chain-folding mechanism, it is not yet known what factors govern the fold length. Although the present observations suggest that the thickness of the melt-grown single crystals depends at least partly on the amount of polymer involved in their crystallization, further work will be necessary for an understanding of the relation between the fold period and heating conditions, similar to that for polyethylene.[8]

3. The Relation of the Present Observations to Previous Studies with PTFE

As mentioned in the introduction, Bunn and co-workers have reported[3] a banded type of structure on fracture surfaces from bulk specimens of both granular and dispersion-based PTFE; these specimens had been cooled slowly from 380°C. and then fractured at liquid nitrogen temperature. In the case of the granular polymer, the bands were about 0.2–1 μ in width and showed a fine structure of parallel striations, separated by varying distances down to about 300 A., in a direction perpendicular to the band length. With specimens from dispersion polymer, similar striated bands were seen, but in these the striations were parallel with the band length. In both cases, optical evidence (the negative sign of the birefringence) showed the molecular chain direction to be perpendicular to the length of the bands. Subsequent studies have shown[9] that perpendicularly striated bands in such fracture surfaces can be observed with both types of polymer.

The considerations of the previous section show beyond reasonable doubt that the melt crystallization of PTFE occurs by chain folding to give plate-like crystals or lamellae in which the folded chain segments are oriented perpendicular to the base of the plate. Although the work was confined to dispersion polymer, there is no reason to believe there would be any basic difference in the behavior of the higher molecular weight granular material, and so this new information may be applied for further interpretation of the previous observations made with both types of polymer.

The present evidence is thought to support Bunn and co-workers' suggestion[3] that the perpendicularly striated bands may be sheets seen edgewise, and it is now suggested that these bands represent the outlines of crystal plates which have been fractured in planes perpendicular to their

bases, and so along the chain direction. The sharpness which they observed for the edges of the bands would thus be a consequence of the uniformity of the chain-fold length. Also, the negative sign they reported for the birefringence of these bands would be in accordance with the optical properties expected for an edge view of a uniaxial positive crystal plate, described earlier in this paper. In the present work with dispersion polymer, the greatest thickness of a plate for which a single crystal electron diffraction pattern was obtained was about 900 A., corresponding to chain segments of molecular weight about 34,500. Although Bunn reports typical band widths of 7000–8000 A., corresponding to segment molecular weights of about 300,000, it is possible that crystal plates of this greater thickness and chain-fold length might be formed in the interior of the higher molecular weight granular polymer and with the different temperature conditions used. The origin of the striations across the band width is not yet entirely clear. However, electron micrographs of this type of band (e.g., Figure 1 of reference 3) suggest that many of the individual striations are not coplanar with the overall fracture surface, the bands having a sawtooth type of appearance. They may perhaps result from cleavage of the plates in a random manner along different planes parallel with the chain direction.

The longitudinally striated bands seen on fracture surfaces from the dispersion polymer appear to be similar structures to the separate needle-like crystals and the bands on the surfaces of films observed in the present work with the same polymer. This is suggested by the similar appearance and also by the negative sign of the birefringence of all three forms. Thus, it seems probable that these fracture bands also consist of stacks of overlapping thin sheets of polymer, in which the striations represent edge views of the individual sheets, as suggested by Bunn and co-workers. Here it is interesting to note that the 1000 A. spacing which they observed for the striations is about the same as the 900 A. seen now for the thickness of single crystal plates of this polymer. Such longitudinally striated bands in fracture surfaces are presumably formed when the fracture occurs along planes approximately parallel with the broad surfaces of the crystal sheets, with superimposed sheets in the stacks being split apart in the process. In other words, such bands probably result when the fracture is predominantly interlamellar, rather than intralamellar, as in the cases where the perpendicularly striated bands are observed.

References

1. Keller, A., *Makromol. Chem.*, **34**, 1 (1959).
2. Symons, N. K. J., *J. Polymer Sci.*, **51**, S21 (1961).
3. Bunn, C. W., A. J. Cobbold, and R. P. Palmer, *J. Polymer Sci.*, **28**, 365 (1958).
4. Bunn, C. W., and E. R. Howells, *Nature*, **174**, 549 (1954).
5. Doban, R. C., A. C. Knight, J. H. Peterson, and C. A. Sperati, paper presented at 130th Meeting, American Chemical Society, Atlantic City, N.J., Sept. 1956.

6. Madorsky, S. L., et al., *J. Res. Natl. Bur. Std.*, **51**, 327 (1953).

7. Siegle, J. C., and L. T. Muus, paper presented at 130th Meeting, American Chemical Society, Atlantic City, N.J., Sept. 1956.

8. Statton, W. O., and P. H. Geil, *J. Appl. Polymer Sci.*, **3**, 357 (1960).

9. Geil, P. H., unpublished information.

Résumé

La cristallisation à partir de l'état fondu du polytétrafluoroéthylène dispersé en quantités variant de simples particules dispersées à des films continus, a été étudiée au microscope électronique par diffraction des électrons et par microscopie optique. On admet que la dégradation thermique du polymère durant la cristallisation peut être négligée en raison de l'emploi d'une température ne dépassant pas 350°C. Grâce à l'utilisation de très faibles quantités de polymère, des monocristaux d'une épaisseur allant de 150 à 900 A. ont pu être obtenus. Dans ces derniers les chaînes moléculaires sont orientées perpendiculairement au plan de base du cristal; ceci indique que la cristallisation à partir de l'état fondu du polytétrafluoroéthylène s'effectue par un mécanisme de plissement des chaînes, ainsi qu'il a été démontré précédemment pour d'autres hauts polymères. Ces connaissances nouvelles permettent une interprétation plus positive des structures en bandes striées observées précédemment sur les surfaces produites lors de la rupture de spécimens bruts de ce polymère tant sous forme granulée que sous la forme de dispersion. De telles bandes montrant des striations perpendiculaires à leurs longueurs représentment probablement des plaques cristallines individuelles formées par fracture suivant des plans perpendiculaires à leurs bases. Des bandes montrant des striations longitudinales, par contre, résultent de la séparation d'amas de telles plaques ou lamelles suivant des plans de fracture approximativement parallèles à leurs surfaces. Ces observations réalisées sur des monocristaux isolés et bien définis à partir du polymère fondu distinct d'une solution peuvent être considérées comme vraiment nouvelles. Quoiqu'observée jusqu'ici uniquement dans le cas du polytétrafluoroéthylène, la croissance de tels monocristaux à partir de l'état fondu peut être possible pour d'autres polymères à condition d'étudier ces derniers en quantités très faibles.

Zusammenfassung

Die Kristallisation von Polytetrafluoräthylen auf Dispersionsbasis in Mengen von einzelnen Dispersionsteilchen bis zu kontinuierlichen Folien aus der Schmelze wurde durch Elektronenmikroskopie, Elektronenbeugung und optische Mikroskopie untersucht. Da die angewendete Maximaltemperatur nur 350°C betrug, kann angenommen werden, dass der thermische Abbau während der Kristallisation zu vernachlässigen ist. Bei Verwendung sehr geringer Polymermengen wurden Einkristalle mit Dicken zwischen 150 und 900 A. beobachtet, deren Molekülketten senkrecht zur Basisebene des Kristalls orientiert sind; das zeigt, dass die Schmelzkristallisation von Polytetrafluoräthylen, so wie früher schon für andere Hochpolymere beschrieben, über einen Kettenfaltungsmechanismus verläuft. Diese neue Erkenntnis erlaubt eine positivere Interpretation der früher an Bruchflächen von Proben dieses Polymeren auf Dispersionsbasis und vom gekörnten Typ beobachteten gestreiften Bandstrukturen. Solche Bänder, die Streifung senkrecht zu ihrer Längserstreckung zeigen, stellen wahrscheinliz individuelle Kristallplättchen vor, welche in einer zur Basis senkrechten Ebene gebrochen wurden, während Bänder mit longitudinaler Streifung durch Abspaltung von solchen gestapelten Platten oder Lamellen entlang einer Bruchebene parallel zur Oberfläche zustandekommen. Die jetzige Beobachtung isolierter und wohldefinierter Einkristalle aus einer Polymerschmelze, im Gegensatz zur Lösung, scheint völlig neu zu sein. Das Wachstum solcher Einkristalle aus der Schmelze wurde zwar bis jetzt nur an Polytetrafluoräthylen beobachtet, dürfte aber auch bei anderen Polymeren möglich sein, wenn diese nur in sehr kleinen Mengen untersucht werden.

The Effect of Molecular Weight Distribution on the Optical Properties of Polystyrene in the Transition Region

J. F. RUDD and E. F. GURNEE, *Physical Research Laboratory, The Dow Chemical Company, Midland, Michigan*

Synopsis

Birefringence measurements during relaxation of stress have been made on five narrow molecular weight distribution (anionic) polystyrenes at temperatures of 91.5, 95.0, and 98.5°C. One broad distribution (isothermal) polystyrene was measured at 91.5°C. The birefringence vs. log time curves obtained are observed to pass through a maximum, the magnitude of the maximum being independent of molecular weight above $\bar{M}_w = 154,000$ and increasing with temperature at constant $\bar{M}_w$. Increasing molecular weight heterogeneity causes the birefringence decay curves to shift to later times and broaden slightly, and the magnitude of their maxima to decrease. Decay data previously obtained on a plasticized commercial polystyrene are presented and shown to be in agreement with present findings. No substantial change in energy of activation associated with the decay process ($E_a = 150$ kcal./mole) is observed with either broadening of molecular weight distribution or with plasticization.

Introduction

The effect of molecular weight and molecular weight distribution on the viscoelastic properties of polymeric materials has been discussed by several authors.[1-4] The influence of molecular weight distribution, in particular, has been investigated by both creep[5] and stress relaxation techniques.[6,7] The influence of molecular weight distribution on the optical effects associated with viscoelastic properties, on the other hand, has not received a great deal of attention to date (with the exception of one study of creep, recovery, stress relaxation, and birefringence of polystyrene in the rubbery state[8]). In view of the scarcity of published information dealing with optical properties in the region where retarded elastic mechanisms predominate, the investigation of the effect of molecular weight and molecular weight distribution upon such properties was felt to be useful both from a practical standpoint as well as from a theoretical one.

One way of doing this might be to measure the birefringence changes accompanying relaxation of stress over a suitable temperature and molecular weight range. This could be accomplished rather easily if the material selected for investigation had a transition region somewhere between
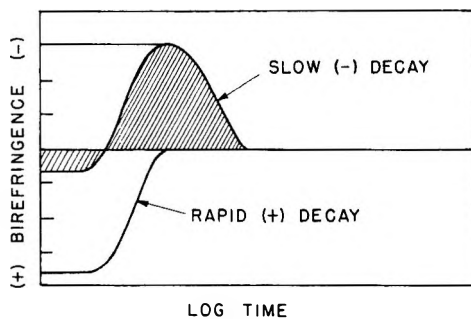
Fig. 1. Mechanism for birefringence decay of polystyrene.

25° and 100°C.* and lacked the complicating optical effects produced by crystallinity changes during stretching. One polymer which satisfied these requirements was polystyrene. In addition, it was capable of being produced in varying degrees of molecular dispersity when suitable polymerization techniques were employed.

It had been previously observed,[12] although it was not recognized at that time, that the birefringence decay curve for polystyrene does not show a simple monotonic decrease with time. Rather, it increases relatively rapidly at first from a positive value (or one close to zero), reaches a maximum at some time, which, in general, varies inversely with the temperature, and then decays toward zero. Such a curve can be considered to be the algebraic sum of two exponential terms, one with a larger positive coefficient, the other with a smaller negative coefficient. The relaxation times associated with the exponential terms determine the rates at which the positive and negative birefringence contributions decay. The birefringence maximum results when the positive contribution has decayed completely or when it reaches some constant nonzero value. This is shown schematically in Figure 1 where positive, negative, and net birefringence are plotted against log time. The relaxation times for the two component decay curves shown in this figure may be assumed to differ by 2 or 3 orders of magnitude.

Samples and Experimental Method

Five anionically polymerized, narrow molecular weight polystyrenes ranging in molecular weight from 125,000 to 267,000 were detained from H. W. McCormick and F. Brower of this Company. These materials had been polymerized under carefully controlled conditions with a butyl-lithium–benzene catalyst system and were devolatilized upon completion of the polymerization to remove the residual solvent. Characterization as to molecular weight was accomplished by ultracentrifugation in cyclohexane at 35°C.[13] Intrinsic viscosities were determined in toluene at 25°C. and

* Not only mechanical but also optical properties of high polymers are known to be temperature-sensitive in the transition region. Indeed, in the case of crosslinked polyethyl acrylate,[9] polymethyl methacrylate,[10] and polystyrene[11] there is a change in sign of the birefringence produced by an applied stress, time effects being much in evidence.

TABLE I

Polystyrene Samples

Material	$[\eta]^a$	η_1, poise[b]	Heat distort., °C.	$\bar{M}_w$	$\bar{M}_n$	$\bar{M}_w/\bar{M}_n$
			Anionic polystyrene			
S103	0.520	1,400	103	124,700	118,000	1.05
S105	0.606	2,600	101	153,000	147,500	1.04
S109	0.701	5,000	102	193,000	182,000	1.06
S111	0.777	7,800	100	239,000	221,000	1.08
S108	0.872	12,200	105	267,000	247,000	1.08
			Isothermal polystyrene			
B4	0.787	3,450	104	255,000	130,000	1.96
			Thermal polystyrene			
Extr. 666	0.905	1,720	86	320,000	78,000	4.0

[a] Determined in toluene at 25°C.

[b] Determined at 227°C. (see ref. 15).

heat distortion measurements were made in an effort to assess volatile content according to the method of Hierholzer and Boyer.[14] Melt viscosities of these materials at 227°C. have been reported previously.[15]

Besides the five narrow-distribution polystyrenes, a broad-distribution polymer which had been prepared under isothermal conditions was also measured. Intrinsic viscosities, melt viscosities, (η_7), heat distortions, and molecular weight data for all materials used are given in Table I.

Test specimens were rectangular bars which measured 6 in. $\times$ $1/2$ in. $\times$ $1/10$ in. These were cut oversize from compression-molded sheets and then reduced to final dimensions by hand filing and polishing. All specimens possessed essentially zero orientation, as revealed by examination with polarized light.

Birefringence measurements during relaxation of stress were made in a continuous fashion by using the optical portion of a special apparatus which has been described elsewhere.[12] Birefringence was measured at temperatures of 91.5, 95.0, and 98.5°C., temperature being maintained to within 0.25°C. by means of a mercury-type temperature controller located in the oil bath surrounding the viewing chamber.

Test specimens were suspended in the apparatus at least 12 hrs. prior to an experiment, in order to allow any small internal stresses introduced during sample preparation to relax out. The lower end of a specimen was clamped, as before, to a connecting rod which passed down through the bottom of the viewing chamber. This rod was not, however, attached to the lever arrangement shown in Figure 1 of reference 12, but rather was fastened to a system of fairly stiff springs which permitted one to approach a condition of "instantaneous" stretch. Predetermined elongations were obtained by setting a stop on the connecting rod with the aid of a feeler gauge.

Experimental Results and Discussion

The general type of birefringence curve obtained for polystyrene in the transition region is shown in Figure 2 where birefringence/strain ratio is plotted against log time for one of the narrow distribution materials (S105). The two types of points shown are indicative of the approximate reproducibility of the method. The data are plotted as a ratio rather than simply as birefringence, to facilitate comparison of data obtained at different levels of strain (stop settings were adjusted so as to obtain an optimum birefringence effect for each molecular weight and temperature).

It will be noticed in Figure 2 that the birefringence/strain ratio increases at first in a negative sense, passes through a maximum, and then decreases monotonically toward zero. Since the observed maximum is in the negative direction, it is necessary to assume that the positive birefringence decays more rapidly than the negative. It must be remembered that only the *total* curve can be observed experimentally. Furthermore, it can be seen that the maximum will only be obtained over a limited temperature region. If the temperature is too high, the positive birefringence will decay before the measuring equipment can respond; if it is too low, the maximum will still occur, but at inconveniently long times.

The positive birefringence in polystyrene is associated with the twisting of the phenyl groups so that their axes become parallel to the direction of the applied stress, while the negative birefringence is associated with chain orientation which causes the axes of the phenyl groups to become perpendicular to the direction of the applied stress. (A little manipulation with a molecular model will indicate how the chain motion tends to align the phenyl groups at right angles to the direction of stretch, while side group twisting results in the phenyl groups being partially aligned in the same direction as the stress.) The fact that the positive birefringence decay is more rapid than the negative is consistent with the assumptions that chain
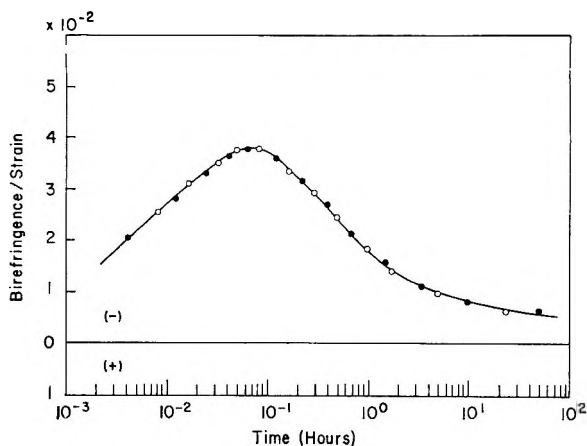

Fig. 2. Birefringence/strain ratio vs. log time for narrow-distribution polystyrene (S105) at 91.5°C.
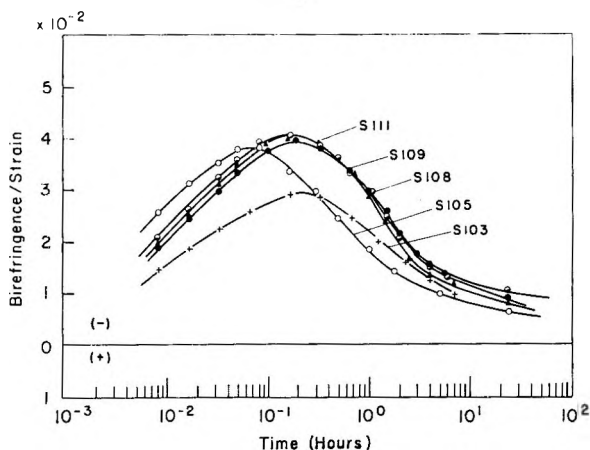
Fig. 3. Birefringence/strain ratio vs. log time for five narrow-distribution polystyrenes at 91.5°C.
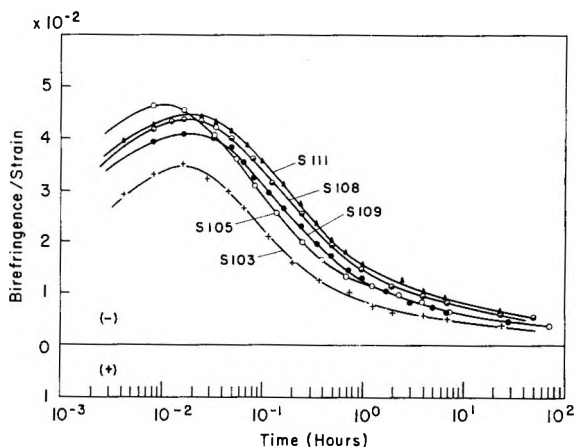

Fig. 4. Birefringence/strain ratio vs. log time for five narrow-distribution polystyrenes at 95.0°C.

motion involves many molecular segments, is much more involved and, therefore, requires a longer time to accomplish.

The effect of molecular weight on birefringence decay rate is shown in Figures 3–5, where decay curves are plotted for five narrow molecular weight polystyrenes at temperatures of 91.5, 95.0, and 98.5°C., respectively. It will be observed in Figures 3 and 4 that the magnitude of the birefringence–strain maximum, which may be used as a rough index of the amount of orientation introduced during the stretching process, increases with molecular weight up to $\bar{M}_w = 154{,}000$, remaining constant at higher molecular weights. An apparent exception to this observation is the 154,000 molecular weight curve at 95.0°C. (Fig. 4), which exhibits a higher maximum than any of the other materials shown in this figure. This
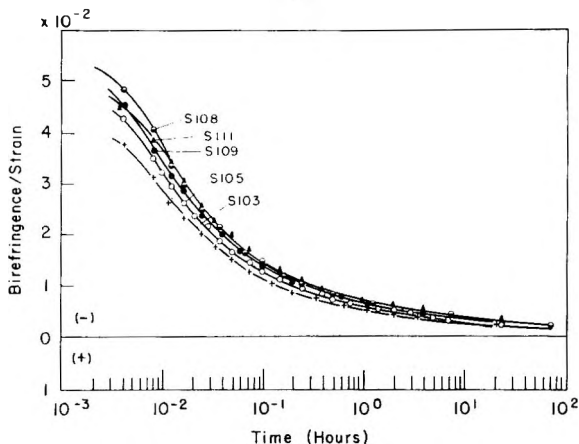
Fig. 5. Birefringence/strain ratio vs. log time for five narrow-distribution polystyrenes at 98.5°C.
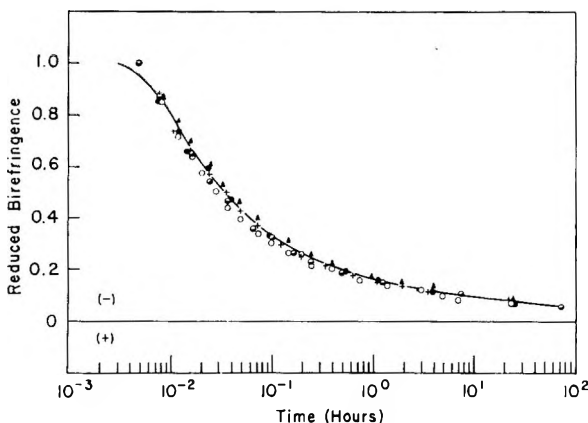
Fig. 6. Reduced birefringence vs. log time for five narrow-distribution polystyrenes at 98.5°C.

discrepancy was checked by running triplicate experiments, birefringence decay curves which essentially reproduced the one shown in Figure 4 being obtained. In this connection it may also be observed that the time at which the birefringence–strain maximum occurs for this material differs by about $1/2$ log cycle from the maximum times of the other polystyrenes, pointing to a definite difference in optical behavior.

A comparison of the maximum time values for the same material at two different temperatures (Figures 3 and 4) indicates a shift in the peak of approximately 0.3 log cycle/°C. This is in substantial agreement with birefringence decay data obtained previously on an extruded sheet made from a commercial polystyrene[16] which contained less than 1% plasticizer (Extr. 666).

The effect of molecular weight on decay rate is more clearly seen in Figure 5, where the longer-time portion of the curves is in greater evidence than

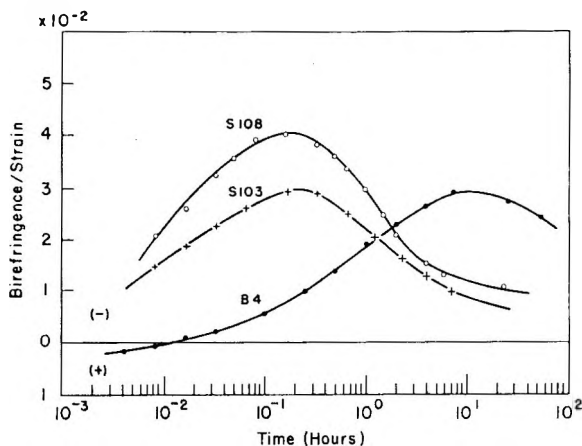Fig. 7. Birefringence/strain ratio vs. log time for broad (●) and narrow (+, O) distribution polystyrenes at 91.5°C.

in either of the two previous figures. It is apparent from inspection of the curves in Figure 5 that molecular weight has very little effect upon decay rate in the molecular weight range covered. In fact, if the data be replotted as reduced birefringence (birefringence referred to its value at some arbitrary time, in this case 0.005 hr.) versus log time, as has been done in Figure 6, what is virtually a single curve is the result.

In order to study the effect of molecular weight distribution on optical properties, birefringence decay curves for two of the narrow-distribution polystyrenes (S103 and S108) were compared with the decay curve for a broad distribution polystyrene (B4) at a single temperature (91.5°C.). The results are shown in Figure 7 plotted as birefringence/strain ratio versus log time. A rather remarkable point to be noticed here is that, although the broad-distribution polymer has approximately the same heat distortion temperature as those of the two narrow-distribution materials, the birefringence maximum of the former occurs about two decades later in time than the maxima of the latter. Hence it would appear that birefringence decay rate does not correlate solely with heat distortion temperature, as has often been assumed.

Another interesting feature of Figure 7 is the disparity of the birefringence/strain maxima between the three materials. S108 and B4 have almost the same weight-average molecular weight, while S103 and B4 have about the same number-average molecular weight. From this one may conclude that the magnitude of the birefringence peak correlates with $\bar{M}_n$ whereas the time at which the peak occurs, $t_{max\Delta}$, depends upon $\bar{M}_w$ or some higher molecular weight average.

In order to check these conclusions further, the limiting birefringence curves obtained for the narrow-distribution polystyrenes at 91.0, 95.0, and 98.5°C. were compared with similar decay curves for a commercial broad-distribution polystyrene (Extr. 666) which had been obtained previously.[16]
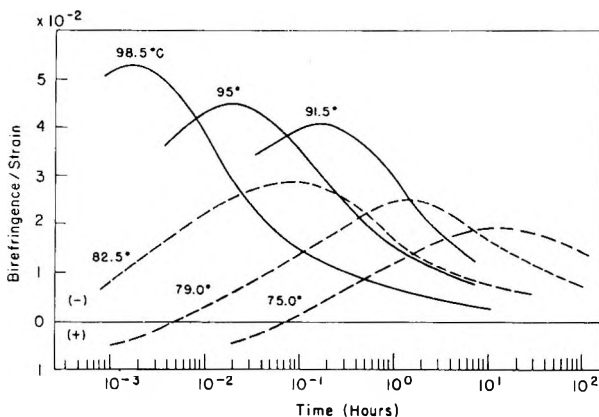
Fig. 8. Birefringence/strain ratio vs. log time for commercial broad- (- - -) and narrow-
(—) distribution polystyrenes.

Because the commercial material contained a small amount of plasticizer (estimated from weight loss upon precipitation in methanol to be less than 1%) it had both a lower heat distortion temperature and a lower high-shear melt viscosity than a narrow-distribution polystyrene of approximately the same weight-average molecular weight (see Table I). Since the presence of even a small amount of low molecular weight material has a marked effect upon the mechanical and rheological properties of high polymers, an attempt was made to eliminate this effect by comparing birefringence decay curves for the plasticized polymer with limiting curves for the narrow-distribution polystyrenes, referring each to its respective heat distortion temperature. (The heat distortion temperature for the plasticized polymer was 86°C. while that for the narrow distribution polystyrenes, 102°C., was obtained by averaging heat distortion values for the separate polymers.) These curves are shown, plotted in the usual way, in Figure 8.

Several features of this figure deserve comment. The failure of the birefringence/strain maxima of the two types of polymer to coincide in time—even though the curves have been chosen in such a way as to minimize differences in internal mobility due to plasticizer—is not surprising when one considers the range of molecular weights encompassed in each case. The range for each of the narrow-distribution polymers is less than 200,000 while for the broad-distribution material it is 1,400,000.

The fact that the birefringence/strain maxima of the commercial polystyrene occur at later times than those of the narrow-distribution polymers is indicative of the importance of the high molecular weight "tail" of the former. Abnormal prolongment of the relaxation time spectrum brought about by high molecular weight species had previously been observed in the case of concentrated polyisobutylene solutions by Ferry and co-workers.[17] The importance of high molecular weight material in bulk polymers was also noted by Bueche,[18] who first suggested that the rapid increase of the
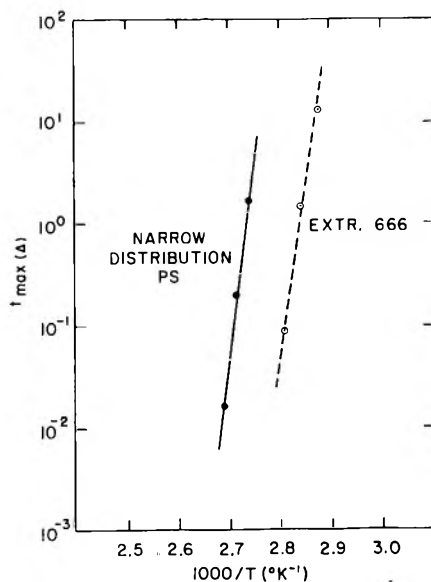
Fig. 9. Arrhenius plots of $t_{max\Delta}$ for commercial broad- and narrow-distribution polystyrenes.
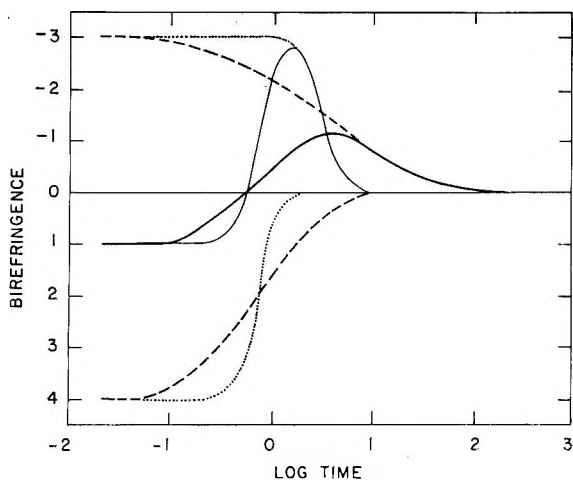
Fig. 10. Birefringence decay curves for a monodisperse ($\cdots$) and a polydisperse (- - -) polymer exhibiting positive and negative birefringence.

segmental friction coefficient with molecular weight was due to coupling by molecular entanglement.

The temperature dependence of the time at which the birefringence maximum occurs ($t_{max\Delta}$) appears at first glance to be slightly greater for the narrow-distribution polymers. That this is not the case can be seen by plotting the logarithm of $t_{max\Delta}$ versus $1/T$ for the two types of polymers, as

is done in Figure 9. Since this plot yields reasonably straight lines over the temperature range covered, one may write

$$t_{max\Delta} = Ae^{E_o/RT}$$

where E_a has an approximate value of 150 kcal./mole. This value agrees fairly well with energies of activation for various polymer systems determined from stress relaxation experiments in the transition region and above,[19] and is in good agreement with the activation energy of polystyrene obtained from retraction measurements[20] in the range 75–95°C. However, it is clear that these curves cannot be rigorously superimposed by shifting.

The decrease in the magnitude of the birefringence maxima with increasing molecular weight heterogeneity may be explained in the following way. The observed birefringence decay curve for polystyrene may be considered to be made up of two separate decay curves, as was shown in Figure 1. One of these is positive in sign and is associated with twisting of the phenyl groups, the other is negative and is associated with molecular configuration changes. For a system of molecules which is monodisperse there will be a distribution of optical relaxation times for each of these decay curves, reflecting the participation of differently sized polymer segments in the relaxation process (see ref. 1, pp. 148–152). For a system of molecules which is polydisperse, there will be an even broader distribution of optical relaxation times for each of the birefringence curves, since both spectra will incorporate a range of optical contributions. The net birefringence curve will, in consequence, show a maximum which is both less in magnitude and displaced to longer times in comparison with the net birefringence curve for the monodisperse system. That this result is due solely to the greater dispersion of the separate decay curves may be seen in Figure 10 where birefringence is plotted against log time for a monodisperse and a polydisperse system. (These curves do not represent actual optical distributions but are merely meant to illustrate the explanation presented above. An explanation somewhat different from that given here must be used to account for the decrease in the magnitude of the birefringence maxima with decreasing temperature. Such an explanation would involve, among other things, a difference in the energies of activation between the positive and negative birefringence contributions.)

References

1. Alfrey, T., *Mechanical Behavior of High Polymers*, Interscience, New York–London, 1948, pp. 145, 148.

2. Andrews, R. D., N. Hofman-Bang, and A. V. Tobolsky, *J. Polymer Sci.*, **3**, 669 (1948); Brown, G. M., and A. V. Tobolsky, *J. Polymer Sci.*, **6**, 165 (1951).

3. Tobolsky, A. V., and J. R. McLoughlin, *J. Polymer Sci.*, **8**, 543 (1952); McLoughlin, J. R., and A. V. Tobolsky, *J. Colloid Sci.*, **7**, 555 (1952).

4. Schmieder, K., and K. Wolf, *Kolloid-Z.*, **134**, 149 (1953).

5. Van Holde, K. E., and J. W. Williams, *J. Polymer Sci.*, **11**, 243 (1953); Swanson, D. L., and J. W. Williams, *J. Appl. Phys.*, **26**, 810 (1955).

6. Ninomiya, K., *J. Colloid Sci.*, **14**, 49 (1949).

7. Tobolsky, A. V., and K. Murakami, *J. Polymer Sci.*, **40**, 443 (1959); *ibid.*, **47**, 55 (1960).

8. Nielsen, L. E., and R. Buchdahl, *J. Colloid Sci.*, **5**, 282 (1950).

9. Stein, R. S., S. Krimm, and A. V. Tobolsky, *Textile Res. J.*, **19**, No. 1 (1949).

10. McLoughlin, J. R., Ph.D. Dissertation, Princeton University (1951).

11. Andrews, R. D., and J. F. Rudd, *J. Appl. Phys.*, **28**, 1091 (1957).

12. Gurnee, E. F., L. T. Patterson, and R. D. Andrews, *J. Appl. Phys.*, **26**, 1106 (1955).

13. McCormick, H. W., *J. Polymer Sci.*, **36**, 341 (1959).

14. Hierholzer, G. A., and R. F. Boyer, *ASTM Bulletin* No. 134, 37 (1945).

15. Rudd, J. F., *J. Polymer Sci.*, **44**, 459 (1960).

16. Gurnee, E. F., unpublished results.

17. Ferry, J. D., I. Jordan, W. W. Evans, and M. F. Johnson, *J. Polymer Sci.*, **14**, 261 (1954).

18. Bueche, F., *J. Chem. Phys.*, **20**, 1959 (1952); *J. Appl. Phys.*, **26**, 738 (1955).

19. Ninomiya, K., and H. Fujita, *J. Colloid Sci.*, **12**, 204 (1957).

20. Andrews, R. D., *J. Appl. Phys.*, **26**, 1061 (1955).

Résumé

On a effectué des mesures de biréfringence au cours de la rélaxation de tension sur cinq échantillons de polystyrène (anionique) de distribution de poids moléculaire resserre, et ce à 91,5°, 95.0° et 98.5°C. On a mesuré une large distribution (isotherme) de polystyrène à 91.5°C. On observe que les courbes obtenues de la biréfringence en fonction du log du temps passent par un maximum, la grandeur de ce maximum étant indépendante du poids moléculaire au-dessus de $\bar{M}_w = 154.000$ et il augmente avec la température pour un $\bar{M}_w$ constant. Une augmentation de l'hétérogénéité du poids moléculaire cause un glissement des courbes de perte de biréfringence vers des valeurs de temps plus élevées; elle cause un faible élargissement de la courbe et une diminution du maximum. Les données concernant la perte de biréfringence obtenues antérieurement sur des matériaux plastifiés, du polystyrène commercial, sont présentées et sont en accord avec les résultats présents. On n'observe pas de changement substantiel dans l'énergie d'activation associée au processus de perte ($E_a = 150$ kcal/mole) ou à l'élargissement de la distribution du poids moléculaire ou à la plastification.

Zusammenfassung

Doppelbrechungsmessungen werden an fünf Polystyrolen mit enger Molekulargewichtsverteilung (anionisch) während der Spannungsrelaxation bei Temperaturen von 91,5°, 95.0° und 98,5° ausgeführt. Ein breit verteiltes Polystyrol (isotherm) wurde bei 91,5°C vermessen. Die erhaltenen Kurven Doppelbrechung gegen log Zeit gehen durch ein Maximum; die Grösse des Maximums ist oberhalb $\bar{M}_w = 154000$ vom Molekulargewicht unabhängig und nimmt mit der Temperatur bei konstantem $\bar{M}_w$ zu. Mit zunehmender Molekulargewichtsheterogenität verschieben sich die Kurven für den Rückgang der Doppelbrechung zu späteren Zeiten, verbreitern sich schwach und die Grösse ihrer Maxima nimmt ab. Früher an weichgemachtem, handelsüblichem Polystyrol erhaltene Daten werden mitgeteilt; sie sind mit den jetzt gewonnenen Befunden in Einklang. Weder bei der Verbreiterung der Molekulargewichtsverteilung noch bei der Weichmachung wird eine wesentliche Änderung der Aktivierungsenergie des Abfallprozesses ($E_a = 150$ kcal/Mol) beobachtet.

Long-Chain Branching Frequency in Polyethylene*

J. E. GUILLET, *Research Laboratories, Tennessee Eastman Company, Division of Eastman Kodak Company, Kingsport, Tennessee*

Synopsis

A study was made of the long-chain branching frequency of polyethylene by using data on polyethylene fractions reported by Moore and co-workers. It was found that the frequency of long-chain branching does not increase with increasing molecular weight, as predicted by Beasley's theory, but remains relatively constant. This means that molecular weight distributions calculated by assuming the validity of the Beasley relations will be broader than those determined experimentally. It was also found that the viscosity–molecular weight relation for branched fractions can be constructed from a knowledge of g, a parameter related to the mean square radius of gyration of the molecules, assuming only the validity of the relation $g^{3/2} = [\eta]_{br}/[\eta]_{lin}$. A method was developed for determining γ^*, which is the frequency of long-chain branches corrected for short-chain branching. Since the value of γ^* is nearly constant throughout the distribution, determination of γ^* for a high molecular weight fraction allows the construction of the complete viscosity–molecular weight relation for all fractions of the same polymer. This relation can then be used to characterize the molecular weights of the fractions and hence the shape of the actual molecular weight distribution curve.

Introduction

The polyethylene molecule, when synthesized by a typical high-pressure process, is believed to be a branched structure containing both short-chain and long-chain branches.[1] The short-chain branches are from two to six carbon atoms in length and are probably formed by intramolecular chain transfer during the polymerization. The long-chain branches are formed by intermolecular chain transfer, in which an active radical abstracts a hydrogen atom from a "dead" polymer chain and the resulting radical can grow by further addition of ethylene units, giving a long branch attached at some random position along the length of the original polymer chain. According to Beasley's theory[2] the number of these long branches will increase with the average molecular weight of the polymer molecule; this prediction has been confirmed qualitatively by the experimental results of a number of authors.[3–6]

The exact manner in which the frequency of branching (i.e., the number of branches per unit length) changes with molecular weight depends on the kinetics of the polymerization reaction. Based on a relatively simple kinetic scheme, Beasley's theory predicts that the frequency of branching

---

* Presented in part at the 141st National Meeting of the American Chemical Society, Washington, D.C., March 20–29, 1962.

also increases with molecular weight. It is very important to know the exact manner in which the long-chain branching frequency changes with molecular size, because this has decided effects on the shape of the theoretical molecular weight distribution curve.

Billmeyer[3] proposed a long-chain branching index, n, for polyethylene calculated from the value of g obtained by means of the relation:

$$g^{3/2} = [\eta]_{br}/[\eta]_{lin} \tag{1}$$

where $[\eta]_{br}$ is the intrinsic viscosity of a branched polymer, $[\eta]_{lin}$ is the intrinsic viscosity of a linear polymer of the same weight-average molecular weight, and g is the ratio of the mean square radii of branched and linear molecules of the same molecular weight.[7] The weight-average molecular weights for the polyethylene were calculated from light-scattering data. It was subsequently shown by Moore[8] that the method used in estimating these weight-average molecular weights was incorrect because of the necessity of extrapolating the results to zero angle. Further, it is difficult to obtain consistent values for weight-average molecular weights by light scattering because of the presence of small amount of very high molecular weight polymer, or "microgel," and the very high values obtained show little correlation with values calculated from distribution curves obtained by fractionation.[9,10] Also, the values of weight-average molecular weights obtained by light scattering frequently do not show the expected correlations with the rheological properties of the polymer, whereas values obtained by other methods, such as by fractionation, do.

In view of this, it is apparent that an independent method is needed for estimating long-chain branching in polyethylene. Recently, Moore and co-workers[6] developed a method of estimating long-chain branching in polyethylene fractions which was based on solution viscosity measurements and sedimentation constants obtained from ultracentrifuge data. Moore published values of g, obtained by this method, for a series of fractions reported by Guillet and co-workers,[9] who used a chromatographic fractionation method. With these data it is now possible to compare the expected frequency of long-chain branching calculated from Beasley's kinetic treatment with experimental data. The present paper is concerned with the results of such a comparison and the significance of this in terms of the interpretation of molecular weight distribution curves obtained by fractionation.

Results and Discussion

Fractionation Data

The polymer studied in this work was a typical high-pressure polyethylene made by the I.C.I. process and was designated polymer A in a previous paper.[9] It is characterized by a density of 0.917, a melt index of 1.62, and a number-average molecular weight of 26,100 (by ebulliometry).[11] Infrared measurements indicated a branching frequency of 2.4 methyl groups per hundred carbon atoms. Data on its molecular weight distribution and

TABLE I
Branching Data on Fractions from Polymer A

$[\eta]^a$	g	$\bar{M}_v$	m	γ	m^*	γ^*
0.31	0.848	9,830	1.9	2.7	0.62	0.88
0.43	0.804	17,200	2.6	2.1	1.26	1.02
0.82	0.783	42,300	3.0	1.0	1.58	0.52
0.91	0.787	49,900	2.9	0.81	1.52	0.43
1.00	0.709	68,300	4.6	0.81	2.87	0.59
1.11	0.672	91,100	5.7	0.88	3.7	0.57
1.33	0.657	123,000	6.4	0.73	4.0	0.46
1.82	0.518	311,000	13.7	0.62	9.4	0.42
1.99	0.491	392,000	16.1	0.57	11.2	0.40
2.11	0.410	614,000	26.3	0.60	21.0	0.48

[a] Intrinsic viscosity in tetralin at 100°C. calculated from inherent viscosity, corrected for solvent density and kinetic energy.

ultracentrifuge data on the fractions are also given in the previous paper.[9] On the basis of ultracentrifuge data, the fractions appeared to be quite sharp. Fractions of linear polyethylene obtained by the same method have been demonstrated[12] to have a ratio of weight-average molecular weight to number-average molecular weight, $\bar{M}_w/\bar{M}_n$, of 1.04.

Data on fractions of this polyethylene sample are given in Table I, along with the values of g reported by Moore and co-workers[6] and the values of m (the number of long-chain branches per molecule) as calculated from the relations proposed by Zimm and Stockmayer.[13]

Correction for Short-Chain Branching

In calculating his values of m, Moore assumed that short-chain branching does not affect the value of g and hence the difference observed is due entirely to long-chain branching. There is good reason to believe that the value of g may also be affected by short-chain branching. A theoretical expression for g in terms of the number and frequency of short-chain branches was proposed by Billmeyer[3] and was used by Trementozzi[5] in correcting measured values of g for short-chain branching:

$$g = (1/S + 1)[1 + S(1 - 2f + 2f^2 - 2f^3) + S^2(-f + 4f^2 - f^3)] \quad (2)$$

where S is the number of branches per molecule and f is the fractional length of the branch. If one assumes that the short-chain branches contain four carbon atoms, the calculated value of g will vary with short-chain branching frequency, as shown in Figure 1. The values shown were calculated for a molecular weight of 10,000. The value is nearly independent of molecular weight, however, and hence Figure 1 can be used to determine g to a close approximation for a molecule of any molecular weight containing only short-chain branches.

The corrected value of g can be calculated from the relation:

$$g^* = g_{obs}/g' \quad (3)$$

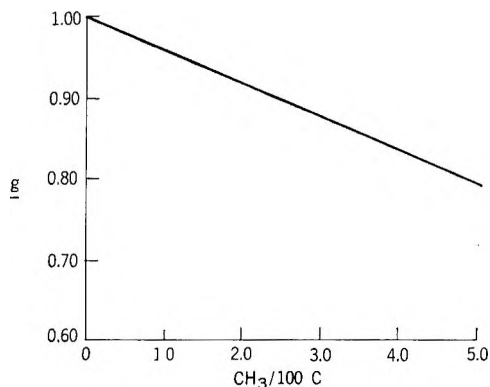where g^* is the value of g of the sample relative to a linear molecule con-

Fig. 1. Variation of g with short-chain branching (mol. wt. $= 10,000$).

taining only short-chain branches, g_{obs} is the value of g obtained by experiment, and g' is the value of g of the short-chain-branched molecule in Figure 1. The corrected value of m, which is denoted m^*, is then obtained from the Zimm-Stockmayer relation and is also included in Table I.

Calculation of Branching

It was shown by Thurmond and Zimm[7] that the intrinsic viscosities of linear and branched molecules in a theta solvent are related by eq. (1). More recently, Zimm and Kilb[14] proposed that a more correct relation is obtained by using $g^{1/2}$ in place of $g^{3/2}$ in this equation:

$$g^{1/2} = [\eta]_{\text{bi}} / [\eta]_{\text{lin}} \qquad (4)$$

This relation has received experimental support from the data of Orofino and Wenger[15] on polystyrene trifunctional star molecules. However, there is some doubt that the relation applies to the highly branched molecules found in high-pressure polyethylene. For example, Tung[16] has published data on the ratio of intrinsic viscosities of branched and linear fractions of polyethylene. These data are shown in Table II along with calculations of the number of branches per molecule, m^*, and the branching frequency, γ^* (corrected for short-chain branching), obtained by using the two rela-

TABLE II
Branching Data on Polyethylene Fractions

Frac-tion[16]	$\bar{M}_w$	$[\eta]$	$[\eta]_{\text{br}}/[\eta]_{\text{lin}}$	Branching data[a]			
				By eq. (4)		By eq. (1)	
				m^*	γ^*	m^*	γ^*
C-4	175,000	1.05	0.36	150	12	11	0.88
C-5	120,000	0.98	0.44	94	11	6.8	0.79
C-6	99,500	0.92	0.48	74	10	5.4	0.76
C-7	62,500	0.80	0.58	36	8	3.4	0.76

[a] Values of g were corrected for short-chain branching assumed to be 2.4 methyl groups per 100 carbon atoms.

tions. It is apparent that if one assumes the validity of the $g^{1/2}$ relation the number of long-chain branches per molecule becomes very large indeed—considerably larger than can be accounted for by any of the conventional kinetic explanations for long-chain branching in polyethylene. Similar conclusions may be drawn from the work of Trementozzi.[5] It is possible that these discrepancies are due to the fact that, when the viscosities were measured, a good solvent, tetralin, as opposed to a theta solvent was being used. However, Orofino and Wenger[15] showed that the ratio they obtained for linear and trifunctional star molecules of polystyrene was the same, regardless of whether it was measured with a good solvent or with a theta solvent.

In the present work it has been assumed that for branched molecules of the type found in high-pressure polyethylene the $g^{3/2}$ relation is more nearly appropriate. In the first place, it gives branching values closer to those expected from polyethylene and, second, this type of relation is implicit in the derivation of Moore's equation relating branching to viscosity and ultracentrifuge data. While future work may develop a more accurate branching equation which may alter the absolute values of the number of branches and branching frequencies reported in this paper, it is believed that the general conclusions obtained in this work will still be valid.

Calculation of Molecular Weights

Since the ultracentrifuge results have given an independent measure of g, it is possible to estimate the viscosity molecular weight of each fraction by calculating the inherent viscosity of the linear molecule of equivalent molecular weight from the Thurmond-Zimm relation, eq. (1). The molecular weight can then be obtained from the known relation between inherent viscosity and molecular weight for linear fractions. In the present work, Tung's relation was used:[17]

$$[\eta] = 5.10 \times 10^{-4} M^{0.725} \tag{5}$$

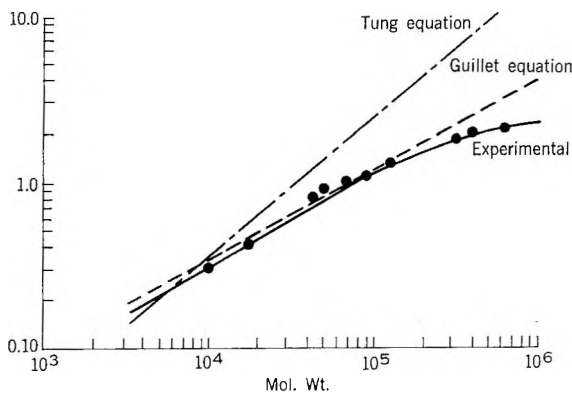The results are also included in Table I.

Fig. 2. Viscosity–molecular weight relations for linear and branched polyethylenes.

The data allow one to construct the viscosity–molecular weight relation for these branched fractions by plotting log $[\eta]$ as a function of log $\bar{M}_r$ in the usual manner.   Such a plot is shown in Figure 2 along with the relation obtained from ebulliometric molecular weight data on similar fractions reported by Guillet and co-workers.[9]   For molecular weights below 200,000, which is the upper limit of the ebulliometric measurements, the agreement is surprisingly good.   This agreement represents experimental corroboration of both the measured g values and the assumptions involved in the use of the Stockmayer relation.   At molecular weights above 200,000 the curve deviates markedly from linearity, as expected from the high degree of long-chain branching.   This effect was shown by Trementozzi[5,18] and is discussed from an empirical point of view by Mussa.[19-21]

Long-Chain Branching Frequency

By means of the molecular weights of the fractions derived from the ultracentrifuge data it is now possible to study the frequency of long-chain branches.   The frequency of long-chain branches is given by the relation:

$$\gamma = 14{,}000m/M \tag{6}$$

where γ is the long-chain branching frequency expressed in terms of branch points (or end groups) per 1000 carbon atoms and M is the molecular weight of the fraction.   Values of γ and γ^* for the various fractions are shown in Table I.   Here γ^* is the value of γ calculated from m^*, the number of long-chain branches corrected for short-chain branching.   It can be seen that the uncorrected values for long-chain branching frequency lead to unusually high values for long-chain branching in the low molecular weight fractions. The frequency gradually decreases as the molecular weight increases.   On the other hand, the values of γ^* are more nearly constant and the values for long-chain branching in the low fractions are considerably reduced by the correction for short-chain branching.   Both γ and γ^* show a significant decrease with increasing molecular weight.   This is opposed to the prediction of Beasley's theory.   Beasley's theory[2] predicts that, for all molecules having a molecular weight M, the average number of branch points, $G(m,\beta)$, is given by the relation:

$$G(m,\beta) = [(M/M_0) - 1/\beta \ln (1 + \beta M/M_0)] \tag{7}$$

where β is a branching parameter. M_0 is given by:

$$\bar{M}_n = M_0/(1 - \beta) \qquad \text{if } \beta < 1 \tag{8}$$

The weight-average molecular weight is given by:

$$\bar{M}_w = 2M_0/(1 - 2\beta) \qquad \text{if } \beta < {}^1/_2 \tag{9}$$

The ratio of the two average molecular weights is given by:

$$\bar{M}_w/\bar{M}_n = 2[(1 - \beta)/(1 - 2\beta)] \tag{10}$$

Figure 3 shows the theoretical variation of γ^* with M as calculated for
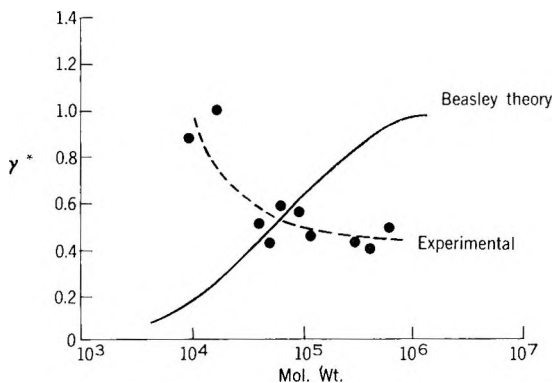
Fig. 3. Variation of γ^* with molecular weight for fractions.

polymer A, the measured value of $\bar{M}_n = 26,100$ being used and a value of $\beta = 0.50$ assumed (this value gives the closest fit to the observed distribution curve, as discussed in a later section). The experimentally determined values of γ^* are also plotted on the same scale. It is evident that the experimental values are quite different from the theoretical prediction in that they start relatively high and decrease with molecular weight to a nearly constant value, whereas the theoretical relation predicts just the opposite. The use of weight-average molecular weights (e.g., those from light scattering) in the calculation of γ would tend to magnify this difference rather than reduce it.

In the development of his theory, Beasley assumed that the polymerization system was homogeneous and that the rate of intermolecular chain transfer was independent of molecular weight. Since the former should be a reasonably good assumption for the particular polymer studied in the present work, one must assume that the marked divergence of the experimental values from theory is due to the invalidity of the latter. Possibly, the larger molecules become shielded from transfer by coiling or partial precipitation from the reaction medium, so that their effective concentration is reduced. This was also considered by Beasley.

Molecular Weight Distribution

The most important effect of a breakdown of the Beasley theory with regard to the frequency of long-chain branching in polyethylene is on the shape of the molecular weight distribution curve. Because of the predicted increase in branching frequency with molecular weight, the Beasley distributions are characterized by having extremely long, high molecular weight "tails." The fact that the branching frequency actually decreases with molecular weight means that the actual distribution curve cuts off more sharply at the high molecular weight end of the distribution. This will cause a marked difference between the actual values of $\bar{M}_w$ and of $\bar{M}_w/\bar{M}_n$ and those calculated by assuming a Beasley type of distribution. Figure 4 shows the experimental distribution curve (I) for sample A ob-
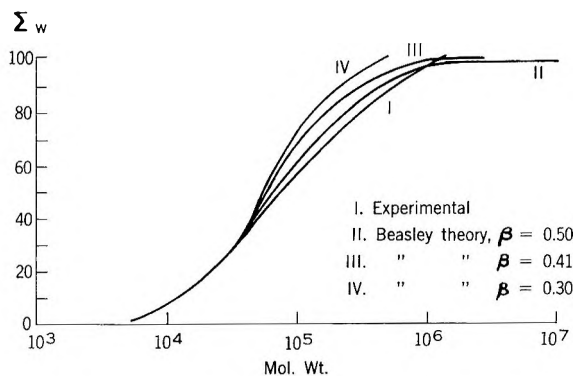
Fig. 4. Molecular weight distribution curve for polymer A.

tained from fractionation data; ultracentrifuge data were used in calculating the molecular weights, as described in a previous section. With the measured value of $\bar{M}_n$ a series of Beasley distributions was calculated for various values of β.

The closest fit to the experimental data was obtained with a value of $\beta = 0.5$; this theoretical distribution curve (II) is also shown in Figure 4. The curves agree reasonably well over most of the total weight per cent of the polymer. The divergence is most important for the upper 5% of the distribution. Since the value of β is 0.5, the theoretical value of $\bar{M}_w$ is infinite for the Beasley distribution. Graphical evaluation of $\bar{M}_w$ from the experimental curve gives a value of 190,000 and an $\bar{M}_w/\bar{M}_n$ ratio of only 6.88. This demonstrates clearly the importance of experimental determination of the long-chain branching frequency for the high molecular weight fractions in polyethylene. On the basis of eq. (10) a value of $\bar{M}_w/\bar{M}_n = 6.9$ corresponds to a value of $\beta = 0.415$. The theoretical distribution curve III is not as good a fit to the experimental data as is the curve for the high value of β.

Mussa[20] proposed a semiempirical method of fitting fractionation data to the Beasley equation. Application of Mussa's method to our data indicated a value of $\beta = 0.30$. This gives a lower value of the weight-average molecular weight ($\bar{M}_w = 92,000$) and the calculated distribution curve IV is far removed from the experimental one. This discrepancy is due presumably to the limitations of the Beasley distribution in describing the experimental situation with regard to long-chain branching frequency and to the assumptions involved in Mussa's treatment.

Baskett found similar discrepancies between the Beasley distribution and experimental distributions determined from crosslinking experiments.[4] A comparison of the two distributions is shown in Figure 5. Again, the experimental curve does not show the extended "tail" characteristic of the Beasley distribution.

One may conclude from the above considerations that the experimental distribution curves for polyethylenes do not, in general, have the extremely
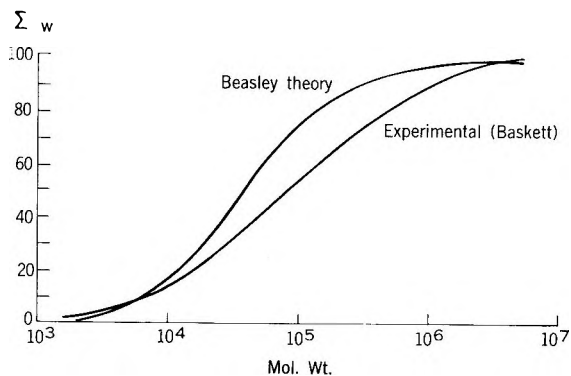
Fig. 5. Comparison of experimental and theoretical distribution curves.[4]

long, high molecular weight "tails" characteristic of the Beasley distribution, and hence values of $\bar{M}_w$ and $\bar{M}_w/\bar{M}_n$ ratios calculated by assuming this type of distribution will lead to values which are unrealistically high.

Molecular Weight–Viscosity Relation

In evaluating the actual shape of the molecular weight distribution curve from fractionation data on branched polyethylenes, the largest source of error lies in the determination of the molecular weight of the high molecular weight fractions. The use of inherent viscosity or intrinsic viscosity measurements, although by far the simplest experimentally, is complicated by the effect of long-chain branching. In the present case, an independent measurement of g allowed a correction to be made for this effect, and an accurate intrinsic viscosity–molecular weight equation could be established. Because the error in assuming a linear relation of the form $\log [\eta] = \log K + \alpha \log M$ is greatest for the high molecular weight fractions, the values of $\bar{M}_w$ and, hence, the $\bar{M}_w/\bar{M}_n$ ratio will be too low when such an equation is used. In a previous paper[9] the use of the linear equation gave a value of $\bar{M}_w/\bar{M}_n = 3.86$, whereas correction of the data for branching in the highest fractions now gives a value of 6.88 for the same polymer from the same fractionation data. Unfortunately, since the degree of long-chain branching may be expected to vary from polymer to polymer, the relation found experimentally for polymer A will not apply generally to other polyethylenes. The amount of work involved in obtaining such a relation would prevent this method from being of general application.

If, however, other polyethylenes are similar to polymer A in showing a relatively constant frequency of branching in the upper fractions, a single determination of branching frequency for a high molecular weight fraction by an independent method would be sufficient to establish the entire shape of the viscosity–molecular weight relation for all fractions of that particular polymer, with the use of eq. (1). The value of g can be obtained by interpolation of the data given by Zimm and Stockmayer when the value of m^* is calculated from the branching frequency γ^* for each molecular weight.
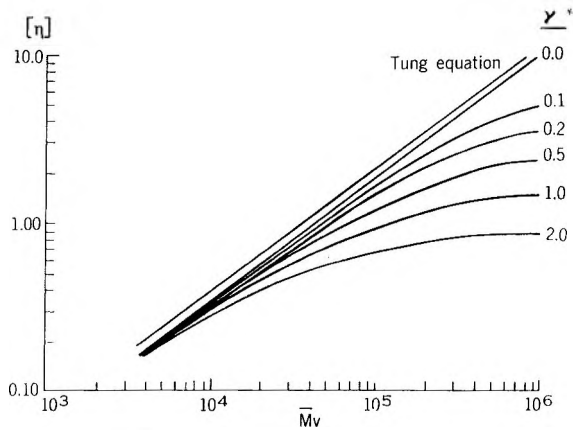
Fig. 6. Theoretical $[\eta]$ vs. $\bar{M}_v$ relations for various branching frequencies (short-chain branching $= 2.4$ CH$_3$/100 C).
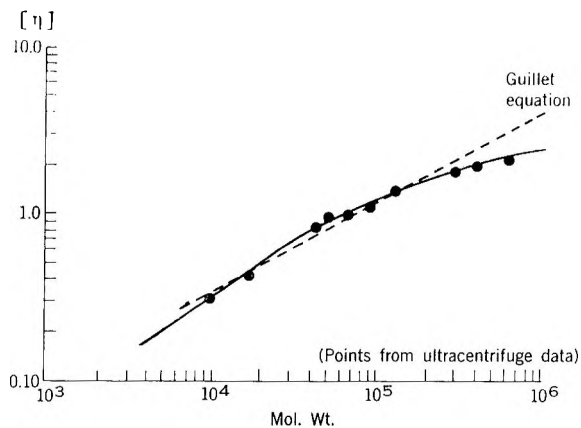

Fig. 7. Theoretical branching curve for $\gamma = 0.44$ (short-chain branching $= 2.4$ CH$_3$/100 C).

The value of $[\eta]_{lin}$ can be obtained from the Tung equation, eq. (5), and should be corrected for short-chain branching frequency by the Stockmayer relation in the manner described previously.

With this method a set of theoretical viscosity–molecular weight relations was calculated for polyethylenes having a short-chain branching frequency of 2.4 methyl groups per 100 carbon atoms and various constant branching frequencies. Typical curves for $\gamma^* = 0.0, 0.1, 0.2, 0.5, 1.0$, and 2.0 methyl groups per 1,000 carbon atoms are shown in Figure 6. In actual practice, curves of this type give an excellent fit to the experimental data. The average value of γ^* for the last four fractions of polymer A is 0.44. Figure 7 shows the experimental points obtained from all fractions of polymer A by using the ultracentrifuge data for calculating molecular weights. The broken line is the theoretical curve for $\gamma^* = 0.44$ with 2.4 methyl groups per

100 carbon atoms short-chain branches. The theoretical curve fits the data to well within the precision of the measurements involved.

Preliminary results with other polymers indicate that this approximation may be valid for a considerable number of commercial polyethylenes. If one can estimate the branching frequency, whether by direct measurement from ultracentrifuge methods, or from melt viscosity studies,[22] or from a knowledge of the method of preparation, it should be possible to select an appropriate viscosity–molecular weight relation and establish accurate molecular weight distributions from intrinsic viscosity measurements of polymer fractions.

Conclusion

It is concluded from this study that the frequency of long-chain branching in fractions of a typical commerical polyethylene does not increase with increasing molecular weight, as predicted by the Beasley theory, but remains relatively constant. As a result, the distribution calculated by assuming the validity of the Beasley relation is broader than that determined experimentally. The parameter β of Beasley's theory appears to provide a good fit to the experimental distribution curve for the first 90% of the polymer, but should not be used in calculating $\bar{M}_w$ or $\bar{M}_w/\bar{M}_n$ because of the apparent invalidity of the theory in predicting the branching (and hence molecular weight) of the highest fractions.

The branching frequency γ^*, which is the frequency of long-chain branches corrected for short-chain branching, represents a useful parameter from which one can construct the viscosity–molecular weight relation for fractions of branched polyethylene. This relation can then be used to characterize the molecular weights of the fractions and hence the shape of the actual molecular weight distribution curve.

References

1. Roedel, M. J., *J. Am. Chem. Soc.*, **75**, 6110 (1953).
2. Beasley, J. K., *J. Am. Chem. Soc.*, **75**, 6123 (1953).
3. Billmeyer, F. W., Jr., *J. Am. Chem. Soc.*, **75**, 6118 (1953).
4. Baskett, A. C., *Intern. Symp. Macromol. Chem., Milan and Turin. Ricerca Sci.*, **25** (1955).
5. Trementozzi, Q. A., *J. Polymer Sci.*, **22**, 187 (1956).
6. Moore, L. D., Jr., G. R. Greear, and J. O. Sharp, *J. Polymer Sci.*, **59**, 339 (1962).
7. Thurmond, C. D., and B. H. Zimm, *J. Polymer Sci.*, **8**, 477 (1952).
8. Moore, L. D., Jr., *J. Polymer Sci.*, **20**, 137 (1956).
9. Guillet, J. E., R. L. Combs, D. F. Slonaker, and H. W. Coover, Jr., *J. Polymer Sci.*, **47**, 307 (1960).
10. Nicolas, L., *J. Polymer Sci.*, **29**, 191 (1958).
11. Glover, C. A., and Ruth R. Stanley, *Anal. Chem.*, **33**, 447 (1961).
12. Guillet, J. E., R. L. Combs, D. F. Slonaker, J. T. Summers, and H. W. Coover, Jr., *SPE Trans.*, **2**, 164 (1962).
13. Zimm, B. H., and W. H. Stockmayer, *J. Chem. Phys.*, **17**, 1301 (1949).

14. Zimm, B. H., and R. W. Kilb, *J. Polymer Sci.*, **37**, 19 (1959).

15. Orofino, T. A., and F. Wenger, *Dilute Solution Properties of Branched Polymers. Polystyrene Trifunctional Star Molecules*, Am. Chem. Soc., Washington, D.C., March 26–29, 1962.

16. Tung, L. H., *J. Polymer Sci.*, **46**, 409 (1960).

17. Tung, L. H., *J. Polymer Sci.*, **24**, 333 (1957).

18. Trementozzi, Q. A., *J. Polymer Sci.*, **23**, 887 (1957).

19. Mussa, C., I.V., *J. Polymer Sci.*, **23**, 877 (1957).

20. Mussa, C., I.V., *J. Polymer Sci.*, **26**, 67 (1957).

21. Mussa, C., I.V., *J. Polymer Sci.*, **28**, 587 (1958).

22. Schreiber, H. P., and E. B. Bagley, *The Newtonian Melt Viscosity of Polyethylene— An Index of Long-Chain Branching*, Intern. Symp. Macromol. Chem., Montreal, July 27–Aug. 1, 1961.

Résumé

On étudie la fréquence de ramification en longue chaîne de polyéthylène à partir des résultats de Moore et collaborateurs, concernant les fractions de polyéthylène. On en déduit que la fréquence de ramification en longue chaîne n'augmente pas en fonction du poids moléculaire suivant la théorie de Beasley, mais demeure relativement constante. Ceci signifie que les distributions de poids moléculaires calculées sur la base des relations de Beasley, sont plus étendues que celles déterminées expérimentalement. On en déduit également que la relation viscosité-poids moléculaire des fractions ramifiées peut être déterminée en connaissant g, paramètre relatif en carré du rayon moyen de gyration des molécules, basé uniquement sur la validité de la relation $g^{3/2} = [\eta]_{\text{ramifie}}/[\eta]_{\text{lineaire}}$. On développe une méthode de détermination de γ^*, facteur de fréquence de ramification à longue chaîne, corrigé pour les ramifications à courtes chaînes. Puisque la valeur de γ^* est à peu près constante tout au long de la distribution, sa détermination pour une fraction de haut poids moléculaire permet la construction d'une relation viscosité-poids moléculaire valable pour toutes les fractions du même polymère. On emploie cette relation pour caractériser les poids moléculaires des fractions et, à partir de là, la forme de la courbe de la distribution de poids moléculaire actuelle.

Zusammenfassung

Eine Untersuchung der Häufigkeit der Langkettenverzweigung von Polyäthylen wurde mit Hilfe der von Moore und Mitarbeitern an Polyäthylenfraktionen gefundenen Daten durchgeführt. Die Häufigkeit der Langkettenverzweigung nimmt nicht, wie es nach der Theorie von Beasley zu erwarten wäre, mit steigendem Molekulargewicht zu, sondern bleibt ziemlich konstant. Das bedeutet, dass die unter Annahme der Gültigkeit der Beasley-Beziehungen berechneten Molekulargewichtsverteilungen breiter sind als die experimentell bestimmten. Weiters liess sich die Viskositäts-Molekulargewichtsbeziehung für verzweigte Fraktionen bei Kenntnis von g, einem zum mittleren Quadrat des Gyrationsradius der Moleküle in Beziehung stehenden Parameter, bloss unter Annahme der Gültigkeit der Beziehung $g^{3/2} = [\eta]_{\text{verzweigt}}/[\eta]_{\text{linear}}$ konstruieren. Eine Methode zur Bestimmung von γ^*, der für Kurzkettenverzweigung korrigierten Häufigkeit der Langkettenverzweigung, wurde entwickelt. Da der Wert von γ^* über die ganze Verteilung nahezu konstant bleibt, erlaubt die Bestimmung von γ^* an einer hockmolekularen Fraktion die Konstruktion der vollständigen Viskositäts-Molekulargewichtsbeziehung für alle Fraktionen des gleichen Polymeren. Diese Beziehung kann dann zur Ermittlung des Molekulargewichts der Fraktionen und damit der Gestalt der tatsächlichen Molekulargewichtsverteilungskurve verwendet werden.

Acid Behavior of Carboxylic Derivatives of Cellulose.   Part I.   Carboxymethylcellulose

F. H. CHOWDHURY* and S. M. NEALE, *Department of Chemistry, College of Science and Technology, Manchester, England*

Synopsis

The potentiometric and viscometric behavior of carboxymethylcellulose have been studied with solutions containing potassium chloride. It has been found that the titration results can be described by the modified form of the Henderson equation $pH = pK_m + n_{\log} \alpha/(1 - \alpha)$, the values of pK_m and n being dependent on the concentration of both carboxymethylcellulose and the concentration of potassium chloride in the system. Extrapolation of the straight-line pK versus α to $\alpha = 0$ yields a value of 3.42 for pK_0 which is identical with the pK value of galacturonic acid. The concentration dependence of pH for any given value of α can be described by the equation $[pH]_c{}^\alpha = [pH]_0{}^\alpha - 0.52\sqrt{c}$ where $[pH]_0{}^\alpha$ is the pH at a concentration c and degree of dissociation α, and $[pH]_0{}^\alpha$ is the corresponding value extrapolated to infinite dilution. Both the viscosity and the potentiometric results show that the carboxyl groups in CMC are not free from electrostatic interactions but that at a salt concentration of $1M$ electrostatic effects almost disappear.

Introduction

It was observed by Kern[1] for polyacrylic acid that the "dissociation constants," as defined by the equation,

$$K = [H^+] [-A^-]/[-HA] = [H^+]\alpha/(1 - \alpha)$$

decreased with increasing degree of dissociation. Since then the acid behavior of other soluble polyelectrolytes, e.g., polymethacrylic acid,[2,3] carboxymethylcellulose,[4] copolymers of crotonic acids with vinyl acetate,[5] pectic acids,[6,7] etc., have been studied. It is now generally recognized that the acid behavior of the carboxyl groups in polyelectrolytes may be described by a modified form of the Henderson equation,

$$pH = pK_m + n_{\log}\alpha/(1 - \alpha)$$

where pK_m is the value of pH at half neutralization and n an empirical index of the intramolecular electrostatic interactions. The values of pK_m and n have been found to depend on the nature of the polymer, on the concentration of neutral salts in the system, on the concentration of the polyion itself, and on the distance between the carboxyl groups along the polymer backbone.

* Present address: Department of Chemistry, Rajshahi University, East Pakistan.

Since the values of pK_m and n are dependent on concentration it is necessary to extrapolate the results to infinite dilution in order to obtain an unequivocal value. Following this procedure, Oth and Doty[3] obtained, for polymethacrylic acid, values of pK_m and n which were much higher than the values reported earlier by Katchalsky and Spitnik.[2]

To account for the acid behavior of carboxymethylcellulose (CMC) Kagawa and Katsura[4] suggested the following relation:

$$a_H{}^2/c_p(1 - \alpha) = K = K_s(1 - \alpha/\alpha)^m$$

where c_p is the concentration of CMC, K a new dissociation constant, and m the variation exponent. This equation seems to represent the data of the authors for various concentrations, but because of the logarithmic dependence of pH on concentration, it can only be valid over a limited concentration range. The effect of neutral salts cannot be explained by this equation. Moreover, Kagawa's equation leads to pK values which appear to be too high for this type of polyelectrolyte and much higher than the known pK values of uronic acids and carboxylic derivatives of cotton cellulose.[9]

In order to throw further light on the matter, the potentiometric and the viscometric behavior of CMC have been studied in dilute solutions and the results are reported in this paper.

Experimental

Materials

Samples of NaCMC of different degrees of substitution (Imperial Chemical Industries Limited) were purified by first filtering aqueous solutions through glass wool. NaCMC was then precipitated by the dropwise addition of alcohol and filtered through a filter cloth. The operation was repeated several times and finally the sodium salt was washed repeatedly with 75% (v/v) ethanol till it was completely free from chloride ions. The samples were then dried in vacuum over P_2O_5 until constant weight was obtained. The degree of substitution, defined as the number of carboxyl groups per glucose unit, was determined by igniting the samples with concentrated sulphuric acid. The free acid (CMC) was prepared by slowly passing a solution of the sodium salt through an ion exchange column containing the cation exchange resin Amberlite IR-120(H). The efficacy of the process was followed by pH measurements and the operations were continued until a steady pH was obtained. The ash contents of the samples thus prepared were less than 0.04% expressed on the weight of CMC.

pH Measurements

For the pH measurements a Cambridge pH meter in conjunction with a glass electrode and a saturated calomel electrode was employed. The pH

meter was calibrated with a buffer solution of $0.05M$ potassium hydrogen phthalate (pH = 3.97) and checked by a solution of $0.01N$ HCl in $0.09N$ KCl (pH = 2.07) and $0.05M$ borax (pH = 9.27). As the glass electrode gives erratic results in the presence of sodium ions, carbonate-free potassium hydroxide solution was used throughout.

Viscosity Measurements

The viscosities of CMC solutions were measured with Ostwald viscometers in a water thermostat at $25 \pm 0.05°C$. Calibration was carried out by measuring the time of flow of distilled water or standard sugar solutions. To study the effect of rate of shear, the viscosity of the most concentrated solution of CMC was measured in several viscometers. As the results agreed within 0.3% this point was not pursued further.

CMC solution in 30-ml. portions was taken in each of a series of 50-ml. conical flasks. The required amount of potassium chloride was then added and the flasks were shaken well. Different amounts of standard potassium hydroxide solution were then added from a microburette to give a series of pH and viscosity readings over the entire neutralization curve. The conical flasks were stoppered, shaken well, and allowed to stand for 6 hrs. in an atmosphere of nitrogen. The pH and viscosity readings were then taken for each of these solutions and in this way the neutralization and the viscosity curves for different degrees of dissociation were determined. For the calculation of dynamic viscosities, densities of CMC solutions were determined with a specific gravity bottle at $25 \pm 0.05°C$.

Unless otherwise stated, all viscometric and potentiometric results refer to a sample of CMC of degree of substitution 0.49.

Calculation of Dissociation Constants

Assuming that CMC behaves as a weak monobasic acid, the thermodynamic dissociation constant of the carboxyl groups may be defined as follows:

$$K_{th} = a_{H^+} a_{-COO^-}/a_{-COOH}$$

The hydrogen ion activity, a_{H^+}, can be determined experimentally, but nothing definite is known about the activity of the $-COO^-$ ions. To overcome this difficulty, a "concentration dissociation constant" has been defined as

$$K_c = ([H^+][-COO^-])/[-COOH]$$

The bracketed quantities represent the concentrations in equivalents per liter. The following values of activity coefficients of hydrogen ions in potassium chloride solutions have been estimated by Harned et al.[10,11] and have been used to calculate the concentration of hydrogen ions from measured hydrogen ion activity.

Ionic strength	Activity coefficient of hydrogen ions
0.02	0.8989
0.11	0.8492
1.01	0.9354

The total concentration of the carboxyl groups in equivalents per liter was determined from the equivalence point of the potentiometric curve. Concentration of the —COO$^-$ ions was calculated from the equation $[H^+] + [K^+] = [COO^-] + [—OH^-]$ in accordance with the requirements of the electrical neutrality of the system. Here $[K^+]$ represents the concentration of the potassium ions in the solution derived from the amount of KOH added. $[OH^-]$ may be neglected, since the concentration of hydroxyl ions in acid solution is negligibly small. The degree of dissociation, α, has been defined as $[—COO^-]/[—COOH]$, pK_c as log K_c, and pK_m as the value of pK_c when $\alpha = 0.5$.

Results and Discussion

The viscosity of an aqueous solution of CMC was measured at different pH values, the initial pH of the solution (2.84) being varied either by the addition of KOH or HCl. It was found, as shown in Figure 1, that the viscosity increases with increasing pH, goes through a maximum at a pH of about 7, and then decreases. The increase in viscosity with increasing pH has also been observed with other synthetic polyelectrolytes[12] and has been attributed to the uncoiling of the polyanion due to electrostatic repulsion between like charges. As the pH of the aqueous solution is decreased by the addition of HCl, viscosity is considerably reduced and finally attains
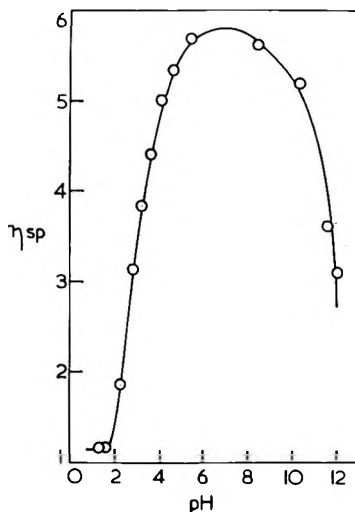

Fig. 1. Variation of specific viscosity with pH for CMC solution.

a steady value. This may be attributed to the suppression of the dissociation of the carboxyl groups.

When free alkali is present (above pH 8), the cations begin to function by reducing interanionic electrostatic repulsions, and the chains coil up again.

Effect of Neutral Salts

Figure 2 shows the variation of pK_c with α for different salt concentrations. The pK values increase; i.e., the dissociation constants decrease with increasing values of α, clearly demonstrating that the carboxyl groups in CMC are not free from electrostatic interactions. With increasing salt concentration the acid behavior of CMC gradually approaches that of a monobasic acid, the value of pK_c becoming almost independent of α. This may be attributed to the shielding of the negative charges in the polyanion by the positively charged potassium ions present in excess. Extrapolation of the $\alpha\ pK_c$ curve to $\alpha = 0$ in the absence of added salt yields a value of 3.42 which is identical with the experimentally determined pK value of galacturonic acid. Thus pK_0 (intrinsic dissociation constant) for CMC may be taken as equal to 3.42.

In Figure 3 some pH values for different salt concentrations have been plotted against $\log \alpha/(1 - \alpha)$ in accordance with the modified form of the Henderson equation. The values of n, which may be taken as a measure of the electrostatic interactions, and of pK_m, are shown below.

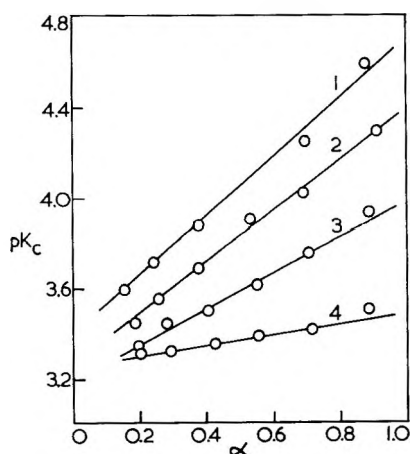| KCl concn.	pK_m	n
0.00	4.05	1.63
0.01	3.87	1.56
0.10	3.68	1.38
1.00	3.38	1.12

Fig. 2. Variation of pK_c with degree of dissociation for different concentrations of KCl: (1) zero; (2) 0.01N KCl; (3) 0.1N KCl; (4) 1.00N KCl.

As expected, the values of both pK_m and n decrease with increasing concentration of potassium chloride. At a salt concentration of $1.00N$ the value of n is 1.12, indicating a close approach to the behavior of a monomeric acid $(n = 1)$. The value of pK_m, at this salt concentration, is also
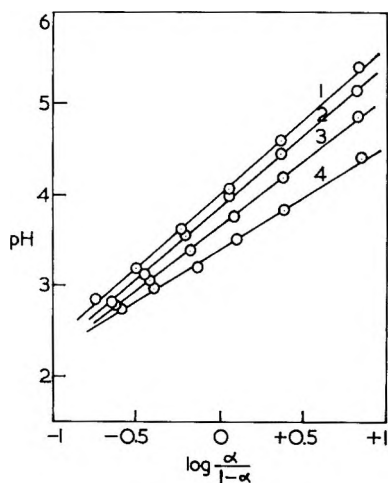
Fig. 3. Plots of pH vs. $\log \alpha/(1-\alpha)$ in accordance with the modified form of the Henderson equation: (1) water; (2) 0.01N KCl; (3) 0.10N KCl; (4) 1.00N KCl.
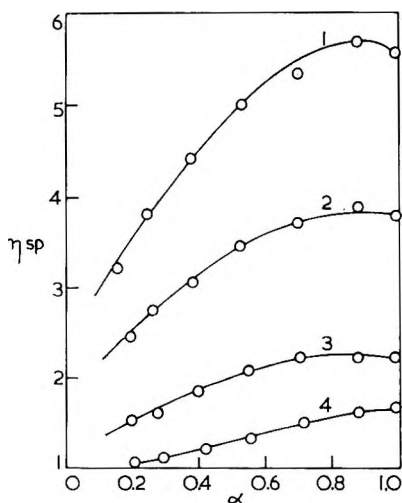
Fig. 4. Variation of specific viscosity with degree of dissociation for different concentrations of KCl: (1) water; (2) 0.01N KCl; (3) 0.10N KCl; (4) 1.00N KCl.

very close to the pK value for galacturonic acid (3.42) or the pK_0 value for CMC (3.42, see above). Thus, it is evident that the presence of a large excess of neutral salt suppresses, almost completely, the electrostatic interactions in the CMC molecule.

The effects of degree of dissociation and of neutral salt on the viscosity are shown in Figure 4, where η_{sp} (specific viscosity) values have been plotted against α. It will be seen that viscosity increases with increasing amounts of —COO$^-$ ions and that the rate of increase of viscosity decreases with increasing salt concentration.

Effect of CMC Concentration

It will be seen from Figure 5 that η_{sp}/c values for CMC, in agreement with the behavior of other polyelectrolytes, rises sharply with dilution. For NaCMC this has been attributed[13] to the uncoiling of the polymer chain due to the increasing ionization and consequent electrostatic repulsion. The
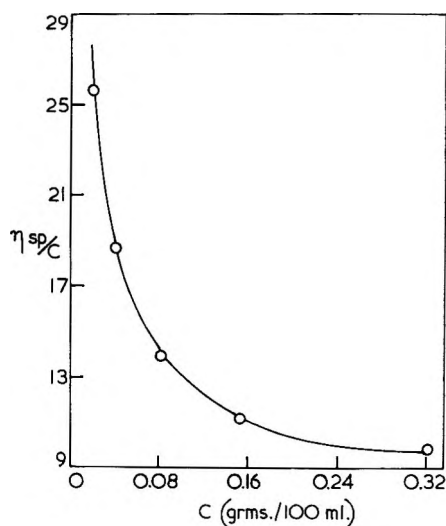
Fig. 5. Variation of η_{sp}/c vs. c for CMC solution.

probability of hydrogen ions escaping from the polymer coil into the external aqueous phase also increases with increasing dilution, resulting in an increase in the interanionic repulsions. An increase in the net charge on the polyanion would make further dissociation of the carboxyl groups more difficult, and hence both pK_m and n are expected to increase with increasing dilution. For the same reason the rate of variation of viscosity with α is also expected to increase with increasing dilution. Figure 6 shows that the viscosity of CMC solutions does, in fact, behave in the manner predicted.

Figure 7 shows the titration behavior of CMC at two different concentrations. The values of pK_m and n taken from Figure 7 are as follows:

Concn., equiv./l.	pK_m	n
0.0095	4.05	1.63
0.0045	4.20	1.71
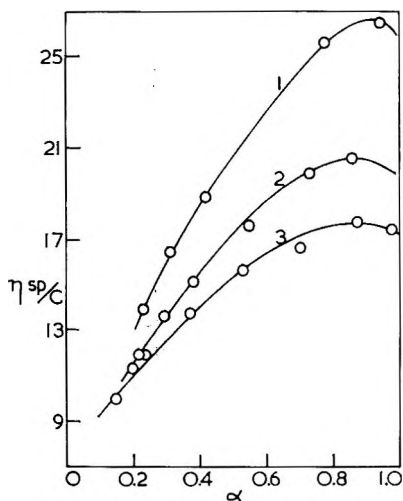
Fig. 6. Variation of η_{sp}/c against degree of dissociation for different concentrations of CMC: (1) 0.0815 g./100 ml.; (2) 0.1532 g./100 ml.; (3) 0.3210 g./100 ml.
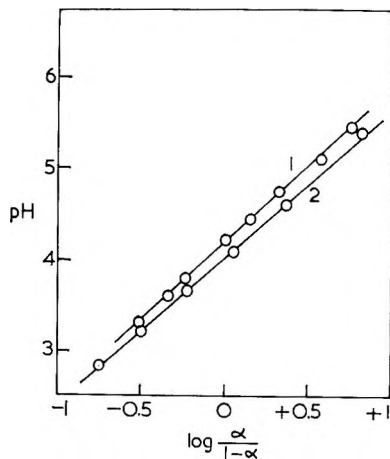
Fig. 7. Plots of pH vs. $\log \alpha/(1-\alpha)$ for different concentrations: (1) 0.0095N; (2) 0.0045N.

Since pK_m and n are dependent on polyacid concentration, it is necessary to extrapolate the results to infinite dilution, to obtain the unequivocal titration equation. To make this possible, potentiometric titrations of CMC have been carried out in dilute solutions at five different concentrations. From the titration results it has been found (Fig. 8) that the concentration dependence of pH for different values of α can be represented by

$$[\text{pH}]_c^{\alpha} = [\text{pH}]_0^{\alpha} - A\sqrt{c}$$

where c is the concentration of carboxyl groups, in equivalents per liter, $[\text{pH}]_c^{\alpha}$ is the pH at a concentration c and degree of dissociation α, $[\text{pH}]_0^{\alpha}$
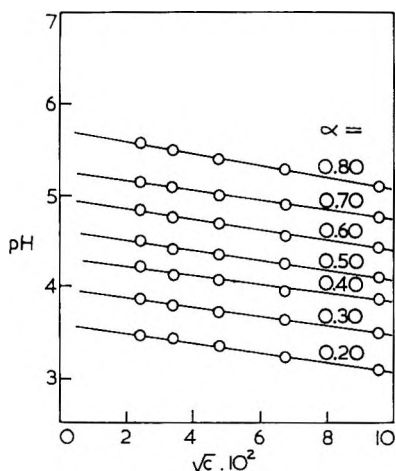
Fig. 8. Plots of pH vs. concentration of carboxyl groups for different values of α.
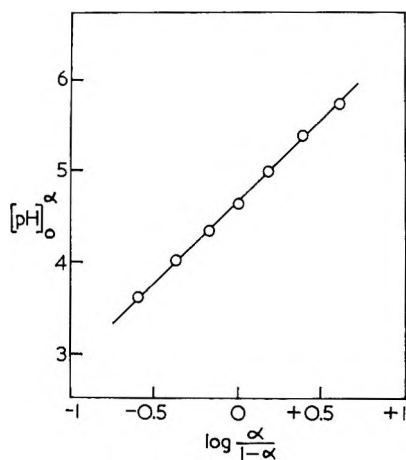
Fig. 9. Plots of $[pH]_0\alpha$ vs. log $\alpha/(1-\alpha)$ for CMC of degree of substitution 0.49.

is the pH extrapolated to infinite dilution and degree of dissociation α. A has been found to have a value of 0.52 ± 0.04 identical with the Debye-Hückel constant for electrolytes in water at $25\,°C$.

Values of $[pH]_0^\alpha$ obtained by extrapolation from Figure 8 have been plotted against log $\alpha/(1-\alpha)$ in Figure 9. It is thus seen that the "infinite dilution titration equation" for CMC of degree of substitution of 0.49 is

$$pH = 4.64 + 1.80 \log \alpha/(1-\alpha)$$

Effect of Degree of Substitution

Figure 10 shows the titration behavior of CMC of three different degrees of substitution. It will be seen from the table below and also from Figure 10 that both pK_m and n increase with increasing degree of substitution.

Degree of substitution	pK_m	n
0.49	4.00	1.61
0.70	4.17	1.76
0.81	4.38	1.83
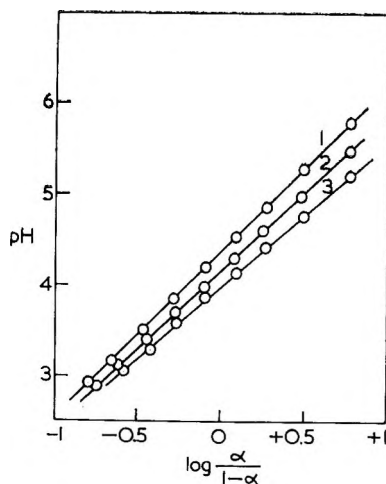
Fig. 10. Plots of pH vs. $\log \alpha/(1-\alpha)$ for CMC of following degrees of substitution: (1) 0.81; (2) 0.70; (3) 0.49.

With increasing degree of substitution the distance between the carboxyl groups decreases. This causes increased electrostatic interactions, dissociation of the carboxyl groups becoming more difficult and, as a result, both pK_m and n increase with increasing degree of substitution.

References

1. Kern, W., *Z. Physik. Chem.*, **A181**, 249 (1938).
2. Katchalsky, A., and P. Spitnik, *J. Polymer Sci.*, **2**, 432 (1947).
3. Arnold, R., and J. Th. G. Overbeeck, *Rec. Trav. Chim.*, **69**, 192 (1950).
4. Kagawa, I., and K. Katsura, *J. Polymer Sci.*, **7**, 89 (1951).
5. Johanson, S., *Svensk Kem. Tidskr.*, **60**, 122 (1948).
6. Speiser, R., C. H. Hills, and C. R. Eddy, *J. Phys. Colloid, Chem.*, **49**, 328 (1945).
7. Schultz, T. H., H. Lotzaker, and H. S. Owens, *J. Phys. Colloid Chem.*, **49**, 554 (1945).
8. Oth, A., and P. Doty, *J. Phys. Chem.*, **43**, 56 (1952).
9. Chowdhury, F. H., and S. M. Neale, *J. Polymer Sci.*, **A1**, 2893 (1963).
10. Harned, H. S., *J. Am. Chem. Soc.*, **42**, 1808 (1920).
11. Harned, H. S., and N. J. Brunbaugh, *J. Am. Chem. Soc.*, **4**, 2729 (1922).
12. Katchalsky, A., *J. Polymer Sci.*, **7**, 393 (1951).
13. Fujita, H., and T. Homa, *J. Polymer Sci.*, **15**, 276 (1955).

Résumé

On étudie le comportement potentiométrique et viscosimétrique de la carboxyméthylcellulose, en solution contenant du chlorure de potassium. On en déduit que les résultats titrimétriques sont décrits par une forme modifiée de l'équation d'Henderson: pH =

$pK_m + n_{\log} \alpha/(1 - \alpha)$. Les valeurs de pK_m et de n sont dépendantes de la concentration en cellulose carboxyméthylée et aussi de la concentration en chlorure de potassium dans le système. L'extrapolation de la droite pK en fonction de α, jusque $\alpha = 0$ donne une valeur de 3.42 pour pK_0 qui est identique à la valeur de pK de l'acide galacturonique. La dépendance de la concentration du pH, pour n' importe quelle valeur de α, s'exprime par l'équation: $[pH]_c^{\alpha} = [pH]_c^{\alpha} - 0.52\sqrt{c}$, où $[pH]_c^{\alpha}$ est le pH à la concentration c et au degré de dissociation α, et $[pH]_0^{\alpha}$ est la valeur correspondante extrapolée à dilution infinie. Les résultants viscosimétriques et potentiométriques montrent tous deux que les groupes carboxylés dans la CMC ne sont pas libres d'interactions électrostatiques, mais qu' à une concentration molaire en sel les effets électrostatiques disparaissent presque complètement.

Zusammenfassung

Das potentiometrische und viskosimetrische Verhalten von Carboxymethylcellulose in Kaliumchlorid-hältigen Lösungen wurde untersucht. Die Titrationsergebnisse können durch eine modifizierte Henderson-Gleichung $pH = pK_m + n_{\log}(\alpha/1 - \alpha)$ dargestellt werden, wo die Werte von pK_m und n von der Konzentration der Carboxymethylcellulose und auch von der Kaliumchloridkonzentration im System abhängen. Lineare Extrapolation von pK gegen α auf $\alpha = 0$ liefert für pK_0 einen Wert von 3,42, der mit dem pK-Wert von Galacturonsäure identisch ist. Die Konzentrationsabhängigkeit des pH kann für jeden gegebenen Wert von α durch die Gleichung $[pH]_c^{\alpha} = [pH]_0^{\alpha} - 0,52\sqrt{c}$ beschrieben werden, wo $[pH]_c^{\alpha}$ das pH bei einer Konzentration c und einem Dissoziationsgrad α und $[pH]_0^{\alpha}$ der entsprechende auf unendliche Verdünnung extrapolierte Wert ist. Viskosimetrische und potentiometrische Ergebnisse zeigen, dass die Carboxylgruppen in CMC nicht frei von elektrostatischen Wechselwirkungen sind, dass aber bei einer Salzkonzentration von 1 Mol/Liter die elektrostatischen Einflüsse praktisch verschwinden.

Acid Behavior of Carboxylic Derivatives of Cellulose. Part II. Oxycellulose

F. H. CHOWDHURY* and S. M. NEALE, *Department of Chemistry, College of Science and Technology, Manchester*

Synopsis

The acid behavior of nitrogen dioxide, periodate–chlorite, and alkaline hypobromite oxycelluloses in presence of potassium chloride solutions of different concentrations has been studied. Experimental results indicate that the carboxylic groups in oxycelluloses are not free from mutual electrostatic interactions. In agreement with the behavior of carboxymethylcellulose and other soluble polyelectrolytes, the pK values increase with increasing degree of dissociation and decrease with increasing concentration of potassium chloride in the system. The titration results can be described by the modified form of the Henderson equation $pH = pK_m + n \log \alpha/(1 - \alpha)$, the value of n being always greater than unity. Experimental results have also been treated in an entirely new way, that of splitting the system into two equipotential phases: (*1*) the internal phase consisting of both the oxycellulose and its imbibed solution and (*2*) the external fluid phase. The Donnan theory of membrane equilibrium has been applied in calculating the internal pH values. It has been found that although the measured external pH values decrease considerably with increasing salt concentration, the calculated internal pH values are independent of salt concentration.

Introduction

It is now generally accepted that samples of purified cellulose possess as part of their chemical structure a few carboxyl groups which, when suspended in water, are capable of ionization according to the following equilibrium:

$$-COOH \rightleftharpoons -COO^- + H^+$$
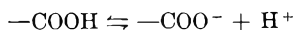
The dissociation of the carboxyl groups leaves the cellulose molecule negatively charged, since the $-COO^-$ ions form part of the cellulose structure. That the intrinsic negative charge shown by cellulose in neutral aqueous solutions is due chiefly to the presence of carboxyl groups has been demonstrated by Neale and Standring,[1] who measured the Donnan potentials across cellophane membranes of different carboxyl content, between two solutions of potassium chloride of different concentrations. The electric potentials were found to decrease with decreasing pH and disappeared completely at a pH of 2.5. Neale and co-workers[2-4] have also shown that the effect of the pH, of neutral salts, and of the nature of the fiber on equilibrium

---

* Present address: Department of Chemistry, Rajshahi University, East Pakistan.

dyeing can be explained by assuming that cellulose is negatively charged in aqueous solution, because of the dissociation of the carboxyl groups.

Although the important role played by the carboxyl groups in equilibrium dyeing and other related processes has generally been recognized, very little is known about their dissociation equilibrium. A systematic quantitative study of the acid behavior of different types of carboxylic derivatives of cellulose was, therefore, undertaken. Results obtained with oxycelluloses (carboxylic derivatives of cotton cellulose) are reported in this paper.

Different Types of Oxycellulose

It is now known that there are some specific oxidants which oxidize only one type of hydroxyl group in the cellulose molecule, so that it is possible to prepare oxycelluloses which are chemically homogeneous and to which a definite chemical structure can be ascribed. The action of periodic acid[5] followed by chlorous acid[6] has been shown to produce an oxycellulose in which the secondary hydroxyl groups have been converted into carboxyl groups with the simultaneous rupture of the pyranose ring. The structure of the periodate–chlorite oxycellulose (as it is called) may, therefore, be represented as follows:
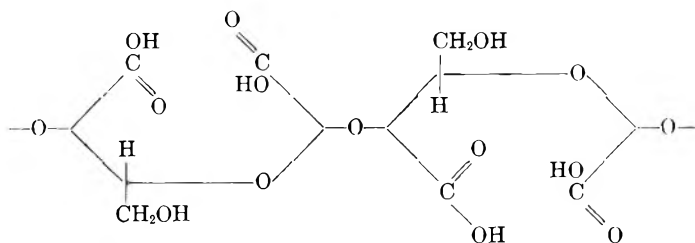
On the other hand, nitrogen dioxide[7] produces an oxycellulose in which the primary hydroxyl groups have been converted into carboxyl groups:
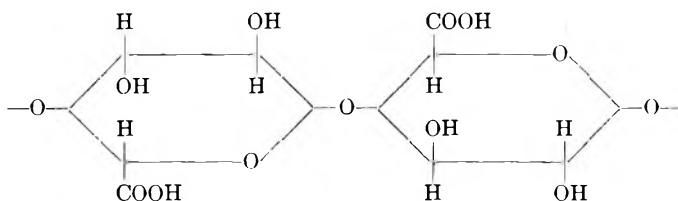
It is therefore possible to study the behavior of the carboxyl groups with respect to their position in the cellulose molecule.

The action of alkaline hypobromite oxycellulose has also been studied.

Experimental

Purification

Raw Egyptian cotton was purified by boiling with a 2% caustic soda solution, in the absence of air, and by subsequently washing with 2% acetic

acid. The purified air-dried sample had the following characteristics: cuprammonium fluidity,[8] 4.72; Copper number,[10] 0.02; total carboxyl content,[11] 1.8 mequiv./100 g. These data show that the cellulose had undergone very little degradative and oxidative transformation.

Preparation of Oxycelluloses

Alkaline hypobromite oxycellulose was prepared according to the method suggested by Clibbens.[9] The hypobromite solution was $0.1N$ with respect to free alkali and $0.1N$ with respect to its oxidizing value. Oxycelluloses of the highest carboxyl content prepared by this method had a carboxyl content of 26.16 mequiv./100 g. Further oxidation produced a gel-like substance which was not suitable for our purpose.

Following the procedure of Davidson[12] periodate-chlorite oxycelluloses were prepared by oxidizing cotton cellulose with sodium metaperiodate followed by chlorous acid.

Nitrogen dioxide oxycelluloses were prepared by the action of gaseous nitrogen dioxide in an all-glass apparatus, as described by Nevell.[13] Oxycelluloses of various carboxyl content were prepared by varying either the time of oxidation or the concentration of the oxidant or both.

All samples of oxycelluloses were made cation-free by being immersed in $0.1N$ HCl for 2 hr. and then washed with numerous changes of distilled water until the filtrates were neutral to bromocresol purple. The samples were then air-dried, cut into small pieces (1 mm. length), and stored in glass-stoppered bottles.

Bone-Dry Weight

The bone-dry weights of the air-dried samples were determined by drying a small portion at 110° in an electric oven for 24 hr. Assuming that the moisture content of a sample of air-conditioned oxycellulose stored in a glass bottle is the same throughout, bone-dry weights were calculated.

Potentiometric Titrations

Potentiometric titrations were carried out in a 250-ml. lipless beaker fitted with a rubber bung through which passed the tip of a microburette, a glass electrode, a saturated calomel electrode, a mercury seal stirrer, and an inlet for bubbling nitrogen through the solution; an outlet guarded against the CO_2 of the atmosphere by a soda lime tube. The pH readings were taken with a Cambridge pH meter which was previously calibrated with standard buffer solutions. As the glass electrode gives erratic results in the presence of sodium ions, a carbonate-free potassium hydroxide solution was used throughout. A 1-g. quantity of oxycellulose was taken in 100 ml. of KCl solution for every titration.

It was found almost impossible to carry out a potentiometric titration in the absence of added salt, because of a very slow downward drift in the pH readings. In the presence of salts, up to about 80% neutralization, steady

pH readings were obtained. Beyond this point, there was a slow but definite downward drift, which was especially pronounced in the neutralization region. It was found that readings in the neutralization region became steady 30 min. after the addition of alkali; accordingly, these readings were taken every 30 min. The total carboxyl content of the oxycelluloses was checked by the iodometric method.[11] The iodometric result was always found to correspond to a pH of 8.5 on the neutralization curve.

Results and Discussion

Homogeneous Distribution

Making the artificial assumption of a homogeneous distribution of all the ions throughout the whole system, and equating the activity coefficients to unity, the dissociation constant K has been calculated according to the following equation:

$$K = [H^+] [-COO^-]/[-COOH]$$

where the bracketed quantities represent the concentration, in equivalents per liter. The degree of dissociation α has been defined as $[-COO^-]/[COO^-] + [-COOH]$, pK as $-\log K$, and pKS as $-\log K$ when $\alpha = 0.5$.

Figures 1, 2, and 3 show the variation of pK values with degree of dissociation for the three different types of oxycellulose. It will be seen that the pK values increase with increasing degree of dissociation and that for any degree of dissociation the pK values decrease with increasing salt concentration. In this respect the behavior of the carboxyl groups is similar to that of carboxymethylcellulose and other soluble polyelectrolytes. An increase in the pK values with increasing degree of dissociation was observed by Hirsch[14] for oxycelluloses prepared by the action of nitric acid and
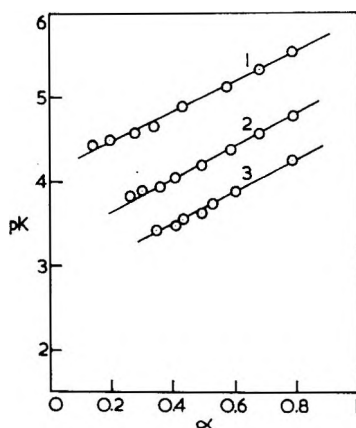
Fig. 1. Variation of pK with degree of dissociation for nitrogen dioxide oxycellulose: (1) 0.01N KCl; (2) 0.10N KCl; (3) 0.00N KCl. Carboxyl content of the oxycellulose, 16.12 mequiv./100 g.

Fig. 2. Variation of pK with degree of dissociation for hypobromite oxycellulose: (1) 0.01N KCl; (2) 0.10 KCl; (3) 1.00N KCl. Carboxyl content of the oxycellulose, 26.16 mequiv./100 g.
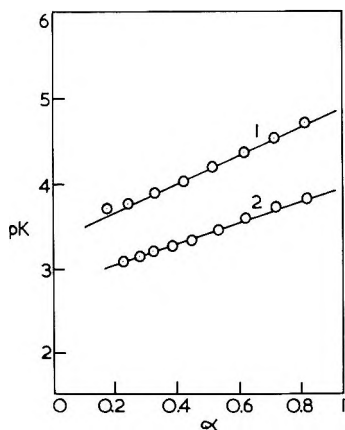
Fig. 3. Variation of pK with degree of dissociation for periodate–chlorite oxycellulose: (1) 0.10N KCl; (2) 1.00N KCl. Carboxyl content of oxycellulose, 120.4 mequiv./100 g.

nitric oxide. In Figures 4, 5, and 6 the pH values for the three different types of oxycellulose are plotted against log $\alpha/(1 - \alpha)$ in accordance with the modified form of the Henderson equation:

$$\text{pH} = \text{p}K_m + n \log \alpha/(1 - \alpha)$$

where pK_m is the value of pK when $\alpha = 0.5$ and n is an empirical index of the intramolecular electrostatic interactions. It will be seen that straight-line relationships are obtained between pH and log $\alpha/(1 - \alpha)$. The slopes of the straight lines (n values) are very similar in all cases, and are as follows:

	KCl concn.		
	0.01	0.1	1.0
Figure 4	1.7	1.7	1.8
Figure 5	1.7	1.7	1.6
Figure 6	1.5	1.6	1.7

These show that the carboxylic acid groups are not free from electrostatic interaction, even in the presence of $1N$ potassium chloride. This contrasts with the behavior of carboxymethylcellulose, with which the n value decreases rapidly with salt addition.[15] In these insoluble oxycelluloses the
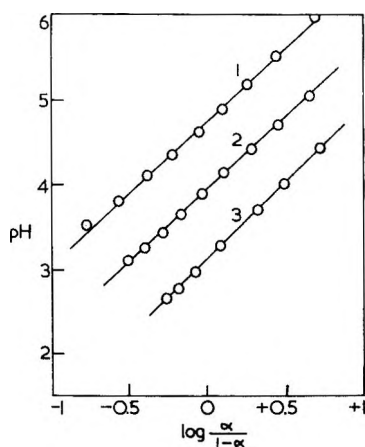
Fig. 4. Plots of pH vs. log $\alpha/(1 - \alpha)$ or nitrogen dioxide oxycellulose: (1) 0.10N KCl; (2) 0.10N KCl; (3) 1.00N KCl. Carboxyl content of the oxycellulose, 59.48 mequiv./100 g.
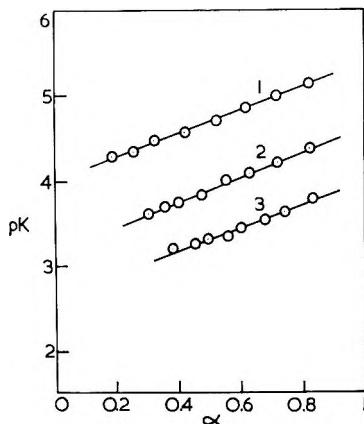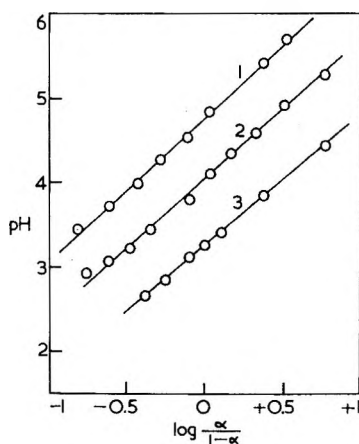

Fig. 5. Plots of pH vs. log $\alpha/(1 - \alpha)$ for periodate–chlorite oxycellulose: (1) 0.01N KCl; (2) 0.10N KCl; (3) 1.00N KCl. Carboxyl content of the oxycellulose, 74.84 mequiv./100 g.
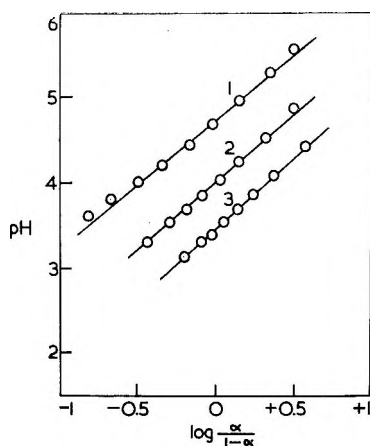
Fig. 6. Plots of pH vs. log $\alpha/(1 - \alpha)$ for hypobromite oxycellulose: (1) 0.01N KCl; (2) 0.10N KCl; (3) 1.00N KCl. Carboxyl content of the oxycellulose, 18.88 mequiv./100 g.

values of n do not appear to follow any definite trend with rising salt concentration.

Oxycellulose as a Two-Phase System

In this alternative and more realistic treatment the assumption is made that the oxycellulose with its imbibed solution may be regarded as one equipotential phase. The system is thus split up into two equipotential phases, as follows:

Phase 1, oxycellulose with its imbibed solution		Phase 2, external aqueous phase
—COOK	$[H^+]_1$	$[K^+]_2$
—COOK	$[K^+]_1$	$[H^+]_2$
	$[Cl^-]_1$	$[Cl^-]_2$
—COOH	H_2O	H_2O

The distribution of the mobile ions according to the Donnan theory of membrane equilibrium will be given by the relation:

$$a\,(H^+_1)/a\,(H^+_2) = a\,(K^+_1)/a\,(K^+_2) = a\,(Cl^+_2)/a\,(Cl^-_1) \qquad (1)$$

Assuming equality of activity coefficients in both phases, it is permissible to replace activity by concentrations. Equation (1) may then be written as follows:

$$[H^+]_1/[H^+]_2 = [K^+]_1/[K^+]_2 = [Cl^-]_2/[Cl^-]_1 = \lambda \qquad (2)$$

Since both the phases must be, to a close approximation, electrically neutral, it is possible to write

$$[K^+]_2 + [H^+]_2 = [Cl^-]_2 \qquad (3)$$

$$[H^+]_1 + [K^+]_1 = [Cl^-]_1 + [—COO^-] \qquad (4)$$

As the concentration of OH^- ions is very small, it has been neglected.

Now let V_1 and V_2 represent the volume of the solvent for the internal and the external phases, respectively. By equating the total potassium ion content of the system to the total chloride ion content.

$$V_1[K^+]_1 + V_2[K^+]_2 = V_1[Cl^-]_1 + V_2[Cl^-]_2$$

or

$$V_1[K^+]_1 - [Cl^-]_1 = V_2[Cl^-]_2 - [K^+]_2 \qquad (5)$$

Combining eq. (3) and eq. (5).

$$[K^+]_1 - [Cl^-]_1 = (V_2/V_1)[H^+]_2 \qquad (6)$$

From eq. (2):

$$[K^+]_1 [Cl^-]_1 = [K^+]_2 [Cl^-]_2 \qquad (7)$$

From eqs. (6) and (7), $[K^+]_1$ can be determined:

$$[K^+]_1 = (V_2/V_1)[H^+]_2 + \sqrt{((V_2/V_1)[H^+]_2)^2 + 4m^2}/2 \qquad (8)$$

where m is the molality of the potassium chloride solution.

As an approximation, the molality of the potassium ions in the external phase may be taken to be equal to m. This approximation does not introduce serious errors when salt concentration is not too low. From eq. (2), therefore,

$$[K^+]_1/[K^+]_2 = [H^+]_1/[H^+]_2 = [K^+]_1/m = \lambda$$

so that, when the value of λ is known, $[H^+]_1$, the concentration of hydrogen ions in the internal phase, can be calculated.

The above equations are applicable before the addition of alkali to the system. When, however, alkali is added, eq. (6) can be written as:

$$[K^+]_1 - [Cl^-]_1 = (V_2/V_1)[H^+]_2 + w/V_1$$

Fig. 7. Variation of external and internal pH with milliequivalents of alkali bound for nitrogen dioxide oxycellulose: (1) external pH in 0.10N KCl; (2) external pH in 1.00N KCl; (3) internal pH in 0.10N KCl and 1.00N KCl. Carboxyl content of the oxycellulose 59.48 mequiv./100 g.

where w represents the milliequivalents of alkali added. From this the values of internal pH for the whole titration curve can be calculated.

Water of Imbibition

To be able to calculate the ionic concentrations in the internal phase, it is necessary to know the amount of water imbibed by cellulose. Employing the centrifugal technique, Coward and Spencer[16] found that the water retained was 55 g./100 g. cellulose, which was later confirmed by Neale and Farrar.[17] This value has been used for all calculations on the basis of a two-phase system. It is emphasized, however, that this is purely an arbitrary value and is regarded as the one giving the most satisfactory agreement with theory.
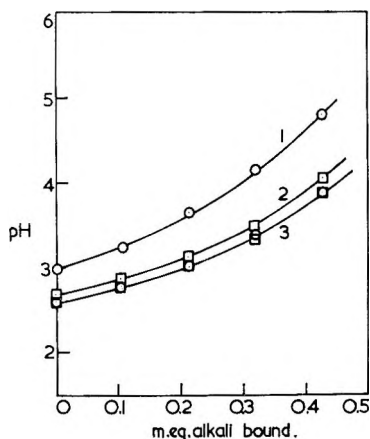
Fig. 8. Variation of external and internal pH with milliequivalents of alkali bound for periodate–chlorite oxycellulose: (1) external pH in 0.10N KCl; (2) external pH in 1.00N KCl; (3) internal pH in 0.10N KCl and 1.00N KCl. Carboxyl content of the oxycellulose, 74.84 mquiv./100 g.
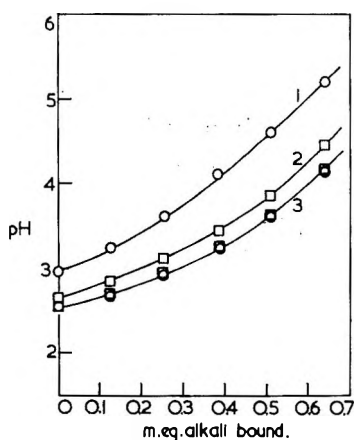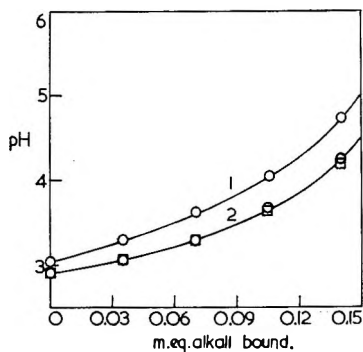

Fig. 9. Variation of external and internal pH with milliequivalents of alkali bound for hypobromite oxycellulose: (1) external pH in 0.10N KCl; (2) external pH in 1.00N KCl and internal pH in 0.10N KCl and 1.00N KCl.

Since the approximations made in the method of calculation do not apply when the salt concentration is low, internal pH values corresponding to $0.01N$ KCl have not been calculated. The external pH values and the cor-

TABLE I
Internal pH Values for Nitrogen Dioxide Oxycellulose (1 g./100 ml. soln.) (—COOH content of oxycellulose: 59.48 mequiv./100 g.)

KOH added, mequiv.	External pH		Internal pH	
	0.10N KCl	1.00N KCl	0.10N KCl	1.00N KCl
0	2.98	2.68	2.61	2.60
0.109	3.26	2.86	2.74	2.77
0.218	3.66	3.12	3.00	3.01
0.327	4.16	3.4S	3.37	3.34
0.436	4.79	4.04	3.88	3.87

TABLE II
Internal pH Values for Periodate–Chlorite Oxycellulose (1 g./100 ml. soln.) (—COOH content of oxycellulose: 74.84 mequiv./100 g.)

KOH added, mequiv.	External pH		Internal pH	
	0.1N KCl	1.00N KCl	0.1N KCl	1.00N KCl
0	2.95	2.66	2.56	2.57
0.128	3.24	2.86	2.68	2.76
0.256	3.64	3.12	2.92	2.99
0.384	3.11	3.44	3.25	3.28
0.512	4.61	3.87	3.63	3.67
0.640	5.22	4.46	4.15	4.20

TABLE III
Internal pH Values for Hypobromite Oxycellulose (1 g./100 ml. soln.)
(—COOH Content of oxycellulose: 18.88 mequiv./100 g.)

KOH added, mequiv.	External pH		Internal pH	
	0.10N KCl	1.00N KCl	0.10N KCl	1.00N KCl
0	3.30	3.14	3.11	3.12
0.036	3.54	3.32	3.30	3.29
0.072	3.87	3.54	3.54	3.53
0.107	4.31	3.89	3.92	3.85
0.142	4.96	4.44	4.49	4.39

responding internal pH values for $0.1N$ KCl and $1.0N$ KCl have been tabulated in Tables I–III and shown graphically in Figures 7–9. It will be seen that, although the external pH values decrease considerably with increasing

salt concentration, the calculated internal pH values are independent of this quantity.

It may be inferred, therefore, that the Donnan theory treatment does account for the variation with salt concentration of the external pH. However, plots of internal pH against $\log \alpha/(1 - \alpha)$ do not yield n values very much different from those quoted in the preceding section. It must be concluded, therefore, that the behavior of the insoluble oxycelluloses is essentially different from that of the soluble carboxymethylcelluloses, but it does resemble that of the fibrous proteins, investigated by Peters[18] and Gilbert and Rideal.[19]

References

1. Neale, S. M., and P. T. Standring, *Proc. Roy. Soc.*, **A213**, 530 (1952).

2. Neale, S. M., and W. A. Stringfellow, *Trans. Faraday Soc.*, **29**, 1167 (1933).

3. Neale, S. M., and J. Harrison, *Trans. Faraday Soc.*, **30**, 386 (1934).

4. Neale, S. M., and W. A. Stringfellow, *J. Soc. Dyers Colourists*, **17, 56** (1940).

5. Jackson, E. L., and C. S. Hudson, *J. Am. Chem. Soc.*, **59**, 2049 (1937).

6. Rutherford, H. A., F. W. Minor, A. R. Martin, and M. J. Harris, *J. Res. Natl. Bur. Std.*, **29**, 131 (1942).

7. Yakel, E. C., and W. O. Kenyon, *J. Am. Chem. Soc.*, **64**, 121 (1942).

8. Howlett, F., and D. Belward, *J. Textile Inst.*, **40**, T399 (1949).

9. Clibbens, D. A., *J. Textile Inst.*, **16**, T13 (1925).

10. Clibbens, D. A., and A. Geake, *J. Textile Inst.*, **15**, T27 (1924).

11. Nabar and Padmanabhan, *Proc. Indian Acad. Sci.*, **31**, 371 (1950).

12. Davidson, G. F., *J. Textile Inst.*, **46**, T407 (1955).

13. Nevell, T. P., *J. Textile Inst.*, **24**, 148 (1950).

14. Hirsch, P., *Rev. Trav. Chim.*, **71**, 999 (1952).

15. Neale, S. M., and Chowdhury, F. H., *J. Polymer Sci.*, **A1**, 2881 (1963).

16. Coward, H. F., and L. Spencer, *J. Textile Inst.*, **14**, T32 (1923).

17. Neale, S. M., and J. Farrar, *J. Colloid Sci.*, **7**, 186 (1952).

18. Peters, L., *J. Soc. Dyers Colourists'*, **75**, 63 (1949).

19. Gilbert, G. A., and E. K. Rideal, *Proc. Roy. Soc.*, **A182**, 335 (1944).

Résumé

On étudie le comportement acide d'oxycelluloses obtenues au moyen de dioxyde d'azote, de periodate-chlorite et d'hypobromite alcalin, en présence de solutions de chlorure de potassium à diverses concentrations. Les résultats expérimentaux montrent que les groupes carboxyliques des oxycelluloses ne sont pas libres d'interactions électrostatiques mutuelles. En accord avec le comportement de la carboxyméthylcellulose et d'autres polyélectrolytes solubles, les valeurs de pK augmentent avec un degré de dissociation croissant et diminuent avec l'augmentation de concentration du chlorure de potassium dans le système. Les résultats titrimétriques sont donnés par la forme modifiée de l'équation d'Henderson: $pH = pK_m + n \log \alpha/1 - \alpha$, dans laquelle la valeur de n est toujours supérieure à l'unité. Les résultats expérimentaux ont été également considérés de façon entièrement différente par scission du système en deux phases équipotentielles; (*1*) la phase interne constituée d'oxycellulose et de sa solution d'imbibition et (*2*) la phase liquide externe. On applique la théorie de l'équilibre de membrane de Donnan au calcul des valeurs du pH. Bien que les valeurs externes de pH mesurées décroissent fortement avec l'augmentation de concentration saline, les valeurs de pH internes calculées sont indépendantes de la concentration en sel.

Zusammenfassung

Das Säureverhalten von Stickstoffdioxyd-, Perjodat-Chlorit- und Alkalihypobromit-oxycellulose wurde in Gegenwart verschieden konzentrierter Kaliumchloridlösungen untersucht. Die Versuchsergebnisse zeigen, dass die Carboxylgruppen in Oxycellulose nicht frei von gegenseitiger elektrostatischer Wechselwirkung sind. In Übereinstimmung mit dem Verhalten von Carboxymethylcellulose und andern löslichen Polyelektrolyten, nehmen die pK-Werte mit steigendem Dissoziationsgrad zu und mit steigender Kaliumchloridkonzentration im System ab. Die Titrationsergebnisse lassen sich durch eine modifizierte Hendersongleichung pH = pK_m + n log $\alpha/(1 - \alpha)$ beschreiben, wo der Wert von n immer grösser als eins ist. Die Versuchsergebnisse wurden auch in einer völlig anderen Weise behandelt, nämlich durch Aufspaltung des Systems in zwei Phasen von gleichem Potential, (1) die innere, aus Oxycellulose und der imbibierten Lösung bestehende Phase und (2) die äussere, flüssige Phase. Zur Berechnung der inneren pH-Werte wurde die Theorie des Membrangleichgewicht von Donna verwendet. Obgleich die gemessenen äusseren pH-Werte mit steigender Salzkonzentration beträchtlich abnehmen, sind die berechneten, inneren pH-Werte von der Salzkonzentration unabhängig.

Proton Magnetic Resonance in Natural Rubber: Comparison with Dielectric Measurements*

HAZIME KUSUMOTO, *Hitachi Central Research Laboratory, Kokubunzi, Tokyo, Japan*, and H. S. GUTOWSKY, *Noyes Chemical Laboratory, University of Illinois, Urbana, Illinois*

Synopsis

Proton magnetic resonance studies have been made of cured natural rubber containing up to 31% combined sulfur. Line shapes and spin-lattice relaxation times were observed at temperatures between −190 and 180°C. In the line shape studies, the main effect of the combined sulfur was upon the temperature at which the line width is narrowed by the molecular segmental motions. The temperature at the onset of the major line width narrowing increases from −50°C. for raw rubber to about 10°C. for 31% combined sulfur. A relation was found between the dependence upon sulfur content of the line width changes and the second-order transition temperature. The proton spin-lattice relaxation time T_1 was measured for three cured samples in the temperature range above the motional narrowing region. The T_1 vs. temperature curves agree qualitatively with the theory of Kubo and Tomita. The general features of the T_1 curves are consistent with a distribution of correlation times which broadens with increasing sulfur content. Energies of activation were computed from these results and they are compared with the dielectric relaxation data obtained previously. The effect of a distribution of correlation time is discussed.

I. INTRODUCTION

Several studies on natural rubber[1-5] have been made by means of proton magnetic resonance techniques. The effects of curing[2,5] and elongation[4] on the molecular motions in natural rubber have been observed in measurements of line shapes and spin-lattice relaxation times as a function of temperature. Line shape studies[5] on cured rubber having up to 9% combined sulfur showed major narrowing of the line widths at temperatures above −50°C., and this was assigned to the segmental motions. Also, there was observed a gradual narrowing of line widths in the temperature range between −150 and −50°C. It was proposed that this type of line width change is related to the CH_3 group rotation. The temperature dependence of the proton spin-lattice relaxation time T_1 showed the general features described by the theories of Bloembergen, Purcell, and Pound[6] and Kubo and Tomita.[7] Also, the T_1 versus temperature curves were found to depend on the sulfur content in a manner qualitatively similar to the line shapes and their temperature dependence.

However, there were quantitative discrepancies[5] between experiment and theory, and these seemed to be due to the assumption that the relaxation was caused by random molecular motions with a single correlation time.[6,7] Moreover, the discrepancies appeared to increase with the sulfur content. In the present experiments, the line width and T_1 measurements were extended to samples containing up to 31% combined sulfur. It was hoped that in samples with such extremely large sulfur content, and discrepancies would be correspondingly larger than in the previous samples having a maximum of 9% sulfur, and that the nature and origin of the discrepancies would be more readily apparent.

In our experiments, raw Hevea rubber and seven samples of cured Hevea rubber containing 1.9–31.0% of combined sulfur were examined in the temperature range from −190 to 180°C. In the line shape studies both gradual narrowing at low temperatures, upon warming, and more abrupt narrowing at high temperatures were found in all cases. The temperature regions in which the line width changes occur clearly depend on the content of combined sulfur. Moreover, a relation was found between the dependence upon sulfur content of the transition temperature region in NMR and the so-called second-order transition temperature. This relation appears to be concerned with the mechanism of curing.

Information on the molecular motions at higher temperatures was obtained also from T_1 measurements. Energies of activation for the motions were computed from both the line shape and T_1 data under the assumption of a single correlation time. These values are compared with the results obtained in dielectric measurements[8-10] on samples with similar sulfur contents. In treating these results the effect of a distribution of correlation times is considered, and the theoretical aspects are presented.

II. EXPERIMENTAL

1. Samples

The materials investigated were raw Hevea rubber and seven specimens of cured Hevea rubber differing in the combined sulfur content. The first step in the preparation of the cured samples was the mastication of a batch of raw Hevea rubber (100 parts by weight) with accelerator (mercaptobenzothiazole, 1 part) and antioxidant (phenyl-β-naphthylamine, 1 part).

TABLE I

Preparation and Composition by Weight of the Cured Rubber[a]

	Sample No.						
	1	2	3	4	5	6	7
Curing temp., °C.	140	140	140	140	140	140	140
Curing time, hr.	2	2	2	3	4.5	4.5	4.5
Mixed sulfur, %	2	4	8	14	20	25	32
Combined sulfur, %	1.9	3.9	7.8	13.8	19.4	24.1	31.0

[a] The accelerator used in the preparation of the samples was mercaptobenzothiazole (1 phr), and the antioxidant was phenyl-β-naphthylamine (1 phr).

Samples from this batch were then mixed with sulfur and cured as described in Table I. The composition and curing conditions were chosen to give the maximum amount of combined sulfur. Crystallization and hysteresis effects were minimized by annealing the sample for several hours at 30°C. prior to a set of measurements.

2. Equipment and Experimental Procedures

The proton absorption line shape was observed for all samples from liquid nitrogen temperature to temperatures high enough that the width narrowed to about 0.1 gauss. The line shape observations were performed with a regenerative spectrometer[11] operating at a fixed frequency of 26.8 Mcycles/sec. Also, the proton spin-lattice relaxation time T_1 was measured on three samples, (1, 3, and 6) between approximately −40°C. and 130°C. These measurements of T_1 were made with a spin-echo[12] apparatus at 20 Mcycles/sec. In addition, T_1 was determined at 28 Mcycles/sec. for all seven cured samples at room temperature. The T_1 values were measured by the 180−90° pulse method of Carr and Purcell.[13] Two cryostats were used to regulate the sample temperature. A variable heat-leak cryostat[11] was used for the line shape measurements, and a gas-flow type[11] was used in the T_1 measurements. In all experiments the temperature was measured with a copper–Constantan thermocouple placed directly in the sample.

III. RESULTS AND DISCUSSION

1. Line Shape Studies at Low Temperatures

Derivative curves of samples 3 and 7 at −190°C. are reproduced in Figure 1. The absorption lines are simple and bellshaped without any notable structure. However, the peaks of the derivative curves become flatter, as shown in Figure 1, with increasing combined sulfur. At the same time, the line width between the maximum and minimum slope, ΔH_{msl}, seemed to increase with increasing combined sulfur, though accurate values could not be determined for ΔH_{msl} because of the flatness of the peaks. It seems likely that the line widths of the heavily cured samples are likely to increase below liquid nitrogen temperatures. Measurements at lower temperatures would be desirable to make sure of this tendency.

At the lowest temperature the second moments obtained for the eight samples ranged between 17.5 and 19.0 gauss². The contribution of the protons in the monomer of rubber molecule, $-CH_2CH_2C(CH_3)-CH-$, to the total second moment may be calculated assuming that the C–H distance is 1.09 A. and that all the angles are tetrahedral. The monomer may be considered to consist of two rigid methylene groups, each of which has an intragroup second moment of 10.2 gauss², and a group consisting of the methyl protons and the isolated proton at the double bond. The value of the second moment of this group is 17.1 gauss². The net intramolecular contribution from these groups to the second moment is

$$\Delta H_2{}^2 = (4/8) \times 10.2 + (4/8) \times 17.1 = 13.7 \text{ gauss}^2$$
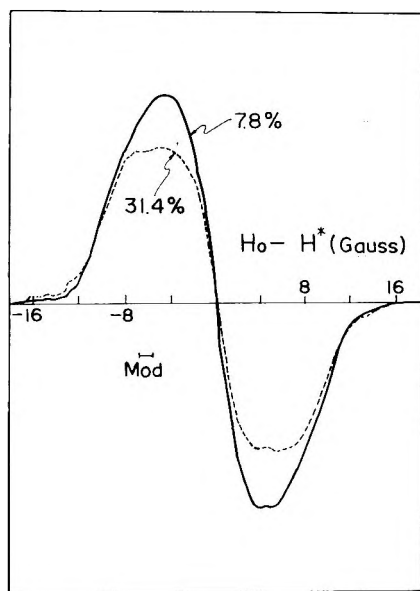
Fig. 1. The first derivative of the proton absorption observed at $-190°C.$ in cured Hevea rubber samples containing 7.8% and 31.0% by weight of combined sulfur. The arrow indicates the amplitude of the audio-frequency modulation of the magnetic field. The center of the derivative curve corresponds to an applied magnetic field of about 6325 gauss.

The difference of 4–6 gauss[2] between this calculated value and those observed should come from the dipolar interactions between protons in adjacent groups either in the same or different molecules. About 5 gauss[2] could be a reasonable value[15] for such intergroup and intermolecular interactions in polymers. On this basis the molecules may be considered to be effectively in a rigid lattice at liquid nitrogen temperature.

The vulcanization of natural rubber is an extremely complex process, the principal features of which have been investigated extensively by Farmer et al.[16] In general, the role of combined sulfur has been believed to be the formation of intermolecular and intramolecular crosslinks at the double bond of the monomer:
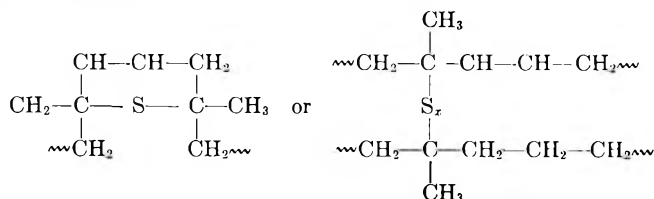
These crosslinks affect the local arrangement of molecules. The intermolecular crosslinks would affect the intermolecular dipolar interaction, and the intramolecular ones would have effects on the intramolecular interaction. Actually, vulcanization of rubber causes decrease of specific volume.[14] Since the dipolar interaction is proportional to the inverse third

power of the proton–proton distance, such decreases in the intermolecular distances with sulfur content increase the intermolecular contribution to the second moment.   The effect may be reasonably large and should increase with increasing combined sulfur content, although exact estimation is difficult because of the complicated arrangement of the molecules and a lack of knowledge of the exact number of crosslink of both types.   In any case, the line shapes shown in Figure 1 indicate that broader lines occur in samples with more combined sulfur.

2. Temperature Dependence of the Line Width and the Second Moment

The first derivative of the absorption line was recorded for the eight samples throughout the entire temperature range studied.   No appreciable structure was observed in any of the absorption lines.   At the first time the
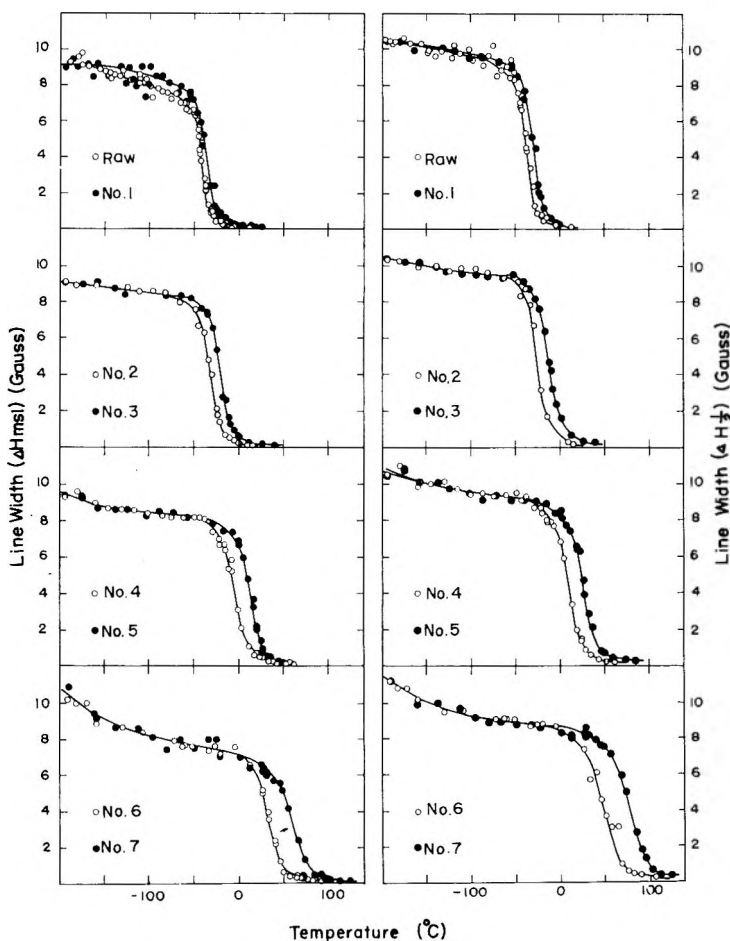
Fig. 2. Half-height line widths ($\Delta H_{1/2}$) and maximum slope line widths (ΔH_{msl}) of the proton absorption as a function of temperature for a sample of raw natural rubber and seven vulcanized samples.   The sample numbers indicated in each section refer to those in Table I.
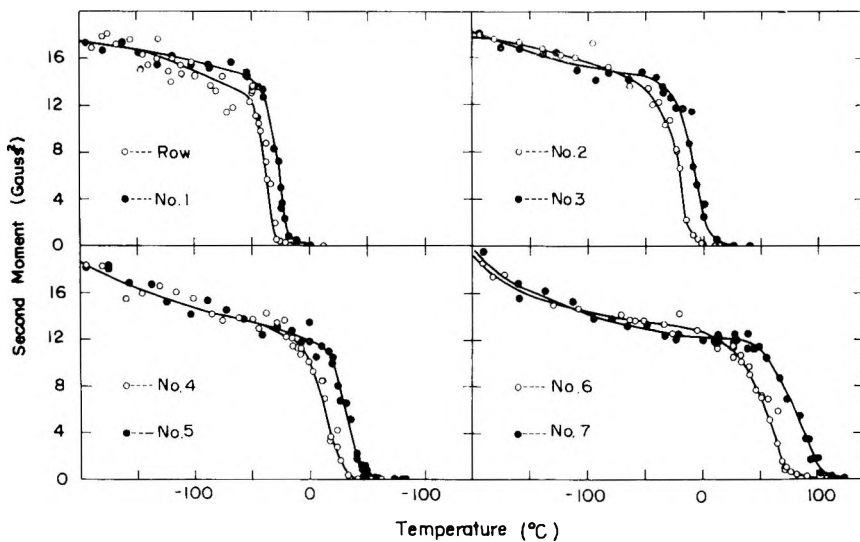
Fig. 3. Second moments of the proton absorption as a function of temperature for a sample of raw natural rubber and seven vulcanized samples. The sample numbers indicated in each section refer to those in Table I.

maximum and minimum slope line width, ΔH_{msl}, was obtained directly from recorded first derivatives. The second moment, $\Delta H_2{}^2$, was calculated from these first derivatives. The half-height line width, $\Delta H_{1/2}$, was measured from absorption lines obtained by integrating derivative curves numerically. $\Delta H_{1/2}$ and $\Delta H_2{}^2$ are plotted against temperature in Figures 2 and 3, respectively.

The general features of these curves are similar to those observed in the previous studies[2,5] on natural rubber. All samples showed a gradual narrowing in the low temperature range. The line width decreased from 11.5–10.5 gauss at the lowest temperature to 8–9 gauss for $\Delta H_{1/2}$, and from 16.5–20 gauss² to 12–13 gauss² for $\Delta H_2{}^2$. The reduced values and the temperatures where the gradual narrowing ceased depended upon the combined sulfur content. This gradual narrowing upon warming, ended at −50°C. for raw rubber and at about 10°C. for the cured sample 7. Except for the case of raw rubber, the transition temperature from the gradual narrowing to the major one was difficult to determine. This tendency increased with increase of the combined sulfur content.

Such a gradual narrowing may occur as a result of a localized motion in the rubber molecule. The rotation of the CH_3 group about the C_3 symmetry axis may cause such narrowing. This interpretation, proposed previously,[2] is very tempting. In fact, the second moment decreased to 12–13 gauss². These values could be predicted, assuming that all the methyl groups rotate around their C_3 axis.[18]

However, it was found that the proton absorption of some high polymers having no rotating group also showed the gradual narrowing below the temperature range where the major narrowing takes place. Such a narrow-

TABLE II

The Reduction in the Line Widths and Second Moments due to the Minor Narrowing in Some Amorphous High Polymers Having No Rotating Methyl Group[c]

| | Temperature | Neoprene[a] | Thiokol rubber[b] | | |
			A	ST	FA
ΔH_{msl}	Liquid N_2 temperature.	12.8	11.3	14.1	13.5
$\Delta H_{1/2}$		11.6	—	—	—
ΔH_2^2		16.7	19	20	18.5
ΔH_{msl}	Temperature where the	9.9	10.0	11.6	11.2
$\Delta H_{1/2}$	major narrowing	9.9	—	—	—
ΔH_2^2	takes place.	13.0	15	15	14.5
Temp. of major narrowing, °C.		−36	−35	−37	−55

[a] Data of Kusumoto.[19]

[b] Data of Kusumoto.[20]

[c] ΔH is in gauss and ΔH_2^2 is in gauss^2.

ing was observed on some amorphous polymers like neoprene,[19] polysulfide rubber,[20] Buna N,[21] and crystalline polymers like polyamide.[22] The line width data at liquid nitrogen temperature and those at the onset of the major narrowing on neoprene[19] and thiokol rubber[20] are summarized in Table II. For these materials, the extent of reduction in line width is comparable with that of natural rubber.

This narrowing may be caused also by the vibrational motion of the chain segments around their axes. The second moment for highly cured rubber seemed to have a tendency to be still increasing at the lowest temperature studied. These results lead us to suggest that the methyl groups rotate even at the lowest temperature studied and the gradual narrowing is assigned to the vibrational motion of the segments. In this point of view, it would be expected that the line width for raw rubber and for weakly cured rubber would increase at lower temperatures. The strongest argument against this hypothesis may be that the second moment observed at the lowest temperature was close to that expected for the rigid molecule. An experimental value of the second moment much larger than expected for the rigid state was observed[23] on polyethylene at liquid nitrogen temperature. A decrease in the H–H distance was a likely explanation for such a large value of the second moment. The increase of the second moment on the heavily cured rubber below liquid nitrogen temperature might be understood in the same way as in the case of polyethylene. In order to make sure of the correctness of these hypotheses, line shape measurements below liquid nitrogen temperatures should be carried out. Also T_1 and dielectric measurements for the temperature region of gradual narrowing would serve to elucidate further properties in this region.

The temperature region in which the major line width change occurs depends upon the combined sulfur content. As expected, the region shifted to higher temperature with increase in the combined sulfur content. This is a quite reasonable tendency, because the crosslinking should hinder the segmental molecular motions. In Figure 4 these "transition temperatures"
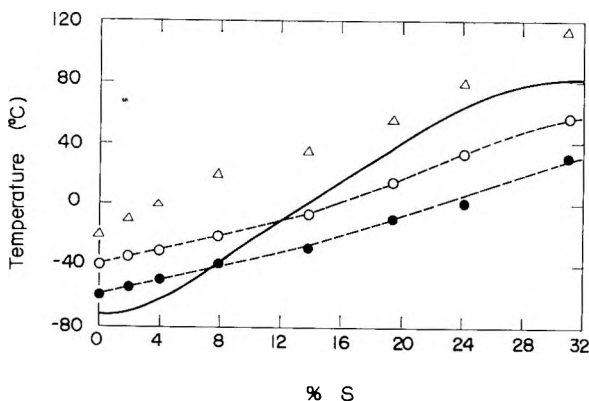
Fig. 4. Relation between T_g, T_n, and $T_n{}^*$ and the combined sulfur content: (———)
dependence upon the combined sulfur content of the second-order transition temperature,
T_g; (O) T_n; and (●) $T_n{}^*$; (△) temperature where $\Delta H_{1/2}$ reduces to 0.5 gauss.

are compared with the so-called second-order transition temperature, T_g,
against the sulfur content reported by Boyer and Spencer.[24] The tempera-
ture coefficient of heat capacity, specific volume, and expansion coefficient
change discontinuously at T_g. In Figure 4 are also plotted against the
combined sulfur the temperatures T_n at which the absorption lines begin
to narrow, and those $T_n{}^*$ where the values of $\Delta H_{1/2}$ reduce to $2(\ln 2\Delta H_2{}^2)_{1/2}$.
The definition of T_n and $T_n{}^*$ may be arbitrary. However, an interesting
relation between T_g and T_n is found there. T_n and the transition range
in NMR are located above T_g for low sulfur content, but for high sulfur
content the former exist below T_g. It is usual that T_g does not coincide
with T_n for polymers. One of few exceptions was silicon rubber for which
T_g ($-123°C$.) agreed well with T_n.[25] The apparent discrepancies of the two
kinds of transition temperature may be attributed to the difference in time
scale for the two measurements and to the different distribution of correla-
tion time in NMR and relaxation time in dielectric measurements.

3. Temperature Dependence of the Spin-Lattice Relaxation Time T_1

The proton spin-lattice relaxation time T_1 was measured for samples 1, 3,
and 6 in the temperature range where the major motional narrowing takes
place. Few attempts were made to measure T_1 at lower temperatures for
sample 6. T_1 values obtained are plotted against reciprocal temperatures
in Figure 5. The main features of the curve in all cases may be interpreted
on the basis of the theory of Kubo and Tomita:[7]

$$1/T_1 = (3/10)\gamma^4\hbar^2 \sum_j r_j{}^{-6}\{[\tau_c/(1 + \omega^2\tau_c{}^2)] + [4\tau_c/(1 + 4\omega^2\tau_c{}^2)]\} \quad (1)$$

where γ is the proton magnetogyric ratio, r_j are the distances to the neigh-
boring protons, ω is the angular resonance frequency ($= 2\pi\nu$), and τ_c
is the correlation time for the random reorientational motion of molecules
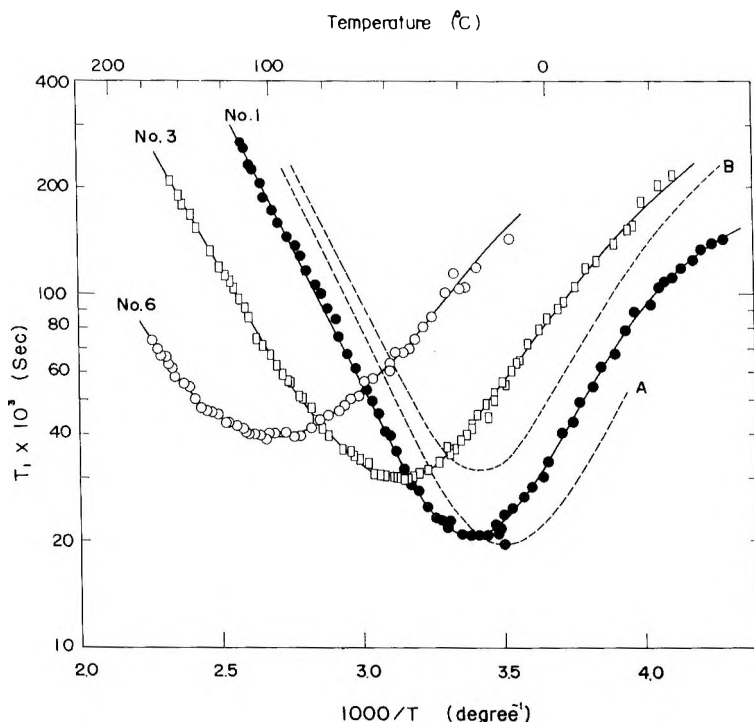
Fig. 5. The proton spin-lattice relaxation time as a function of temperature for three vulcanized samples of Hevea rubber (samples 1, 3, and 6) at resonance frequency of 20 Mcycles/sec.: (A) and (B) T_1 data on uncured Hevea rubber (reproduced from Gutowsky et al.[5]). Measurement frequencies are 20 Mcycles/sec. and 28 Mcycles/sec. for A and B, respectively.

producing the relaxation. Equation (1) gives a minimum T_1 value when $\omega\tau_c = 0.6158$. The minimum value of T_1 is obtained from[5]

$$1/T_{1\min} = 0.4275(\gamma^4 h^2/\omega) \sum r_j^{-6} \qquad (2)$$

Each sample was found to have such a minimum T_1 value. The magnitude and temperature of $T_{1\min}$ were found to depend on the combined sulfur content. This feature is similar to those found in the previous study.[5] All the V-shaped T_1 curves are located approximately in the temperature range of the major motional narrowing. The major narrowing of line width should be associated with random reorientations of the chain segments of the molecules and the minimum in T_1 is also attributable to the same mechanism. A few T_1 values measured below 0°C. showed there would exist another minimum in T_1 around -100°C. A type of molecular motion may be suggested for this temperature range. This would correspond to rotation of the CH_3 groups or to the vibrational motion of the segments as mentioned above. The T_1 minimum values are likely to depend upon the sulfur content. Average distances of the nearest neighbor for each proton are estimated to be about 1.8 A., and at these temperatures the methyl

groups are assumed to rotate so rapidly that their contribution to T_1 may be negligible. This average proton–proton distance would not be affected by curing. Thus, eq. (2) gives a T_{1min} value of 17.7 msec. for all the samples measured. This value is in good agreement with the experimental values (20.5 msec. for the cured rubber containing 1.9% sulfur and 18.8 msec. for raw rubber[5]). However, the minimum value of T_1 observed for the sample containing 26% sulfur was 40 msec. This result suggests that the average value of r_j is not correct for this case or that eq. (1) under the condition of the single τ_c cannot be applied for these polymeric systems.

The shape of the log T_1 versus $1/T$ curve also depends upon the sulfur content. The T_1 curve for the heavily cured sample was shallower and flatter than that observed for the weakly cured rubber. Applicability of eq. (1) may not be adequate for the heavily cured rubber. More detailed discussion of these results is given in the following section.

IV. GENERAL DISCUSSIONS AND CONCLUSIONS

1. Comparison of NMR Line Width Changes and Dielectric Relaxation

As previously described, the major narrowing of the absorption takes place when the inverse frequency width of line[6,18] $(2\pi\delta\nu)^{-1}$, approaches the correlation time, τ_c, for the segmental motions of rubber molecules. In the case of rather slow motion near the transition temperature, eq. (3) is given by the theory of Kubo and Tomita[7] for describing the narrowing:

$$(\Delta H_{1/2})^2 = (16 \ln 2/\pi) \langle \Delta H_2{}^2 \rangle_{rigid} \tan^{-1} [(\alpha\pi/8 \ln 2) \tau_c \, \gamma\Delta H_{1/2}] \quad (3)$$

where $\langle \Delta H_2{}^2 \rangle_{rigid}$ is the second moment before the narrowing takes place and α is a correction factor depending upon the line shape which is unity for Gaussian line shape. Only one responsible correlation mechanism represented by τ_c is assumed for deriving this equation. If one further assumes that this τ_c varies with temperature as

$$\tau_c = \tau_{0c} \exp \{\Delta E/RT\} \quad (4)$$

corresponding to a thermal process with an activation energy ΔE, combining eqs. (3) and (4), we can obtain the energies of activation from the line width data.

On the other hand, the segmental motions of cured rubber can be studied by the dielectric measurement. Crosslinking caused by combined sulfur produces electric dipoles in molecules and between molecules as shown above. For such systems, dielectric measurements are useful to investigate the motion of the dipoles. The applied electric field forces the dipoles to rotate under hindrance by combined molecules. Such dielectric behavior of cured rubber is described qualitatively by Debye's theory.[26] In this point of view the motions of the electric dipole are closely related to those of the segments and it should be quite interesting to compare the results of the dielectric measurement with those of NMR.

According to Debye's theory, the dielectric constant ϵ' and the dielectric loss factor ϵ'' are described as

$$(\epsilon' - \epsilon_\infty)/(\epsilon_0 - \epsilon_\infty) = (1 + \omega^2 \tau_D^2)^{-1} \qquad (5)$$

$$\epsilon''/(\epsilon_0 - \epsilon_\infty) = \omega \tau_D/(1 + \omega^2 \tau_D^2) \qquad (6)$$

where ϵ_0 is the statically measured dielectric constant, ϵ_∞ is the dielectric constant measured at frequencies much greater than the relaxation rate, $\nu_D = (2\pi\tau_D)^{-1}$, and ω denotes the angular frequency of measurements. Only one significant relaxation time, τ_D, is assumed for the motions of the dipole as well as τ_c. An equation similar to eq. (4) is given also for temperature dependence of τ_D:

$$\tau_D = \tau_{0D} \exp \{\Delta E/RT\} \qquad (7)$$

τ_D is directly obtained from eqs. (5) and (6) for the observed values ϵ', ϵ'', ϵ_0, and ϵ_∞. In the limiting cases of $\omega\tau_D \ll 1$ and $\omega\tau_D \gg 1$, $\epsilon''/(\epsilon_0 - \epsilon_\infty)$ is directly proportional to τ_D and τ_D^{-1}, respectively. Thus, combined with eqs. (5) and (6), eq. (7) gives energies of activation for the motions of electric dipoles.

T_1 measurements also serve as a means of investigating the segmental motions of rubber molecules. If the term $\Sigma_j r_j^{-6}$ in eq. (1) is known, T_1 gives τ_c. As in the case of eq. (6), eq. (1) also is reduced to simple forms as

$$1/T_1 = \omega\tau_c$$

and

$$1/T_1 = C/(\omega^2 \tau_c^2) \qquad (8)$$

for the two limiting cases, $\omega\tau_c \ll 1$ and $\omega\tau_c \gg 1$, respectively. We obtain energies of activation from eqs. (4) and (8).

Thus, under the assumption of a single correlation time τ_c and a single dielectric relaxation time τ_D, energies of activation for the motions of segments and dipoles can be found from the experimental data of ϵ', ϵ'', $\Delta H_{1/2}$, and T_1 independently of each other.

Extensive dielectric measurements on cured rubber differing in the combined sulfur content in the range from 2 to 32% have been carried out by Scott et al.[8] for the frequency range from 60 cycles/sec. to 300 kcycles/sec. in the temperature region from −75 to 320°C. Energies of activation were computed from these results by using the slopes of the high temperature linear portion of plots of log ϵ'' versus $1/T$ and are listed in Table IIIB; those obtained from the data of T_1 and $\Delta H_{1/2}$ by using eqs. (1) and (3)–(8) are listed in Table IIIA.

The values of ΔE in Table III are dependent upon the combined sulfur content and the method of measurement. ΔE obtained by NMR is not consistent with that obtained from the dielectric data for the same content of combined sulfur. As previously pointed out,[10] the values of ΔE from dielectric measurements show a marked dependency upon frequency and

TABLE IIIA

Values of ΔE Obtained from NMR Measurements

Sample No.	S, %	ΔE, kcal./mole	
		From $\Delta H_{1/2}$	From T, (at 20 Mcycles/sec.)
0	0	13.8	7.7[a]
1	1.9	13.8	7.3
2	3.9	12.2	—
3	7.8	12.5	6.3
4	13.8	13.9	—
5	19.4	13.9	—
6	24.1	12.4	5.3
7	31	13.5	—

[a] Data of Gutowsky et al.[5]

TABLE IIIB

Values of ΔE Obtained by Use of Dielectric Measurements of Scott et al.[8]

S, %	ΔE, kcal./mole						
	300 kcycles/ sec.	100 kcycles/ sec.	3 kcycles/ sec.	1 kcycle/ sec.	60 cycles/ sec.	This work[a]	Kauz-mann[b]
2	10.7	10.7	10.7	10.7	13.2	24	25.2
4	10.6	10.1	11.6	12.5	11.7	25	26.1
8	8.6	9.7	11.4	13.4	14.7	28	28.6
14	6.2	10.8	12.8	12.7	14.2	33	32.3
23	11.4	10.3	15.2	16.0	16.8	45	46.0

[a] Calculated from the temperature dependence of τ_{D0} in Figure 6.
[b] Calculated by Kauzmann[10] on the basis of measurements of Scott et al.[8]

temperature. In NMR measurements ΔE from T_1 is almost one-half the value obtained from the line width data. The values of ΔE from $\Delta H_{1/2}$ do not seem to show significant variation with combined sulfur contents. In T_1 measurements ΔE has a clear tendency to decrease with increased combined sulfur content. It may be a reasonable prediction that the combined sulfur reduces the freedom of segmental motions and consequently would cause increase of activation energies for both NMR and dielectric behavior. Some of the ΔE values shown in Table III exhibit such trends, but others do not and thereby they indicate that the matter is not so simple.

2. Effects upon T_1 of the Distribution of Correlation Time

It is well known[9] that the frequency dependence of ϵ' and ϵ'' on high polymers deviates considerably from that predicted by eqs. (5) and (6). This fact has been observed on cured rubber,[10] and it has been confirmed[10] that the unreasonable values of ΔE should be ascribed to neglect of the distribution of relaxation time. In order to interpret the discrepancies of results of the dielectric measurements for high polymers it has been proposed[10] that eqs. (5) and (6) of the simple Debye model under the assump-
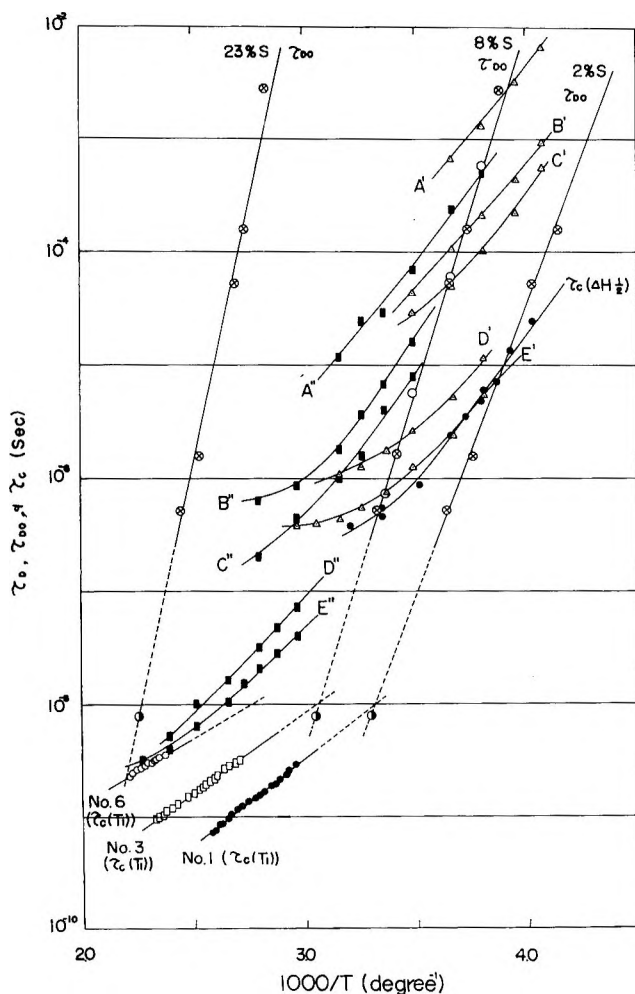
Fig. 6. NMR correlation times and the dielectric relaxation times obtained by various methods: ($\otimes$) curves for 2, 8, and 23% S are τ_{Dmax} determined from $\omega \tau_D = 1$ as described in text (the measuring frequencies are 60 cycles/sec., 1 kcycle/sec., 3 kcycles/sec., 100 kcycle/sec., and 300 kcycle/sec. from top to bottom); (O) on the τ_{D0} curve for 8% S are the most probable relaxation times deduced from frequency dependence of ϵ'' at corresponding temperatures; (◑) on the τ_{D_0} curves are calculated τ_D max values for measurements at 1 Mcycle/sec.; (■) $\tau_D(\epsilon')$ obtained from temperature dependence of ϵ' (A', B', C', D', and E' correspond to measuring frequencies of 60 cycles/sec., 1 kcycle/sec., 3 kcycles/sec., 100 kcycles/sec., and 300 kcycles/sec., respectively); ($\triangle$) $\tau_D(\epsilon'')$ obtained in the same way as $\tau_D(E')$ (A'', B'', C'', D'', and E'' have the same meaning as A', etc.); (●) $\tau_c(\Delta H_{1/2})$ denotes τ_c obtained from line width data; (●), (□), and (O) curves for $\tau_c(T_1)$ are deduced from T_1 measurements for the samples 1, 3, and 6, respectively.

tion of the single τ_D are inadequate to characterize the complicated behavior of high polymeric systems and that the distribution of the dielectric relaxation time should be considered for such polydisperse systems.

Several types of distribution function to fit the experimental ϵ'' curves

to the theoretical ones have been proposed.   One of them is a Gaussian type function proposed by Wagner[9,12] and has been applied to interpret the dielectric properties of cured rubber.   The following function of τ_D has been given for a distribution:

$$k(\tau_D)d\tau_D = (b/\sqrt{\pi}) \exp\{-b^2z^2\}dZ \qquad (9)$$

where b is a constant which determines the width of the distribution; Z is defined as $\ln(\tau_D/\tau_{D0})$, with τ_{D0}, the most probable relaxation time, assumed to have a temperature dependence similar to eq. (7).   The results based upon introducing the distribution function into eqs. (5) and (6) have been reported.[10]   The theoretical ϵ' and ϵ'' versus frequency curve showed quite considerably good agreement with experimental values on cured rubber, showing that the assumed distribution of τ_D is a reasonable modification of Debye's theory for such polydisperse system. τ_{D0} is determined from the frequency dependence of ϵ'' at the temperature studied, i.e., τ_{D0} is defined as $(2\pi)^{-1}$ times the inverse frequency giving the maximum loss factor at the temperature.   The apparent energies of activation are obtained from the temperature dependence of τ_{D0}, assuming

$$\tau_{D0} = \tau^*_{D0} \exp\{\Delta E/RT\} \qquad (10)$$

Values of obtained ΔE from the dielectric data on cured rubber are listed in Table III.   The increase in ΔE with increasing combined sulfur content appears to be very reasonable.

Meanwhile, $\tau_{D\max}$, which is determined by $\omega\tau_D = 1$ for the maximum value of ϵ'' on a ϵ'' versus temperature curve, gives τ_{D_0} at a given temperature.   This fact is clear on the cured rubber sample containing 8% sulfur.[8]   In Figure 6 are plotted values of τ_D, $\tau_{D\max}$, and τ_{D_0} obtained by various methods against reciprocal temperature.   The temperature dependence of $\tau_{D\max}$ agrees well with that of τ_{D_0} on the sample containing 8% sulfur.   Therefore, the apparent energies of activation are obtained from the temperature dependence of τ_{D_0} and $\tau_{D\max}$ by eq. (10).   In all events, the effects of the distribution of τ_D is shown obviously in Figure 6.

Similar investigations of the distribution of τ_c would be worthwhile in order to investigate effects upon eqs. (1) and (3).   Several authors[5,28-32] have studied on this problem related to high polymers.   Certain types of distribution function have been proposed[5,29-32] and their effects upon T_1 versus the average correlation time[29,31] τ_c curve and on energies of activation have been discussed.[5,25,28]   We also have examined the effects of a correlation time distribution, upon the temperature dependence of T_1.   Introducing the distribution function to eq. (9), we obtain the eq. (11) for $1/T_1$, as proposed previously:[5,29]

$$\frac{1}{T_1} = \frac{3}{10}\gamma^4\hbar^2 \sum_j r_j^{-6} \frac{1}{\omega}\left[\int_0^\infty \frac{k(\tau_c)\omega\tau_c d\tau_c}{1+\omega^2\tau_c^2} + 2\int_0^\infty \frac{2k(\tau_c)\omega\tau_c d\tau_c}{1+4\omega^2\tau_c^2}\right] \qquad (11)$$

where

$$k(\tau_c)d\tau_c = (b/\sqrt{\pi}) \exp\{-b^2z^2\}dZ$$

$$Z = \ln (\tau_c/\tau_{c_0})$$

$$\tau_{c_0} = \tau_{c_0}{}^* \exp \{\Delta E/RT\}$$

where each notation has similar meaning as in eq. (9). Studies on dielectric properties of cured rubbers[10] have shown that the constant b is dependent upon temperature. For this reason, it may be necessary that the frequency dependence of T_1 at a fixed temperature should be examined for a wide frequency range. Rewriting eq. (11), we obtain

$$(T_1/\omega)C = \left[\int_0^\infty \frac{k(\tau_c)\omega\tau_c d\tau_c}{1 + \omega^2\tau_c^2} + 2 \int_0^\infty \frac{2k(\tau_c)\omega\tau_c d\tau_c}{1 + 4\,\omega^2\tau_c^2}\right]^{-1} \tag{12}$$

where

$$C = (^3/_{10}\,\gamma^4\,\hbar^2 \sum_j r_j{}^{-6})^{-1}$$

At a fixed temperature, C is constant and determined only by the molecular structures. For the values of the definite integrals given by Yager,[9] the values of $(T_1/\omega)C$ are plotted against $\omega\tau_c$ for various values of the parameter b in Figure 7. The curve for $b = \infty$ corresponds to a single correlation time. If there is a distribution of the correlation time, the curve becomes flatter and shallower. The tendency is quite analogous to that of the ϵ'' versus frequency curves. The most probable correlation time, τ_{c_0}, may be determined from the condition that $(T_1/\omega)C$ have its minimum value at $\omega\tau_c = 0.6158$. The temperature dependence of τ_{c_0} thus obtained would give the apparent energies of activation.

Also the values of b would be obtained by selecting the most fitted curve and plotting $(T_1/\omega)C$ against frequencies. Unfortunately, it is almost impossible in NMR measurements to perform observations at frequencies varying over a range of three decades or more.

The frequency dependence of the T_1 versus $1/T$ curve on raw Hevea rubber has been reported[5] as shown in Figure 5. In this case, the shapes of the high temperature portion of the curves depend upon the resonance frequency for measurements contrary to eq. (8), showing that a distribution of τ_c might exist. Therefore, if the distribution function for τ_c would be similar to eq. (9), there should be found a set of experimental values of the parameter b. However, a linear plot of log $(T_1/\omega)C$ versus ln $\omega\tau_c$ obtained from the experimental values[5] of T_1 for measurements at 20 and 28 Mcycles/sec. had a slope which was steeper than that of the curve for $b = \infty$ in Figure 7. This result suggests that the distribution function assumed in eq. (11) is inadequate for the raw Hevea rubber.

Nonetheless, the results for the temperature and frequency dependence of T_1, summarized in Figure 5, do support, in two ways, the existence of a distribution function for τ_c in the cured rubber. First, it may be seen that the minimum T_1 value becomes larger with increasing sulfur content. Second, the T_1 curve has a broader, shallower minimum at higher sulfur contents. Both trends imply[5] an increasingly wide distribution of τ_c, which seems reasonable. It should be noted that the average correlation time, $\bar{\tau}_c$,
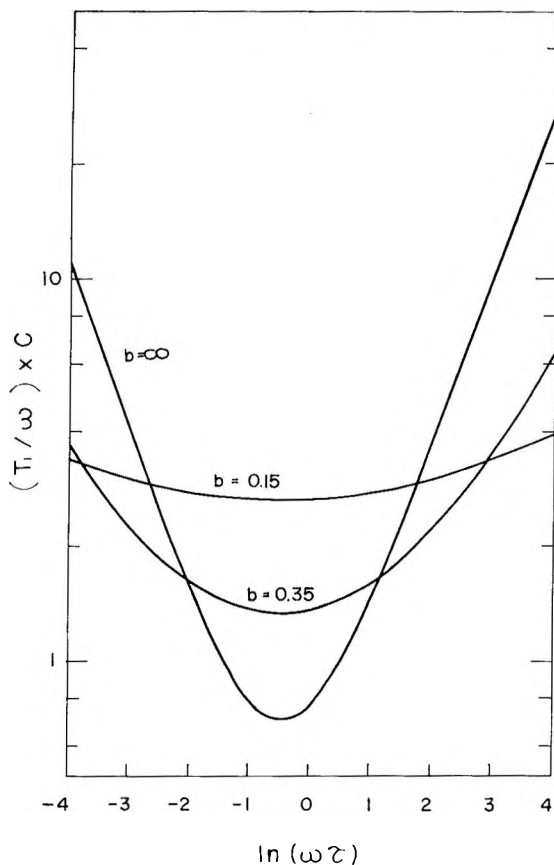
Fig. 7. Effects of various distributions of the correlation time, τ_c, upon the frequency dependence of T_1, according to eq. (11).

obtained for the distribution[29,31] has been considered in analyzing T_1 results and it has been pointed out[30] that the apparent energies of activation from T_1 data are directly proportional to those obtained from NMR line width data using eq. (3).

3. Effect upon the Correlation between τ_c and τ_D of their Distributions

The correlation between NMR and the mechanical and dielectric measurements has been investigated on some high polymer[32] and organic compounds.[34,35] Introduction of a distribution of the correlation times in the interpretations of NMR results was found to improve the correlation. It was shown for polyisobutylene[32] that the temperature dependence of τ_c in NMR giving quite different activation energies from those obtained from the dielectric and mechanical measurements would approach that of the most probable relaxation times in the latter methods. In this section we also will discuss this point, comparing the NMR results with those from dielectric measurements on cured rubber. Since distributions are indicated

by the dielectric measurements,[10] activation energies obtained from temperature dependence of τ_D and τ_c in simple theories no longer have any significance for describing molecular motions in such polydisperse systems. The apparent energies of activation should be accepted for the most probable motions. They are now obtained from τ_{D_0} versus temperature curves. This situation has been shown for the 8% S sample in Figure 6.

Plotted in Figure 6 are the correlation time τ_c obtained from the line width data of the sample 1; the correlation time τ_c calculated from T_1 data on samples 1, 3, and 6; the relaxation time τ_D and the most probable relaxation time $\tau_{D_{max}}$ computed from ϵ'' data[8] on a sample containing 8% S; and the most probable relaxation time τ_{D_0} obtained from ϵ'' data[8] for the samples containing 2, 8, and 23% S. A value of $\alpha = 1$ in eq. (3) was assumed for calculation of τ_c. The results show that the most probable relaxation times obey eq. (12), and that apparent energies of activation obtained from the curves may be given as potential barriers against the most probable motions.

In Figure 6 it can be seen how the distribution of τ_D affects the single correlation theory, i.e., all the τ_D curves obtained for the 8% S sample by use of eqs. (5) and (6) intersect the τ_{D_0} curve. The most interesting feature of $\tau_D(\epsilon')$ curves (A', B', C', D', and E' in Fig. 6) is that they intersect the τ_{D_0} line near the points where the values of τ_{D_0} are given by the relation, $\omega\tau_D = 1$ (where ω is the frequency of measurements of ϵ'). This indicates distribution of τ_D. The relaxational mechanism represented by $\tau_D = \omega^{-1}$ should be most effective on ϵ' in measurements with a frequency of $\omega/2\pi$. Analogous features have been shown also by the $\tau_D(\epsilon'')$ curves (A'', B'', C'', D'', and E'' in Fig. 6). The curves also intersect the τ_{D_0} curve near the points where τ_{D_0} is given by $\omega\tau_{D_0} = 1$. As shown previously,[10] a distribution of τ_D did not affect values of ϵ' calculated by eq. (5). On the other hand, values of ϵ'' obtained by eq. (6) should be larger than those observed[10] if a distribution exists. This is one of the reasons why $\tau_D(\epsilon'')$ curves intersect the τ_{D_0} curve approximately near the points. In any way, because of a distribution, curves of τ_D (ϵ' and ϵ'') obtained from eqs. (5) and (6) intersect the τ_{D_0} curve at the points where the values of τ_{D_0} are the inverse of the measuring frequency ω. On introducing an appropriate distribution function into eqs. (5) and (6), the τ_D curves would form a band superposed on the τ_{D_0} curve.

An analogous consideration would be interesting for $\tau_c(T_1)$ and $\tau_c(\Delta H_{1/2})$ curves in Figure 6. $\tau_c(T_1)$ curves obtained for the results of sample 3 are shown in this figure. The extrapolated curve intersects the τ_{D_0} curve at about $\tau_{D_0} = (2\pi \times 20 \times 10^6)^{-1}$ sec., and the values of τ_c at $T_{1\,min}$ falls at a point near $\tau_{D_0} = 10^{-8}$ sec. Therefore, it may be suggested that the motion having the correlation time of ω^{-1} would be most effective for the relaxation mechanism for a measuring frequency of ω. As in the case of the τ_D (ϵ'') curve, introducing an appropriate distribution function $\tau_c(T_1)$ curves would form a band superposed on the τ_{D_0} curve and τ_c at $T_{1\,min}$ would coincide with τ_{D_0} given by $\tau_{D_0} = 0.6158\,\omega$. If it is possible to change

the resonance frequencies for a wide range (two or three decades), a set of $\tau_c(T_1)$ curves as well as τ_D curves may be plotted from eq. (1).

The temperature dependence of line width is independent of the measuring frequencies, and narrowing of the absorption takes place when the correlation time τ_c becomes of the order of $(\gamma \Delta H/2\pi)^{-1}$. If τ_c is distributed over some range, as expected from the consideration of $\tau_D(\epsilon'')$, the most effective motion for the narrowing would have the correlation time given by $\tau_c = \omega^{-1}$, where ω is the frequency of measurements. However, the functional form relating the NMR line narrowing, eq. (3), to τ_c differs considerably from the equations describing the dielectric relaxation. And, therefore, one expects only limited similarities between $\tau_c(\Delta H_{1/2})$ and τ_D. Yet correspondence is not bad, as may be seen by comparing the curve for $\tau_i(\Delta H_{1/2})$ with curve D' and E', which are for dielectric measurements bracketing those responsible for the NMR line narrowing. Actually, the values of τ_c obtained from the data of second moment, using a similar equation to eq. (3), were about ten times those of $\tau_c(\Delta H_{1/2})$. From these results, we may understand that the effect upon the $\tau_c(\Delta H_{1/2})$ curve of the distribution of correlation time appears in the same manner as τ_D curves. Some corrections have been made in NMR experiments[32, 34] on $\tau_c(\Delta H_{msl})$ curves introducing a distribution function. The results showed that the $\tau_c(\Delta H_{msl})$ curve should be replaced by a band having a steeper gradient. These results may not be quantitative but strongly show the effect of the distribution of correlation times.

The τ_{D_0} curve obtained[10] for the sample containing 23% should be compared with the $\tau_c(T_1)$ curve for sample 6. The intersection is located at a temperature much higher than $T_{1\ min}$ temperature, while the intersection of the curve for the sample containing 8% S with that for sample 3 is, in contrast, found at a little higher temperature than that of its $T_{1\ min}$. These features give some information on the distribution of τ_c and τ_D. In heavily cured rubber τ_D would be nonequivalent to τ_c, for the distribution of τ_D would be much different from that of τ_c. This tendency may be reasonable, since the rather short-range motions of molecules are responsible for the relaxation mechanism in NMR, and the dielectric relaxation is governed by those over a wide range. From these considerations it would be naturally expected that, if there is an adequate distribution function of correlation times, $\tau_c(T_1)$ may give larger values of ΔE for heavily cured rubber than for weakly cured rubber as in the case of dielectric measurements.

From the discussions described above it seems to be absolutely necessary in studies on molecular motions in high polymer by means of NMR techniques to measure the temperature dependence of the spin lattice relaxation time for a very wide range of frequency and compare the temperature dependence of τ_{c_0} with that of the most probable relaxation time in the other type of measurements, e.g., dielectric, mechanical, ultrasonic, etc. measurements. Finally, analysis of the NMR results would be easier if only intramolecular interactions were important, and for this reason it would be well

to study samples having a simple molecular structure such as polyvinylidene chloride, $(-CH_2CCl_2-)_n$.

References

1. Holroyd, L. V., R. S. Codrington, B. A. Mrowca, and E. Guth, *J. Appl. Phys.*, **22**, 696 (1951).

2. Gutowsky, H. S., and L. H. Meyer, *J. Chem. Phys.*, **22**, 2122 (1953).

3. Honnold, V. R., F. McCaffery, and B. A. Mrowca, *J. Appl. Phys.*, **25**, 1219 (1954).

4. Oshima, K., and H. Kusumoto, *J. Chem. Phys.*, **24**, 913 (1956).

5. Gutowsky, H. S., A. Saika, M. Takeda, and D. E. Woessner, *J. Chem. Phys.*, **27**, 534 (1957).

6. Bloembergen, N., E. M. Purcell, and R. V. Pound, *Phys. Rev.*, **73**, 679 (1948).

7. Kubo, R., and K. Tomita, *J. Phys. Soc. Japan*, **9**, 888 (1954).

8. Scott, A. H., McPherson, A. T., and Curtis, H. L., *J. Res. Natl. Bur. Std.*, **11**, 173 (1933).

9. Yager, W. A., *Physics*, **7**, 434 (1936).

10. Kautzman, W., *Rev. Mod. Phys.*, **14**, 12 (1942).

11. Gutowsky, H. S., L. H. Meyer, and R. E. McClue, *Rev. Sci. Instr.*, **24**, 644 (1953).

12. Buchta, J. C., H. S. Gutowsky, and D. E. Woessner, *Rev. Sci. Instr.*, **29**, 55 (1958).

13. Carr, H. Y., and E. M. Purcell, *Phys. Rev.*, **94**, 630 (1954).

14. Andrew, E. R., and R. G. Eades, *Proc. Roy. Soc. (London)*, **A216**, 398 (1953).

15. Powles, J. G., *Proc. Phys. Soc.*, **B69**, 281 (1956).

16. See for example, P. J. Flory, *Principles of Polymer Chemistry*, Cornell Univ. Press, Ithaca, N.Y., 1953.

17. Curtis, H. L., A. H. Scott, and A. T. McPherson, *Natl. Bur. Std. Sci. Paper*, **22**, 383 (1927).

18. Gutowsky, H. S., and G. E. Pake, *J. Chem. Phys.*, **18**, 162 (1950).

19. Kusumoto, H., *J. Phys. Soc. Japan*, **11**, 1015 (1956).

20. Kusumoto, H., unpublished data. ΔH_{msl} vs. temperature curves have been quoted by A. Odajima in *High Polymers*, **7**, 474 (1958).

21. Nohara, S., *Kobunshi Kagaku*, **13**, 531 (1956).

22. Slichter, W. P., *J. Appl. Phys.*, **26**, 1099 (1955).

23. Slichter, W. P., and E. R. Mandell, *J. Appl. Phys.*, **29**, 1438 (1958).

24. Boyer, R. F., and R. S. Spencer, *Advan. Colloid Sci.*, **2**, 8 (1946).

25. Kusumoto, H., I. J. Lawrenson, and H. S. Gutowsky, *J. Chem. Phys.*, **32**, 724 (1960).

26. Debye, P., *Polar Molecules*, Chemical Catalog Co., 1929.

27. Wagner, K. W., *Ann. Physik*, **40**, 817 (1913); *Archiv Elektrotech.*, **3**, 83 (1914).

28. Miyake, A., *J. Polymer Sci.*, **28**, 476 (1958).

29. Odajima, A., *Progr. Theoret. Phys. (Kyoto)*, Suppl., **10**, 142 (1959).

30. Nolle, A. W., and J. J. Billings, *J. Chem. Phys.*, **30**, 84 (1959).

31. McCall, D. W., D. C. Douglass, and E. W. Anderson, *J. Chem. Phys.*, **30**, 1272 (1959).

32. Powles, J. G., and K. Luszcynski, *Physica*, **25**, 455 (1959).

33. Powles, J. G., *J. Polymer Sci.*, **22**, 79 (1956).

34. Luszcynski, K., and J. G. Powles, *Proc. Phys. Soc. (London)*, **74**, 408 (1959).

35. Luszcynski, K., J. A. Kail, and J. G. Powles, *Proc. Phys. Soc. (London)*, **75**, 243 (1960).

Résumé

On a étudié la résonance magnétique du proton sur du caoutchouc naturel vulcanisé contenant jusqu'à 31% de soufre combiné. On observe les formes des raies et les temps de rélaxation des spins à des températures entre −190 et 180°C. Dans les études des formes des raies, on trouve que le principal effet du soufre combiné repose sur la température à laquelle la largeur des raies se reserre par les mouvements des segments moléculaires. La température à partir de laquelle la diminution de largeur des raies augmente, est de −50°C. pour le caoutchouc brut à environ 10°C. pour 31% de sourfre combiné. On trouve une relation entre la dépendance de la teneur de soufre et du changement de largeur des raies et la température de transition du second ordre. Le temps de rélaxation du réseau du spin électrique T_1 a été mesuré pour trois échantillons vulcanisés dans un domaine de température au-dessus de la région de limitation des mouvements. Les courbes T_1 en fonction de la température s'accordent qualitativement avec la théorie de Kubo-Tomita. Les caractéristiques des courbes T_1 dépendent de la teneur en soufre combiné. On a estimé les énergies d'activation à partir de ces résultats et on les a comparées avec les résultats de rélaxation diélectrique obtenus précédemment. On discute l'effet d'une distribution du temps de corrélation.

Zusammenfassung

Protonmagnetische Resonanz-Untersuchungen wurden an vulkanisiertem Kautschuk mit bis zu 31% gebundenem Schwefel ausgeführt. Die Liniengestalt und die Spin-Gitter-Relaxationszeiten wurden bei Temperaturen zwischen −190 und 180° C. beobachtet. Bei der Untersuchung der Liniengestalt zeigte sich, dass der Haupteinfluss des gebundenen Schwefels sich auf die Temperatur erstreckt, bei welcher die Linienbreite durch die Bewegung der Molekülsegmente verringert wird. Die Temperatur der beginnenden Linienverengung steigt von −50°C. bei Rohkautschuk auf etwa 10°C. bei 31% gebundenem Schwefel. Eine Beziehung zwischen der Abhängigkeit der Linienbreitenänderung vom Schwefelgehalt und der Umwandlungstemperatur zweiter Ordnung wurde gefunden. Die Protonspin-Gitter-Relaxationszeit, T_1, wurde an drei vulkanisierten Proben im Temperaturbereich oberhalb des Gebietes der Bewegungsverengung gemessen. Die Kurve T_1 gegen Temperatur stimmt qualitativ mit der Theorie von Kubo-Tomba überein. Der Verlauf der T_1-Kurven hängt vom Gehalt an gebundenem Schwefel aü. Aktivierungsenergien wurden aus den Ergebnissen berechnet und werden mit den früher erhaltenen Daten über dielektrische Relaxation verglichen. Der Einfluss einer Verteilung der Korrelationszeit wird diskutiert.

Stereoregulated Poly-dideuteroethylene I.   Polymers of *trans*-1,2-Dideuteroethylene and *cis*-1,2-Dideuteroethylene by a Ziegler Catalyst

SAKUJI IKEDA, AKIO YAMAMOTO, and HIROSHI TANAKA,
*Research Laboratory of Resources Utilization, Tokyo Institute of
Technology, Okayama, Meguro, Tokyo, Japan*

Synopsis

Polydideuteroethylenes having some stereoregulated structure were prepared by polymerizing *trans*- and *cis*-1,2-dideuteroethylene using a Ziegler catalyst. *trans* and *cis*-dideuteroethylene were prepared by reducing dideuteroacetylene with chromous chloride solution and copper activated zinc dust, respectively.   Infrared spectra of the two polymers obtained showed significant differences particularly in the bending vibration bands of CHD groups.   Bands at 1335 and 1288 cm.$^{-1}$ were observed only in polymers of the *trans* isomer, and a band at 1305 cm.$^{-1}$ was observed only in polymers of the *cis* isomer.   Densities, melting points, intrinsic viscosities, and crystallinities of the polymers were measured and compared with those of normal polyethylene.   The x-ray diffraction patterns of the polydideuteroethylenes were almost identical with that of normal polyethylene.

INTRODUCTION

Although di-isotactic polydeuteropropylenes have been prepared from *trans*- and *cis*-1-deuteropropylene by Natta and co-workers[1] and the effect of a stereoregulating catalyst on the configuration of the CHD groups resulting from the polymerization has been discussed by them, no attempt has been made, so far as we know, to obtain the simplest stereoregular deuteropolymer—polydeuteroethylene.

To obtain the stereoregular polydeuteroethylene, we have synthesized *trans*- and *cis*-1,2-dideuteroethylene and carried out the polymerization with a Ziegler catalyst which is known to be a stereoregulating catalyst for many vinyl monomers.

For the stereoregulated structures of poly-1,2-dideuteroethylene, three structures are considered, as shown in Figure 1: erythro-di-isotactic(e-DI), threo-di-isotactic (t-DI) and disyndiotactic (DS) by Natta's nomenclature.[2]

It is not to be expected that the polymer obtained from dideuteroethylene, even using only a single monomeric isomer, would have a structure with complete regularity as considered above, for the monomer has no substituted group which will induce steric hindrance and/or specific polar-
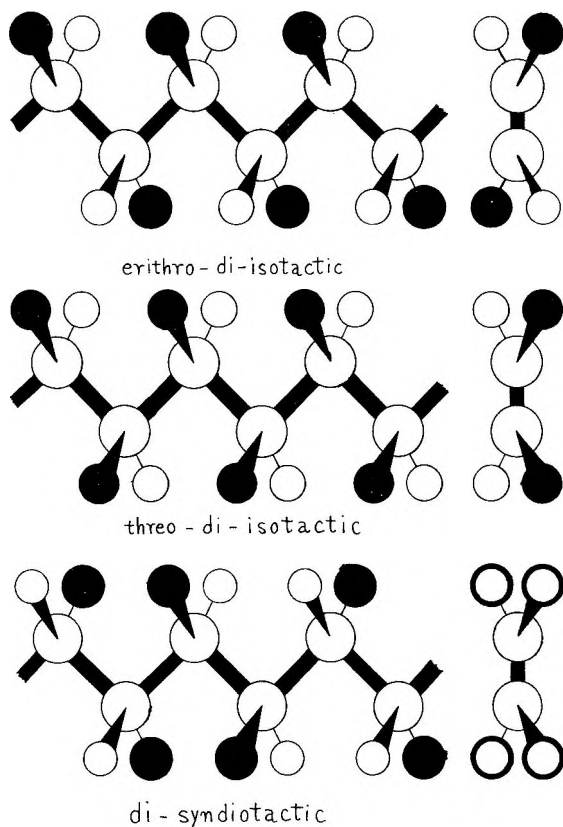
Fig. 1. Stereoregulated structures of poly-1,2-dideuteroethylene.

ization in the C—C bond of the monomer in the polymerization. However, if in each propagation step the addition of ethylene proceeds in a defined configuration to the polymer chain and free rotation of the monomer C—C bond is inhibited, we may obtain the poly-1,2-dideuteroethylene having some stereoregulated structure. The structure may be either (e-DI) plus (DS) or (t-DI) plus (DS), according to the kind of monomer used. The type of double bond opening: *cis* or *trans*, may decide the structure of the polymer obtained.[3]

In the present paper, the methods of preparation, the infrared spectra, and some physical properties of the poly-1,2-dideuteroethylenes obtained are reported.

PREPARATION AND POLYMERIZATION OF DIDEUTERO-ETHYLENE

Dideuteroacetylene was prepared by the reaction of pure calcium carbide with deuterium oxide in a vacuum system. Acetylene obtained by the hydrolysis of calcium carbide contains some impurities such as phosphine,

TABLE I
The Extent of Deuteration and the Principal Impurities in the Deutero Compounds

Compounds	Extent of deuteration, g.-atom-$\%_C{}^a$	Principal impurities[b] and contents, mole-$\%$
C_2D_2	98.9	$CH{\equiv}CD$, 2.5
trans-$C_2H_2D_2$	48.4	$CH_2{=}CHD$, 3
cis-$C_2H_2D_2$	47.9	trans-$C_2H_2D_2$, 1
		$CH_2{=}CHD$
C_2D_4	90.0	$CHD{=}CD_2$
		cis-$C_2H_2D_2$
		$CH_2{=}CHD$

[a] By mass spectrometry.
[b] By infrared spectrophotometry, the values were determined approximately.

ammonia, hydrogen sulfide, and other hydrogen or sulfur compounds. Since the complete purification of acetylene without hydrogen–deuterium exchange is difficult and since some of these impurities are removed during the reduction procedure, the acetylene was used directly for reduction to ethylene without further purification. The ethylene was then submitted to a purification step (Table I).

trans-1,2-Dideuteroethylene was prepared by the reduction of the deuteroacetylene with chromous chloride solution which is a chemical reducing agent reported to give *trans*-isomers.[4] *cis*-1,2-Dideuteroethylene was prepared by the reduction with copper-activated zinc dust and water, a catalyst known to give the *cis* form.[4]

The polymerization of the ethylene was carried out with a Ziegler catalyst prepared from triethylaluminum and titanium tetrachloride in a *n*-hydrocarbon solution. Melting points, densities, and data from x-ray diffraction analysis of the polymers obtained are shown in Table II.

TABLE II
Melting Points, Densities, and X-ray Diffraction Data of Polyethylene

Polymers	M.p., °C.	X-ray analysis		Density at 18°C., g./cm.[a]
		$2\theta°$	Crystallinity $\%$	
Poly-(C_2H_4)	127–132	21.4, 23.7	80	0.9774
Poly-(trans-$C_2H_2D_2$)	127–132	21.4, 23.7	81	1.030
Poly-(cis-$C_2H_2D_2$)	129–133	21.6, 23.8	77	1.018
Poly-(C_2D_4)	129–132	21.4, 23.7	84	1.076

The x-ray diffraction patterns of the poly(*trans*-$C_2H_2D_2$) and poly-(*cis*-$C_2H_2D_2$) were almost identical with that of normal polyethylene.

INFRARED SPECTRA OF POLY-1,2-DIDEUTEROETHYLENE

Typical spectra of poly-(C_2H_4), poly-(*trans*-$C_2H_2D_2$), and poly-(*cis*-$C_2H_2D_2$) in the NaCl region and the major part of the KBr region are shown in Figure 2. As these samples contained traces of silicone oil used

Wave length　μ
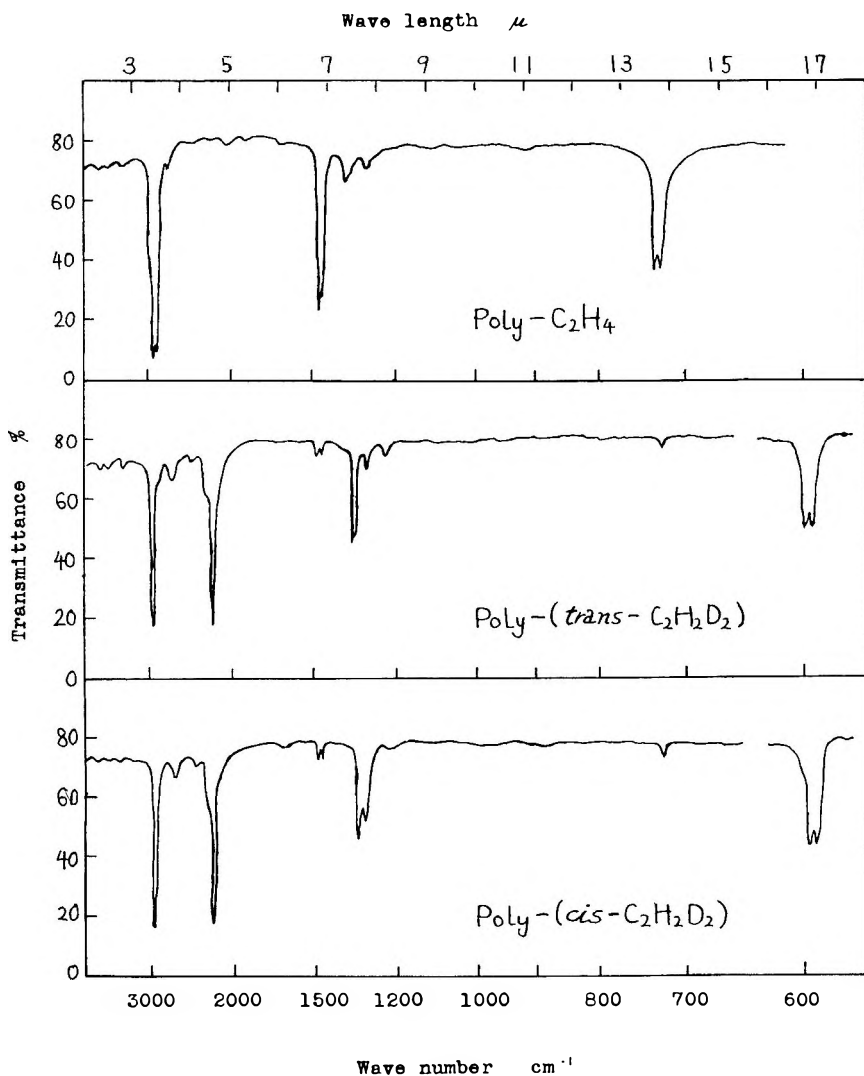
Fig. 2. Infrared spectra of polyethylene, poly-*cis*- and poly-*trans*-1,2-dideuteroethylene.

in the synthesis apparatus as well as decomposition compounds of the catalyst, absorption bands in the regions near 800 cm.$^{-1}$ and 1000–1150 cm.$^{-1}$ are not reliable.

By the substitution of deuterium in place of hydrogen in the methylene group, absorption bands due to methylene vibrations are observed to be shifted in the spectra of poly-$(C_2H_2D_2)$ in comparison with the corresponding bands of poly-(C_2H_4). Half of the bands near 2900 cm.$^{-1}$, bands near 1464 cm.$^{-1}$ and near 725 cm.$^{-1}$ disappeared, and new bands at 2146 cm.$^{-1}$, near 1325 cm.$^{-1}$ and near 590 cm.$^{-1}$ appeared in the spectra of poly-$(C_2H_2D_2)$. The frequency shifts upon isotopic substitution can be char-
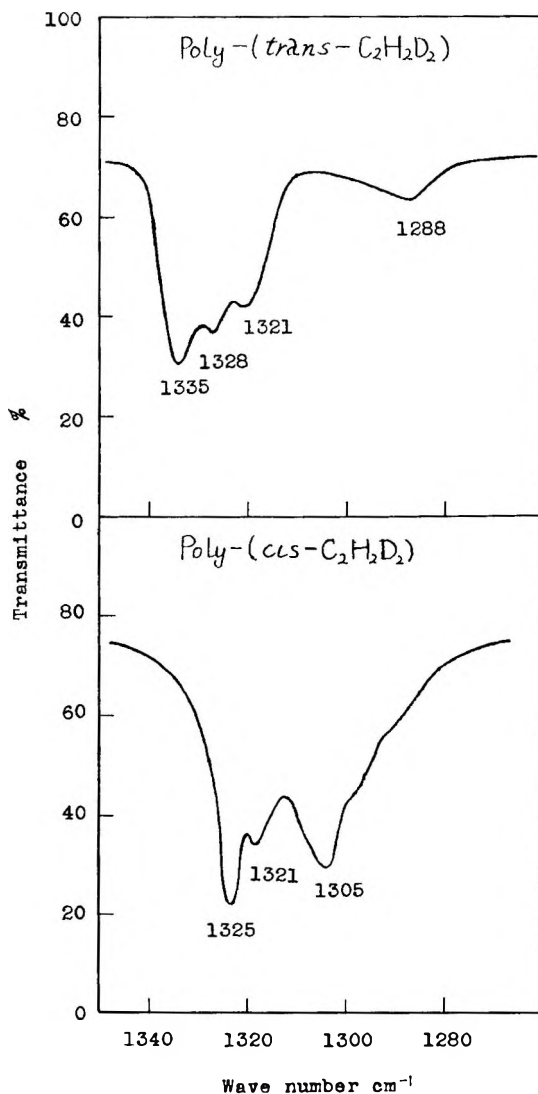
Fig. 3. Infrared spectra of poly-*trans*- and poly-*cis*-1,2-dideuteroethylene.

acterized by the ratios $\nu_H/\nu_D = 1.25$ for the stretching vibration, $\nu_H/\nu_D = 1.2$ for the bending vibration and $\nu_H/\nu_D = 1.2$ for the rocking vibration.

Of particular interest are the bending vibration bands observed near 1325 cm.$^{-1}$ in poly-(*trans*-$C_2H_2D_2$) and poly-(*cis*-$C_2H_2D_2$). In Figure 3 details of this region measured using a grating spectrometer are given. In poly-(*trans*-$C_2H_2D_2$), bands at 1335, 1328, 1321, and 1288 cm.$^{-1}$ were observed, while in poly-(*cis*-$C_2H_2D_2$) the bands at 1335 and 1288 cm.$^{-1}$ were not observed, but a band at 1305 cm.$^{-1}$ was observed instead. In the spectra of the polymers from the *trans*-$C_2H_2D_2$ containing other isomeric

ethylene, e.g., the mixture of 95% $trans$-$C_2H_2D_2$ and 5% C_2H_4 or of 50% $trans$- and 50% cis-$C_2H_2D_2$, the bands at 1335 and 1288 cm.$^{-1}$ were always observed. In the spectra of the polymers from cis-$C_2H_2D_2$ containing monomers, e.g., 50% $trans$- and 50% cis-$C_2H_2D_2$ or C_2D_4 which contained several per cent of cis-isomer resulting from the method of preparation, the band at 1305 cm.$^{-1}$ was always observed.

From the above observations, we can attribute the absorption bands at 1335 and 1288 cm.$^{-1}$ to polymers of the $trans$-isomer and the band at 1305 cm.$^{-1}$ to polymers of the cis-isomer.

Differences between the spectra of the two polymers were also observed in the KBr region. The bands due to rocking of CHD groups were observed at 594 and 586 cm.$^{-1}$ in poly-($trans$-$C_2H_2D_2$) and at 597 and 590 cm.$^{-1}$ in poly-(cis-$C_2H_2D_2$). These bands show strong perpendicular infrared dichroism upon stretching of the sample and changed to single band on melting. In poly-(C_2H_4) a similar splitting of the rocking vibration is observed at 720 and 731 cm.$^{-1}$ The band with the higher frequency is known as a crystallization-sensitive band; however, it could not be decided which is the crystallization-sensitive band in poly-($C_2H_2D_2$).

Bands at 1465, 1453, and 725 cm.$^{-1}$ observed in the spectra of the deuteropolymers indicate the presence of a small fraction of CH_2 groups in the polymers. The bands at 1465 and 725 cm.$^{-1}$ are due to bending and rocking vibrations of CH_2 in poly-(C_2H_4) produced from C_2H_4 liberated from triethylaluminum during the preparation of the catalyst. The absence of the crystallization-sensitive band is due to the absence of crystallites of —$(CH_2)_n$— in the deuteropolymers. The band at 1453 cm.$^{-1}$ can be assigned to the bending of CH_2 groups in the chain of the deuteropolymers, from the fact that its intensity has no correlation to the intensity of the band at 725 cm.$^{-1}$ and from the increase of intensity with increase of protium content in the monomer. The contribution to these bands of the —CH_2CH_3 end group introduced by the catalyst is small, since the CH_3 band observed at 1375 cm.$^{-1}$ is very weak.

The infrared evidence showing the difference between the structures of polymers obtained from cis-$C_2H_2D_2$ and from $trans$-$C_2H_2D_2$ suggests that the double bond opening takes place in the same way for either cis or $trans$. Studies of the structure of the two polymers will be discussed in another paper.

EXPERIMENTAL

Synthetic Procedures

Dideuteroacetylene was prepared in a vacuum system by the distillation of deuterium oxide (deuterium, 99.6 atom-%) into pure calcium carbide using liquid nitrogen. The calcium carbide had previously been heated *in vacuo* for several hours at about 450°C. The dideuteroacetylene produced was collected with liquid nitrogen and used directly for the reduction to ethylene without purification.

trans-1,2-Dideuteroethylene was prepared by reducing the dideuteroacetylene with chromous chloride solution. The chromous chloride solution was prepared by dissolving 70 g. of $CrCl_3 \cdot 2H_2O$ in 40 ml. of water and 80 ml. of concentrated HCl followed by reduction with 30 g. of zinc dust. Dideuteroacetylene (0.1 mole) was collected *in vacuo* in a 1.5 liter flask using liquid nitrogen, and the chromous chloride solution was added into the flask under reduced pressure. After the flask was shaken vigorously for 100 hr., it was again attached to the vacuum line, and the reduced product was collected in a trap cooled with liquid nitrogen after water and less volatile matter had been removed in a Dry Ice–methanol trap.

cis-1,2-Dideuteroethylene was prepared by reducing the dideuteroacetylene with zinc dust activated with copper. Arsenium-free zinc dust (50 g.) was added to 200 ml. of 4% $CuSO_4$ solution. After washing with water several times the activated zinc dust was filtered off and dried *in vacuo*. The dideuteroacetylene was collected in a flask which contained 50 g. of the activated zinc dust and 30 ml. of water. After the flask had been shaken vigorously for 100 hr. at 70°C., the reduced product was collected in a trap by the same procedure described above. (When deuterium oxide was used instead of water, tetradeuteroethylene was obtained.)

Purification of the dideuteroethylene was accomplished by shaking the ethylene successively with ammoniacal cuprous chloride solution, ferric chloride solution, 85% sulfuric acid, and 15% NaOH solution. During the purification no hydrogen–deuterium exchange was observed.

Polymerization was carried out at constant volume in a glass apparatus. High-boiling aliphatic hydrocarbons were used as the solvent. *n*-Cetane or *n*-hydrocarbon (with a suitable boiling range) were shaken with fuming sulfuric acid many times, dried over calcium chloride and calcium hydride and then fractionated under reduced pressure. In making up the catalyst solution, measured volumes of the triethylaluminum and titanium tetrachloride solutions were mixed in a previously dried and nitrogen-flushed reaction vessel with a magnetic stirrer and immersed in a constant temperature bath. Sufficient solvent was added to bring the total volume to 50 ml. In a typical experiment 1.622 mmole of $Al(C_2H_5)_3$ and 0.700 mmole of $TiCl_4$ were used. The vessel was then attached to a vacuum manifold and pumped out for 30 min. The reaction vessel was kept at 0°C., and 300 ml. (at STP) of the ethylene was introduced. The rate of decrease of ethylene pressure was followed using a mercury manometer. After 3 hr., over 95% of the ethylene was polymerized. Butanol and methanol were added into the reaction vessel to destroy the catalyst. The polymer was washed thoroughly with methanol, ethanol, and finally an ethanol–hydrogen chloride mixture, and dried *in vacuo*.

Melting Point, Density, and Viscosity Measurements

The melting range of the polyethylene was determined by viewing a thin film of the polymer on a heated stage of a polarizing microscope. The

TABLE III

Infrared Spectra of the Polymers Obtained from *trans*- and *cis*-1,2-Dideutero-
ethylene using a Ziegler Catalyst

Poly-(*trans*-$C_2H_2D_2$)		Poly-(*cis*-$C_2H_2D_2$)		
Frequency, cm.$^{-1}$	Intensity	Frequency, cm.$^{-1}$	Intensity	Assignment
4180	vw	4170	vw	
3480	w	3460	w	
2957	vw	2957	vw	$\nu_{as}(CH_3)$
2923	vw	2923	vw	$\nu(CH_2)$
2897	vs	2900	vs	$\nu(CH)$ in CHD
2882	vs	2880	vs	$\nu(CH)$ in CHD
2849	w	2849	w	$\nu_s(CH_2)$
2590	w	2590	w	
2152	sh	2155	sh	$\nu(CD)$ in CHD
2133	vs	2137	vs	$\nu(CD)$ in CHD
1465	w	1465	w	$\delta(CH_2)^a$
1453	w	1453	w	$\delta(CH_2)^b$
1335	m			
1328	m	1325	m	
1321	m	1321	w(sh)	$\delta(CHD)$
		1305	m	
1288	w			
1230	vw			
725	w	725	w	$r(CH_2)^a$
594	m	597	m	$r(CHD)$
586	m	590	m	$r(CHD)$

[a] Due to poly-(C_2H_4) produced from C_2H_4 liberated from triethylaluminum.

[b] Due to —CH_2— groups in the chain of poly-($C_2H_2D_2$).

density of the polyethylene was measured by a suspension method in a mixture of ethanol and water or in NaCl solution.

The intrinsic viscosity of the polyethylene was measured at 120°C. in a modified Ubbelohde-type viscometer. Purified decalin was used as a solvent. The intrinsic viscosities of polyethylenes obtained were in the range of 5–8.

X-ray Analysis

X-ray diffraction data were obtained at 20°C. with Phillips x-ray diffractometer equipped with a proportional counter. The sample was made by pressing the molten polyethylene into a flat sheet of approximately 0.5 mm. thickness. The extent of the amorphous part of the polymer was obtained from the ratio of the integrated intensity of the amorphous scattering to the integrated intensity of amorphous scattering and crystalline peaks.

Infrared Spectra

Films for the infrared measurements were prepared by evaporating xylene solutions of the polymers over hot plate heated at 120°C. Infrared spec-

tra were recorded principally by a Shimazu Model IR double-beam spectrometer equipped with a rock-salt prism, in part by a Perkin-Elmer Model 112G single-beam grating spectrometer equipped with a KBr fore-prism and in part by a Perkin-Elmer Model 112 single-beam spectrometer equipped with a KBr prism. Observed frequencies and assignments are shown in Table III.

References

1. Natta, G., *Makromol. Chem.*, **35**, 94 (1960); G. Natta, M. Farina, and M. Peraldo, *Atti Accad. Nazl. Lincei, Rend. Classe Sci. Fis., Mat. Nat.*, [8] **25**, 424 (1958).
2. Natta, G., M. Farina, and M. Peraldo, *J. Polymer Sci.*, **43**, unpaged (1960).
3. Natta, G., *J. Polymer Sci.*, **48**, 219 (1960).
4. Rabinovitch, B. S., and F. S. Looney, *J. Am. Chem. Soc.*, **65**, 2652 (1953).

Résumé

Des polydideutéroéthylènes stéréoréguliers sont préparés par polymérisation du *trans* et *cis*-1,2-dideutéroéthylènes a l'aide du catalyseur de Ziegler. Les *trans*- et *cis*-dideutéroéthylènes sont préparés par réduction du dideutéroacétylène, par le chlorure chromeux en solution et du zinc en poudre activé par du cuivre respectivement. Les spectres infra-rouges des deux polymères obtenus montrent des différences significatives particulières dans les bandes de vibration dues aux vibrations CHD. On observe les bandes de 1335 et 1288 cm.$^{-1}$ uniquement dans le polymère provenant de l'isomere *trans* et une bande a 1305 cm.$^{-1}$ est observée uniquement dans les polymères provenant de l'isomere *cis*. On mesure les densités, les points de fusion, la viscosité intrinsèque et la cristallinité des polymeres et on la compare avec celle du polyéthylene normal. Les diagrammes des rayons-X des polydideutéroéthylenes sont identiques avec ceux du polyéthylene normal.

Zusammenfassung

Sterisch regelmässige Polydideuteroäthylene wurden durch Polymerisation von *trans*- und *cis*-1,2-Dideuteroäthylene mit einem Ziegler-katalysator dargestellt. *trans*- und *cis*-Dideuteroäthylen wurden durch Reduktion von Dideuteroactylen mit Chrom-2-chloridlösung bzw. kupferaktivierten Zinkstaub dargestellt. Die Infrarotspektren der beiden Polymeren wiesen charakteristische Unterschiede, besonders in den Knickschwingungsbanden der CHD-Gruppe auf. Banden bei 1335 und 1288 cm.$^{-1}$ wurden nur bei Polymeren des *trans*-Isomeren und eine Bande bei 1305 cm.$^{-1}$ nur bei Polymeren des *cis*-Isomeren beobachtet. Dichte, Schmelzpunkt, Viskositätszahl und Kristallinität des Polymeren wurde gemessen und mit den entsprechenden Grössen von normalem Polyäthylen verglichen. Das Röntgenbeugungsdiagramm der Polydideuteroäthylene war mit dem von normalem Polyäthylene nahezu identisch.
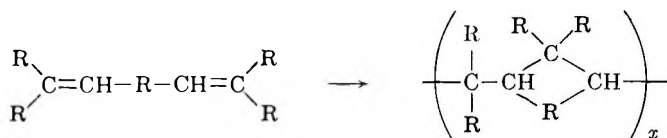
Transannular Polymerization of 1,5-Cyclooctadiene*

BERND REICHEL† and C. S. MARVEL, *Department of Chemistry, University of Arizona, Tucson, Arizona*, and R. Z. GREENLEY, *Department of Chemistry and Chemical Engineering, University of Illinois, Urbana, Illinois*

Synopsis

The polymerization of 1,5-cyclooctadiene to a low molecular weight polymer utilizing a Ziegler-type catalyst composed of triisobutylaluminum and titanium tetrachloride is reported. Although the structure of the polymer has not been definitely established its spectral and other physical properties suggest it to be poly-2,6-bicyclo(3,3,0)octane. Under the same conditions 1,4-cyclohexadiene did not undergo a transannular polymerization reaction but rearranged and yielded poly-1,3-cyclohexadiene.

While there are known a considerable number of inter-intramolecular polymerization reactions[1] of the type

in which a new intramolecular C—C bond is formed under ring closure by the polymerization reaction, a "transannular polymerization" is a new feature of the polymerization of diolefins. Here the intramolecular bond is formed within the ring of a cyclodiolefin, yielding a polymer bicyclic system.
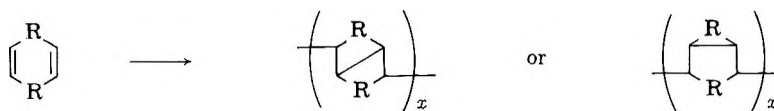
As far as is known, only one example for this type of polymerization has hitherto been verified.[2] The polymerization there is believed to occur according to the following scheme:

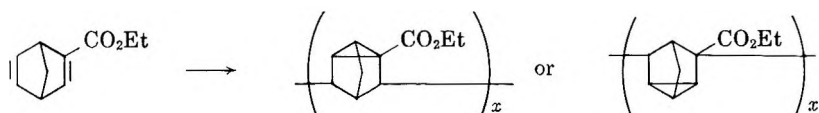In the work reported in this paper, *cis, cis*-1,5-cyclooctadiene (I)[3] was chosen as it seemed most suitable for a transannular polymerization since the transannular reactions were discovered with eight-membered rings,[4] and because of its ready commercial availability. A Ziegler-type catalyst was applied, composed of triisobutylaluminum and titanium tetrachloride. A molar aluminum/titanium ratio of 0.5 was found to give the best yields and any variations in either direction lessened the monomer conversion. Another important experimental condition was the molar ratio of titanium tetrachloride to monomer which was found to be best at 0.06. Some variations of details in the preparation and application of the catalyst (addition of component *A* to component *B* or vice versa, vigorous stirring during slow addition or just pouring together, aging of the catalyst for different times from 1 to 60 min. before addition of the monomer, and shaking during polymerization or standing still) did not seem to have any essential influence on the yield of polymer or its properties. However, when the catalyst was formed in presence of the monomer the conversion increased considerably.

This, together with the unusual ratio of triisobutylaluminum to titanium tetrachloride of 0.5, indicates that the actual initiating system was somewhat different from a regular Ziegler catalyst, but since both components were necessary and since a Ziegler catalyst cannot still be defined exactly it seems justified to talk about a Ziegler-type catalyst.

The yield also increased with elevation of temperature, being negligible at $-20°C.$, and with monomer concentrations in the heptane series. By far the highest conversions (up to 78%) were obtained with benzene as a solvent.

Replacement of titanium tetrachloride by vanadium trichloride or titanium tetrabutyloxide failed to yield any polymer. So did the application of boron trifluoride etherate as initiator at $-80°C.$

Titanium tetrachloride alone without triisobutylaluminum yielded only oligomers soluble in methanol, and boron trifluoride in methylene chloride at $-80°C.$ gave a polymer conversion of 1%.

The per cent conversion versus polymerization time was followed, and it was found that the monomer conversion stopped after approximately 150 hr. at $0°C.$ with heptane as a solvent (Fig. 1).

The polymer was a white powder, soluble in benzene and other hydrocarbons and chlorinated hydrocarbons and partially soluble in ethyl ether. In some cases small fractions were insoluble. About one-third of the

amount of polymer was only oligomerized and soluble in methanol. The rest of the monomer that had failed to polymerize was proved to be unchanged in structure by means of vapor phase chromatography.

The polymers exhibited melting points between 100 and 180°C. The inherent viscosity of the polymer solutions in benzene was always below 0.1, usually in the range of 0.02 to 0.04. A correlation between the intrinsic viscosity and the molecular weight of this type of polymer has not been determined. However, an approximate calculation of the average viscosity molecular weight using an intrinsic viscosity of 0.034 and the values of K and α as determined for polyisobutylene in benzene at 24°C.[5] or for polystyrene in benzene,[6] respectively, gives a molecular weight of the order of 2000 to 3000.
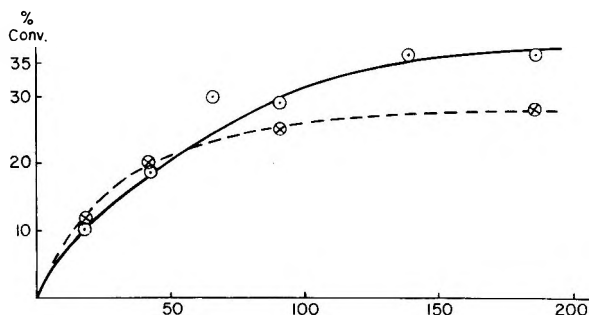
Fig. 1. (⊙) Runs 1–6 with 2 g. of heptane, 48 mg. of triisobutylaluminum, 91 mg. of TiCl₄, and 0.86 g. of monomer. Al/Ti = 0.5. Six moles TiCl₄ per 100 moles monomer; (⊗) Runs 7–10 as above except 3 g. of heptane was used as solvent.

Impurities other than 4-vinylcyclohexene in the monomer in the total amount of less than 1% were found to prevent the polymerization completely. 4-Vinylcyclohexene, however, which is present in every commercial cyclooctadiene, did not negatively affect the polymerization but, on the contrary, prevented or lessened partial crosslinking which occurred under certain conditions.

Bromine and potassium permanganate could not be used to detect unsaturation in the polymer as those agents reacted with its tertiary hydrogens. The nuclear magnetic resonance spectrum of the homopolymer showed no unsaturation within the limits of error, but the infrared spectrum did. A quantitative comparison of the carbon-carbon double bond peak at 1660 cm.$^{-1}$ of monomer and polymer solutions of known concentrations indicated that about 10 to 15% of the monomer units which were incorporated in the monomer chain retained one double bond. This high degree of saturation together with the solubility of the polymer rules out any other than the transannular way of polymerization, as the independent polymerization of each single double bond would lead to crosslinkage.

An x-ray transmission pattern revealed some crystallinity in the polymer.

According to the two theoretical possibilities indicated above for a trans-annular polymerization reaction, two possible structures (II and III) would be expected for the polymer:

(I)   (II)   or   (III)
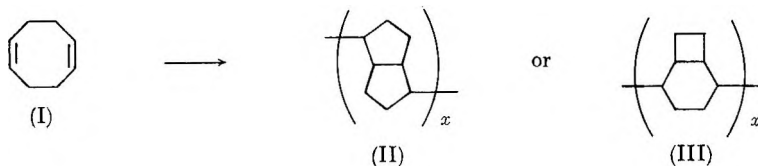
Structure III could be eliminated, as the infrared spectrum of the polymer had not a single peak in common with that of bicyclo(4,2,0)octane[7] but showed a certain similarity to that of cis-bicyclo(3,3,0)octane.[8]

The fact that five monomer units can form a ring as readily as five carbon atoms, which is revealed by the model, might account for the considerable fraction of oligomers soluble in methanol.

A side reaction which probably accounts for the small amount of cross-linkage as well as for part of the residual unsaturation can be explained by the following considerations: there are two conformations of the cis,cis-1,5-cyclooctadiene, the tub form (IV) and the chair form (V). (A third one can be built by Fischer-Hirschfeld models, but as two pairs of hydrogen atoms

(IV)   (V)

come close together this conformation is probably not found in nature.) It was found by dipole measurement[9] that 85% of 1,6 dichloro-1,5-cyclooctadiene exists in the tub form IV despite the dipole-dipole repulsion of the chlorine atoms. Thus the tub form must have an ever greater statistical weight in the unchlorinated hydrocarbon. This is—as the double bonds are very close together in this form—in favor of the transannular reaction. Yet there is certainly a small amount of the chair form V where the double bonds are far apart, and it is probably this conformation in which the double bonds cannot undergo a transannular reaction but react independently, leaving cyclic double bonds in the polymer or leading to a crosslinked polymer, respectively.

The rest of the unsaturation is believed to be due to the end groups.

When 1,4-cyclohexadiene (VI) was polymerized in the same way the polymer exhibited an infrared spectrum identical to that of poly-1,3-cyclohexadiene[10] (VIII). Obviously a rearrangement to 1,3-cyclohexadiene (VII) was here preferred to a transannular reaction.

(VI)

(VII)

(VIII)
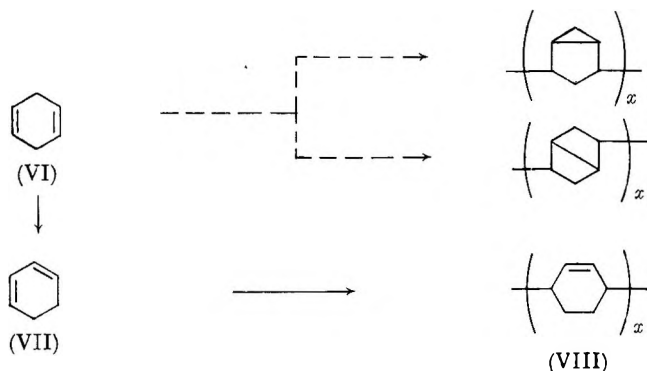
Experimental

Yields are based on the amount of polymer obtained after two precipitations from benzene with methanol and referred to the amount of monomer allowed to react.

Preparation of Reagents

All 1,5-cyclooctadiene samples obtained from different commercial sources contained several impurities which, except for 4-vinylcyclohexene, inhibited polymerization even in amounts of a fraction of a per cent. Absolute purification was accomplished, after reflux over sodium, by carefully fractionated distillation under nitrogen using a heated $5/8$ by 50 in. column filled with glass helices at a reflux ratio of about 1:50 (approximately 1 liter per week). The sodium had to be removed before by simple distillation as it caused foaming and slow formation of a brown tar soluble in methanol which was not due to impurities but to the cyclooctadiene itself.

1,4-Cyclohexadiene was obtained from benzene by the method of Tom and Greenlee.[11]

n-Heptane and benzene were purified by repeated shaking with concentrated sulfuric acid for several hours at room temperature (benzene shorter than heptane as the mixture got warm while being shaken). After washing with a bicarbonate solution and with water the predried solvents were refluxed over sodium for 24 hr. and distilled under a nitrogen atmosphere.

Titanium tetrachloride was purified as described by Clabaugh et al.[12] Triisobutylaluminum (Texas Alkyl) was not purified further.

Ziegler Polymerization Studies

The catalyst for the polymerizations was made up in a dry box by mixing the heptane or benzene solutions, respectively, of the desired amounts of titanium tetrachloride and triisobutylaluminum in a polymerization bottle. The monomer was then added to the dark brown suspension of catalyst which had formed, and the bottles were sealed and left alone at the desired temperature. The polymerization was stopped by pouring the reaction

TABLE I
Variations in the Catalyst Aging Time

Run No.	Heptane, g.	Al(i-Bu)₃, mg.	TiCl₄, mg.	Monomer, g.	Moles Al(i-Bu)₃/ moles TiCl₄	Moles Ti/100 moles monomer	T, °C.	t, hr.	Aging of catalyst, min.	4-Vinyl-cyclohexene, %	Conversion, % Insol.	Conversion, % Sol.
1a	10	80	65	5	1.16	0.76	0	100	60	1	—	1
1b	10	80	65	5	1.16	0.76	0	100	1	1	—	1
1c	10	80	65	5	1.16	0.76	0	100	0[a]	1	—	4.8
2a	10	240	455	4.3	0.5	6.0	0	100	30	1	n[b]	8.4
2b	10	240	455	4.3	0.5	6.0	0	100	0[a]	1	n[b]	19.1
Benzene												
3a	10	80	65	5	1.16	0.76	25	200	30	1	0.5	1.7
3b	10	80	65	5	1.16	0.76	25	200	0[a]	1	0.1	11.2
4a	10	240	455	4.3	0.5	6.0	45	100	30	1	—	75.5
4b	10	240	455	4.3	0.5	6.0	45	100	0[a]	1	—	78

[a] Formation in presence of the monomer.
[b] Here n means negligible.

TABLE II. Influence of Temperature

Run No.	Heptane, g.	Al-(i-Bu)$_3$, mg.	TiCl$_4$, mg.	Monomer, g.	Moles Al(i-Bu)$_3$/ moles TiCl$_4$	Moles Ti/100 moles monomer	T, °C.	t, hr.	Aging of catalyst, min.	4-Vinyl-cyclo-hexene, %	Conversion, % Insol.	Conversion, % Sol.
1a	10	80	65	5	1.16	0.76	0	100	0[a]	1	—	4.8
1b	10	80	65	5	1.16	0.76	25	100	0[a]	1	n[b]	14
1c	10	80	65	5	1.16	0.76	67	100	0[a]	—	7.4	24.7
2a	10	240	455	4.3	0.5	6.0	−20	900	30	0	n[b]	n[b]
2b	10	240	455	4.3	0.5	6.0	0	100	30	1	n[b]	8.4
2c	10	240	455	4.3	0.5	6.0	25	100	30	—	0.5	16
3a	10	240	455	4.3	0.5	6.0	0	100	0[a]	1	n[b]	19.1
3b	10	240	455	4.3	0.5	6.0	25	100	0[a]	1	n[b]	23.3
3c	10	240	455	4.3	0.5	6.0	67	100	0[a]	—	1.1	32.5
Benzene												
4a	10	240	455	4.3	0.5	6.0	25	200	30	1	—	65.5
4b	10	240	455	4.3	0.5	5.0	45	100	30	1	—	75.5

[a] Formation in presence of monomer.
[b] Here n means negligible.

TABLE III. Influence of Solvent

Run No.	Benzene, g.	Heptane, g.	Al-(i-Bu)$_3$, mg.	TiCl$_4$, mg.	Monomer, g.	Moles Al(i-Bu)$_3$/ moles TiCl$_4$	Moles Ti/100 moles monomer	T, °C.	t, hr.	Aging of catalyst, min.	4-Vinyl-cyclo-hexene, %	Conversion, % Insol.	Conversion, % Sol.
1a	—	10	240	455	4.3	0.5	6	67	100	0[a]	0	1.1	32.5
1b	10	—	240	455	4.3	0.5	6	45	100	0[a]	1	—	78
2a	—	10	240	455	4.3	0.5	6	25	100	30	0	0.5	16
2b	10	—	240	455	4.3	0.5	6	25	200	30	1	—	65.6

[a] Formation in presence of monomer.

mixture into approximately 350 ml. of methanol in which the metal methoxides from the catalyst were soluble. The precipitated white or sometimes yellow powder was collected, dried, dissolved in the smallest possible amount of benzene, filtered (for the purpose of analysis repeated filtration through an extra fine paper was necessary), and precipitated again in the same way. If the precipitate was sticky or even an oil it was treated with ethyl ether in which part of it was soluble, and the rest was taken up in benzene. From both of these solutions the polymer could be precipitated as a powder. See Tables I, II, and III for details of experiments. It was lyophilized and dried in a high vacuum for two days at 100°C.

ANAL.: Calcd. for C_8H_{12}: C, 88.90; H, 11.10. Found: C, 88.44; H, 11.22.

The infrared spectrum of the polymer was very simple, exhibiting only two main peaks from methylene at 1460 and 2940 cm.$^{-1}$ with a shoulder at 2880 cm.$^{-1}$, two small peaks at 1660 and 725 cm.$^{-1}$ from residual unsaturation and methylene, respectively, and three weak peaks which are unexplained but in accordance with the spectrum of monomer cis-bicyclo (3,3,0)-octane[3] at 1362 (sharp), 1305 (broad), and 915 cm.$^{-1}$ (broad).

The resolution of a proton magnetic resonance spectrum obtained from a polymer solution in deuterated chloroform on an A-60 Varian spectrometer was, like that of any polymer, poor. It exhibited, however, three peaks or shoulders at 2 ppm, 1.5 ppm, and 0.88 ppm, that is in the same region as those reported by Moniz and Dixon[13] for cis-bicyclo(3,3,0)octane (at 2.38, 1.45, and 1.38 ppm with a shoulder at 1.25 ppm from tetramethylsilane).

Cationic Polymerization Studies

A 100-ml., three-necked flask, equipped with a desiccant tube and a gas inlet tube, was charged with 2 ml. of 1,5-cyclooctadiene in 20 ml. of methylene chloride. It was filled with nitrogen and cooled in a Dry Ice-acetone bath. After boron trifluoride had been passed slowly into the solution for 3 min. it was left in the cooling bath for 3 hr. and then poured into an excess of methanol. Purification of the white solid gave the polymer (191 mg.) in 1.1% conversion, PMT 165–86°C., n_{inh} (0.04% in benzene) 0.09.

When the usual Ziegler polymerization procedure was followed with heptane as a solvent but with titanium tetrachloride only (without triisobutylaluminum), no precipitate was obtained by pouring the reaction mixture into methanol. When the methanol solution was poured into water an organic white solid precipitated which apparently consisted of very low molecular weight polymer. It was not further investigated.

References

1. Marvel, C. S., and R. D. Vest, *J. Am. Chem. Soc.*, **79**, 5771 (1957); **81**, 984 (1959); G. B. Butler and R. J. Angelo, *J. Am. Chem. Soc.*, **79**, 3128 (1957); J. F. Jones, *J. Polymer Sci.*, **33**, 15 (1958); C. S. Marvel and J. K. Stille, *J. Am. Chem. Soc.*, **80**, 1740 (1958);

J. K. Stille and D. A. Frey, 135th Am. Chem. Soc. Meeting, Boston, Mass., April 1958; C. S. Marvel and W. E. Garrison, *J. Am. Chem. Soc.*, **81**, 4737 (1959); C. S. Marvel and E. J. Gall, *J. Org. Chem.*, **25**, 1784 (1960); S. G. Matsoyan, *J. Polymer Sci.*, **52**, 189 (1961).

2. Graham, P. J., E. L. Buhle, and N. Pappas, *J. Org. Chem.*, **26**, 4658 (1961).

3. Two modifications of 1,5-cyclooctadiene are known. The *cis, cis*-product is the stable one. The other one which spontaneously polymerizes (*a*) or dimerizes, respectively, under formation of a four-membered ring ⬡═⬡ (*b*) is now generally regarded as being *trans, trans* though some chemical properties (*c*) demanding the *cis, trans*-configuration are still waiting for an explanation. (*a*) Willstätter, R., and H. Veraguth, *Ber. deut. chem. Ges.*, **38**, 1975 (1905); **40**, 957 (1907); (*b*) Ziegler, K., H. Sauer, L. Bruns, H. Froitzheim-Kühlhorn, and J. Schneider, *Ann. Chem.*, **589**, 125 (1954); (*c*) Ziegler, K., H. Sauer, L. Bruns, H. Froitzheim-Kühlhorn, and J. Schneider, *Ann. Chem.*, **589**, 125 (1954); K. Ziegler and H. Wilms, *ibid.*, **567**, 14 (1950).

4. Cope, A. C., S. W. Fenton, and C. F. Spencer, *J. Am. Chem. Soc.*, **74**, 5884 (1952).

5. Flory, P. J., *Principles of Polymer Chemistry*, Cornell Univ. Press, Ithaca, N. Y., 1953, p. 312.

6. Sorenson, W., and T. W. Campbell, *Preparative Methods of Polymer Chemistry*, Interscience, New York, 1961, p. 36.

7. Cope, A. C., and F. A. Hochstein, *J. Am. Chem. Soc.*, **72**, 2519 (1950).

8. Cope, A. C., and W. R. Schmitz, *J. Am. Chem. Soc.*, **72**, 3061 (1950); J. D. Roberts and W. F. Gorham, *ibid.*, **74**, 2281 (1952).

9. Roberts, J. D., *J. Am. Chem. Soc.*, **72**, 3300 (1950).

10. Marvel, C. S., and G. E. Hartzell, *J. Am. Chem. Soc.*, **81**, 448 (1959).

11. Tom, T. B., and K. W. Greenlee, *Am. Petrol. Inst. Rept.*, **45**, 4 (1948).

12. Clabaugh, W. S., R. T. Leslie and R. Gilchrist, *J. Res. Natl. Bur. Std.*, 261 (1955).

13. Moniz, W. B., and J. A. Dixon, *J. Am. Chem. Soc.*, **83**, 1674 (1961).

Résumé

On décrit la polymérisation du 1,5-cyclooctadiène en polymères de faible poids moléculaire en employant un catalyseur du type Ziegler composé de triisobutylaluminium et de tétrachlorure de titane. La structure du polymère obtenu n'a pas été établie définitivement; cependant l'examen du spectre et d'autres propriétés physiques semble indiquer qu'il s'agit de poly-2,6-bicyclo(3,3,0)-octane. Dans les mêmes conditions le 1,4-cyclohexadiène ne conduit pas à une réaction de polymérisation transannulaire mais subit un réarrangement pour fournir du poly-1,3-cyclohexadiène.

Zusammenfassung

Über die Polymerisation von 1,5-Cyclooctadien zu einem niedermolekularen Polymeren mit einem Ziegler-Katalysator aus Triisobutylaluminium und Titantetrachlorid wird berichtet. Die Struktur des Polymeren wurde noch nicht endgültig aufgeklärt, seine spektralen und andere physikalische Eigenschaften sprechen aber für eine Poly-2,6-bicyclo-(3,3,0)-octanstruktur. Unter den gleichen Bedingungen ging 1,4-Cyclohexadien keine transannulare Polymerisation ein, sondern lagerte sich um und lieferte Poly-1,3-cyclohexadien.

Structure Effects and Related Polymer Properties in Polybutadiene.   I. Preparation and Characterization

M. BERGER and D. J. BUCKLEY, *Esso Research and Engineering Company, Central Basic Research Laboratory, Linden, New Jersey*

Synopsis

Stereoregular polybutadienes, of both high *trans* and high *cis* contents, were isomerized to provide polymers of varying *cis-trans* content.   These isomerizates were used to study structural effects on physical properties.   The isomerizations were carried out under photosensitized conditions in benzene solution at 25°C.   The reaction was controlled to deliver polymers over the range 0–95% *trans* content.   This range was selected to provide crystalline and semicrystalline polymers whose structures could be examined in terms of sequencing or blocking by established x-ray techniques.   Isomer contents were measured accurately by infrared traces.   Isomerizations reached an equilibrium of 77% *trans* regardless of whether the reaction started with high *trans* or high *cis* polybutadienes.   Intrinsic viscosity was found to increase regularly with *trans* content in conformity with the larger size of the *trans* unit. η_{sp}/c versus c relations were observed to give a complicated form and this subject was deferred for further study.   Crystallinity decreased regularly with reduced *trans* content as the equilibrium of 77% *trans* was approached.   Continued isomerization at the point of equilibrium produced a completely amorphous polymer.   The melting temperatures of the crystalline polymers were studied in detail by x-ray camera and counting techniques.   These polymers exhibited two crystal forms.   One form was stable up to 60°C. and invariant with *cis-trans* content in the range 80–95% *trans*.   Below 80% *trans* the melting point of this form decreased with further reduction in *trans* content.   The melting temperature of the other crystal form was dependent on *trans* content and decreased with decreased *trans* content until it coincided with the melting temperature of the other form.   The distributions of *trans* and *cis* units and sequences of them were calculated through construction of matrices of transition probabilities.   Copolymer theory was invoked to calculate pseudo reactivity ratios for the *trans* and *cis* forms.   The melting temperatures of the two crystals were found to follow the predicted curves for random copolymers, although not simultaneously.   This behavior is discussed.   The crystallinity of the isomerizates of high *trans* content was found to be similar to block copolymers in spite of the fact that the method of their preparation would require that they be characterized as random.   The importance of a crystal transition in this case is stressed along with the general effects due to the amount and type of the noncrystallizable unit.

INTRODUCTION

In the recent past a great deal of attention has been paid to the effect of stereoregular sequences which occur in the molecular chains of copolymers.[1-4]   Included in these studies are polybutadiene[4] and polypropylene,[2] although not copolymers in the usual sense, can be treated as such by considering each stereoisomer (*cis*, *trans*, *l*, *d*, etc.) as a separate species.

Many workers[2,5,6] have attempted to determine the distribution of l and d units in polypropylene using various modifications of the copolymer equations. Some work concerned with the sequencing of cis units has been done with polybutadienes of high cis and low trans contents.[4] The present paper deals with the effect of stereostructure in polybutadienes whose trans contents vary from 0 to 95%, and with particular attention to the range 70–95%.

In order to determine the sequencing of units or the degree of isotacticity in a homogeneous copolymer, there are at least two quantities which should be available experimentally. These are (1) the compositional ratio of the copolymer, and (2) the crystallinity (i.e., per cent crystallinity, melting temperature, etc.). Use of the various copolymer equations demands knowledge of these factors. The composition of polybutadienes can be readily determined by infrared absorption. In addition, trans-polybutadienes are crystalline over a wide range of temperatures and over a considerable spread of copolymer compositions. Thus crystallinity can be measured conveniently in relation to copolymer composition. Neither polypropylene nor cis-polybutadiene meet both of these requirements.

EXPERIMENTAL PROCEDURES

Polymer Preparation

All polymers used in this work were prepared by isomerizing a high trans (95%) or a high cis (95%) polybutadiene. The isomerization technique is essentially that developed by Golub.[7] The starting polymer is dissolved in benzene so as to make a 1% polymer solution. Phenyl disulfide, at 55 wt.-% on polymer is then added. The solution is irradiated with ultraviolet light for a prescribed length of time, after which the polymer is precipitated in methanol and then dried. During the reaction oxygen must be excluded to avoid degradation. It was our general practice to sweep the system with nitrogen prior to and during the course of the reaction.

Although the techniques employed by us were fashioned after Golub, our results using apparently the same reaction are quite different from those he reported. Golub states that, in the initiated photoisomerization, the isomerization goes completely to essentially all trans content. We find that, at room temperature, the equilibrium is reached at approximately 75% trans content. It is apparent that if this were not the case, we would not be able to prepare the polymers which are the basis of the present paper. It is interesting that Golub[8] later found that a noninitiated isomerization using γ-radiation attains an equilibrium of 80% trans content. This value is essentially in agreement with the equilibrium attained in our initiated isomerization.

The advantages of preparing polymers of different structure in this manner, rather than by direct polymerization, are considerable and have been discussed to some extent by Trick.[9] Briefly, the method insures con-

sistency of molecular weight, and most important, certainty that the polymer is a true copolymer of *cis* and *trans*. Polymerizations usually employed to produce high *cis* or high *trans* content polybutadienes are highly suspect as to their ability to make completely true copolymers.

The starting polymer for most of this work was Trans-4. This polymer, which is supplied by Phillips Petroleum Company, contains 94% *trans*-1,4, 4% 1,2, and 2% *cis*-1,4 structures. In some cases we have used Cis-4 polybutadiene which is also supplied by Phillips and consists of 94% *cis*-1,4, 4% 1,2, and 2% *trans*-1,4 structures.

Infrared Examination

The *cis*, *trans*, and 1,2 contents in the polybutadienes were determined by infrared absorption using the extinction coefficients calculated by Hampton.[10] They are, for *cis*-1,4, 0.608 at 724 cm.$^{-1}$; for 1,2, 3.285 at 911 cm.$^{-1}$; for the *trans*-1,4, 2.608 at 967 cm.$^{-1}$. These values were checked using an essentially 100% *cis*-polybutadiene supplied by Chemische Werke Hüls. In addition, the sum of the calculated weights of each isomer checked the measured weight of polymer in solution to within 3%. Unsaturation measurements on the polymer show that it has in excess of 98.5% of the theoretical value. All analyses were obtained on polymer dissolved in carbon disulfide.

Of the three absorptions the *cis*-1,4 is by far the most difficult to resolve. In addition to having the lowest extinction coefficient, it has a fairly broad absorption band compared to the *trans*-1,4 and 1,2 structures. This gave us some difficulty, particularly since the polymers of primary interest were those of relatively high *trans* content. These difficulties were reduced somewhat by ensuring that a common solvent source (carbon disulfide) was used for both the solution and reference liquid. We found that if this practice was not observed, there would be serious fluctuations in the *cis* absorption band.

Increased accuracy was also obtained by making use of the fact that the absorption for the 1,2 structure is very sharp and uneffected during isomerization. Hence it was used as a standard to insure uniformity in measuring the isomeric contents of various runs. For samples of extremely low *cis* content the following procedure was used. Two infrared absorption traces were obtained on a given sample, one with a moderate concentration of polymer in carbon disulfide, the other with a high concentration. The sample of high concentration would emphasize the *cis* absorption to a point where it could be conveniently measured. At this concentration, the absorption in the *trans* band would invariably be so strong that no reliable measure could be made of it. However, the absorption at the 1,2-band could be measured for both the high and moderate concentration traces. Thus, one calculates the 1,2 and *cis* contents for the high concentration and the 1,2 and *trans* contents for the low concentration. This permits accurate calculation of the per cent *cis*, *trans*, and 1,2 contents. There did not appear to be an appreciable concentration effect on extinction coeffi-

cients in the range of concentrations used. Difference techniques were not used in the calculation because of the possibility of adducting occurring during the isomerization. If phenyl disulfide or solvent molecules adducted on the polymer chain, it would not be detected by using a difference technique to calculate isomer content.

Intrinsic Viscosity

Viscosity determinations were made in a constant temperature bath at $25°C. ±0.02°C$. Dilute solutions of the polymers were made up in benzene and measured in the usual way in Ubbelohde type tubes. The proper kinetic energy corrections were applied to the data. Plots of η_{sp}/c were found to be satisfactorily linear (when the relative viscosity was maintained <2) and were extrapolated to infinite dilution. Crystalline polymers were dissolved by refluxing in benzene and allowed to cool to $25°C$. These polymers then remained in solution indefinitely.

X-Ray Examination

X-ray crystallinity was obtained by photographic and counting techniques. The counting was done by means of a goniometer with a G.M. tube counter. The percentage of crystallinity was determined by the method of Hermans and Weidinger.[12] This consists principally of integrating or finding the area under the intensity diffraction trace for the partially crystalline material and doing the same for the corresponding amorphous material. The value for the area of the latter is subtracted from that of the former and the ratio of this difference to the entire area obtained for the crystalline polymer is found. Samples were prepared from solution, and allowed to dry for one week before x-ray examination.

RESULTS

Isomerization

The isomerization of an all *cis*- and an all *trans*-polybutadiene as a function of time is shown in Figure 1. The rate of isomerization is not particularly significant, since it depends on the intensity of the ultraviolet source, its distance from the reaction vessel, the reaction vessel shape, and experimental details such as the ultraviolet absorption of the solvent. It is important to note, though, that both the polymers of originally high *cis* content and originally high *trans* content are capable of being isomerized at room temperature. Moreover, a common equilibrium point ($\sim$77% *trans* content) is attained regardless of the starting polymer. As mentioned earlier, these results are at variance with those reported by Golub. Elucidation of the reaction and its mechanism is not the primary objective of the present work. Therefore no future reference to this disagreement will be made in this paper. The general mechanism advanced by Golub, involving complexing and disassociation of mercaptyl radicals with subsequent establishment of the more thermodynamically favored isomeride appears reasonable to us.
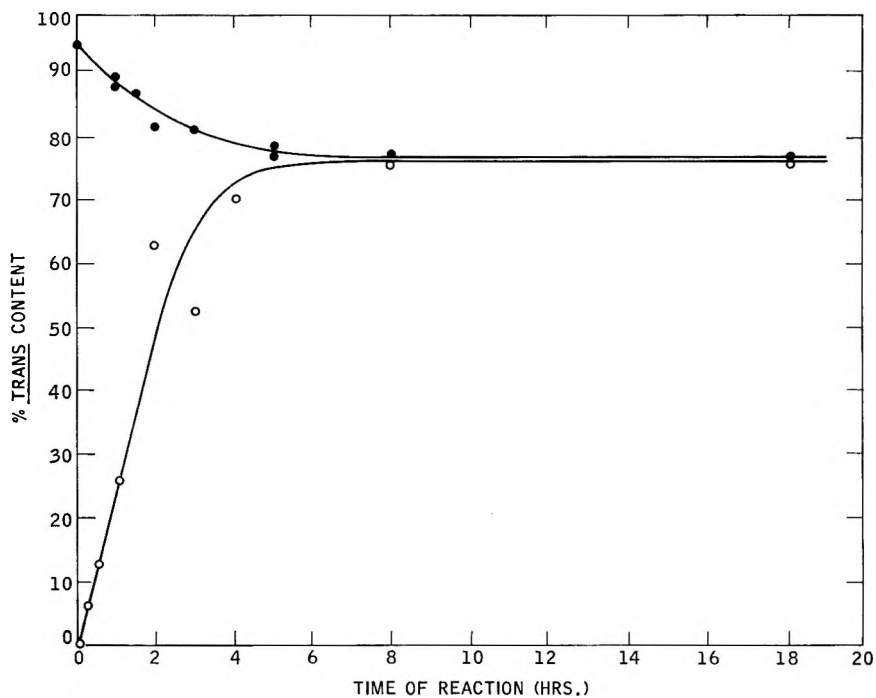
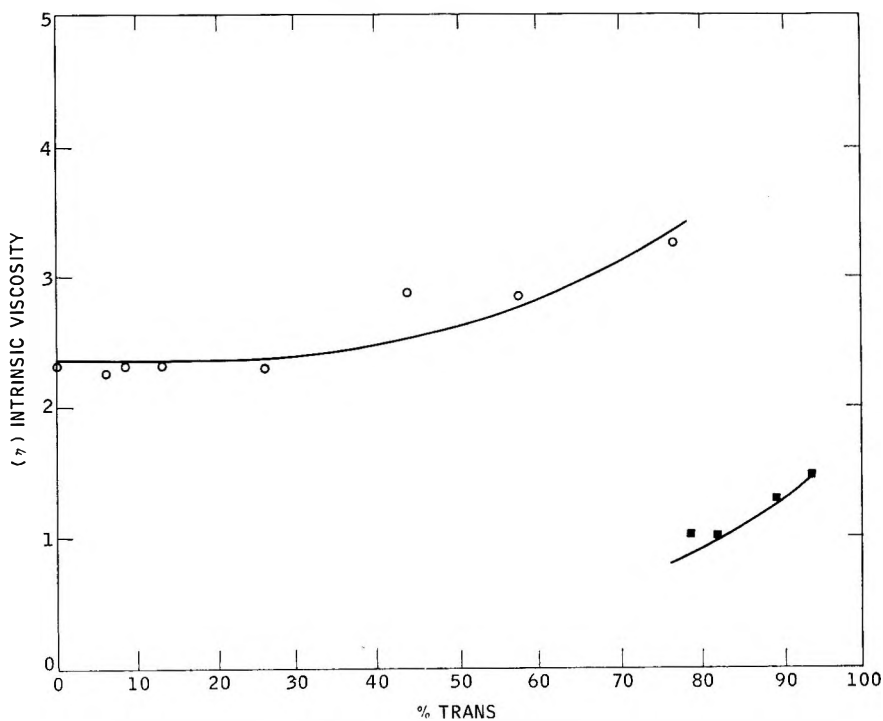Fig. 1. Isomerization of (O) all *cis* and (●) all *trans* polybutadienes.

Fig. 2. Intrinsic viscosity of polybutadienes of varying *cis* and *trans* content in benzene at 25°C.: (O) *Cis*-4 and its isomerates; (●) *Trans*-4 and its isomerizates.

Viscosity

The intrinsic viscosities of the various isomerides are shown in Figure 2. From this curve it appears that the reaction has not resulted in molecular weight breakdown. The data also show that the molecular weight of the original *trans*-polybutadiene is considerably lower than that of the original *cis*-polybutadiene. In order to examine the solution properties of the polymers, we must take cognizance of the starting molecular weights. Therefore, we have shifted the curve for the *trans* polymer upward so as to coincide with that of the *cis* polymer at 75% *trans* (since the 75% *trans* isomeride arrived at from the *cis* and *trans* end should be the same). The data so obtained are shown in Figure 3. The curve shown in this figure is determined from the theoretical relation of intrinsic viscosity to a function of the spherical volume occupied by a coiled polymer molecule.[11] In the application of this theory we make the assumption that the solvent–polymer interaction is identical for both *cis* and *trans* polymer and the isomerizate. Since the *trans* unit is 4.8/4.1 longer than the *cis* unit, the intrinsic viscosity should increase with increasing *trans* content, as is observed. The excellent agreement seems to support the assumption of

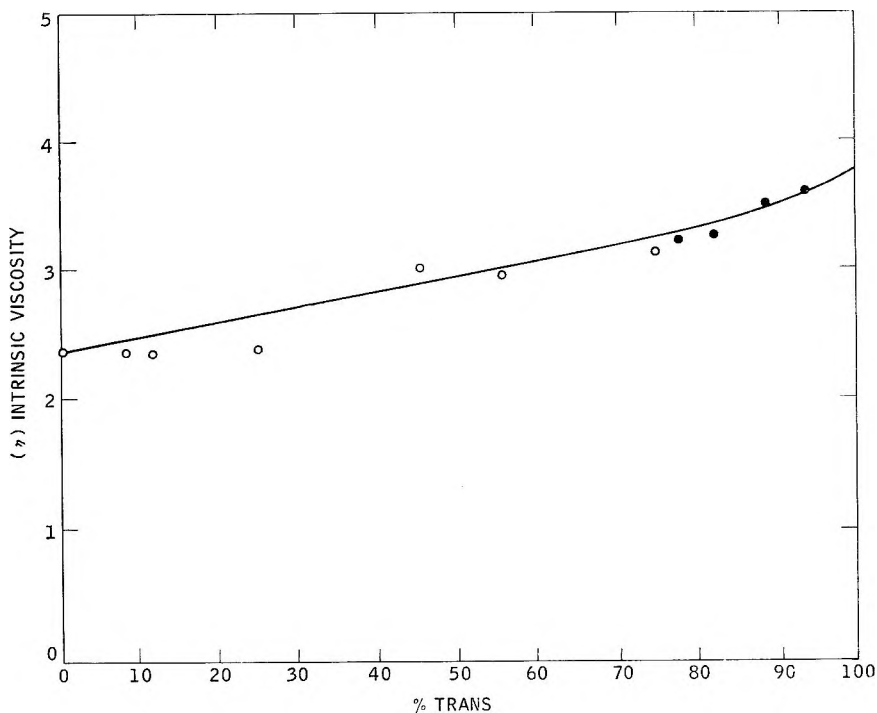Fig. 3. Intrinsic viscosity of polybutadienes of varying *cis* and *trans* content in benzene at 25°C.: (O) Cis-4 and its isomerizates; (●) Trans-4 and its isomerizates. (◐). Values for Trans-4 isomerizates adjusted to compensate for the lower molecular weight of the original polymer. Curve is the theoretical relation between the spherical volume occupied by the polymer and its intrinsic viscosity.

similar solvent–polymer interactions as well as to verify the fact that no
molecular weight breakdown occurred during the isomerization reaction.

As just described, we have observed that the intrinsic viscosity is de-
pendent on the *cis-trans* content in a straightforward manner.   The slopes
of the η_{sp}/c versus c curves over the range of *cis-trans* contents studied here,
appear complicated.   Unfortunately this type of experiment is subject to
errors which limit the precision, and our data cannot be given quantitative
treatment at the present time.   We hope to reexamine this relationship in a
subsequent paper.

Crystallinity

The Trans-4 as received from Phillips is highly crystalline.   As one
would expect, isomerization reduces the crystallinity.   Figure 4 shows a
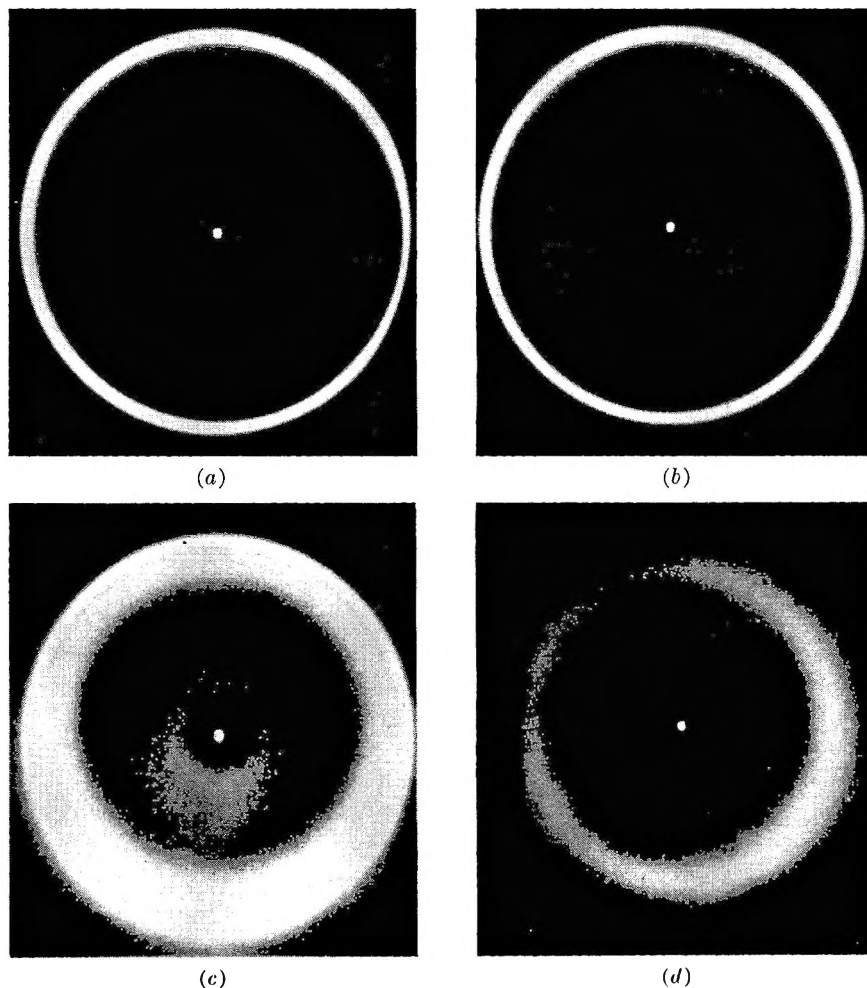

Fig. 4. X-ray diagrams of several isomerizates.   (a) 94% *trans*;   (b) 88% *trans*;   (c)
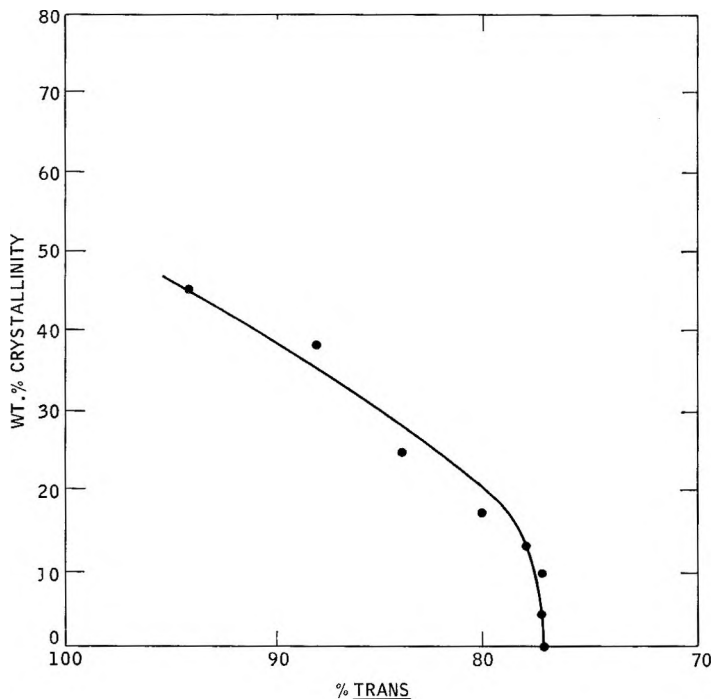82% *trans*;   (d) 78% *trans*.

Fig. 5. The degree of crystallinity for various polybutadiene isomerates made from all *trans*-polybutadiene.

series of x-ray pictures of various isomerizates obtained using the Trans-4 as the starting material. All x-ray data shown here were obtained at room temperature. The structure of the *trans*-1,4 crystal has been described quite adequately by Natta.[13] In his discussion, Natta points out the existence of a first-order crystal–crystal transition. We confirm his observations concerning this transition. The isomerized samples are excellent subjects for studying the nature of this transition. The transition will be discussed in detail later in this report.

Using goniometer techniques we have determined the percentage of crystallinity in the various isomerizates. The percentage of crystallinity versus *trans* content is shown in Figure 5. The most interesting portion of this curve is the region around 75% *trans*. Within the experimentally determined data, it appears that for the same *trans* content, materials exist with a degree of crystallinity anywhere from 0 to 15%. The gross rheological properties of the materials reflect this difference in crystallinity. The 76% *trans* material with 15% crystallinity is a weak, fibrous material best described as "asbestos-like." The 76% *trans* material with zero crystallinity is a tough, extensible elastomer. We feel that the determination of the *trans* content is accurate within 0.5% due to the repeated experiments, material balances, and consistency of the values of the 1,2 content. The crystallinity, as shown in Figure 5, is such as to suggest that the isomeriza-

tion results in long blocks of *cis* and *trans* units rather than a random distribution of these isomers. It would appear that at 76% *trans* content some critical block size of the *trans* units is disrupted and the crystallinity disappears rapidly. On the other hand, the isomerization reaction was chosen on the supposition that it would produce truly random copolymer. At this point it is clear that for complete characterization of the polymer, it is necessary to uniquely describe the distribution of isomeric sequences as affected by the isomerization reaction.

CHARACTERIZATION OF POLYMER STRUCTURE

Distribution of Monomer Units in Chain

The occurrence of crystals in copolymeric materials by its very nature suggests phenomena depending on sequence distribution. As mentioned earlier, polypropylene has been studied extensively with regard to *l* and *d* sequencing, and its effect on crystallinity. It has been shown recently that crystals in various high *cis*-polybutadienes (containing a small amount of *trans*) made from a variety of catalysts have different melting temperatures at the same level of *cis* content. These differences have been attributed to "blocking" or sequencing.[14]

Some work[3] has been done in calculating the distribution of monomer units along the polymer chain as they occur in copolymerization. The critical quantities in these studies are the so-called reactivity ratios. Obviously, there are no reactivity ratios involved in the isomerization. However, the statistics of the isomerization reaction can be handled in such a manner so as to give rise to pseudo reactivity ratios. Using these ratios, it is then possible to calculate *cis-trans* distributions by means of standard copolymerization theory. These pseudo reactivity ratios are the reactivity ratios necessary to polymerize a butadiene polymer to the same *cis-trans* content and distribution as a given isomerizate.

Let us consider the mechanism of isomerization such as Golub has described it. A monomer unit in the polymer chain is "hit" and rises to a metastable state. It then falls back either *cis* or *trans*, depending on thermodynamic conditions. From the results discussed earlier, it would appear that in our reaction the unit falls *trans* 75% of the time and *cis* 25% of the time. Actually our results show 76% *trans*, 4% 1,2, and 20% *cis* at equilibrium; however, for simplicity in analysis we will be considering a polymer of zero 1,2 content and having an equilibrium of 75% *trans*–25% *cis*. In other words, if a *cis* unit is "hit" the chance of its going *trans* is 0.75, and of its staying *cis* 0.25. If a *trans* unit is hit it has a 0.75 chance of staying *trans* and 0.25 chance of going *cis*. This can be represented as shown in (*1*):

	cis	*trans*	
cis	0.25	0.75	(*1*)
trans	0.25	0.75	

Let us now consider an assembly consisting of dimeric molecules,* under conditions where they are subjected to the isomerization reaction. Then using (1) it is possible to construct a matrix of transition probabilities which has the following form:

$$P(t) = \begin{array}{c} \\ TT \\ TC \\ CT \\ CC \end{array} \begin{array}{cccc} TT & TC & CT & CC \\ \begin{vmatrix} A_{11} & A_{12} & A_{13} & A_{14} \\ A_{21} & A_{22} & A_{23} & A_{24} \\ A_{31} & A_{32} & A_{33} & A_{34} \\ A_{41} & A_{42} & A_{43} & A_{44} \end{vmatrix} \end{array} \qquad (2)$$

where A_{11} = fraction of two consecutive monomer units isomerized from *trans-trans* to *trans-trans* at time t, A_{12} = fraction of two consecutive monomer units isomerized from *trans-trans* to *trans-cis* at time t, A_{34} = fraction of two consecutive monomer units isomerized from *cis-trans* to *cis-cis* at time t, etc.

If the ensemble of dimeric molecules started out as all *trans*, then at time t according to eq. (2) a fraction A_{11} of them will still be all *trans*, A_{12} will have the sequence *trans-cis*, A_{13} will have the sequence *cis-trans* and A_{14} will be *cis-cis*. If we now put all the dimeric molecules together to form a long polymer chain, the distribution of *trans-trans*, *trans-cis*, etc. becomes altered due to the effects at the junctures between any two dimeric molecules. The contributions of the junctures can be calculated as follows. A *trans-trans* sequence can occur at a juncture in these arrangements: a *trans-trans* sequence followed by a *trans-trans* sequence, a *trans-trans* sequence followed by a *trans-cis* sequence, a *cis-trans* sequence followed by a *trans-cis* sequence, or a *cis-trans* sequence followed by a *trans-trans* sequence. Thus the probability that a *trans-trans* sequence will occur at a juncture is given by:

$$TT_j = (A_{11})^2 + A_{11}A_{12} + A_{13}A_{12} + A_{13}A_{11} \qquad (3)$$

since $A_{12} = A_{13}$

$$TT_j = A_{11}^2 + 2A_{11}A_{12} + A_{12}^2$$
$$= (A_{11} + A_{12})^2$$

Similarly

$$TC_j = A_{13}^2 + A_{11}A_{14} + A_{13}A_{14} + A_{11}A_{13}$$
$$CT_j = A_{12}^2 + A_{11}A_{14} + A_{14}A_{12}A_{12}A_{11}$$
$$CC_j = (A_{14} + A_{12})^2$$

In a large molecule the probability of finding a *trans-trans* sequence is the

---

* Unfortunately, this is not the best of models for the high polymer. However, the matrix size increases rapidly with the number of units in the chain, thus the arithmetic becomes prohibitive. (For example, analysis of a 5-monomer chain requires a 25 × 25 matrix.) The principal shortcoming of using dimeric molecules is that in a given time interval one or the other unit is "hit." This is, of course, not the case. However, for the point we are trying to establish here, the model appears to be adequate.

sum of the probabilities of it occurring at a juncture and of it occurring as one of the dimeric species, if we call this probability w, we have

$$w = (A_{11} + TT_j)/2 \qquad (4)$$

for a *trans-cis*

$$x = (A_{12} + TC_j)/2$$

for a *cis-trans*

$$y = (A_{13} + CT_j)/2$$

for a *cis-cis*

$$z = (A_{14} + CC_j)/2$$

Pseudo Reactivity Ratios

Now we are in a position to calculate the reactivity ratios necessary to polymerize such a polymer chain. According to copolymer theory, in a copolymer consisting of A and B units, the reactivity ratio may be defined as the ratio of the probability of two A units occurring in a row to that of the probability of an A unit being followed by a B unit. If we consider the *cis-trans* polymer chain as a copolymer of *cis* and *trans*, then applying the above definition and using eqs. (4) we have:

Reactivity ratio for *trans*:

$$\gamma_1 = w/x \qquad (5)$$

Reactivity ratio for *cis*:

$$\gamma_2 = z/y$$

The numerical results of the above analysis are shown in the Appendix and the reactivity ratios for various *trans* levels in Table I. From Table I we see that the polymers derived from isomerization are very close to random copolymers ($\gamma_1\gamma_2 = 1$). These polymers of very high *trans* content appear to be slightly on the "alternation side of randomness" which effect should depress the crystallinity more rapidly than if the polymer were truly random.

Knowing the reactivity ratios we are now in a position to recheck some of the experimental results of the crystallinity study with theory.

TABLE I
Pseudo Reactivity Ratios For a Series of Isomerizates Made From Original All *trans*-Polybutadiene

Ratio	% *trans* content			
	87.5	81.2	76.4	75.2
γ_1	6.47	4.27	3.26	3.0
γ_2	0.0666	0.214	0.206	0.33
$(\gamma_1\gamma_2)$	0.431	0.913	≈ 1	≈ 1

Degree of Crystallinity

According to Flory[15] the fraction of crystalline material is expressed to a good approximation by:

$$W_c = (X_T/p)(1 - p)^2 p\zeta_{cr}\{p(1 - p)^{-2} - e^{-\theta}(1 - e^{-\theta})^{-2}$$
$$+ \zeta_{cr}[(1 - p)^{-1} - (1 - e^{-\theta})^{-1}]\} \quad (6)$$

where

$$\zeta_{cr} = -\{\ln (DX_T/p) + 2 \ln [(1 - p)/(1 - e^{-\theta})]\}/(\theta + \ln p)$$

and

$$p = \gamma_1/(1 + \gamma_1)$$
$$D = \exp \{-2\sigma_e/RT\}$$
$$\theta = \Delta H/R(1/_{Tm} - 1/T_m{}^\circ)$$

and where X_T is the fraction of *trans* units, σ_e is the surface free energy per repeating unit, ΔH is the heat of fusion per mole repeating unit, T_m is the melt temperature of polymer, and $T_m{}^\circ$ is the melt of 100% *trans*.

The theoretical curve of weight-per cent crystallinity versus *trans* content, based on eq. (6), is shown in Figure 6. The values of the reactivity ratios are those shown in Table I. The heat of fusion, ΔH, is taken at 1000 cal./mole, $T_m{}^\circ$ at 135°C. and ln D as -1. Also shown on this plot are the experimental points discussed earlier. It is quite obvious that, even allowing for major errors in ΔH and $T_m{}^\circ$, the shape of the theoretical and experimental curves are quite different. As mentioned earlier, the experimental points are quite similar to what one would expect from a block copolymer (see, for example, Mandelkern).[16] However, the detailed examination of the nature of the reaction discussed shows these polymers are indeed random copolymers. This dilemma is resolved by a study of the melting temperature of the various copolymers.

Melting Temperatures and Crystal Transitions

The melting temperatures are obtained by using the goniometer to note the disappearance of reflections as the temperature of the sample is varied. As noted earlier, the behavior of the *trans* crystal is quite unusual. Below approximately 60°C. the crystal is pseudohexagonal with $a = 4.54$ A. and $c = 4.92$ A. At 60°C. a transition occurs and above this temperature the crystal is still pseudohexagonal, but now the dimensions are $a = 4.88$ A. and $c = 4.68$ A. For convenience we will call the low temperature form α and the high temperature one β. Figures 7 and 8 show the reflections (measured by counts) of both the α and β forms of the crystal as a function of temperature for two of the polymers. It may be noted that the melting temperature of the β form decreases with *trans* content, while the melting temperature of the α form is invariant. From a series of curves of the types in Figures 7 and 8 it appears that for at least polymers of greater than 82% *trans*, the β form indeed arises from the α form since reflections
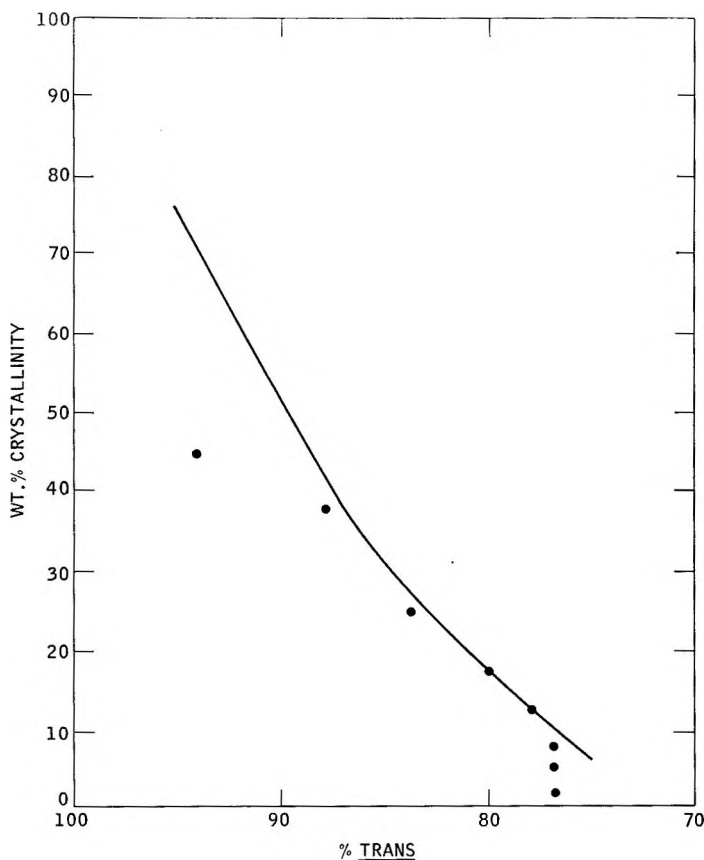
Fig. 6. Theoretical crystallinity content calculated for various *trans* contents on basis of random copolymer equations. Points represent measured values.

from it commence as those from the β form decrease. At approximately 80% *trans*, both the α and β forms have the same melting temperatures. Below 80% the β form can hardly be discerned and the melting temperature of the α form starts to decrease with decreasing *trans* content. A compilation of the melting temperatures of the α and β forms for various *trans* contents is shown in Table II.

This behavior is quite strange, to say the least. Why the melting temperature or transformation of the α form should be invariant with *trans* content until a critical *trans* content is reached is difficult to understand. One would expect both the α and β form to follow the Flory equation[15] simultaneously for random copolymers. This equation is:

$$1/T_m - 1/T_m{}^\circ = R/\Delta H \ln X_T \tag{7}$$

In Figure 9 we have plotted $1/T_m$ (where T_m is taken as the temperature of the highest melting crystal form) and $\ln X_T$. Also shown are Mandelkern's data on the melting temperatures of some emulsion polybutadienes
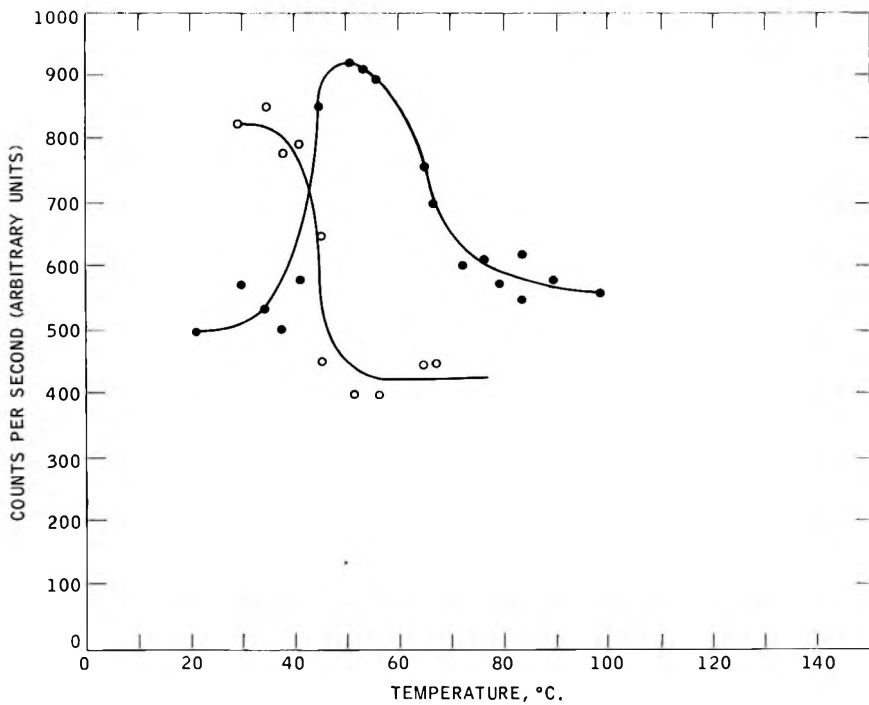
Fig. 7. Plot of peak intensities for (O) α and (●) β forms of 82.4% *trans*-polybutadiene.
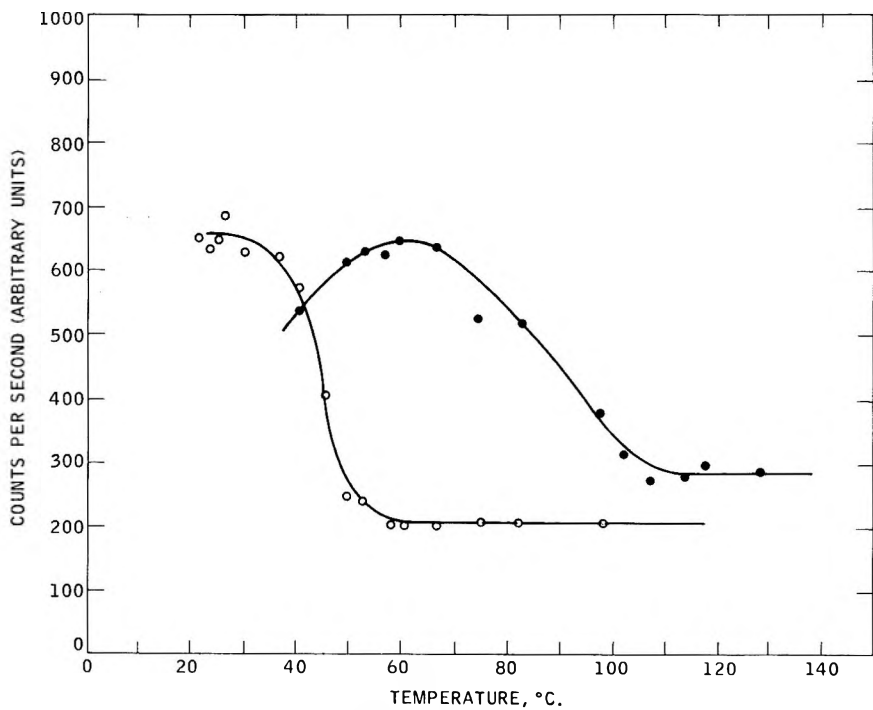

Fig. 8. Plot of peak intensities for (O) α and (●) β forms of 94% *trans*-polybutadiene.

TABLE II

Melting Temperatures of the α and β Crystal Forms in Various Polybutadiene Isomerizates

| | T_m, °C. | | |
% trans	α form	β form	Method
94	60	115.5	Counting
88	65	104.4	Counting
82.4	60	87.7	Counting
81.0	60	71.1	Counting
78.2	65	65	Counting
77.2	51	—	Counting
75	29	—	Photographic
71[a]	7	—	Counting

[a] Isomerized from original high cis-polybutadiene.

in the 60 to 78% *trans* content range. The lower line is a plot of eq. (7) with $T'_m{}^\circ = 148°C.$[18] and $\Delta H = 1000.$[17] The upper line is a best fit for Mandelkern's data. The polymers of high *trans* content appear to fit the theory quite well. However, at about 80% *trans* content the melting temperatures of the polymers drop sharply and the points diverge from the theoretical curve. At 75% *trans* content the melting temperature appears to follow the values obtained by Mandelkern. Some difficulty was experienced in obtaining the melting temperatures of the polymers of low crystallinity using the counting technique. It was therefore necessary to measure the melting temperature of the polymer of lowest crystallinity photographically. In spite of this, it appears that the possible errors are not large enough to alter the description given for the data. The shifting of the melting temperatures from one line to the other appears to take place in the region where the melting temperature of the β form approaches that of the α form. In other words as long as the crystal which melts is the β form the data fall along the lower line, ($T_m{}^\circ = 148°C., \Delta H = 1000$). However, at the lower *trans* content when the melting crystal is the α form the data fall along the upper line ($T_m{}^\circ = 97°C., \Delta H = 1000$). The transition, of course, occurs when the melting temperatures of the α and β forms are close to each other. Thus the melting behavior of both crystals follows the theoretical random copolymer curves though not simultaneously. This confirms the calculation regarding the random nature of the isomeric sequences.

Using this information on the melting crystal we can now, at least in a phenomenological sense, explain the crystallinity vs. *trans* content data shown in Figure 5. At room temperature the crystal form observed is always the α form. For the high *trans* polymers the melting temperature of the α form does not change with *trans* content hence one would not expect the crystallinity to decrease in the normal copolymer manner (eq. 6). Since the melting temperature remains constant it is reasonable to suppose that the crystallinity just decreases in proportion to *trans* content. How-
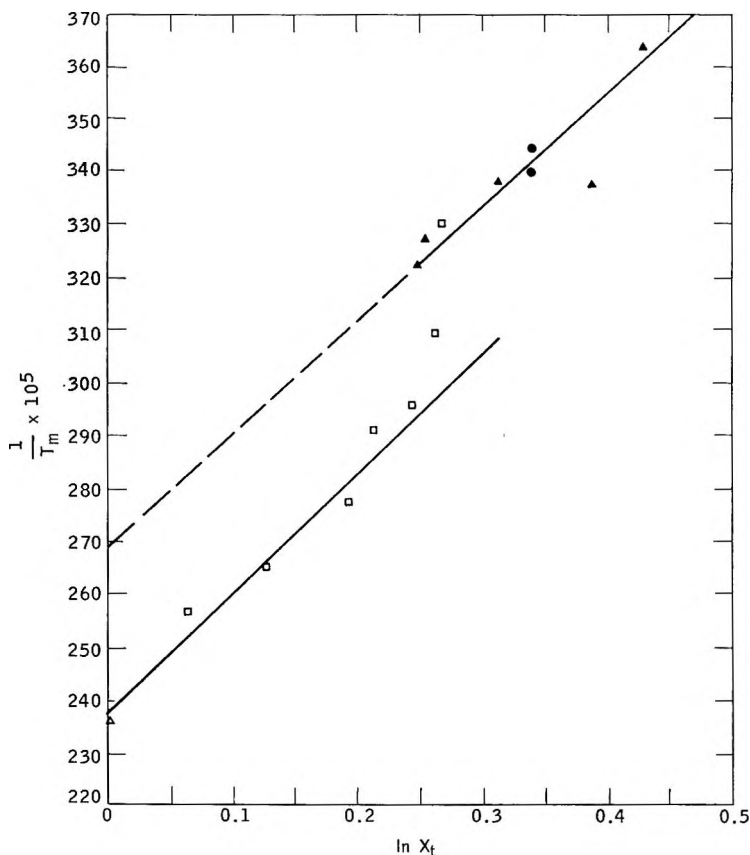
Fig. 9. Plot of melting temperature of polybutadienes as a function of *trans* content: (▲) data of Mandelkern; (●) isomerizate from Cis-4; (□) isomerizate from Trans-4; (△) value of Natta. Upper curve is the best fit of the data of Mandelkern. Lower curve is the theory based on the depression of the melting point of the β form.

ever, at approximately 80% *trans* content the melting temperature of the α form decreases rapidly with *trans* content and thus the crystallinity would drop rapidly. In fact, a very small decrease in *trans* content in this region would effect a major decrease in crystallinity. Thus the crystallinity should decrease linearly with *trans* content until 80% *trans* after which it should decrease at a very fast rate. This is in accord with the data shown in Figure 5. Although we have shown that the random distribution is compatible with crystallinity variations in the copolymer, we have no explanation on a molecular or structural basis for the above phenomenon. We intend to study the implications of Figure 9 in some detail to enable elucidation of the structural factors. We feel that such an understanding is quite important. As will be shown in the second paper of this series, the polymer properties in the transition region undergo profound changes. There is some indication the isomorphism may be playing a major role in the manner in which the crystals behave. The data

shown by Mandelkern were for polybutadienes in which the major non-crystallizing units are vinyl. In the polybutadienes discussed throughout this paper the major noncrystallizing units are *cis*. Some of our recent work shows that two polybutadienes, both of the same *trans* content but with a different stereo isomer (*cis*, and vinyl) as the comonomer have different crystalline properties.

DISCUSSION

We have shown that the crystallinity of high *trans*-polybutadienes with varying amounts of *cis* content behaves very much like the crystallinity of block copolymers. However, since the *trans* content was achieved by chemical modification rather than polymerization it was possible to establish that the distribution of *cis* and *trans* units along the chain is truly random. A detailed study of the melting behavior supports this view. How general these effects are, is still unknown. The existing knowledge of the steric structures of many polymers has been determined through crystallinity studies. The present work suggests very strongly that erroneous conclusions may be made in those cases where transitions can exist and are not investigated thoroughly. It is well known that the secondary crystallization exists for most polymer crystals. Whether or not the secondary crystals have the same structure as that of the primary crystals has not yet been established. It is extremely pertinent to point out that Natta[20] has observed that the nature of the noncrystallizable monomer units affects the crystal structure formed by the crystallizable units in copolymers. In addition, the amount of noncrystallizable units also affects the crystal structure. If any of the latter effects (secondary crystallization or noncrystallizable units) are present, then attempts to characterize chain conformation or distribution of monomer units in copolymers must take them into account.

APPENDIX

In eq. (*1*) in the text, the fixed conditional probabilities are stated. The chance of a *cis* unit going back to *cis* is 0.25, and *cis* going to *trans* is 0.75, *trans* going to *cis* is 0.25 and *trans* going back to *trans* is 0.75. In an ensemble of dimeric molecules let us consider the unit of time to be the average time it takes for one of the dimeric molecules to "flip" *cis* or *trans*. Then, the chance of a *TT* molecule going to *TT* in one unit of time is 0.75, of it going *TC* is 0.125, of going *CT* is 0.125, etc. The chance of molecules which start out *TC* going to *TT* is 0.375, of going to *TC* is 0.5, etc. In fact we can build up a so-called matrix of transition probabilities for determining the fate of all the dimeric molecules in unit time. This is shown in eq. (A1) with proper values:

		TT	TC	CT	CC	$\%\,Trans$	$\%\,Cis$	
	TT	0.75	0.125	0.125	0	87.5	12.5	
	TC	0.375	0.50	0	0.125	62.5	37.5	(A1)
$P_1 =$	CT	0.375	0	0.50	0.125	62.5	37.5	
	CC	0	0.375	0.375	0.25	37.5	62.5	

In addition, the total *trans* and *cis* contents are shown. A number shown in the matrix represents the probability of the corresponding unit in the vertical column *TT*, *TC*, *CT*,

or CC being isomerized to the corresponding unit in the horizontal row TT, TC, CT, or CC in unit time.

To calculate the distribution in two units of time one merely has to multiply the matrix (A1) by itself. The result is shown in eq. (A2):

$$
P_2 = \begin{array}{c} TT \\ TC \\ CT \\ CC \end{array}
\begin{array}{|cccc|cc}
TT & TC & CT & CC & \%\ Trans & \%\ Cis \\
0.656 & 0.156 & 0.156 & 0.0312 & 81.2 & 18.8 \\
0.469 & 0.344 & 0.094 & 0.094 & 68.8 & 31.2 \\
0.469 & 0.094 & 0.344 & 0.094 & 68.8 & 31.2 \\
0.281 & 0.281 & 0.281 & 0.156 & 56.2 & 43.8
\end{array} \qquad (A2)
$$

Multiplying the matrix of P_2 once again by itself gives the result in eq. (A3). Continuation of the procedure gives the values in eq. (A4).

$$
P_4 = \begin{array}{c} TT \\ TC \\ CT \\ CC \end{array}
\begin{array}{|cccc|cc}
TT & TC & CT & CC & \%\ Trans & \%\ Cis \\
0.585 & 0.179 & 0.179 & 0.0547 & 76.4 & 23.6 \\
0.540 & 0.2262 & 0.164 & 0.0704 & 73.5 & 26.5 \\
0.540 & 0.164 & 0.2262 & 0.0704 & 73.5 & 26.5 \\
0.492 & 0.2106 & 0.2106 & 0.0858 & 70.2 & 19.8
\end{array} \qquad (A3)
$$

$$
P_{16} = \begin{array}{c} TT \\ TC \\ CT \\ CC \end{array}
\begin{array}{|cccc|cc}
TT & TC & CT & CC & \%\ Trans & \%\ Cis \\
0.562 & 0.1897 & 0.1897 & 0.0618 & 75.17 & 24.83 \\
0.564 & 0.1894 & 0.1894 & 0.0618 & 75.17 & 24.83 \\
0.564 & 0.1894 & 0.1894 & 0.0618 & 75.17 & 24.83 \\
.557 & 0.1882 & 0.1882 & 0.0633 & 74.50 & 25.5
\end{array} \qquad (A4)
$$

Using the values in eqs. (A1)–(A4) for eq. (3) of the text we have for the case starting with an all-*trans* ensemble of molecules the values shown in Table AI:

TABLE AI

	87.5% *Trans*	81.2% *Trans*	76.4% *Trans*	75.17% *Trans*
TT_j	0.766	0.660	0.585	0.562
TC_j	0.108	0.152	0.179	0.190
CT_j	0.109	0.152	0.179	0.190
CC_j	0.0156	0.035	0.055	0.062

Then we can calculate w, x, y, z using eqs. (4) of the text; the results are shown in Table AII.

TABLE AII

	87.5% *Trans*	81.2% *Trans*	76.4% *Trans*	75.17% *Trans*
w	0.758	0.658	0.585	0.562
x	0.1172	0.154	0.179	1.190
y	0.1172	0.154	0.179	0.190
z	0.0078	0.033	0.055	0.062

With these values and eqs. (5) in the text, it is possible to calculate the reactivity ratios γ_1 and γ_2 shown in Table I of the text.

References

1. Yake, A. M., and R. Chujo, *J. Polymer Sci.*, **46**, 163 (1960).

2. Miller, R. L., and L. E. Nielsen, *J. Polymer Sci.*, **46**, 303 (1960).

3. Sakaguchi, Y., *Kobunshi Kagaku*, **17**, 333 (1960).

4. Lanzavecchia, G., *Chim. Ind. (Milan)*, **43**, 376 (1961).

5. Coleman, B. D., *J. Polymer Sci.*, **31**, 155 (1958).

6. Fordham, J. W., *J. Polymer Sci.*, **39**, 321 (1959).

7. Golub, M. A., *J. Polymer Sci.*, **25**, 373 (1957).

8. Golub, M. A., *J. Am. Chem. Soc.*, **82**, 5093 (1960).

9. Trick, G. S., *J. Polymer Sci.*, **41**, 213 (1959).

10. Hampton, R. R., *Anal. Chem.*, **21**, 923 (1949).

11. Flory, P. J., *Principles of Polymer Chemistry*, Cornell Univ. Press, Ithaca, N. Y., (1953).

12. Hermans, P. H., and A. Weidinger, *J. Appl. Phys.*, **19**, 419 (1948).

13. Natta, G., *Atti Accad. Nazl. Lincei, Rend., Classe Sci. Fis. Mat. Nat.*, **20**, 728 (1956).

14. Seddt, K. W., G. S. Trick, R. H. Mayor, W. M. Saltman and R. M. Pierson, *Rubber Plastics Age*, **42**, 175 (1961).

15. Flory, P. J., *Trans. Faraday Soc.*, **51**, 848 (1955).

16. Mandelkern, L., *Rubber Chem. and Technol.*, **32**, 1392 (1959).

17. Mandelkern, L., M. Tryon, and F. A. Quinn, Jr., *J. Polymer Sci.*, **19**, 77 (1956).

18. Miller, R. I., and L. E. Nielsen, *J. Polymer Sci.*, **44**, 391 (1960).

19. Rybnikar, F., *J. Polymer Sci.*, **44**, 517 (1960).

20. Natta, G., P. Corradini, D. Sianesi, and D. Mrero, *J. Polymer Sci.*, **51**, 527 (1961).

Résumé

On a isomérisé des polybutadiènes stéréoréguliers contenant un pourcentage élevé de segments *cis* et *trans*, afin d'obtenir des polymères avec des taux différentes de segments *cis-trans*. Ces polymères isomérisés ont été employées pour étudier les effets de la structure sur les propriétés physiques. Les isomerisations ont été effectuées par photosensibilisation en solution benzénique à 25°C. La réaction fut controlée afin d'obtenir des polymères qui contiennent des segments *trans* de 0 à 95%. On a choisi cette gamme ainsi pour produire des polymères cristallins et semi-cristallins dont la structure pouvait être intupièetie par des techniques aux petits rayons-x en termes de séquences ou de blocs. On a mesuré méticuleusement le pourcentage des isomères par l'infarrouge; les isomérisations atteignaient un équillibre de 77% trans indépendamment du fait que la réaction des polybutadiènes commence avec un taux élevé de *trans* ou de *cis*. La viscosité intrinséque augmente régulièrement en fonction du pourcentage de *trans* conformément à la taille plus grande d'une unité *trans*. Les relations $\eta_{sp}/c-c$ ont une forme compliquée et ce problème sera étudié plus tard. La cristallinité décroît régulièrement avec la diminution du pourcentage en *trans* quand on s'approche de l'équilibre de 77% de *trans*. En continuant l'isomérisation au moment de l'équilibre, on obtenait un polymère complètement amorphe. Les points de fusion des polymères cristallins ont été étudiés en détail au moyen d'une caméra à rayons-x courts. Ces polymères possèdent deux formes cristallines. La première était stable jusqu'a 60°C. et ne variait pas avec le rapport cis-*trans* dans le domaine 80–95% trans. Au-dessous de 80% *trans* le point de fusion de cette forme diminuait quand le taux de *trans* décroissait. La température de fusion de l'autre forme cristalline dépendait du pourcentage en *trans* et diminuait lorsque le taux de trans décroissait jusqu'a ce qu'il coïncide avec le point de fusion de l'autre forme. On a calculé les distributions des unités et des séquences *trans* et *cis* par des calculs matriciels et des probabilités de transition. On a eu recours à la théorie des copolymères pour calculer les rapports de la pseudo-réactivité pour les formes *cis* et *trans*. Les points de fusion des deux formes cristallines suivent les courbes théoriques pour des polymères statistiques

mais pas en même temps. On discute ce phénomène. La cristallinité des polymères isomérisés à pourcentage en *trans* élevé est similaire à celle de copolymères à blocs bien que la méthode de leur préparation suppose qu'ils soient statistiques. L'importance d'une transition au sein du cristal est soulignée et mise en rapport avec la quantité et le type d'unité non-cristallisable.

Zusammenfassung

Stereoreguläre Polybutadiene mit hohem *trans-* und *cis*-Gehalt wurden isomerisiert um Polymere mit variierendem *cis-trans*-Gehalt zu erhalten. Diese Isomerisierungsprodukte wurden zur Untersuchung des Struktureinflusses auf physikalische Eigenschaften verwendet. Die Isomerisierung wurde mit Photosensibilisierung in Benzollösung bei 25°C. durchgeführt. Die Reaktion wurde so geführt, dass Polymere mit 0 bis 95% *trans*-Gehalt entstanden. Dieser Bereich wurde gewählt, um kristalline uud semi-kristalline Polymere zu erhalten, deren Aufbau aus Squenzen oder Blöcken durch Röntgenaufnahmen überprüft werden konnte. Der Gehalt an Isomeren konnte durch Infrarotmessungen genau bestimmt werden. Die Isomerisierung erreicht bei 77% *trans* ein Gleichgewicht, gleichgültig ob von Polybutadienen mit hohem *trans-*oder *cis*--Gehalt ausgegangen wurde. Die Viskositätszahl zeigte eine regelmässige Zunahme mit dem *trans*-Gehalt, was mit der grösseren Ausdehnung der *trans*-Einheit übereinstimmt. Die Beziehung η_{sp}/c gegen c hatte eine komplizierte Form und bliebt einer weiteren Untersuchung überlassen. Die Kristallinität nahm mit fallendem *trans*-Gehalt bei Annäherung an das Gleichgewicht von 77% *trans* regelmässig ab. Fortgesetzte Isomerisierung beim Gleichgewichtspunkt führte zu einem vollständig amorphen Polymeren. Die Schmelztemperatur des kristallinen Polymeren wurde mit Röntgen- und Zählverfahren genau untersucht. Die Polymeren wiesen zwie Kristallformen auf. Eine Form war bis zu 60°C. stabil und im Bereich von 80–95% *trans* invariant gegen den *cis-trans*-Gehalt. Unterhalb 80% *trans* nahm der Schmelzpunkt dieser Form bei weiterer Verringerung des *trans*-Gehaltes ab. Die Schmelztemperatur der anderen Kristallform war vom *trans*-Gehalt abhängig und nahm mit fallendem *trans*-Gehalt bis zum schliesslichen Zusammenfallen mit der Schmelztemperatur der ersten Form ab. Die Verteilung der *cis-* und *trans*-Einheilten und ihrer Sequenzen wurde durch Konstruktion von Matrizen für die Umwandlungswahrscheinlichkeit berechnet. Die Copolymerisationstheorie wurde zur Berechnung der PseudoReaktivitätsverhältnisse für die *trans-* und *cis*-Form herangezogen. Die Schmelztemperatur der beiden Kristalle folgte, wenn auch nicht gleichzeitig, der für statistische Copolymere berechneten Kurve. Dieses Verhalten wird diskutiert. Die Kristallinität von Isomerisierungsprodukten mit hohem *trans*-Gehalt war, ungeachtet der Tatsache, dass ihre Herstellungsmethode eine Charakterisierung als ungeordnet verlangt, ähnlich der von Blockcopolymeren. Die Bedeutung einer Kristallumwandlung in diesem Fall and die allegemeinen Einflüsse der Menge und Art der nichtkristallisierbaren Einheit werden betont.

Polymerization in Liquid Sulfur Dioxide.   Part XIII. Polymerization of Styrene Derivatives in Liquid Sulfur Dioxide

NIICHIRO TOKURA, MINORU MATSUDA, and YASUO OGAWA,
*The Chemical Research Institute of Non-Aqueous Solutions,
Tohoku University, Sendai, Japan*

Synopsis

p-Bromostyrene, *p*-methylstyrene and α-methylstyrene were subjected to polymerization in liquid sulfur dioxide with α,α'-azobisisobutyronitrile as an initiator at polymerization temperatures of 0–60°C. In case of polymerization of *p*-bromostyrene, only polysulfones of 1:2 molar ratio between sulfur dioxide and *p*-bromostyrene were obtained. No cationic polymerization was observed. In case of polymerization of *p*-methylstyrene polysulfone having 1:2 composition, a radical polymerization product, as well as poly-*p*-methylstyrene, a cationic polymerization product, as obtained, revealing concurrent and competitive occurrence of both polymerizations. The cationic polymerization was explained as the result of the electron-donating property of the *para*-methyl substituent and the catalytic action of sulfur dioxide or sulfurous acid formed with a minute amount of water contained in liquid sulfur dioxide. In liquid sulfur dioxide, the cationic polymerization was perfectly inhibited by DMF and the radical polymerization was not affected by the presence of DMF. In a system in which the radical polymerization alone proceeded in liquid sulfur dioxide, the overall rate of the polymerization was proportional to the concentration of AIBN in the order of 0.7. This was interpreted to indicate that the strong solvation between sulfur dioxide and the terminal radical of the growing radical due to hyperconjugation of the *p*-methyl group may stabilize the terminal radical, leading to a unimolecular termination. In the polymerization of α-methylstyrene, the addition of AIBN did not give polysulfone, but gave poly-α-methylstyrene alone as a result of cationic polymerization.

INTRODUCTION

Radical polymerization of vinyl monomers in liquid sulfur dioxide is known to give polysulfones, except in case of acrylonitrile[1] or related olefin derivatives. The composition of these polysulfones is reported to be fixed in all cases (except in the results of one investigator),[2] and this composition corresponds to a ratio of 1:1 (e.g., SO_2 and isobutene)[3] or 1:2 (e.g., SO_2 and styrene)[4] between sulfur dioxide and the vinyl compound. The difference of these ratios is considered to depend upon the difference in the compositions of the complexes formed between sulfur dioxide and the vinyl monomers before polymerization, which is, in turn, caused by the difference in the degree of interaction of the monomer with sulfur dioxide according to the electron density in the vinyl group. The formation of polyacrylonitrile

but not polysulfone in the case of radical polymerization of acrylonitrile[2] is attributed to the fact that the formation of a complex is impossible because of the strong electrophilicity of the nitrile group and the repulsion between the positive charged vinyl group of the monomer and sulfur dioxide molecules. On the other hand, the cationic polymerization of vinyl compounds in liquid sulfur dioxide gives polyolefins without exception.[5]

The present authors have experimented on the polymerization of styrene derivatives with α,α'-azobisisobutyronitrile as an initiator, and a comparative examination of the effect of substituents on the composition of the polysulfones obtained has been undertaken.

EXPERIMENTAL

Materials

Liquid sulfur dioxide and α,α'-azobisisobutyronitrile (AIBN) were purified by the usual methods as reported earlier.[2] α-Methylstyrene used was a commercial product (Dow Chemical Co.) which had been twice distilled *in vacuo* under nitrogen (b.p. 59.5°C./16 mm. Hg). p-Bromostyrene was prepared from bromobenzene by a series of reactions: acetylation, Meerwein-Ponndorf reduction and dehydration.[6]

ANAL. Calcd.: C, 52.48%, H, 3.88%; Found: C, 52.04%, H, 4.02%; b.p. 89°C./ 13 mm. Hg, n_D^{20} 1.5931 (lit.:[6] b.p. 89°C./13 mm. Hg, n_D^{20} 1.5933).

p-Methylstyrene was synthesized in a similar way.[7]

ANAL. Calcd.: C, 91.53%, H, 8.47%; Found: C, 91.35%, H, 8.64%; b.p. 58.5°C./12 mm. Hg, n_D^{25} 1.5393 (lit.:[7] b.p. 59°C./12 mm. Hg, n_D^{25} 1.5392).

Experimental Technique

The rate of polymerization was measured by the gravimetric method in a glass pressure tube. A definite amount of the monomer containing a known amount of AIBN was pipetted into the tube. The tube was connected to a vacuum line, flushed with dry nitrogen, and filled with purified liquid sulfur dioxide to a definite volume at a definite temperature, as in the usual way.[1] The polymerization temperature was 30-60°C. After the completion of polymerization, the reaction mixture was poured into a large amount of methanol; the polymer precipitated was filtered off and dried under reduced pressure at 45°C. until a constant weight was obtained.

RESULTS AND DISCUSSION

In order to make possible a comparison with the radical polymerization of styrene in liquid sulfur dioxide,[4] similar polymerization conditions were used as in the case of styrene. The time–conversion curves for each reaction are shown in Figure 1.
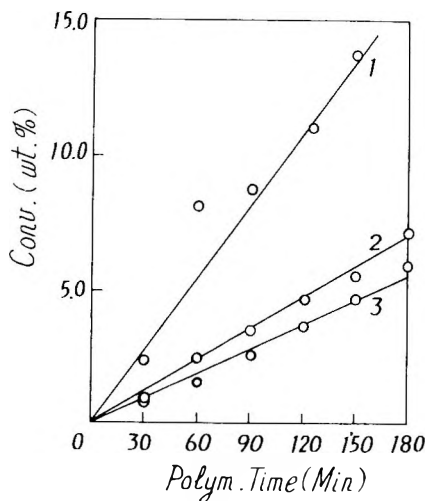
Fig. 1. Time–conversion curves: (*1*) p-methylstyrene; (*2*) styrene; (*3*) p-bromo-styrene. Polymerization conditions: [monomer] = 36.36 vol.-%; [liq. SO_2] = 63.64 vol.-%; [AIBN]$_0$ = 1.09 × 10^{-2} mole/l.; polymerization temperature, 50°C.

Polymerization of p-Bromostyrene

Time-conversion curves obtained at various temperatures in the range 30-60°C. are shown in Figure 2, and an Arrhenius plot is shown in Figure 3. The activation energy of the overall reaction is found to be 13.9 kcal./mole. The results of the elementary analyses of the polymers are given in Table I.
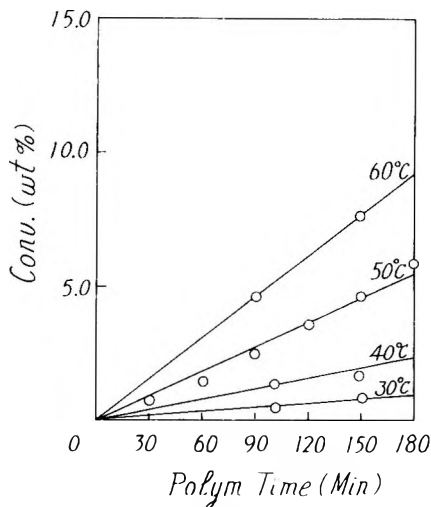

Fig. 2. Time–conversion curves obtained by polymerization of p-bromostyrene. Polymerization conditions: [p-bromostyrene] = 36.36 vol.-%, [liq. SO_2] = 63.64 vol.-%; [AIBN]$_0$ = 1.09 × 10^{-2} mole/l.; polymerization temperature, 50°C.
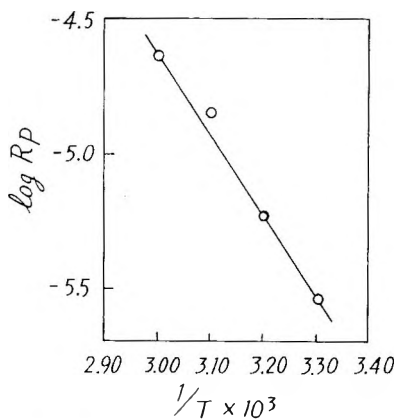
Fig. 3. Arrhenius plot of the overall reaction rate obtained from Fig. 2.

TABLE I

Elementary Analyses of p-Bromostyrene Polysulfone

[p-Bromostyrene], mole/l.	[Liq. SO_2], mole/l.	Polymerization temp., °C.	Conversion, wt.-%	C, %	H, %
1.40	16.53	50	0.46	45.61	3.21
2.80	12.86	50	5.78	46.26	3.20
2.80	11.02	50	0.36	46.25	3.50
4.20	9.19	50	5.27	47.25	3.54
5.60	5.51	50	1.90	47.08	3.53

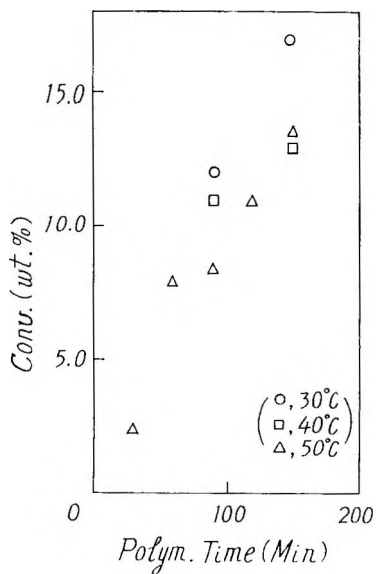

Fig. 4. Time–conversion curves obtained by polymerization of p-methylstyrene. Polymerization conditions: [p-methylstyrene] = 36.36 vol.-%; [liq. SO_2] = 63.64 vol.-%; [AIBN]$_0$ = 1.09 × 10^{-2} mole/l.; polymerization temperature, 50°C.

Polymerization of p-Methylstyrene

Time–conversion curves for polymerizations at 30–50°C. are shown in Figure 4, and the results of elementary analyses of the polymers obtained are given in Table II.

TABLE II

Elementary Analyses of Polymers Obtained by the Polymerization of p-Methylstyrene

[p-Methylstyrene], mole/l.	[Liq. SO₂], mole/l.	Polymerization temp., °C.	Conversion, wt.-%	C, %	H, %
1.39	16.53	50	3.69	85.25	7.66
2.77	12.86	50	19.28	85.92	7.72
4.16	9.19	50	1.02	74.20	6.85
5.54	5.51	50	1.44	71.30	6.61

As has been mentioned above, the radical polymerization of vinyl monomers capable of entering into donor-acceptor interactions with liquid sulfur dioxide molecules gives polysulfone when the reaction is carried out in liquid sulfur dioxide. According to the theory of Dainton et al.,[8] isobutene or cyclopentene, which form 1:1 complexes with liquid sulfur dioxide, yield polysulfones of 1:1 composition.

In radical polymerization of styrene in liquid sulfur dioxide, the present authors have always obtained polysulfone of the 1:2 composition,[4] even when the conditions of polymerization such as temperature, concentration of catalyst, and ratio of liquid sulfur dioxide to the monomer was changed. The same was true even when various solvents which have been proved to show some interaction with liquid sulfur dioxide[10] or various salts[11] were added.
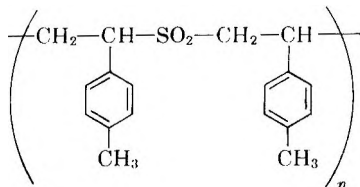
While Barb[2] obtained polysulfones having a ratio more than 1:2 in the polymerization of styrene, it is suspected that the reactions were carried out under such conditions of polymerization as at a very low ratio of liquid sulfur dioxide to styrene; hence the polymerization of styrene alone took place after sulfur dioxide had been consumed. Now, in view of the result of polymerization of p-bromostyrene, and taking account of the polymolecular nature of the products, the results of analysis of the polymers (Table I) can be regarded to agree well with the composition of 1:2 (sulfur dioxide: p-bromostyrene), the calculated values for the polymers of having the structure:
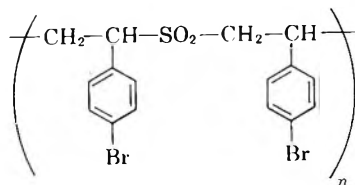
being C 44.63% and H 3.52%.

An activation energy of the overall reaction of 13.9 kcal./mole is a value comparable to 14.7 kcal./mole obtained in the polymerization of styrene.[4] The introduction of a bromine at the *para* position of the vinyl group may be said to have no effect on the composition of the polysulfone.

In the polymerization of *p*-methylstyrene, the analytical values in Table II differ considerably from the calculated values for a 1:2 polysulfone having the structure:

$$\left(\begin{array}{c} -CH_2-CH-SO_2-CH_2-CH- \\ \mid \qquad\qquad \mid \\ \bigcirc \qquad\qquad \bigcirc \\ \mid \qquad\qquad \mid \\ CH_3 \qquad\quad CH_3 \end{array} \right)_n$$

the calculated figures being C, 72.00% and H, 6.67%.

Moreover, in polymerization at various temperatures (Fig. 4), the reproducibility of the results was not so good; however, the higher was the yield, the lower was the temperature. The reason for this anomaly may lie in concurrent occurrence of a competitive cationic polymerization. Therefore, the extraction of the polymer was attempted. Extraction with benzene (Table III) permitted extraction of both poly-*p*-methylstyrene and a part of the polysulfone, but the use of cyclohexane as an extractant yielded polymers containing virtually sulfur, i.e., poly-*p*-methylstyrene alone (Table IV).

TABLE III
Analyses of Polymers Extracted with Benzene

	C, %	H, %	S
Polymer	85.58	7.92	+
Residue	76.51	7.13	+
Extract	85.97	8.07	+

TABLE IV
Analyses of Polymer Extracted with Cyclohexane

	C, %	H, %	S, %
Polymer	82.53	7.85	4.86
Residue	74.21	7.01	10.23
Extract	91.19	9.05	0.26

This indicates that cationic polymerization was evidently taking place concurrently and competitively. Accordingly, polymerization in the presence of a trace of hydroquinone, an inhibitor to radical polymerization, was undertaken. The result is given in Table V. The result is consistent with the theoretical value calculated for poly-*p*-methylstyrene. Although very small

amounts of sulfur were present, this may be regarded to be sulfur dioxide which combined with the polymer molecules during reaction, possibly in the form of sulfinic acid.

The fact that a cationic polymerization takes place in liquid sulfur dioxide in spite of the absence of a cationic catalyst such as Lewis acid may be attributable to the strong electron-donating property of the p-methyl group of the styrene derivative and to the catalytic action of sulfur dioxide itself. Alternatively, sulfur dioxide with a trace of water as a cocatalyst may also be a useful source for the catalyst, as has been reported in the polymerization of isobutene.[12] Perhaps the less reproducible results in the simultaneous (radical and cationic) polymerization are due to the weak acidity and/or the fluctuation of the water content of sulfur dioxide. (Reproducible results were obtained if the radical polymerizations were carried out by the suppression of the cationic polymerization.)

TABLE V
Analyses of the Polymers Obtained in Presence of Hydroquinone[a]

Polymerization time, min.	Conversion, wt.-%	C, %		H, %		S, %	
		Found	Calcd.	Found	Calcd.	Found	Calcd.
50	8.24	91.15	91.47	8.37	8.53	1.01	0
90	5.67	91.23		8.58		0.32	

[a] Polymerization conditions: [p-methylstyrene]$_0$ = 2.29 mole/l.; [liq. SO$_2$]$_0$ = 14.16 mole/l.; [AIBN]$_0$ = 0; polymerization temperature, 50°C.

In addition to p-methylstyrene, α-methylstyrene, methyl vinyl ether,[13] and formaldehyde[14] are known to be monomers which are polymerized cationically by sulfur dioxide alone.

In the next place, radical polymerization alone of p-methylstyrene was arranged to occur by adding dimethyl-formamide (DMF) as an inhibitor for the cationic polymerization. (Addition of both hydroquinone and DMF gave no polymer at all. Addition of DMF had no effect on the rate of the radical polymerization. With regards to the mechanism of inhibition by DMF, the details will be reported elsewhere.) The results are given in Table VI.

To judge only from the results of elementary analyses, it can be seen that the composition of the polysulfone has a definite ratio of 1:2 between sulfur dioxide and p-methylstyrene. The calculated values for a polysulfone of 1:2 ratio are C, 72.00%, H, 6.67%, and S, 10.67%. The fact that the composition of the polysulfone has a ratio of 1:2 as in the case of styrene polysulfone or p-bromostyrene polysulfone leads to the conclusion that the methyl group at the *para* position has no significant effect on the composition of the polysulfone. If the polymerization takes place through formation of a complex between sulfur dioxide and the styrene derivative, the *para*-methyl substituent may be interpreted to have no effect on the composition of the complex. Moreover, the addition of other solvents or salts to the poly-

TABLE VI

Results of Elementary Analyses of Polymers Obtained in Presence of Dimethylformamide (DMF); Polymerization Temperature 50°C.

$[Liq. SO_2]_0$, mole/l.	$[p\text{-Methylstyrene}]_0$, mole/l.	$[AIBN]_0$, mole/l.	$[DMF]_0$, mole/l.	Polymerization time, min.	Conversion, wt.-%	C, %	H, %	S, %
14.72	1.39	5.46×10^{-3}	1.18	150	0.75	71.04	6.81	10.08
11.04	2.78	1.09×10^{-2}	1.18	150	2.40	71.57	6.79	10.59
7.36	4.17	1.64×10^{-2}	1.18	100	1.43	71.36	6.85	10.34
3.68	5.56	2.18×10^{-2}	1.18	100	1.10	72.04	6.81	9.83

merizing system gave no change of the composition of the polysulfones obtained (Table VII).

TABLE VII
Result of Elementary Analyses of p-Methylstyrene Polymer Obtained on Addition of Solvents or Salts in the Presence of DMF[a]

Additive	Additive concn., mole/l.	Polymerization time, min.	Conversion, wt.-%	C, %	H, %	S, %
Benzene	2.79	180	1.64	72.31	6.96	9.97
Toluene	2.34	180	1.77	71.95	6.96	10.06
p-Xylene	2.03	180	1.84	72.21	6.73	10.30
Carbon tetrachloride	2.56	180	1.74	70.82	7.10	9.73
Tetraethylammonium bromide	2.65×10^{-3}	180	2.90	71.18	6.79	10.84

[a] Polymerization conditions: [liq. SO_2]$_0$ = 6.74 mole/l., [p-methylstyrene]$_0$ = 2.54 mole/l., [DMF]$_0$ = 1.08 mole/l., [AIBN]$_0$ = 1.09 $\times$ 10^{-2} mole/l., polymerization temperature, 50°C.

Polymerizations were carried out in the presence of DMF with AIBN of various concentrations as the initiator to examine the effect of concentration of AIBN upon the overall rate R_p of the polymerization. The results are shown in Figure 5.

The rate equation obtained from Figure 5 is

$$R_p = k[\text{AIBN}]_0^{0.7}$$

where [AIBN]$_0$ is the initial concentration of the initiator. For reference, the result of the elementary analyses of the polymers obtained is shown in Table VIII. The number of the order, 0.7 with respect to AIBN concentration, is a value not previously found for radical polymerization of a homogeneous system, and consequently, the unimolecular termination should be considered during the polymerization. However, the unimolecu-
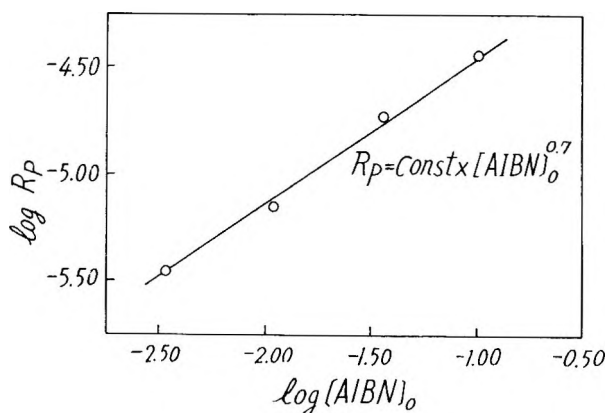

Fig. 5. The log-log plot of overall reaction rate vs. concentration of AIBN.

TABLE VIII
Elementary Analyses of the Polymers

[AIBN]$_0$, mole/l.	C, %	H, %	S, %
1.01×10^{-1}	70.67	6.85	10.47
3.53×10^{-2}	71.45	6.91	10.60
1.09×10^{-2}	71.05	6.75	10.32
3.59×10^{-3}	72.20	6.81	10.13

lar termination in the heterogeneous system of acrylonitrile can be explained as the occlusion of the polymer chains; in the homogeneous polymerization of p-methylstyrene a similar view can not be accommodated. A plausible explanation may be as follows. The terminal radical of the growing chain may have an increase in electron density owing to the hyperconjugation effect of the p-methyl group, and as the result, may be solvated strongly by liquid sulfur dioxide molecule; the terminal radical is thus stabilized, and the polymer chain is terminated unimolecularly:
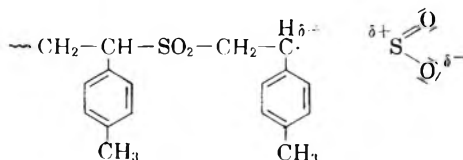
Even in the presence of AIBN, α-methylstyrene in liquid sulfur dioxide does not give the polysulfone, a radical polymerization product, but poly-α-methylstyrene is found as a result of a cationic polymerization. Steric hindrance should be taken into account to explain why polysulfone is not formed. A similar mechanism as in the case of the polymerization of p-methylstyrene in liquid sulfur dioxide may be adopted for the polymerization of α-methylstyrene; however the rate of the polymerization seems very large in the latter, the conversion reaching nearly 90% at 0°C. for 30 min. in liquid sulfur dioxide.

TABLE IX
Results of Elementary Analyses of Poly-α-methylstyrene Obtained in Liquid SO$_2$

[α-Methyl-styrene]$_0$, mole/l.	[Liq. SO$_2$]$_0$, mole/l.	Conversion, wt.-%	Polymerization temp., °C.	[AIBN]$_0$, mole/l.	C, %	H, %	S, %
3.58	10.79	6.41	50	7.64×10^{-3}	91.73	8.62	0
3.58	10.79	7.12	50	2.89×10^{-2}	91.32	8.53	0
3.58	10.79	1.85	50	1.65×10^{-2}	90.71	8.39	0
3.58	10.79	5.56	50	1.65×10^{-2}	91.11	8.54	0
3.58	10.79	17.48	50	1.65×10^{-2}	90.77	8.42	0
5.12	6.74	2.57	0	0	90.35	8.44	0
4.10	9.41	24.90	0	0	91.16	8.66	0

The results of elementary analyses of poly-α-methylstyrene are given in Table IX. Polymerization in the presence of DMF also gave no polymer

TABLE X

Polymerization of α-Methylstyrene in the Presence of DMF; Polymerization Temperature 50°C.

[α-Methyl-styrene]$_0$, mole/l.	[Liq. SO$_2$]$_0$, mole/l.	[DMF]$_0$, mole/l.	[AIBN]$_0$, mole/l.	[BF$_3$·O(C$_2$H$_5$)$_2$]$_0$, mole/l.	Polymer
2.79	11.04	1.18	2.28×10^{-2}	0	None
2.79	11.04	1.18	2.28×10^{-2}	0	None
2.79	11.04	1.18	2.28×10^{-2}	0	None
2.79	11.04	1.18	2.28×10^{-2}	0	None
2.79	11.04	1.18	2.28×10^{-2}	0	None
1.40	14.71	1.18	0	1.14×10^{-2}	None
4.19	7.36	1.18	0	3.42×10^{-2}	None
5.59	3.68	1.18	0	4.56×10^{-2}	None

(Table X). (The addition of DMF inhibited the cationic polymerization entirely, even when BF$_3$ etherate was used as the catalyst.)

The intrinsic viscosities of the polymers obtained are listed in Table XI.

TABLE XI

Intrinsic Viscosities of Polymers Measured in Ubbelohde Viscometer at 30°C. in DMF

Polymer	$[\eta]$, dl./g.
p-Methylstyrene polysulfone	0.37
p-Bromostyrene polysulfone	0.23
Poly-p-methylstyrene	0.04

References

1. Tokura, N., M. Matsuda, and F. Yazaki, *Makromol. Chem.*, **42**, 108 (1960).
2. Barb, W. G., *Proc. Roy. Soc. (London)*, **A212**, 66, 177 (1952).
3. Dainton, F. S., and K. J. Ivin, *Quart. Rev.*, **12**, 16 (1958).
4. Tokura, N., and M. Matsuda, *Kogyo Kagaku Zasshi*, **64**, 501 (1961).
5. Asami, R., and N. Tokura, *J. Polymer Sci.*, **42**, 545, 553 (1960); Tokura, N., M. Matsuda, and Y. Watanabe, *J. Polymer Sci.*, **62**, 135 (1962).
6. Boundy, R. H., and R. F. Boyer, *Styrene. Its Polymers, Copolymers and Derivatives*, Reinhold, New York, 1952, p. 788.
7. Moury, D. T., M. Renoll, and W. F. Huber, *J. Am. Chem. Soc.*, **68**, 1105 (1946).
8. Booth, D., F. S. Dainton, and K. J. Ivin, *Trans. Faraday Soc.*, **55**, 1293 (1959).
9. Tokura, N., M. Matsuda, T. Kawahara, and Y. Ogawa, *Kogyo Kagaku Zasshi*, **65**, 1095 (1962).
10. Andrews, L. J., and R. M. Keefer, *J. Am. Chem. Soc.*, **73**, 4169 (1951).
11. Tokura, N., M. Matsuda, and H. Kichiji, *J. Polymer Sci.*, **61**, S54 (1962).
12. Tokura, N., M. Matsuda, and I. Shirai, *Bull. Chem. Soc. Japan*, **35**, 371 (1962).
13. Reppe, W., and E. Kuhn, U.S. Pat. 2,188,778 (1940).
14. Tokura, N., M. Matsuda, I. Shirai, K. Shiina, Y. Ogawa, and Y. Kondo, *Bull. Chem. Soc. Japan*, **35**, 1043 (1962).

Résumé

On a polymérisé les p-bromostyrène, p-méthylstyrène et alpha-méthylstyrène dans du SO₂ liquide utilisant l'AIBN comme catalyseur dans un domaine de températures de 0 à 60°C. Dans le cas de la polymérisation du p-bromostyrène on obtenait seulement des polysulfones ayant un rapport molaire 0.5 entre le SO₂ et le p-bromostyrène. On n'a pas constaté de polymérisation cationique. Dans le cas de la polymérisation du p-méthylstyrène on obtenait non seulement une polysulfone ayant une composition 0.5, donc le produit d'une polymérisation radicalaire, mais aussi un produit d'une polymérisation cationique, le poly-p-méthylstyrène, ce qui veut dire que les deux genres de polymérisations interviennent d'une manière concurrente et compétitive. On a interprêté la polymérisation cationique comme étant le résultat de propriétés électro-donneuses du groupement méthyle en position *para* et l'action catalytique du SO₂ ou de l'acide sulfureux formé par des traces d'eau contenues dans le SO₂ liquide. Dans le SO₂ liquide la polymérisation cationique fut parfaitement inhibée par le DMF et la polymérisation radicalaire ne fut pas influencée par la présence de DMF. Dans un système où la polymérisation radicalaire se fait toute seule dans le SO₂ liquide, la vitesse totale de la polymérisation était proportionnelle à la concentration d'AIBN à la puissance 0.7. Ceci a été expliqué en admettant que la forte solvation existante entre le SO₂ et le radical terminal de la chaîne en croissance due à l'effet d'hyperconjugaison du groupement *para*-méthyle, pourrait stabiliser le radical terminal, menant aisni à une terminaison monomoléculaire. En polymérisant l'alpha-méthylstyrène au moyen d'AIBN, on n'obtenait pas de polysulfone, mais uniquement du poly-alpha-méthylstyrène à la suite d'une polymérisation cationique.

Zusammenfassung

p-Bromstyrol, p-Methylstyrol und α-Methylstyrol wurden einer Polymerisation in flüssigem Schwefeldioxyd mit α,α'-Azobisisobutyronitril als Starter bei Temperaturen von 0° bis 60°C unterworfen. Bei der Polymerisation von p-Bromstyrol wurden nur Polysulfone mit einem Molverhältnis Schwefeldioxyd zu p-Bromstyrol von 1:2 erhalten. Es wurde keine kationische Polymerisation beobachtet. Im Falle der Polymerisation von p-Methylstyrol wurden zugleich ein Polysulfon mit der Zusammensetzung 1:2, ein Produkt der radikalischen Polymerisation und Poly-p-methylstyrol, ein Produkt der kationischen Polymerisation, erhalten, was zeigt, dass beide Prozesse gleichzeitig und kompetitiv verlaufen. Die kationische Polymerisation wurde durch die Elektronendonoreigenschaft der in *para*-Stellung befindlichen Methylgruppe und die katalytische Wirkung von Schwefeldioxyd oder von der mit spurenweise in flüssigem Schwefeldioxyd vorhandenen Wasser gebildeten schwefeligen Säure erklärt. In flüssigem Schwefeldioxyd wurde die kationische Polymerisation durch DMF völlig verhindert; auf radikalische Polymerisation hatte die Gegenwart von DMF keinen Einfluss. In einem System, in welchem in flüssigem Schwefeldioxyd allein radikalische Polymerisation stattfand, war die Bruttopolymerisationsgeschwindigkeit in bezug auf AIBN von der Ordnung 0,7. Das wurde dahingehend gedeutet, dass die durch den Hyperkonjugationseffekt der *para*-ständigen Methylgruppe hervorgerufene starke Solvatisierung der Radikalendgruppe der wachsenden Kette durch Schwefeldioxyd eine Stabilisierung der Radikalendgruppe bewirkt, was zu einem unimolekularen Kettenabbruch führt. Bei der Polymerisation von α-Methylstyrol verursachte der Zusatz von AIBN keine Polysulfonbildung sondern es entstand als Ergebnis einer kationischen Polymerisation nur Poly-α-methylstyrol.

Swelling of Highly Crosslinked Network Structure

T. K. KWEI, *Interchemical Corporation, Central Research Laboratories, New York, New York*

Synopsis

The swelling of highly crosslinked epoxy polymer films by organic vapor was investigated. The molecular weight per crosslinked unit obtained by applying the equation of rubber elasticity to sorption isotherms is in good agreement with the value estimated from chemical considerations. Thermodynamic functions of solvent–polymer mixing are also presented.

I. INTRODUCTION

Recently the swelling of network structures has been the subject of many investigations. Many of the studies dealt with the swelling of sparsely crosslinked polymers and the extent to which the theory of rubber elasticity can be applied to high crosslinked network structures has not been clearly established. We would like to report some data on the swelling of epoxy-type polymer networks. These highly crosslinked structures, prepared from 4,4'-bisglycidylphenyl-2,2'-propane and various aliphatic amines, are chosen because the reaction between the two components is well understood and the molecular weight per crosslinked unit can be estimated, in some cases, with reasonable certainty from chemical considerations. A comparison of the experimental results with theory can be conveniently made with these systems.

In the present paper, we shall discuss the determination of molecular weight per crosslinked unit M_c and the polymer-solvent interaction parameter χ by the vapor sorption method. Thermodynamic functions for the mixing of the solvent with the polymer are also presented.

According to the current theory, equilibrium swelling can be represented by eq. (1):[1]

$$\ln a_1 = \ln (1 - v_2) + v_2 + \chi v_2{}^2 + \rho(\bar{V}_1/M_c) \, [\langle\alpha\rangle_0^2 \, v_2{}^{1/3} - (2/f)v_2] \quad (1)$$

where $\langle\alpha\rangle_0$ is the dilation factor and the other terms have their usual significance. In the preparation of our polymer, a minimum amount of solvent was used in order that $\langle\alpha\rangle_0^2 \cong 1.0$. Equation (1) can be rearranged according to the method of Rogers, Stannett, and Szwarc:[2]

$$[\ln (a_1/v_1) - v_2]/v_2{}^2 = \chi + \rho(\bar{V}_1/v_2{}^2) \, [v_2{}^{1/3} - (2/f)v_2] \, (1/M_c) \quad (2)$$

If swelling data are available for a range of solvent activities, as in vapor sorption experiments, a plot of $[\ln (a_1/v_1) - v_2]/v_2{}^2$ versus $\rho(\bar{V}_1/v_2{}^2) [v_2{}^{1/3} - (2/f)v_2]$ will be linear with a slope of $1/M_c$ and an intercept equal to χ.

The enthalpy of mixing of the solvent with the polymer can be derived from the temperature coefficient of χ, $d\chi/dT$, according to the relationship:

$$\Delta H_M = -kT^2(d\chi/dT)n_1v_2 \qquad (3)$$

where n_1 is the number of solvent molecules in the mixture.

The partial molar enthalpy of mixing $\Delta \bar{H}_1$ of the polymer network and the liquid solvent can be calculated from eq. (4):

$$(d \ln P/P_0/dT)_{v_2} = -\Delta \bar{H}_1/RT^2 \qquad (4)$$

with the tacit assumption that the enthalpy of network elongation is negligible.

Since the number n_2 of polymer molecules is a mixture of crosslinked network and solvent is to be equated to zero owing to the absence of individual polymer molecules in the network structure,

$$\Delta H_M = n_1 \Delta \bar{H}_1 + n_2\Delta \bar{H}_2 = n_1\Delta \bar{H}_1 \qquad (5)$$

The above relationship is used as a test for the internal consistency of the experiment data.

II. EXPERIMENTAL

Materials

4,4'-Bisglycidylphenyl 2,2'-propane (m.p. 43.5°C.) from Shell Chemical Company, 1,6-hexanediamine (m.p. 39–41°C.) from Matheson Coleman and Bell Company, and Versamid 125 (amine value 298) from General Mills Company were used. Reagent grade solvents were used without further purification.

Film Preparation

A 25-g. portion of 4,4'-bisglycidylphenyl-2,2'-propane and appropriate amount of amine were dissolved in butanone-2 and thoroughly mixed. The mixture polymerized slowly on standing. When the solution viscosity

TABLE I

Polymer	Amine
A	1,6-Hexanediamine (HMDA), 100% stoichiometric amount, 5 g. butanone-2
B	1,6-Hexanediamine (HMDA), 50% stoichiometric amount, 5 g. butanone-2
C	Versamid 125, 75% stoichiometric amount, 10 g. butanone-2

reached a desirable level, films were drawn on tin foil by means of a Gardner gauge. The film was allowed to stand in a desiccator for 24 hr. and then cured at 60°C. for 17 hr.

The extent of reaction between the two components is essentially complete under the above conditions[3,4] for polymers A and B (Table I). For polymer C, spectroscopic results indicate the presence of 10–15% unreacted oxirane rings.

Solvent extraction indicated negligible amount of soluble material in the cured film.

Preliminary Swelling Experiments with Liquid Solvents

Equilibrium swelling values for the polymer were obtained by immersing rectangular piece of polymer films of about 0.5 g. in a solvent at room temperature for at least a weak. The polymer films were then surface dried and weighed in closed vessels. These measurements were carried out for the purpose of selecting suitable solvents for vapor sorption experiments.
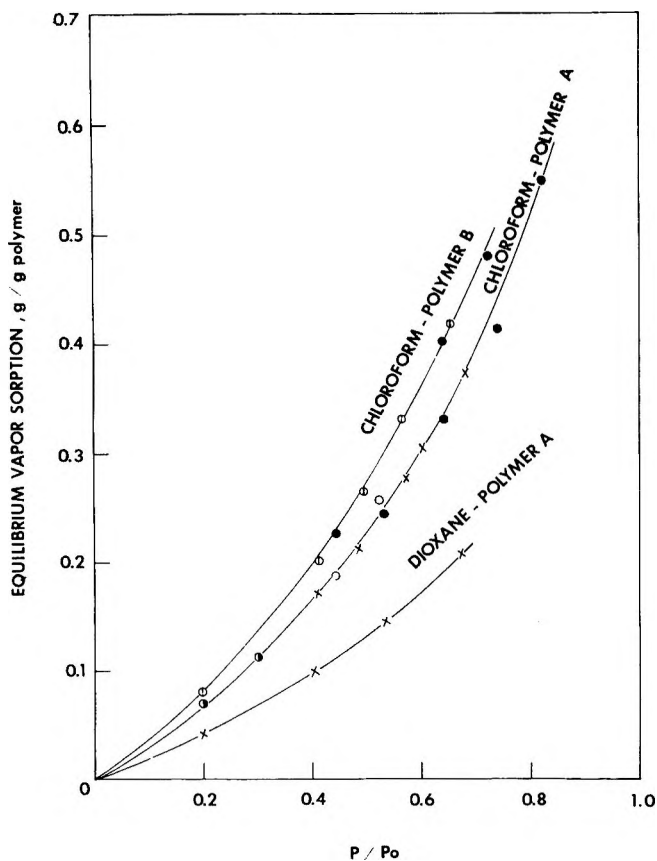
Fig. 1. Sorption isotherms for polymers A and B at various temperatures: (O) 30°C.; (●) 40°C.; (✕) 50°C.; (◍) 50.2°C.; (◑) 60°C.

Among the many solvents used, chloroform and dioxane were chosen for vapor sorption study because of the extensive swelling which resulted.

Vapor Sorption Experiments

The equilibrium vapor sorption by the cured film was measured by means of a quartz helix microbalance (100 mg. capacity, 1 mg./mm. sensitivity) described by Prager and Long.[5] The equilibrium pressure and the weight gain of the sample were recorded after no further change in the extension of the spring was observed overnight. The volume fractions were calculated from the experimentally determined weight fractions.

In the calculation of volume fractions of solvent and polymer, the densities of these two components at each temperature are used:

$$v \text{ (polymer)} = \frac{1}{1 + \dfrac{\rho(\text{polymer})}{\rho(\text{solvent})} \Delta w}$$
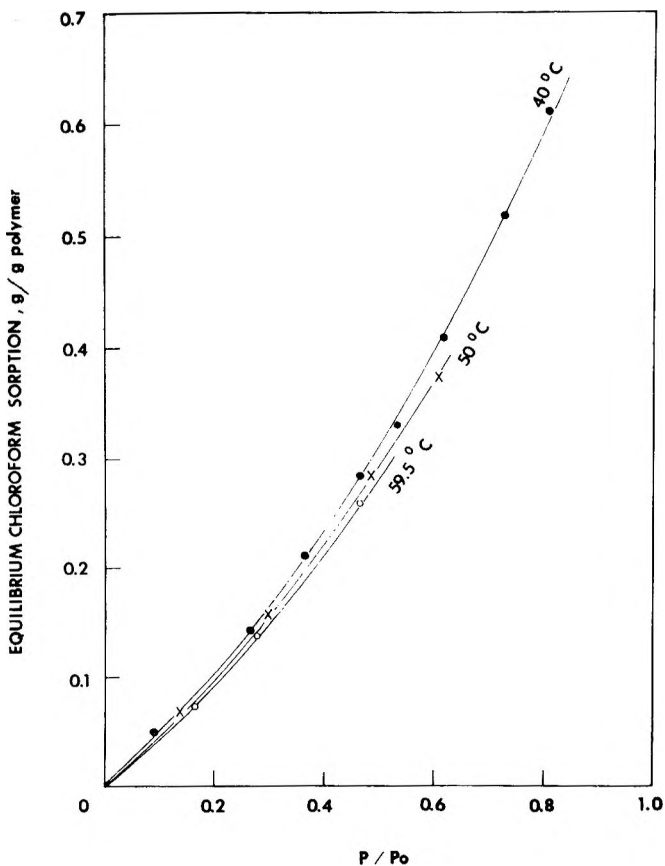
Fig. 2. Sorption isotherms for chloroform–polymer C.

where Δw is the amount of vapor sorbed in g./g. polymer. The density of the polymer was measured by dilatometry.

III. RESULTS

The rate of sorption of chloroform and dioxane vapor by the three polymer films is, in general, very slow at room temperature. A plot of Q/Q_e versus $t^{1/2}$ indicates that the diffusion of the vapors through these films is probably anomalous, in that Fick's Law is not obeyed. Moreover, hysteresis was observed in the equilibrium vapor sorption experiments, notably in the region of low vapor pressures. This is probably due to the fact that the dilatometric transition temperatures of these polymer occur at near 60°C., while some of the experiments were carried out at temperatures below 60°C. It is known, however, that the incorporation of a diluent or solvent into the polymer noticeably reduces the transition tem-
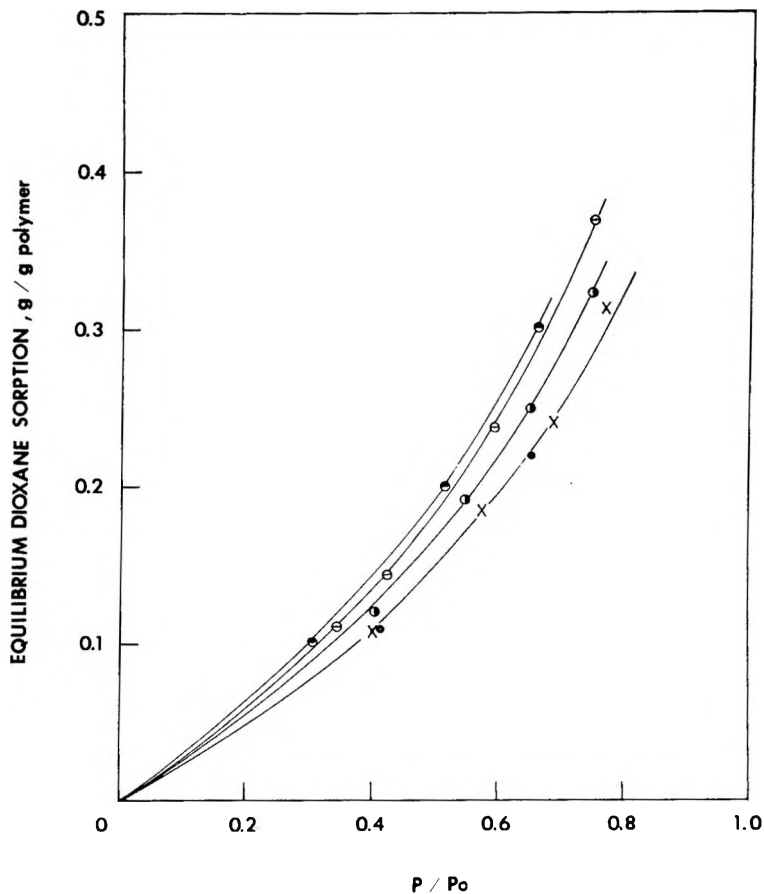
Fig. 3. Sorption isotherms for dioxane–polymer C at various temperatures: (+) 35°C.; (●) 40°C.; (×) 50°C.; (◑) 60°C.; (⊖) 70°C.; (◓) 75°C.

perature. Some theoretical predictions as to the effect of diluent on transition temperature are available in the literature.[6,7] We therefore attempt to eliminate the observed hysteresis by sorption at high vapor pressures followed by subsequent partial desorption to a point where the polymer–solvent mixture will have an estimated transition temperature below that of the experimental temperature. Subsequent sorption and desorption
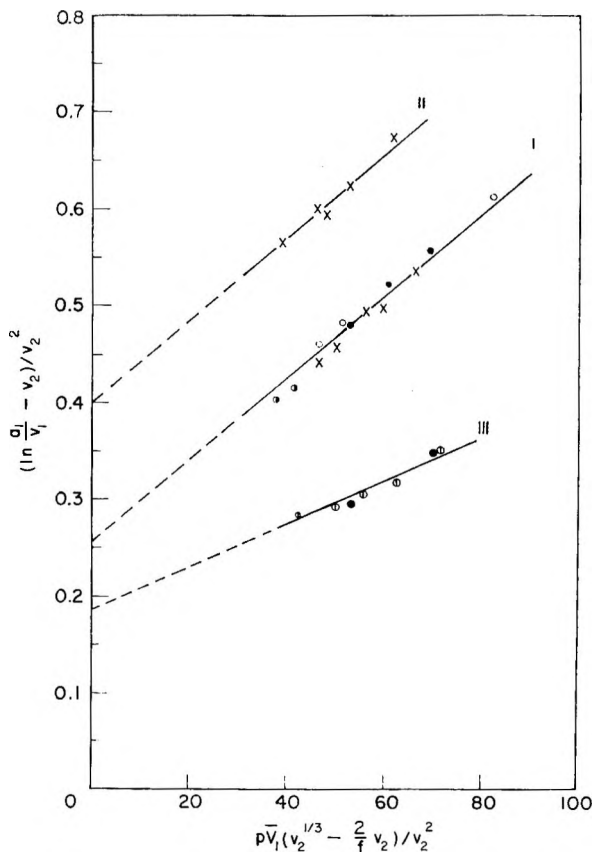

Fig. 4. Plot of vapor sorption data according to eq. (2) for the systems (I) chloroform–polymer A, (II) dioxane–polymer A, and (III) chloroform–polymer B at various temperatures: (O) 30°C.; (●) 40°C.; (X) 50°C.; (①) 50.2°C.; (◑) 60°C.

are found to be reversible. The results reported in this study were obtained after hysteresis were eliminated.

In the temperature range of 30–60°C., the amount of chloroform vapor sorbed by polymers A and B at equilibrium is independent of temperature at a given partial vapor pressure P/P_0 of chloroform (Fig. 1). Hence $\Delta \bar{H}_1$ is zero for these three systems. The temperature coefficient of chloroform sorption by polymer C (Versamid cure, 80% S.A.) is negative in the range 40–60°C. (Fig. 2). For dioxane–polymer C, however, the temperature

TABLE II

Molecular Weight between Crosslinks

Amine	Solvent	Temp., °C.	M_c	χ	$\Delta \bar{H}_1$ kcal./mole	$\dfrac{d\chi}{dT}$	ΔH_M, kcal./mole solvent	$\Delta \bar{S}_1$, e.u.
HMDA, 100% S.A.	Chloroform	30–60	240	0.26	0	0	0	—
HMDA, 100% S.A.	Dioxane	50	240	0.40	—	—	—	—
HMDA, 50% S.A.	Chloroform	40–50	455	0.18	0	0	0	—
Versamid, 75% S.A.	Chloroform	40	100	−0.28	—	—	—	—
		50	100	−0.22	−0.76 (at $v_2 = 0.9$)	4.3×10^{-3}	−0.80	~0
Versamid, 75% S.A.	Dioxane	59.5	100	−0.19	—	—	—	—
		35–50	110	0.15	0	0	0	—
		60	172	0.165	—	—	—	—
		70	205	0.13	1.15 (at $v_2 = 0.9$)	5.0×10^{-3}	1.09	6.2
		75	205	0.09	—	—	—	—

coefficient of equilibrium vapor sorption is essentially zero below 50°C. but is positive above 60°C. (Fig. 3).

Figures 4, 5, and 6 show experimental data plotted according to eq. (2) In the application of eq. (2), f is taken to be three for reasons to be discussed
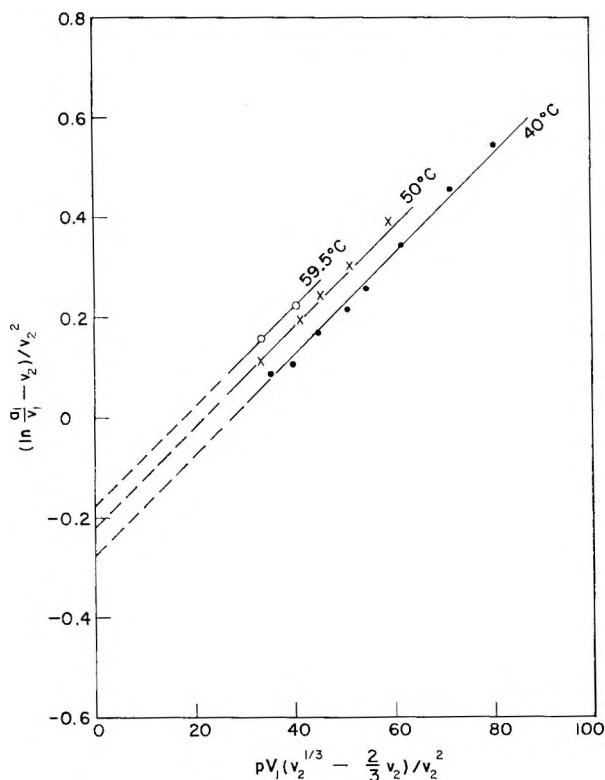

Fig. 5. Plot of vapor sorption data according to eq. (2) for the system chloroform–polymer C.

later. Linear plots are obtained in almost all cases, indicative of the constancy of χ within the concentration range studied. The values of χ, M_c, and various thermodynamic functions are listed in Table II. The agreement between ΔH_M and $\Delta \bar{H}_1$ is satisfactory.

IV. DISCUSSION

The molecular weight per crosslinked unit determined by the sorption method is now compared with calculated value based on structural considerations. A model of polymer A can be constructed, with the assumptions that (1) the predominant reactions in the formation of polymer A are the ones between the amine and the oxirane groups and these reactions are essentially complete under the experimental conditions, and (2) trifunctional nitrogen atoms are the crosslink junctions, i.e., $f = 3$. It can be seen
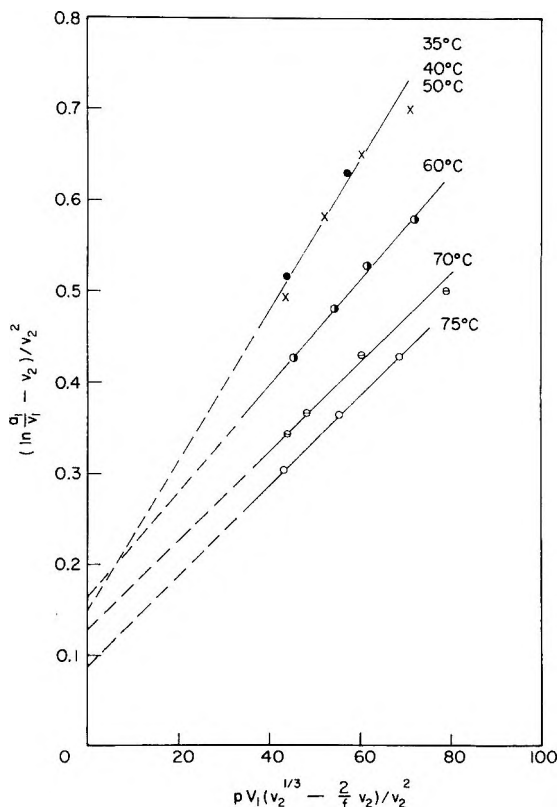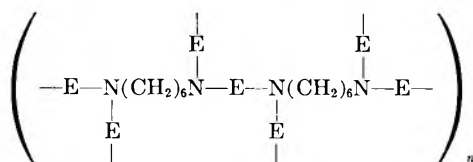
Fig. 6. Plot of vapor sorption data according to eq. (2) for the system dioxane–polymer C.

from the model that the section between crosslinks is either a 4,4′-bisglycidylphenyl-2,2′-propane unit or a 1,6-hexanediamine unit,
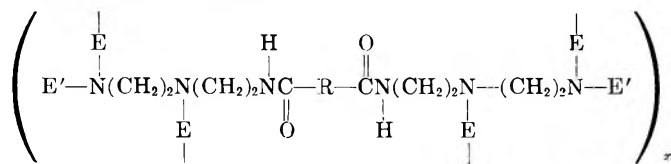
$$\left(\begin{array}{cc} \overset{|}{E} & \overset{|}{E} \\ -E-N(CH_2)_6N-E-N(CH_2)_6N-E- \\ \overset{|}{E} & \overset{|}{E} \\ | & | \end{array} \right)_n$$

where —E— is the 4,4′-bisglycidylphenyl-2,2′-propane unit with both oxirane rings reacted. The average molecular weight per crosslinked unit is $(2 \times 340 + 116)/3 = 265$, in good agreement with the experimentally determined value of 240. The data from dioxane sorption also yields the same M_c value.

Although only 50% stoichiometric amounts of 1,6-hexanediamine were used in the preparation of polymer B, 93% of the oxirane groups have reacted.[3] The etherification of oxirane groups[4] apparently plays, in this case, an important role in the network formation. A completed reacted structure will have an average M_c of approximately $(4 \times 350 + 116)/3 = 492$, in comparison with the experimental value of 455.
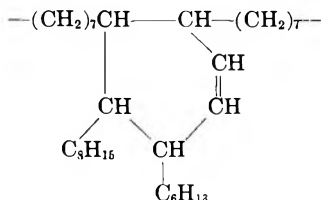
It is possible that the minor difference between the experimental and the theoretical M_c values may in part be ascribed to the fact that the dilation factor $\langle \alpha \rangle$ O is actually somewhat larger than unity, because the crosslinking reaction takes place initially in the presence of solvent. Very close correspondence of the experimental and theoretical M_c value can be achieved if $\langle \alpha \rangle_0^2$ is assigned a value of about 1.05. The correction for chain ends will have very little effect on the calculated values in the above systems.

In the sorption of chloroform by polymer C at 40–60°C., a rather small M_c of 100 was obtained from the plot shown in Figure 4.

About one-third of the 4,4'-bisglycidylphenyl-2,2'-propane molecules will remain as chain ends of the network C because approximately 15% of the oxirane groups are unreacted. A schematic diagram of the network structure can be drawn as follows:

$$\left(\begin{array}{c} \quad\quad\quad E \quad\quad\quad\quad H \quad\quad O \quad\quad\quad\quad\quad E \\ E'\!-\!N(CH_2)_2N(CH_2)_2NC\!-\!R\!-\!CN(CH_2)_2N\!-\!\!-\!(CH_2)_2N\!-\!\!-E' \\ \quad\quad\quad E \quad\quad\quad O \quad\quad H \quad\quad E \end{array} \right)_x$$

where R is

$$-(CH_2)_7CH\!-\!\!-\!\!-CH\!-\!(CH_2)_7\!-\!\!-$$
$$\quad\quad\quad\quad\quad\quad \searrow CH$$
$$\quad\quad\quad CH \quad\quad CH$$
$$\quad\quad C_8H_{16} \quad CH$$
$$\quad\quad\quad\quad\quad C_6H_{13}$$

and E′ is the 4,4'-bisglycidylphenyl-2,2'-propane unit with only one oxirane reacted.

If the chain ends and the pendant aliphatic groups of Versamid, being ineffective in exercising constraint against network swelling, are ignored as part of the network, the average value of M_c is $(2 \times 340 + 536)/5 = 243$.

The small M_c value derived from chloroform sorption seems to suggest that either secondary crosslinks, or physical entanglements of the chains, or both, are effective as constraints against network elongation.

The infrared spectra of Versamid 125, polymer C, and a 1% solution of Versamid 125 in chloroform exhibit characteristic absorption maxima at 3275 cm.$^{-1}$, corresponding to the -NH stretching frequency of *trans* hydrogen-bonded secondary amide.[8] It appears that there exists in polymer C interchain hydrogen bonds which very likely remain intact in the presence of chloroform. These interchain hydrogen bonds presumably may act as secondary constraints against chloroform swelling. If all the amide groups are engaged in interchain hydrogen bonding, the average molecular weight per crosslinked unit can be calculated to be approximately 135. Again, the difference between the theoretical and experimental M_c values may arise from the fact that $\langle \alpha \rangle_0^2$ is greater than unity. In fact, larger quan-

tities of solvent were used in the preparation of polymer C because of the high viscosity of the reaction mixture, and this conceivably could lead to a higher value of $\langle\alpha\rangle_n^2$. An assigned $\langle\alpha\rangle_0^2$ value of about 1.10 would have resulted in very close agreement of experimental and calculated M_c values.

The sorption of dioxane vapor by polymer C presents an interesting case. At temperatures of 35–50°C., $\Delta\bar{H}_1$ is zero and M_c is 110, while at temperatures of 60–75°C., $\Delta\bar{H}_1$ is about 1.1 kcal./mole and M_c increases from 172 to 205. Apparently, rather different mechanisms are involved in the sorption of dioxane at temperatures below and above 50°C. The M_c value of 110 is in reasonable agreement with the calculated value based on the assumption of complete interchain hydrogen bonding, while at higher temperatures the M_c values begin to approach that calculated on the basis for the absence of interchain hydrogen bonding. The ability of dioxane to disrupt amide hydrogen bonds can be verified from infrared data. At room temperature, a 5% and a 0.5% solution of Versamid 125 in dioxane show infrared absorption maxima at 3340 and 3480 cm.$^{-1}$, respectively, but neither solution exhibit absorption peak in the range 3270–3320 cm.$^{-1}$ These spectroscopic results demonstrate the capability of dioxane to disrupt amide hydrogen bonds in Versamid 125. In a lightly swollen network of polymer C, the amide hydrogen bonds apparently remain intact at low temperatures but are destroyed at high temperatures. It appears that in a highly crosslinked network sufficient perturbation of the segments is realized only at comparatively high temperatures such that, dioxane, present in relatively low concentrations, becomes effective in breaking interchain amide hydrogen bonds.

Smaller M_c values are obtained if the swelling equation by Hermans[9] is used to calculate our experimental data.

It is also of interest to notice that the main structural difference between the HMDA-cured polymer and the Versamid-cured polymer is the presence of amide groups in the latter network. It is suggested that the negative ΔN_M for the mixing of chloroform with latter polymer in contrast with $\Delta H = d\,0$ for the same solvent with the HMDA-cured polymer may arise from the specific interaction of the solvent molecules with the amide groups of the polymer. The nature of such polymer–solvent interaction may be similar to the orientation of chloroform by acetone as postulated by Münster.[10] This is also reflected in the smaller $\Delta\bar{S}_1$ in Table II.

In the derivation of the equation for rubber elasticity, the effective chains are assumed to obey a certain probability distribution.[1,11] In the above systems the effective chains are rather short and are not expected to conform to any reasonable probability distribution. Nevertheless, fair agreement between the theoretical and experimental M_c values can be attained. The theoretical implication of this finding is not clear and merits further consideration.

References

1. Flory, P. J., *Principles of Polymer Chemistry*, Cornell Univ. Press, Ithaca, N. Y., 1953, Chapts. XI, XII, and XIII; P. J. Flory, *J. Am. Chem. Soc.*, **78**, 5222 (1956).

2. Rogers, C. E., V. Stannett, and M. Szwarc, *J. Phys. Chem.*, **63**, 1406 (1959).

3. Anderson, H. C., *SPE J.*, **16**, 1241 (1960).

4. Lee, H., and K. Neville, *Epoxy Resins*, McGraw-Hill, New York, 1957, Chap. 2.

5. Prager, S., and F. A. Long, *J. Am. Chem. Soc.*, **73**, 407 (1951).

6. Nielson, L. E., R. E. Pollard, and E. McIntyre, *J. Polymer Sci.*, **6,** 661 (1950).

7. Kelley, F. N., and F. Bueche, *J. Polymer Sci.*, **50,** 549 (1961).

8. Bellamy, R. J., *The Infra-red Spectra of Complex Molecules*, Methuen, London, 1958, Chapter 12.

9. Hermans, J. J., *J. Polymer Sci.*, **59,** 191 (1962).

10. Munster, A., *J. Chem. Phys.*, **49,** 128 (1952); *Trans. Faraday Soc.*, **46,** 165 (1950).

11. Tobolsky, A. V., D. W. Carlson, and N. Indictor, *J. Polymer Sci.*, **54,** 175 (1961).

Résumé

On a étudié le gonflement de films d'époxy-polymère hautement ponté en presence de vapeurs organiques. Le poids moléculaire par unité pontée obtenu par application de l'équation d'élasticité du caoutchouc aux isothermes de la sorption correspond bien à la valeur évaluée par des considérations chimiques. On a présenté également des fonctions thermodynamiques du mélange polymère–solvant.

Zusammenfassung

Die Quellung hochvernetzter Epoxy-Polymerfolien durch organische Dämpfe wurde untersucht. Das durch Anwendung der Gleichung für die Kautschukelastizität auf die Sorptionsisothermen erhaltene Molekulargewicht pro Vernetzungsstelle stimmt gut mit dem auf chemischen Weg erhaltenen überein. Thermodynamische Funktionen für die Lösungsmittel–Polymerischung werden mitgeteilt.

Etude dela Polymérisation des Oléfines catalysee par les Oxydes métalliques.   I.   Méthodes expérimentales d'Etude cinétique; Résultats préliminaires sur la Polymérisation du Propylène par le Système catalytique Phillips

ALAIN GUYOT et JEAN-CLAUDE DANIEL, *Institut de Recherches sur la Catalyse, C.N.R. S., Lyon-Villeurbanne, France*

Synopsis

The kinetics of propylene polymerization catalyzed by chromium oxide on an aluminium silicate carrier was studied by a new method involving use of gas chromatographic analysis of samples removed from the monophase fluid medium surrounding solid catalyst and containing monomer and propane, without any other solvents.   The apparatus and experimental methods are described in detail.   The reaction is first-order with respect to monomer, and also to catalyst if its concentration is high enough.   Between 80 and 120°C, the activation energy is 16 kcal./mole.   The polymerization rate depends on pressure only with respect to monomer concentration, but, when the pressure is low and the temperature high enough, a second process occurs which causes formation of volatile oligomers and retardation of normal polymerization process.   The influence of catalyst and carrier structure and texture will be the subject of a subsequent study.

INTRODUCTION

Certains systèmes catalytiques à base d'oxydes de métaux de transition sont capables de provoquer la polymérisation d'oléfines et de dioléfines dans des conditions modérées de température et de pression.   Jusqu'à présent, seule la polymérisation de l'éthylène a eu des applications industrielles.   Les polymères d'oléfines plus lourdes n'ont pas conduit à des produits possédant une structure régulière, par exemple isotactique.   En conséquence, ces systèmes catalytiques ont été jugés relativement peu intéressants et n'ont pas fait l'objet d'un très grand nombre de travaux. Il n'a donc pas été possible de proposer un mécanisme réactionnel fondé sur des observations expérimentales certaines.

Parmi tous les systèmes catalytiques possibles, le plus simple est incontestablement celui de la société Phillips, qui est de l'oxyde de chrome déposé sur un gel de silice-alumine.   Ce catalyseur convenablement activé par l'air sec à 500°C environ, ou sous vide à plus basse température, permet de polymériser les oléfines, en présence ou non de solvant, à des températures allant de 70 à 300°C et sous des pressions de l'ordre de 40 atmosphères.[1,2]

Il a été particuliérement étudié par l'école russe de Topchiev[3-5] dont les travaux ont porté surtout sur l'activation du catalyseur. Selon ces auteurs, l'activation provoque tout d'abord la déshydratation du support, puis la réduction ménagée du chrome à un état de valence moyen peu inférieur à 6; et enfin, une réaction entre l'oxyde de Cr et le support qui conduirait à la formation d'un chromate d'aluminium. L'influence néfaste de l'eau sur l'activité catalytique a été mise en évidence par Boreskov et ses collaborateurs,[6] celle du degré d'oxydation du chrome a été confirmée par des études magnétochimiques de Mihail[7] et par des travaux utilisant la résonance électronique paramagnétique, dus à Cossee[8] et Pecherskaya.[9] Dans une étude récente sur la polymérisation du propylène, Topchiev[10] a montré qu'il y avait en fait, deux processus concurentiels de polymérisation: l'un, dû au gel mixte silice-alumine, conduit à la formation d'oléfines supérieures de bas poids moléculaire en C_6, C_9, C_{12}, ...; l'autre dû à l'ensemble du catalyseur, conduit aux hauts polymères. L'importance relative de ces deux processus dépend de la composition du système catalytique, le second étant favorisé par l'utilisation d'un cocatalyseur organoaluminique.

Il est remarquable de constater, dans toutes ces études, que l'activité n'est définie que par des estimations qualitatives, ou encore par la quantité de polymère solide produite par gramme de catalyseur au bout d'un temps fixe de l'ordre de quatre heures. Les difficultés technologiques dues aux hautes pressions régnant dans le réacteur ont empêché jusqu'à présent la réalisation de véritables études cinétiques. A notre connaissance, seul Friedlander[11] a publié quelques brefs résultats sur la vitesse de polymérisation de l'éthylène par un système catalytique à base d'oxyde de molybdène; il note, en fonction du temps, la quantité d'éthylène qu'il faut introduire dans le réacteur pour maintenir constante la pression du monomère. Friedlander observe une période d'induction de durée variable, puis ensuite une consommation de monomère proportionnelle au temps et à la concentration en catalyseur. En fonction de la température, il observe, vers 235°C un maximum de l'activité catalytique, qui est à rapprocher de celui qu'a rapporté Topchiev[10] à 105°C dans le cas de la polymérisation du propylène catalysée par l'oxyde de chrome.

L'application d'une méthode originale d'étude cinétique dont nous avons récemment publié le principe,[12] nous permet de présenter ici quelques résultats préliminaires relatifs à l'activité catalytique des catalyseurs Phillips dans la polymérisation du propylène. Notre but est de définir et mesurer expérimentalement la vitesse de polymérisation et de relier quantitativement les nombreux paramètres expérimentaux à cette vitesse. Outre les conditions expérimentales telles que température, pression, concentration et pureté des réactifs, de nombreux paramètres propres au catalyseur peuvent jouer un rôle: composition chimique, surface, distribution de pores, acidité du support, concentration en chrome, état d'oxydation du chrome, teneur en eau du catalyseur.

D'une préparation à une autre, la reproductibilité de ces paramètres est

difficile à obtenir, aussi avons nous été conduits à réaliser une série d'expériences avec de petites quantités d'un même catalyseur, c'est-à-dire qui ait été préparé par un seul cycle d'opérations d'imprégnation, séchage et activation.

METHODES EXPERIMENTALES

1. Matières Premières

Le monomère est un propylène commercial. Pour des raisons liées à notre méthode d'étude cinétique exposée plus loin, le diluant utilisé est le propane. L'analyse chromatographique de ces produits a donné les résultats suivants: Propylène CFR: propylène 92,7%; propane 6,2%; éthane 1,1; Propane ANTAR: propylène 18,4%; propane 80,4%; éthane 1,2.

Les produits contiennent en outre de l'éthylène à l'état de traces.

II. Catalyseur

Selon le procédé Phillips le catalyseur est préparé par imprégnation d'un gel de silice-alumine avec une solution d'acide chromique, séchage à l'air et activation dans un courant d'air à 550°C environ.

Le gel de silice-alumine est un catalyseur de cracking commercial (Ketjen). Il contient 12,9% d'alumine, 0,011% de Na_2O, 0,036% de fer et 0,60% d'ions sulfate. Sa surface est de 500 m²/g. Les pores ont un rayon moyen de 26Å et se répartissent suivant une distribution très étroite.

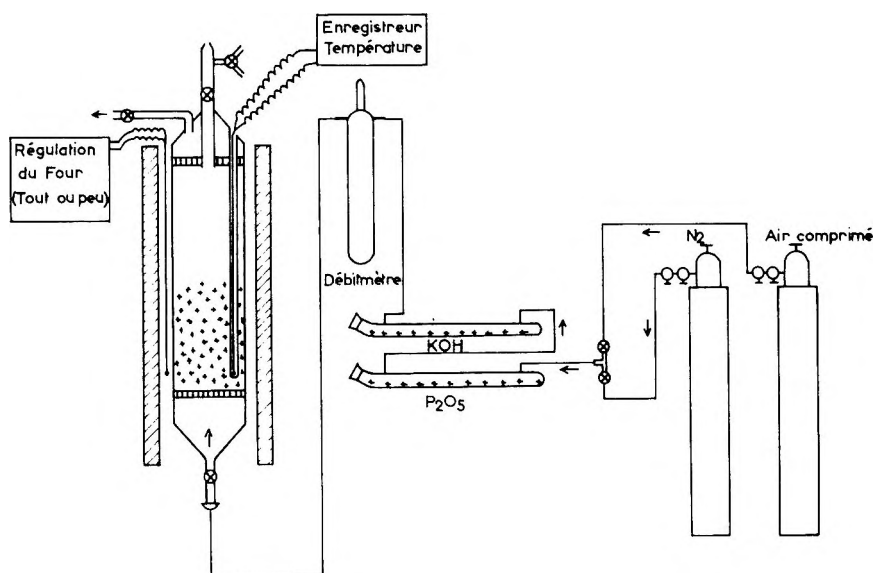Ce gel (200 g) est placé dans un ballon, muni d'un agitateur, dans lequel

Fig. 1. Schéma de l'appareillage d'activation du catalyseur.

on introduit 600 cm³ d'une solution d'acide chromique contenant 9,4 g de chrome. L'ensemble est porté à l'ébullition pendant deux heures. Le gel imprégné est ensuite essoré sur Buchner, séché pendant 24 heures dans une étuve à 110°C, et transféré dans la cellule d'activation. L'appareillage d'activation est schématisé dans la figure 1. Il comprend essentiellement une cellule en verre Pyrex, un four électrique régulé à ± 5°C à 500°C et un système de circulation de gaz (air ou azote).

La cellule est un cylindre comportant dans sa partie inférieure un disque de verre fritté (Pyrex numéro 0) supportant le catalyseur. Une gaine thermométrique permet le contrôle de la température. Le catalyseur est en fait maintenu en suspension fluide par le courant gazeux qui circule de
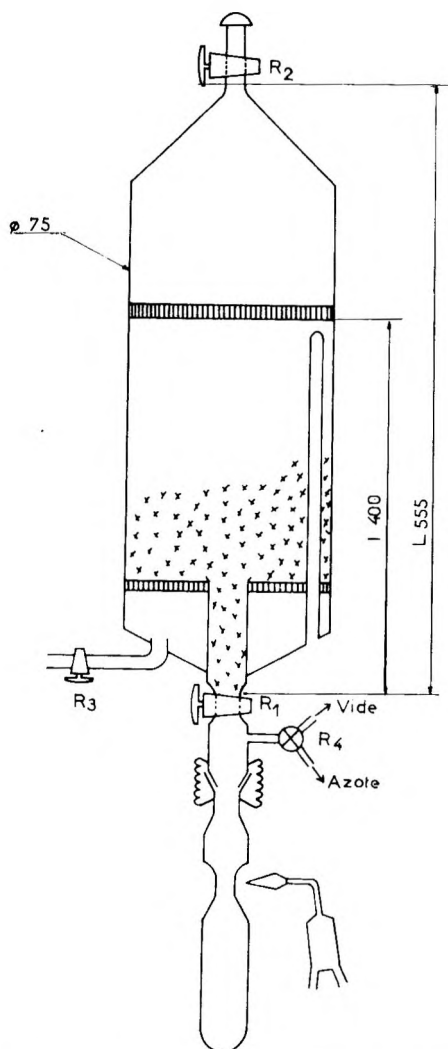
Fig. 2. Cellule d'activation et remplissage des ampoules.

bas en haut. Le débit de ce courant est contrôlé par un débit-mètre placé en amont. Pour éviter que les gaz n'entraînent une trop grande quantité de catalyseur hors de la cellule, celle-ci comporte dans sa partie supérieure un disque de verre fritté (Pyrex numéro 2). Ce disque est traversé d'une part par la gaine thermométrique, d'autre part par une tubulure, munie d'un robinet et qui permet l'introduction du catalyseur. Pendant l'activation, ce robinet R_1 est fermé et les gaz s'échappent par une tubulure latérale après avoir traversé le verre fritté. L'activation est effectuée en faisant circuler dans la cellule un courant d'air sec à 505°C pendant 4 heures, sous un débit de 20 litres/heure. Puis le catalyseur est refroidi au sein de la cellule sous un courant d'azote sec. La cellule est ensuite isolée par la fermeture des robinets d'entrée et de sortie des gaz, puis séparée de l'appareillage d'activation.

Il est absolument nécessaire de manipuler le catalyseur activé à l'abri de l'air ou plus exactement de l'humidité atmosphérique, car l'eau abaisse fortement l'activité catalytique de ce gel très hygroscopique. C'est pourquoi le catalyseur est transféré et stocké dans des ampoules scellées. La figure 2 représente l'appareillage de remplissage des ampoules. La cellule d'activation comporte à l'extrémité de la tubulure d'introduction un robinet latéral à trois voies R_4 et un rodage. L'ampoule est un tube Pyrex à parois minces, rétréci dans sa partie médiane et terminé par un rodage s'adaptant à celui de la cellule. Au moment du remplissage la cellule d'activation est retournée, l'ampoule assemblée est purgée grâce au robinet R_4. En ouvrant le robinet R_1 une certaine quantité de catalyseur (0,5 à 5 g) tombe dans l'ampoule par gravité. Après fermeture de R_1 le vide est réalisé par R_4 et l'ampoule est scellée. Environ trente ampoules sont ainsi remplies, et leur contenu déterminé par pesée. Elles sont stockées en vue d'essais de polymérisation et de dosage sur le catalyseur.

La teneur totale en chrome du catalyseur de couleur vert clair est déterminée selon la méthode de Selwood et Lyon[13], par fusion alcaline et manganimétrie: elle est de 2,52%. Par extraction au Soxhlet à l'eau bouillante, 40,3% de ce chrome sont dissous. Cette proportion de chrome hexavalent est assez faible, et en conséquence l'activité catalytique devrait être modérée.[4]

III. Méthode d'Etude cinétique

Selon le principe que nous avons récemment publié,[12] la méthode d'étude cinétique repose sur l'analyse par chromatographie gazeuse de prélèvements effectués dans la phase gazeuse surmontant le milieu réactionnel, à intervalles de temps convenables. L'autoclave contient, outre sa charge normale, un diluant inerte vis-à-vis de la réaction et dont la tension de vapeur est voisine de celle du monomère. Pour cette raison nous avons choisi le propane. Le prélèvement contiendra surtout propane et propylène et le chromatogramme enregistré présentera donc deux pics essentiels. La composition du prélèvement sera donnée par le rapport des surfaces sous les pics, ou, en première approximation, par le rapport de leur hauteur.
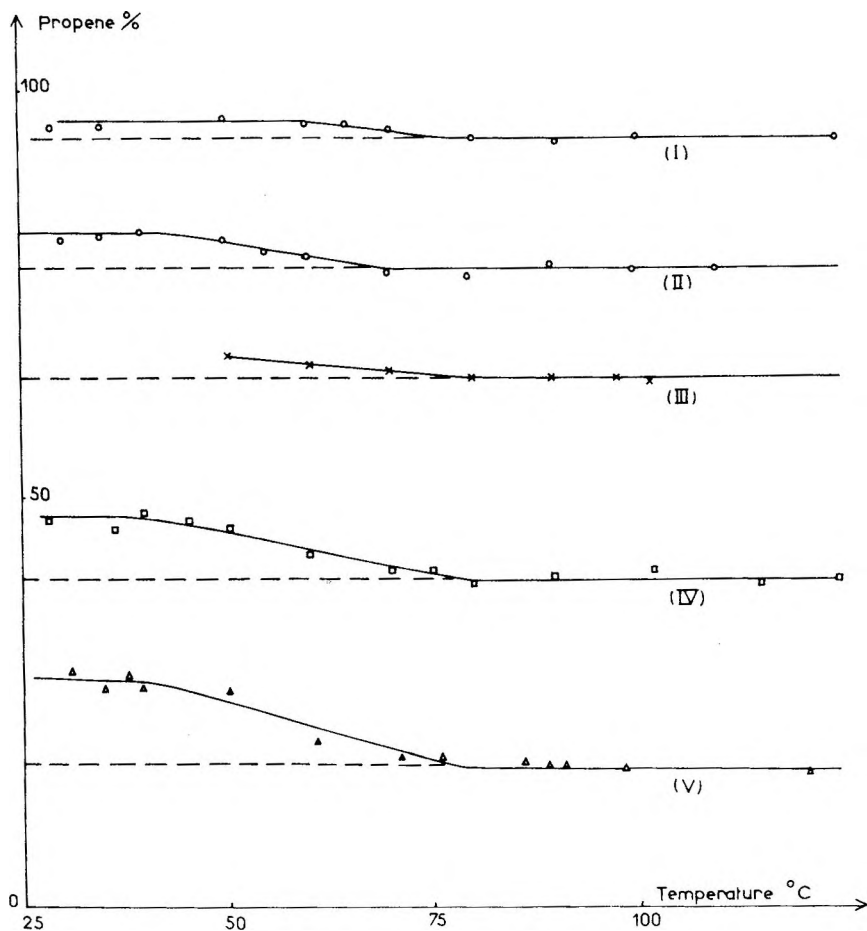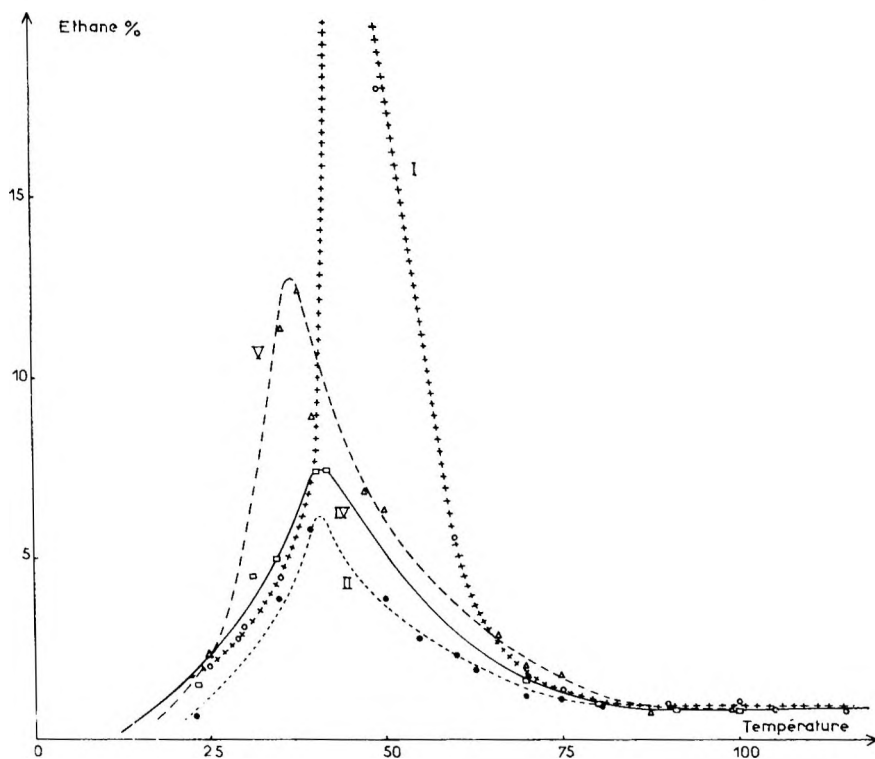
Fig. 3. Teneur en propylène de la phase gazeuse en fonction de la température pour diverses compositions de la charge (tableau I).

Si l'on appelle R_0 et R_t les rapports de ces hauteurs de pic (propylène/propane) à l'instant initial et à l'instant t, le taux de conversion ρ est donné par la relation:

$$\rho\% = 100(1 - R_t/R_0) \tag{1}$$

Cette relation suppose simplement que la composition de la phase vapeur prélevée est, à chaque instant, proportionnelle à la composition globale du milieu réactionnel.

Dans une série d'essais préliminaires, nous avons étudié la composition de la phase gazeuse prélevée dans un autoclave, en fonction de la charge de cet autoclave et de la température. Les résultats sont illustrés par les figures 3 et 4. Dans la figure 3 on a tracé en traits pleins les courbes donnant la proportion de propylène présent dans la phase gazeuse; les proportions de propylène introduites dans l'autoclave sont données par les courbes en

TABLEAU I

Composition de la Charge de l'Autoclave dans les Essais préliminaires de Chroma-
tographie

Numéro de l'essai	Ethane, %	Propane, %	Propylène, %
I	1	6,5	92,5
II	0,8	22	77
III	0,8	36	63
IV	0,8	61,5	37,8
V	0,9	83	16

traits discontinus. Les charges de l'autoclave, dans les cinq séries ef-
fectuées, sont reportées dans le tableau I. Dans un très grand intervalle
de composition de la charge, on peut constater, au-dessus de 80°C l'identité
de ces proportions. En fait, les chromatogrammes comportent un troi-
sième pic correspondant à la faible quantité d'éthane présente dans les
produits. Dans la figure 4, la teneur en éthane des prélèvements gazeux
est aussi étudiée en fonction de la température et de la charge. Les
courbes obtenues présentent un maximum situé entre 25 et 50°C et se
rejoignent au-dessus de 80°C à une ordonnée correspondant à la proportion

Fig. 4. Teneur en éthane de la phase gazeuse en fonction de la température pour diverses
compositions de la charge (tableau I).

réelle de l'éthane introduite. Ceci confirme les résultats décrits dans la figure 3. Les températures critiques du propylène et du propane sont respectivement de 92,3 et 95,6°C, tandis que celle de l'éthane est de 32,1°C. Il semble que la présence d'une proportion d'éthane de l'ordre de 1% abaisse la température critique d'un mélange propane–propylène aux environs de 80°C. Au-dessus de cette température on prélève effectivement une partie du mélange fluide réactionnel et la composition déterminée par chromatographie est celle du fluide environnant le catalyseur solide.

L'intervalle de température où la relation (1) est directement applicable pourrait être étendu en introduisant une proportion plus importante d'éthane.

L'application de la relation (1) suppose en outre la détermination du rapport R_0 de composition initiale, à la température de l'expérience; ceci implique que le catalyseur et le mélange fluide ne doivent entrer en contact que lorsque la température de l'expérience est effectivement établie; cette dernière condition est d'ailleurs nécessaire pour pouvoir mener à bien une étude cinétique.

Ces considérations nous ont amené à élaborer l'appareillage que nous décrivons di-dessous.

IV. Appareillage de Polymérisation

La polymérisation est conduite dans un autoclave à brides en acier inoxydable, de 250 cm³ environ (Fig. 5). Il est équipé d'une gaine thermométrique et de deux vannes. L'une d'elles permet la communication avec un récipient de capacité équivalente, lui-même équipé de deux vannes. Le remplissage du récipient est effectué en premier lieu: le propylène est introduit par piégeage à froid et pesé. Un volume connu de propane liquide est ensuite introduit sous pression, à l'aide d'une burette en verre. Une nouvelle pesée permet de contrôler la composition du mélange. Le récipient est alors adapté à l'autoclave dans lequel a été placée l'ampoule de verre mince contenant le catalyseur; celui-ci est purgé à l'aide de la seconde vanne par l'application successive du vide et de l'azote purifiée (teneur en oxygène et en eau inférieure à 10 ppm). Puis sur les vannes V_0 et V_1 sont adaptés des raccords métalliques munis de rodages sphériques qui permettront les prélèvements. L'ensemble de ces appareillages est alors monté sur le plateau mobile d'une étuve thermostatisée à ± 1°C jusqu'à ce que la température désirée règne à l'intérieur de l'autoclave. Les vannes reliant autoclave et récipient sont alors ouvertes et refermées au bout de quelques instants, dès que les pressions sont équilibrées. La brusque augmentation de pression écrase l'ampoule de catalyseur et la réaction commence. L'agitation de l'autoclave est mise en route, au moyen du plateau mobile.

Les prélèvements sont effectués d'une part par V_0 sur le récipient pour déterminer R_0, et d'autre part par V_1 sur l'autoclave pour déterminer les diverses valeurs de R_t. On utilise des cellules en verre[14] dont la capacité
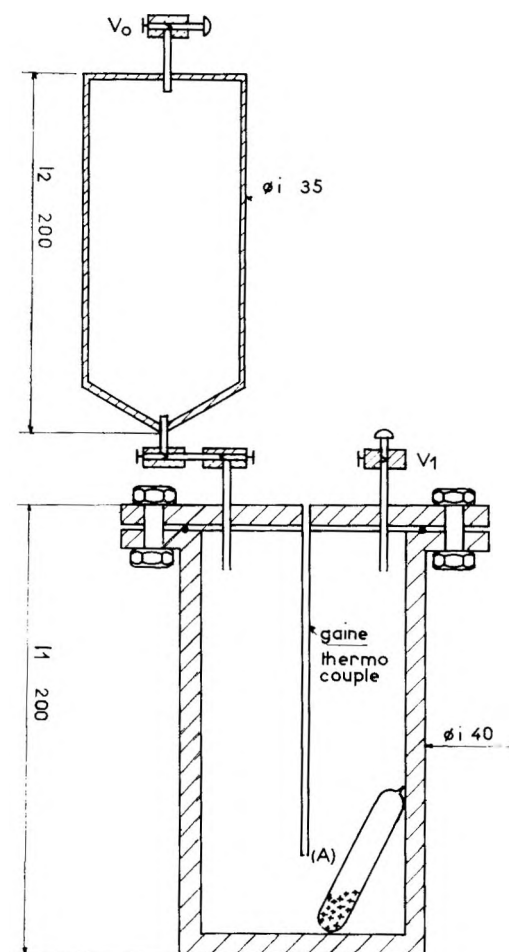
Fig. 5. Appareillage de polymérisation.

utile est de l'ordre de 0,5 cm³.   Elles comportent deux raccords à rodages sphériques femelles dont l'un est adaptable à celui des vannes V_1 ou V_0 et l'autre permet la relation avec un comptebulle, pour limiter le volume prélevé au minimum indispensable.   Ces cellules sont ensuite placées dans le circuit d'un chromatographe[15] illustré schématiquement dans la figure 6. Ce dernier comporte une cellule détectrice à thermistances et une colonne de 4 mm de diamètre et 30 cm de longueur remplie de gel de silice Secagel. Le débit de gaz vecteur (hydrogène) est de 2 litres/heure.   Ainsi le chromatogramme est obtenu en 10 minutes environ.

La polymérisation peut être arrêtée à volonté, par évacuation des produits volatils.   Il est possible de contrôler le rendement final par pesée: le récipient est démonté et pesé séparément, ce qui permet de connaître la quantité de fluide mis en réaction dans l'autoclave; ce dernier, après évacuation des gaz est lui-même pesé.
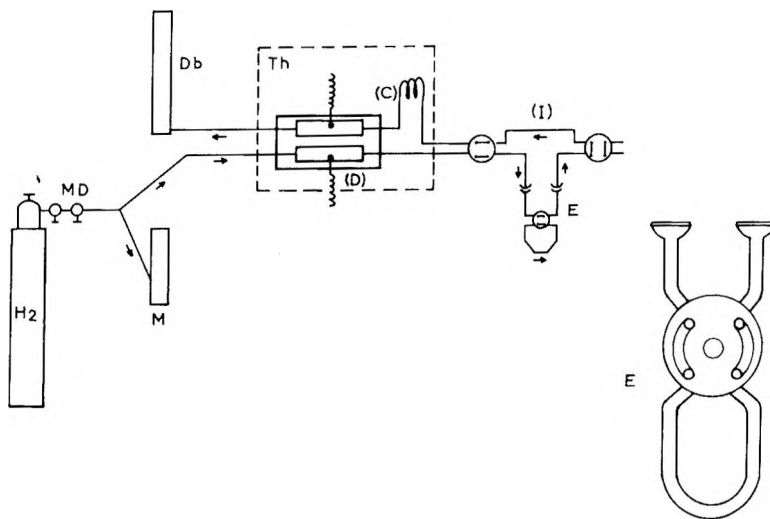
Fig. 6. Appareillage de chromatographie; (MD) manomètre à double détente; (M) manomètre à mercure; (C) colonne; (D) détecteur à thermistances; (Db) débit-mètre; (Th) thermostat à air; (I) circuit d'injection; (E) cellule de prélèvement.

Dans notre étude nous n'avons pas cherché à caractériser les polymères obtenus; ceux-ci sont généralement solides mais contiennent toujours une proportion non négligeable de polymères huileux atactiques.

RESULTATS ET DISCUSSION

Au cours de cette étude préliminaire, nous nous sommes bornés à mesurer la vitesse de polymérisation et à chercher les relations liant cette vitesse aux différents facteurs expérimentaux: concentrations en réactifs, température, pression initiale.

Dans une première série d'expériences, nous avons fait varier la quantité de catalyseur, tout en maintenant fixes la température (100°C) et la charge du récipient en réactifs gazeux (propane 15 g, propylène 22 g) A l'instant initial, l'autoclave contient alors 7,5 g de propane et 11,5 g de propylène: la pression correspondante est d'environ 40 kg/cm². La figure 7 donne le réseau des courbes cinétiques obtenues. Il apparaît qu'il n'existe pas de période d'induction et que la réaction se poursuit régulièrement jusqu'à conversion totale du monomère. Nous avons cherché à déterminer l'ordre de la réaction par rapport au monomère. Pour cela, l'on porte le logarithme de la vitesse instantanée de polymérisation en fonction du logarithme de la concentration en monomère. La vitesse instantanée $-dM/dt$ est liée au taux de conversion par la relation:

$$-dM/dt = (M_0/100)d\rho/dt$$

En coordonnées logarithmiques, nous avons trouvé dans tous les cas une relation linéaire dont la pente est très voisine de l'unité. En portant
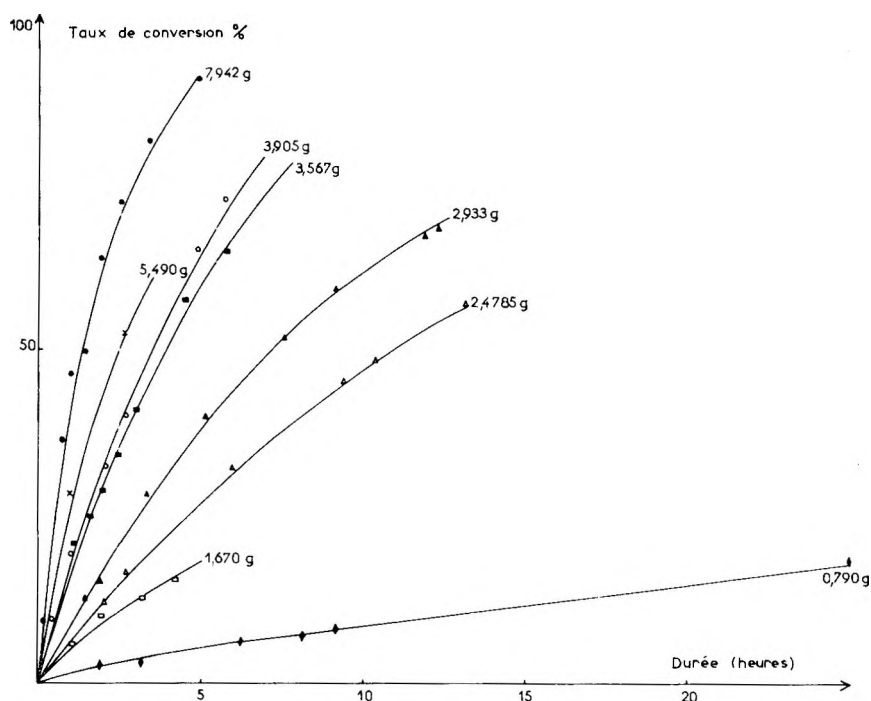
Fig. 7. Taux de conversion (%) en fonction du temps, pour divers poids de catalyseur.

log (M_0/M) en fonction du temps, on obtient, comme le montre la figure 8 un réseau de droites passant par l'origine, ce qui établit que la réaction admet l'ordre 1 par rapport au monomère. Nous avons donc:

$$-dM/dt = k_1 (M) \qquad (2)$$

Chaque expérience de polymérisation peut être caractérisée par la pente k_1 des droites de la figure 8, pente dont la valeur a la signification d'une constante de vitesse.

Dans la suite, nous avons cherché quels sont les facteurs déterminant la valeur de k_1.

Les expériences précédentes permettent de déterminer la relation entre k_1 et la concentration en catalyseur. Dans un diagramme où l'on a porté en ordonnée la valeur de k_1 et en abscisse le poids de catalyseur utilisé, les points expérimentaux se placent sur la courbe décrite dans la figure 9. Cette courbe présente une partie linéaire pour les grandes quantités de catalyseur. Lorsque le rapport pondéral catalyseur/monomère est inférieur à 0,25 les points se placent sur un arc rejoignant l'origine des coordonnées. Il serait évidemment utile de savoir pourquoi la courbe ne présente pas une allure uniforme dans tout le domaine de concentration. Il parait vraisemblable d'admettre que les impuretés inhibitrices présentes dans la charge fluide sont responsables de cet état de chose. Les impuretés entrent en compétition avec le monomère dans l'occupation des sites
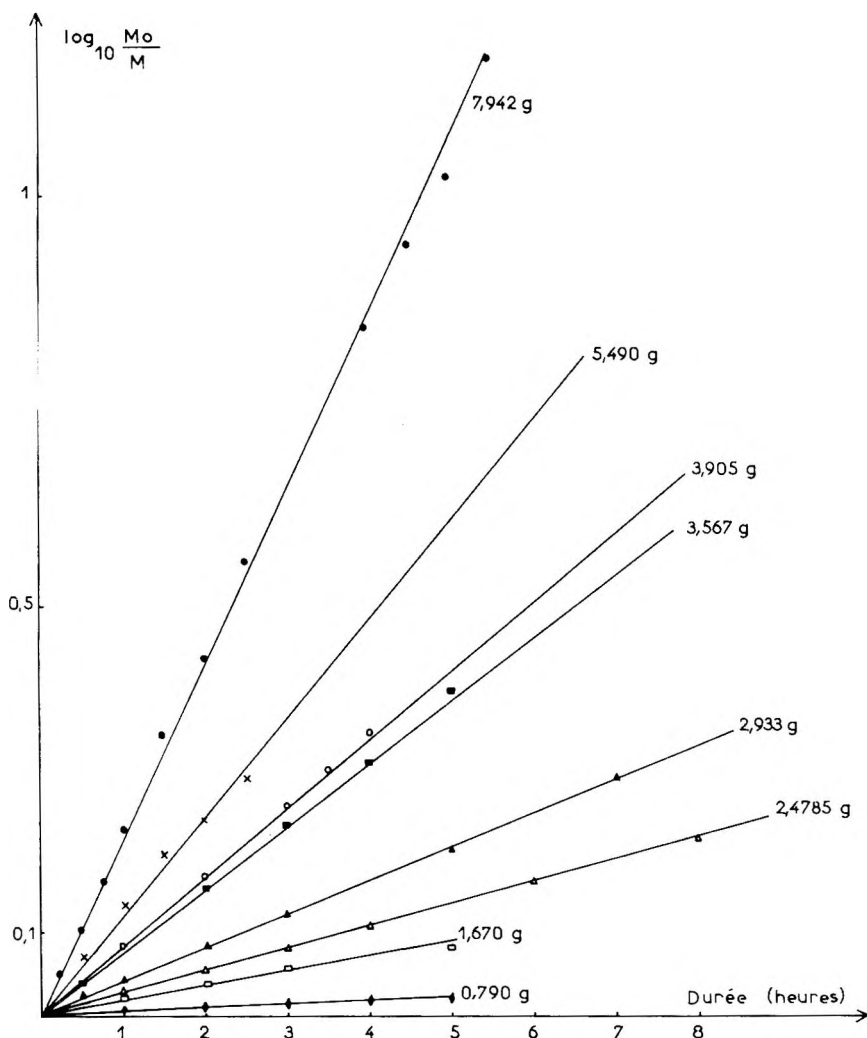
Fig. 8. Transformées linéaires (ordre 1) des courbes cinétiques de la figure 7.

actifs du catalyseur. Leur concentration est fixe dans cette série d'expéri-
ences et elles ne peuvent occuper qu'un nombre restreint de sites. Dès que
la concentration en catalyseur est suffisante on obtient une loi linéaire
(droite D). En l'absence d'impuretés la véritable loi pourrait être repré-
sentée par la droite D' parallèle à D mais passant par l'origine.

Nous retiendrons simplement que, à température et pression initiale
constantes, la cinétique de la réaction peut être représentée par la relation

$$-dM/dt = k_2(C - C_0)(M) \tag{3}$$

lorsque le poids de catalyseur C est supérieur à une valeur critique C'
(fig. 9) Dans une seconde série d'expériences nous avons étudié l'influence de
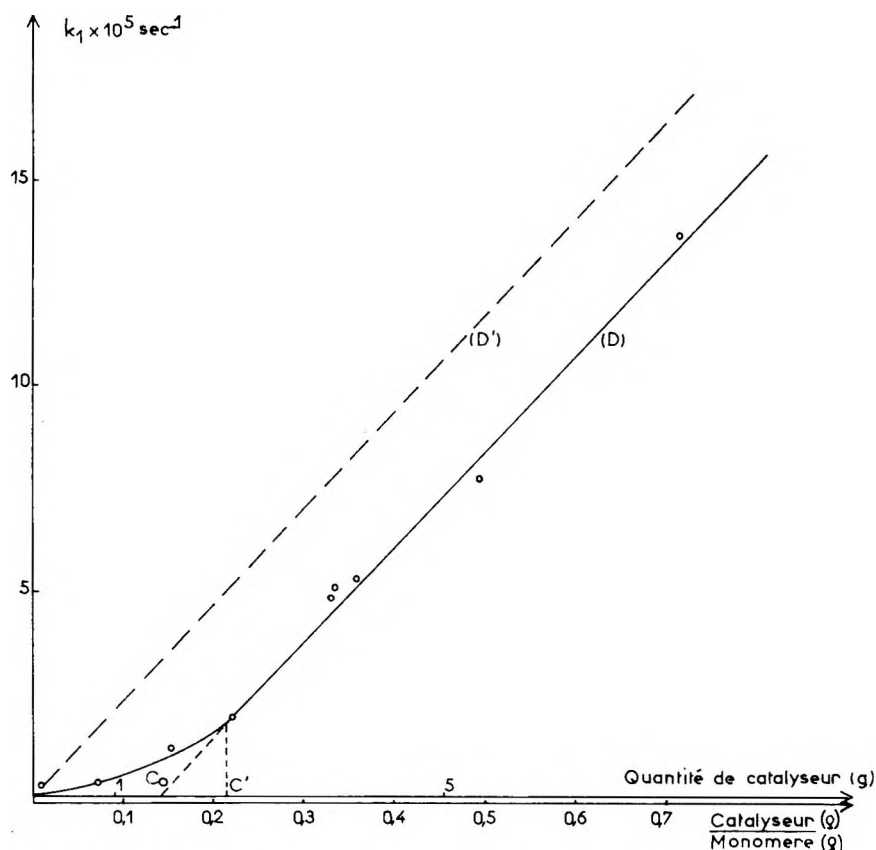la température sur la cinétique de polymérisation; la charge de l'autoclave

Fig. 9. Constante de vitesse k_1 en fonction du poids de catalyseur, et du rapport pondéral: catalyseur/monomère.

en monomère, propane et catalyseur était maintenue constante: les poids de réactifs étant respectivement de 11,5–7,5 et 3,6 ± 0,2 g. Les courbes cinétiques obtenues sont représentées sur la figure 10, tandis que les transformées linéaires (ordre 1) sont tracées sur la figure 11. Ces dernières sont valables dans tout l'intervalle de conversion étudié lorsque la température est inférieure à 100°C; mais si la température est supérieure, les points expérimentaux s'écartent de la droite initiale au bout d'un temps de réaction variable. Ces résultatss ont à rapprocher de ceux obtenus antérieurement par Topchiev[10] qui a observé que le rendement en polymère solide, après 4 heures de polymérisation, passait par un maximum vers 105°C. Ce même auteur signale aussi que le processus de formation d'un polymère solide s'accompagne d'un second processus, dû au support, et qui conduit à des oligomères. Notre méthode cinétique nous permet de suivre la disparition du propylène sans préciser en quelles sortes de produits ce momomère se transforme. Toutefois, rappelons que nous arrêtons les réactions en laissant évacuer par distillation les réactifs volatils. S'il se forme
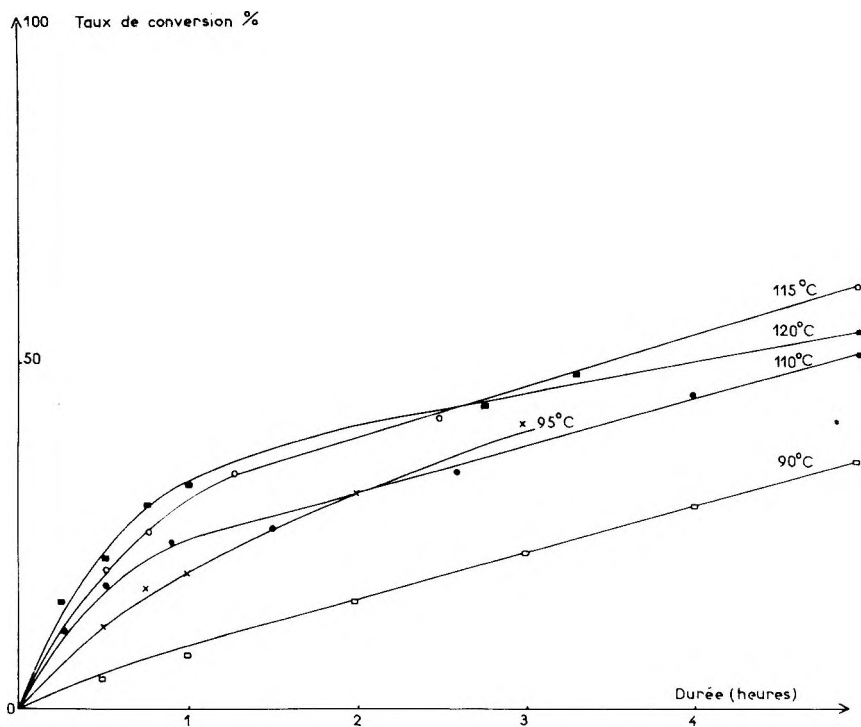
Fig. 10. Taux de conversion (%) en fonction du temps, pour diverses températures.

des oligomères volatils dans ces conditions, ils sont donc éliminés et ce phéno-
mène peut être mis qualitativement en évidence si l'on compare les rende-
ments finaux déterminés par chromatographie et par pesée.   Les résultats
consignés dans le tableau II montrent bien qu'il se forme des quantités
appréciables de produits volatils dès que la tempétature dépasse 100°C
puisqu'alors le rendement gravimétrique est nettement inférieur à celui
déterminé par chromatographie.   Ce processus d'oligomérisation, dont
l'influence est relativement faible lorsque la température est inférieure ou
égale à 100°C., n'est pas indépendant du processus normal de polyméri-

TABLEAU II

Rendements finaux déterminées par Chromatographie et par Gravimétrie, en Fonction
de la Température de l'Expérience

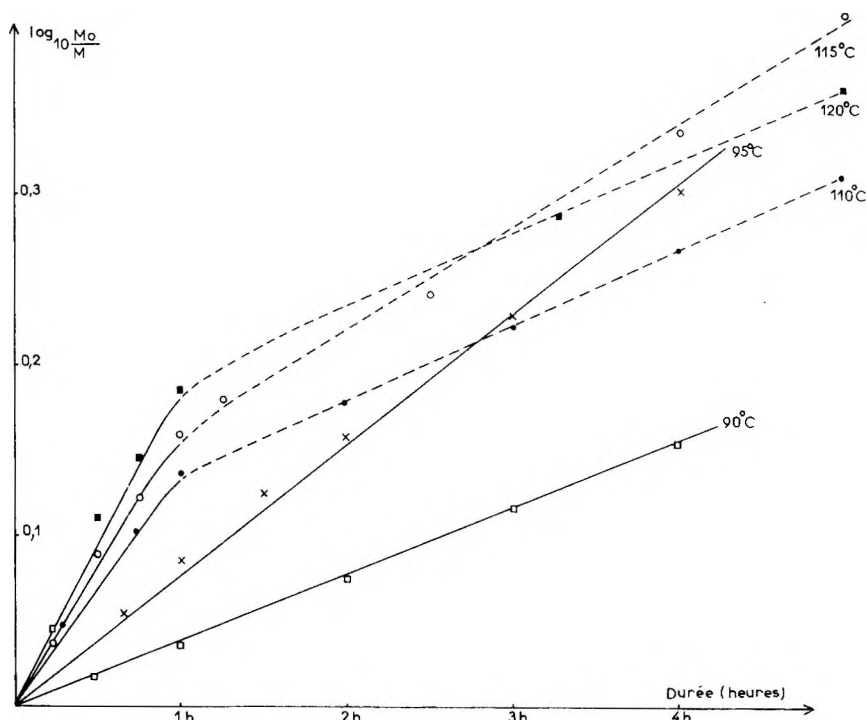| Température, °C	Catalyseur, g	Rendement, %	
		Chromatographie	Pesée
80	3,76	60	62,5
95	4,21	70	74,5
100	3,90	90	87,5
110	3,48	60	42,5
115	3,59	65	55
120	3,58	60	41

Fig. 11. Transformées linéaires (ordre 1) des courbes cinétiques de la figure 10.

sation; en effet, lorsqu'il se manifeste, la vitesse de consommation du monomère est inférieure à sa valeur normale comme le montrent les courbes de la figure 10. En première hypothèse nous pensons que les oligomères peuvent s'insérer dans les chaînes de polymère en croissance et provoquer l'arrêt de la polymérisation en bloquant le centre actif de la croissance. Nous pensons aussi qu'un tel processus pourrait expliquer les résultats cinétiques de Friedlander[11] qui observe un maximum en fonction de la température, dans la vitesse de polymérisation de l'éthylène au moyen d'un catalyseur à base d'oxyde de molybdène. Cet auteur trouvait une énergie d'activation positive de 18 kcal/mole pour une température inférieure à 235°C et une énergie d'activation négative (-14 kcal) ensuite. Il attribuait ces différences au fait qu'à basse température, l'énergie d'activation de l'initiation contrôle la réaction tandis que, à plus haute température, l'énergie libre d'adsorption devient prédominante.

La portion initiale de nos courbes cinétiques, et leurs transformées linéaires permettent de déterminer la relation entre la constante k_1 et la température. La loi d'Arrhenius illustrée par la figure 12 donne une énergie d'activation de 16 kcal. Cette valeur est tout à fait normale, pour une polymérisation. Le point expérimental représentant l'expérience conduite à 80°C s'écarte nettement de la droite. Nous croyons que ceci est simplement dû au fait que cette température représente la limite de validité de notre méthode cinétique; toutefois l'accord assez bon entre les
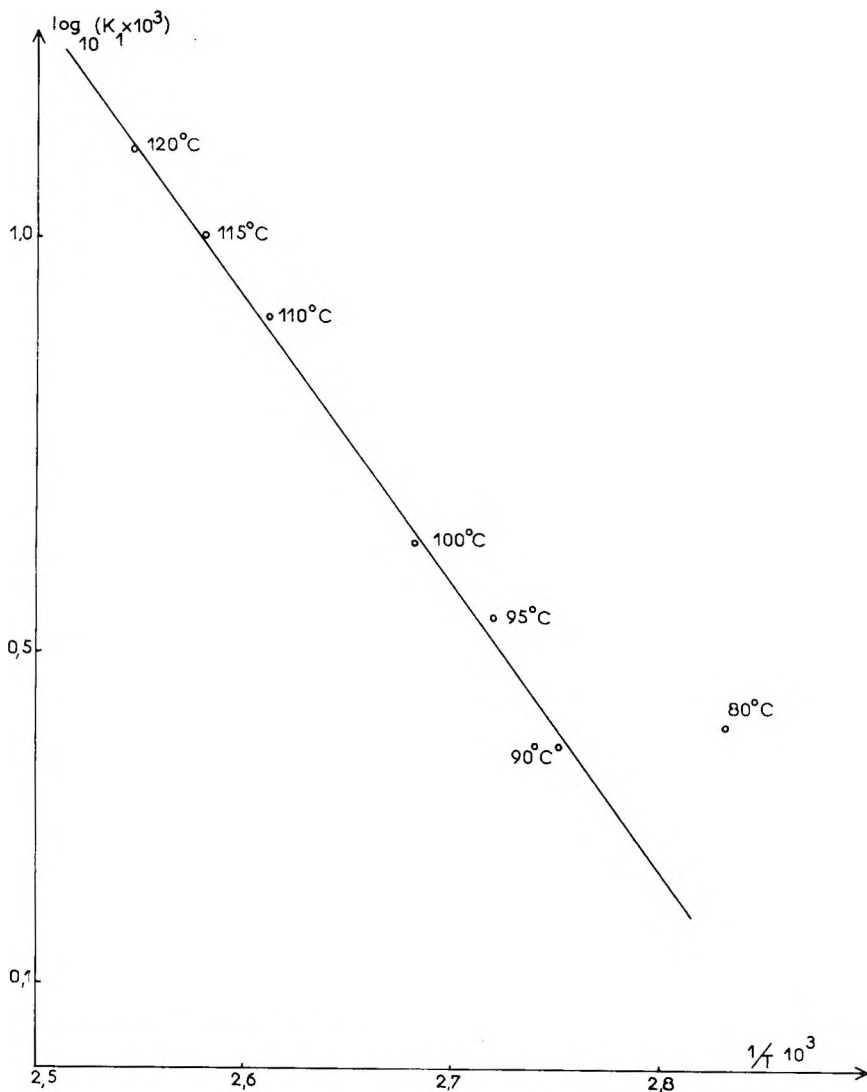
Fig. 12. Diagramme d'Arrhenius (log k_1 en fonction de $1/T°K$).

rendements finaux déterminés par chromatographie et par pesée (tableau II) nous incline à penser qu'il doit exister deux phases fluides à l'intérieur de l'autoclave ce qui favorise la diffusion du monomère vers les centres actifs et augmente la vitesse de polymérisation.

Dans une dernière série d'expériences enfin, nous avons fait varier la pression initiale (non mesurée) en modifiant la charge totale de l'autoclave, sans changer la composition de cette charge. La température a été maintenue fixe à 100°C ainsi que la quantité de catalyseur à 2,7 ± 0,2 g. Les résultats sont illustrés par les courbes cinétiques de la figure 13, ou consignés dans le tableau III.
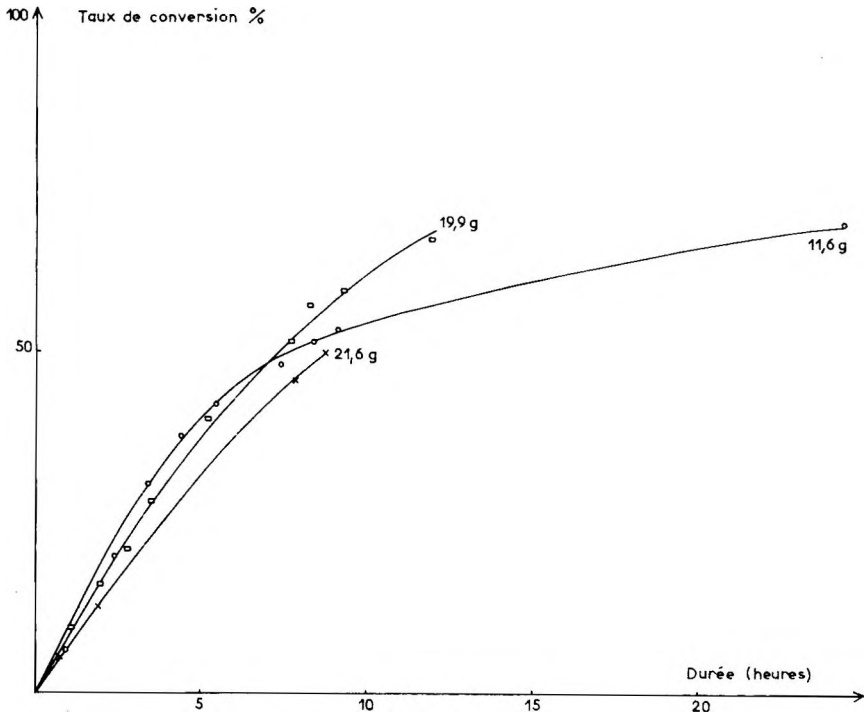
Fig. 13. Taux de conversion (%) en fonction du temps pour diverses valeurs de la charge fluide totale de l'autoclave.

Là encore, le phénomène d'oligomérisation se manifeste nettement lors de la première expérience. Ce processus est donc favorisé non seulement par une élévation de la température mais aussi par un abaissement de la pression.

Les valeurs de la constante k_1 obtenues en utilisant les transformées linéaires de courbes de la figure 13 sont indépendantes de la pression initiale: la vitesse de polymérisation ne dépend de la pression que par l'intermédiaire de la concentration en monomère. Seul le processus d'oligomérisation est susceptible de modifier cette loi. Les écarts entre les valeurs figurant dans la dernière colonne du tableau III sont dus en fait aux différences entre les quantités de catalyseur utilisées, et les points expéri-

TABLEAU III

Influence de la Pression initiale sur les Rendements finaux et Constante de Vitesse (Ordre 1)

Charge totale, g	Catalyseur, g	Rendement final, %		$k_1 \times 10^5$, sec^{-1}
		Chromatographie	Pesée	
11,6	2,83	67,5	46	2,84
19,9	2,93	65,5	65	2,64
21,6	2,61	50	51	2,10

mentaux correspondant à ces expériences se placent normalement sur la courbe de la figure 9 donnant k_1 en fonction de la quantité de catalyseur C.

CONCLUSIONS

La mise au point de notre méthode cinétique nous a permis d'étudier la polymérisation du propylène au moyen d'un catalyseur du type Phillips, sans solvant, en présence de propane comme diluant et dans des conditions où il n'existe qu'une seule phase fluide au sein du réacteur. La réaction admet alors l'ordre 1 par rapport au monomère, ainsi que par rapport au catalyseur lorsque la concentration de ce dernier est suffisante. Dans un domaine de température allant de 80 à 120°C, la réaction possède une énergie d'activation globale de 16 kcal/mole. La vitesse de polymérisation, indépendante de la pression peut être représentée par la relation

$$-dM/dt = A \exp \left\{ -E/RT \right\} (C - C_0)M \tag{4}$$

où $E = 16$ kcal/mole, R est la constante des gaz parfaits, C la concentration en catalyseur, C_0 une concentration en catalyseur limite qui pourrait dépendre de la concentration d'impuretés introduites dans les réactifs, ainsi que de la nature du catalyseur; M enfin est la concentration en monomère. Lorsque la pression baisse jusqu'à une valeur suffisante, valeur qui dépend de la température, un second processus se manifeste; il conduit à la formation d'oligomères volatils, et retarde le processus normal de polymérisation.

Il convient de remarquer que ces résultats ont été obtenus en utilisant divers échantillons d'un même catalyseur et il est probable que les paramètres A, E et C_0 de la relation (4) dépendent d'un certain nombre de facteurs structuraux relatifs à l'oxyde de chrome ainsi qu'au gel de silice-alumine utilisé comme support. D'autres expériences sont en cours à l'heure actuelle dans notre laboratoire, pour préciser ces points et pour mieux connaître le processus d'oligomérisation. Nos résultats sont en accord avec les deux types de mécanisme déjà proposés par Natta[16] et Friedlander[11] et qui impliquent respectivement des catalyses anionique-coordinée et par ion-radical. Pour pouvoir distinguer entre ces mécanismes, ou éventuellement en proposer un troisième, il est indispensable de poursuivre simultanément des études sur la structure et la texture du catalyseur, la cinétique de polymérisation et la structure des polymères formés.

Références

1. Phillips Petroleum Co., Brevet Belge 530.617 (1954); U. S. Pat. 2,825,721 (1958); Brevet Français 1.135.292 (1956).

2. Clark, A., J. P. Hogan, R. L. Blanks, et W. C. Lanning, *Ind. Eng. Chem.*, **48**, 1152 (1956).

3. Topchiev, A. V., B. A. Krentsel, A. I. Perelman, et K. G. Miesserov, *J. Polymer Sci.* **34**, 129 (1959).

4. Topchiev, A. V., B. A. Krentsel, A. I. Perelman, et T. B. Rode, *Izv. Akad. Nauk SSSR, Ot. Khim. Nauk*, **6**, 1079 (1959).

5. Topchiev, A. V., B. A. Krentzel, A. I. Perelman, et V. I. Smetansuk, *Izv. Akad. Nauk SSSR, Otd. Khim. Nauk*, **6**, 365 (1959).

6. Boreskov, G. K., V. A. Zhisku, et T. Ya. Tyulikova, *Dokl. Akad. Nauk SSSR*, **136**, 125 (1961).

7. Mihail, R., P. Cortaleanu, et A. G. Ioneco, *J. Chim. Phys.*, **56**, 568 (1959).

8. Cossee, P., et L. L. Van Reijen, Actes 2ème Congrès International de Catalyse, Paris, Juin 1960, p. 1679.

9. Pecherskaya, Y. I., V. B. Kazanskiĭ, et V. V. Voevodskiĭ, *Actes 2ème Congr. Intern. Catalyse, Paris, Juin 1960*, p. 2121.

10. Topchiev, A. V., *J. Polymer Sci.*, **53**, 195 (1961).

11. Friedlander, H. N., *J. Polymer Sci.*, **38**, 91 (1959).

12. Guyot, A., C. Blanc, J. C. Daniel, et Y. Trambouze, *Compt. Rend.*, **253**, 1795 (1961).

13. Selwood, P. S., et L. Lyon, *Discussions Faraday Soc.*, **8**, 227 (1950).

14. Capony, J., et L. de Mourgues, *Séparation immédiate et chromatographie 1961*, Gams Ed., Paris, 1962, p. 163.

15. de Mourgues, L., et V. Rochina, *Bull. Soc. Chim. France*, **1962**, 729.

16. Natta, G., *Makromol. Chem.*, **16**, 213 (1955).

Résumé

La cinétique de polymérisation du propylène, catalysée par l'oxyde de chrome déposé sur un support de silice-alumine, est étudiée au moyen d'une nouvelle méthode basée sur l'analyse par chromatographie gazeuse de prélévements effectués dans le milieu fluide monophasé qui entoure le catalyseur solide et qui contient le monomère et du propane, à l'exclusion de tout autre solvant. Les appareillages et les méthodes expérimentales sont décrits en détail. La réaction admet l'ordre 1 par rapport au monomère, ainsi qu'au catalyseur, lorsque sa concentration est suffisante. Entre 80 et 120°C, l'énergie d'activation est de 16 kcal/mole. La vitesse de polymérisation ne dépend de la pression que par l'intermédiaire de la concentration en monomère. Toutefois, lorsque la pression est faible et que la température est assez élevée, un second processus se manifeste; il provoque la formation d'oligomères volatils et retarde le processus normal de polymérisation. L'influence des facteurs structuraux et texturaux relatifs au catalyseur et au support sera étudiée prochainement.

Zusammenfassung

Die Kinetik der Polymerisation von Propylen wird mittels eines Katalysators von Chrom-Oxyd auf einem Träger von Aluminium-Siliziumoxyd nach einer neuen Methode untersucht, die auf der Anwendung der Gaschromatographie durch Abnahme der Proben aus dem fluiden einphasigen Medium, das den festen Katalysator umgibt, beruht und welches nur das Monomer und Propan enthält. Die Apparaturen und experimentellen Methoden sind ausführlich beschrieben. Es handelt sich um eine Reaktion erster Ordnung, in Hinblick auf das Monomer sowie den Katalysator, wenn dessen Konzentration ausreichend gross ist. Zwischen 80 und 100°C beträgt die Aktivierungs-

energie 16 kcal/mol. Die Polymerisationsgeschwindigkeit hängt nicht vom Druck sondern vom Mittel der Konzentration des Monomers ab. Dennoch findet eine zweite Reaktion statt, wenn der Druck zu schwach ist und die Temperatur zu niederig; es bilden sich flüchtige Oligomere, die den eigentlichen Polymerisationsprozess verzögern. Der strukturelle sowie texturelle Einfluss des Katalysators und Trägers wird demnächst untersucht.